USAAMRDL-TR-77-16

ADVANCED OVERRUNNING CLUTCH TECHNOLOGY

Jules G. Kish

Sikorsky Aircraft
Division of United Technologies Corp.
Stratford, Connecticut 06602

December 1977

Prepared for

APPLIED TECHNOLOGY LABORATORY
U. S. ARMY RESEARCH AND TECHNOLOGY LABORATORIES (AVRADCOM)
Fort Eustis, Va. 23604

APPLIED TECHNOLOGY LABORATORY POSITION STATEMENT

The objective of this program was to research, design, and test advanced helicopter transmission overrunning clutches (freewheel units) for the purpose of preparing the Design Guide, USAAMRDL-TR-77-18.

Mr. Michael Dobrolet, Propulsion Technical Area, Technology Applications Division, served as the Project Engineer for this effort.

(9) Final Rept. 14 Mar 74-14 Jun 76

(19) Unclassified

SECURITY CLASSIFICATION OF THIS PAGE (When Data Entered)

REPORT DOCUMENTATION PAGE	READ INSTRUCTIONS BEFORE COMPLETING FORM
1. REPORT NUMBER (18) USAAMRDL TR-77-16 ✓	2. GOVT ACCESSION NO. / 3. RECIPIENT'S CATALOG NUMBER
4. TITLE (and Subtitle) (6) ADVANCED OVERRUNNING CLUTCH TECHNOLOGY	5. TYPE OF REPORT & PERIOD COVERED
	6. PERFORMING ORG. REPORT NUMBER
7. AUTHOR(s) (10) Jules G. Kish	8. CONTRACT OR GRANT NUMBER(s) (15) DAAJ02-74-C-0028 ✓
9. PERFORMING ORGANIZATION NAME AND ADDRESS Sikorsky Aircraft DIV ✓ Division of United Technologies Corp. Stratford, Connecticut 06602	10. PROGRAM ELEMENT, PROJECT, TASK AREA & WORK UNIT NUMBERS (16) 62209A 1F262209AH76 (17) 00-006-EK
11. CONTROLLING OFFICE NAME AND ADDRESS Eustis Directorate ✓ U.S. Army Air Mobility R&D Laboratory Fort Eustis, Virginia 23604	12. REPORT DATE (11) December 1977
	13. NUMBER OF PAGES 311 (12) 316 p.
14. MONITORING AGENCY NAME & ADDRESS(if different from Controlling Office)	15. SECURITY CLASS. (of this report) Unclassified
	15a. DECLASSIFICATION/DOWNGRADING SCHEDULE

16. DISTRIBUTION STATEMENT (of this Report)

Approved for public release; distribution unlimited.

17. DISTRIBUTION STATEMENT (of the abstract entered in Block 20, if different from Report)

18. SUPPLEMENTARY NOTES

19. KEY WORDS (Continue on reverse side if necessary and identify by block number)

Clutches
Helicopters
Freewheel Unit
One Way Clutch
Overrunning Clutch
Spring Clutch
Sprag Clutch
Ramp-Roller Clutch

20. ABSTRACT (Continue on reverse side if necessary and identify by block number)

This report documents a study to find overruning clutch concepts suitable for use in helicopters. Ten designs were selected for in-depth evaluation, and from these, three were selected for fabrication and testing: the spring, the sprag, and the ramp-roller clutches. These performed satisfactorily in the tests, and a design guide was compiled for them (USAAMRDL-TR-77-18).

DD FORM 1 JAN 73 1473 EDITION OF 1 NOV 65 IS OBSOLETE

Unclassified

SECURITY CLASSIFICATION OF THIS PAGE (When Data Entered)

323 800 ✓ JOB

PREFACE

This program was conducted by Sikorsky Aircraft, Division of United Technologies Corporation, Stratford, Connecticut, for the U. S. Army Air Mobility Research and Development Laboratory* under Contract DAAJ02-74-C-0028. The period of performance was from March 14, 1974 to June 14, 1977.

U. S. Army technical direction was provided by Mr. M. Dobrolet of the Eustis Directorate.

Acknowledgement is made to the engineering staff of Borg Warner Corporation, Bellwood, Illinois, for technical assistance in the design of the sprag clutch, fabrication of the sprag unit, and consultation during the test program. Acknowledgement is also made to the engineering staff of the Curtiss-Wright Corporation, Caldwell, New Jersey for the design and fabrication of the spring clutch and technical support during the test phase of the program. Acknowledgement is also given to the engineering staff of the Avco Lycoming Division, Stratford, Connecticut, for the conduct of the test program in its entirety, including design and fabrication of test facilities, operation of the tests, and organization of test data and results.

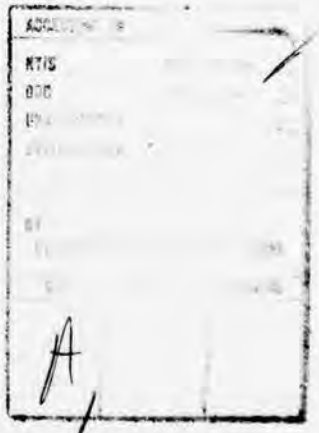

*On 1 September 1977, the Eustis Directorate, U. S. Army Air Mobility Research and Development Laboratory was redesignated the Applied Technology Laboratory, U. S. Army Research and Technology Laboratories (AVRADCOM).

TABLE OF CONTENTS

TABLE OF CONTENTS (Cont'd)

TABLE OF CONTENTS (Cont'd)

LIST OF ILLUSTRATIONS

LIST OF ILLUSTRATIONS (Cont'd)

LIST OF ILLUSTRATIONS (Cont'd)

LIST OF ILLUSTRATIONS (Cont'd)

LIST OF ILLUSTRATIONS (Cont'd)

LIST OF ILLUSTRATIONS (Cont'd)

LIST OF ILLUSTRATIONS (Cont'd)

LIST OF ILLUSTRATIONS (Cont'd)

LIST OF ILLUSTRATIONS (Cont'd)

LIST OF ILLUSTRATIONS (Cont'd)

LIST OF TABLES

LIST OF TABLES (Cont'd)

INTRODUCTION

During the preliminary design phase of this contract, general mechanisms were examined to produce new ideas and concepts that would be applicable to helicopter overrunning clutches. Patents of overrunning clutch designs were examined. Commercial designs and current helicopter freewheel units were studied to see what improvements could be made. Out of this preliminary investigation, ten different designs emerged that were considered worthy of evaluation. A layout was made and analysis performed on each of the ten designs. The design parameters were:

Speed	20,000 rpm
Endurance design horsepower	1500 hp
Static design horsepower	3000 hp
Minimum oil inlet temperature	195°F
Maximum oil inlet pressure	100 psig
Lubricant	MIL-L-7808

After the ten different preliminary designs were examined, an evaluative process was conducted using a weighted-factor method. Fourteen different criteria were evaluated for each clutch design, these being

Weight
Cost
Reliability
Maintainability
Centrifugal effects
Vibration
Transient torque
Thermal effects
Start-up control
Failure modes
Operation limits
Unusual testing
Multi-engine
Bearing brinelling

Many of these evaluation criteria were further subdivided. For example, reliability was divided into number of parts, fail-safety, overrunning wear life, driving fracture possibility, and confidence factor. After the evaluation of each of the fourteen criteria, a single factor, termed the figure of merit, was established for each clutch. From the figure of merit, three candidate clutches were chosen for

further evaluation, fabrication, and test. These were the spring clutch, the sprag clutch, and the ramp-roller clutch. Detail designs were conducted on these three overrunning clutches, and hardware was manufactured.

A comprehensive test program was conducted with identical tests on each of the three clutch designs so that data could be compared on an equal basis. The test phase was divided into two tasks. In Task I, the amount of testing was planned to be just sufficient to "wring out" the weak links in each clutch design. A period was reserved for redesign and retest so that, at the start of Task II testing, each clutch was ready in its final configuration.

For the first time, the clutches were tested in a turbine test rig that was capable of simulating helicopter ground operating conditions of full-speed overrun, differential-speed overrun, operation with rotor inertia, high-speed engagements and disengagements, start-up from rest, torsional forced vibration, and hot and cold environments. The turbine test rig was equipped with a flywheel to simulate rotor head, transmission, and blade inertia, and a water brake capable of absorbing full engine power. The turbine test stand could also simulate full flight operation. During Task II, the following tests were conducted on each clutch

- full-speed overrun, 50 hours
- differential-speed overrun, 30 hours
- dynamic load tests, 750 engagements
- dynamic cyclic, 10,400 cycles
- high-temperature environment, 300°F
- low-temperature environment, -40°F
- static cyclic, 10^7 cycles
- static overload to failure.

A design guide was also compiled that gives the criteria, methods, formulas, curves, charts, figures, etc., for designing a spring, sprag, or a ramp-roller clutch for helicopter use in any speed, power, and torque condition. See "Helicopter Freewheel Unit Design Guide," USAAVLABS Technical Report 77-18.[1]

1. Kish, Jules G., HELICOPTER FREEWHEEL UNIT DESIGN GUIDE, Sikorsky Aircraft, USAAMRDL Technical Report TR-77-18, Eustis Directorate, U. S. Army Air Mobility Research and Development Laboratory, Fort Eustis, Virginia, October 1977.

DESIGN SELECTION

The following pages discuss each of the ten clutch designs prepared during the program. The principle of operation for each clutch is explained both for the driving and the overrunning modes. Manufacturing problems are discussed along with the key features of each design.

SPRING CLUTCH

The principle of operation of the spring clutch is depicted in Figure 1. A spring of rectangular cross section is positioned between two concentric internal shaft diameters. The end coils of the spring are of a larger diameter than the central coils and are in contact with the bores of the shafts. When the two shafts are twisted relative to each other so as to wind the spring tighter, the coil diameters contract and the end coils slip on the shaft bores. When the two shafts are twisted so as to unwind the spring, the spring expands and grips the shaft bores along its entire length. In this position the spring is able to transmit torque from one shaft across the gap to the other shaft.

The center coil of the spring, which bridges the gap between shafts, must transmit the full torque through its cross section. The load along the length of the spring then gradually decreases as the torque is transmitted into the housing.

The least expensive spring to manufacture has a coil of constant-section wire, heat treated, and finish machined. Since the center section must carry the full torque and the wire is of constant section, the end coils have very low stress. However, with this design, the spring is excessively long. The constant cross-section spring is therefore unacceptable for aircraft use. A constant-stress spring is the lightest solution. In a constant-stress spring clutch, the thickness of the spring will vary exponentially with length. If the radial thickness is varied, the spring will still be excessively long; hence, the best solution is to vary the axial thickness of each coil. In practice, an approximation to an exponential distribution is easier to manufacture.

The candidate spring overrunning clutch is shown in cross section in Figure 2. Note that in this design the spring thicknesses in both the axial and radial dimensions are varied to obtain an approximation of a parabolic constant-stress function. The central coils of the spring are relieved. During overrunning, the spring contacts only on the end coils, which are designed with an interference fit. The spring guide arbor holds the spring in alignment during overrunning and forces the slippage to occur on the end coils of the shaft opposite to the shaft attached to the arbor.

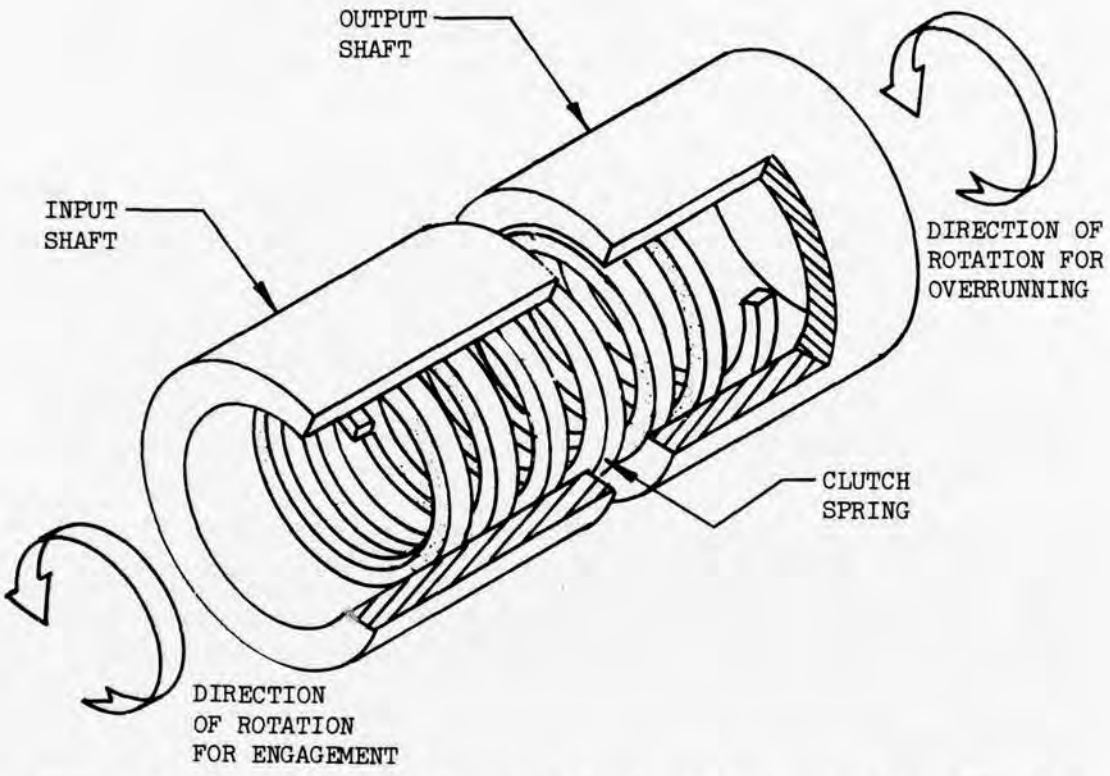

Figure 1. Principle of Operation, Spring Overrunning Clutch.

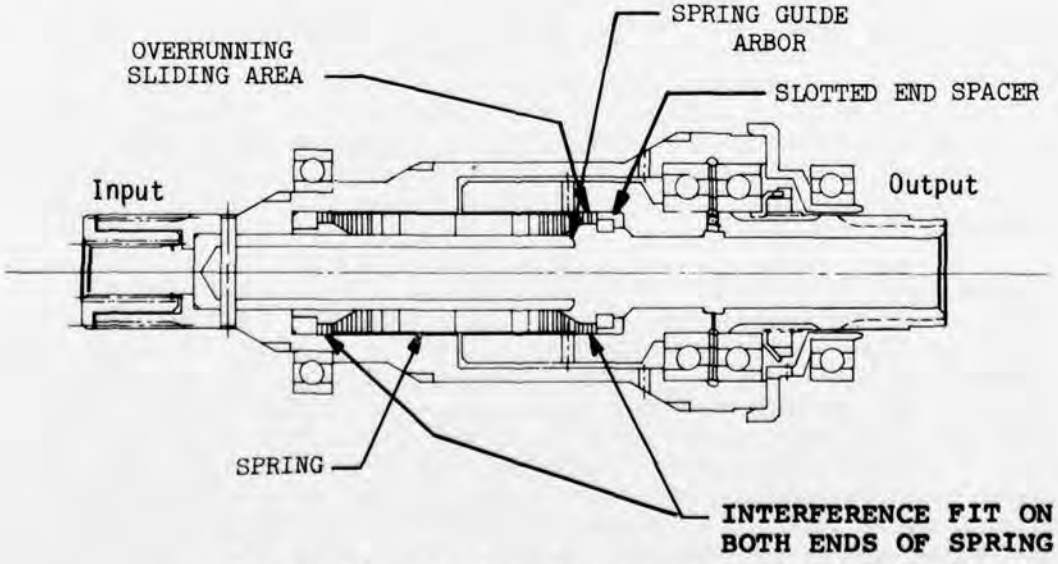

Figure 2. Spring Overrunning Clutch.

The clutch's outer housing member is provided with two bearings that support the clutch output shaft independently of the input shaft. Relative rotation between input and output clutch shafts is permitted by the preloaded tandem bearings between the two members. Bearing brinelling is minimized with this bearing arrangement.

Lubricant is fed through either end of the clutch to the inner shaft member where it will feed past the slotted end spacer, over the end coils of the spring, which are also slotted, and through the drain holes in the output shaft bore. During overrunning, the oil must pass over only the portion of the spring that is rubbing, thereby assuring proper lubricant flow to the area of the spring and housing which are contacting. The duplex bearings are also lubricated through central holes in the input shaft and through slots at the bearing interfaces. The outer support bearings are lubricated by fixed jets in the support housing.

Other designs of spring clutches are also feasible. For example, the central coil can be manufactured to be integral with either the input or output shafts. In practice, this type of design is difficult to manufacture and induces high stresses at the shaft-spring interface and is, therefore, not recommended.

SPRAG CLUTCH

The sprag clutch is probably the most widely used type of overrunning clutch in commercial and aircraft applications today. The sprag clutch operates on the principle of the wedge. The inner and outer shafts are concentric circular cylinders, which are the least expensive type of shaft to manufacture. However, the sprag unit is itself complex and involves precision machining and tolerances. Several different firms specialize in the manufacture of sprag units and offer inexpensive prices due to the high quantities used in industrial applications. Two different types, "A" and "B", are depicted in Figure 3.

In the type A design, a ribbon spring located between two sprag carriers keeps the sprags in contact with the inner and outer shafts, while a garter-type spring accomplishes the same purpose in the type B design. Driving action is obtained by wedging the sprags between the inner- and outer-shaft races. Drag devices hold the sprag unit to either the inner or outer race. During overrunning, the sprags slide on the inner or outer race depending on which race is not held frictionally to the sprag unit. A unique feature of the type B design is the sprag abutment feature, which comes into play during a static overload. In an overload condition, the sprags contact each other, forming a solid unit that cannot "roll over." The

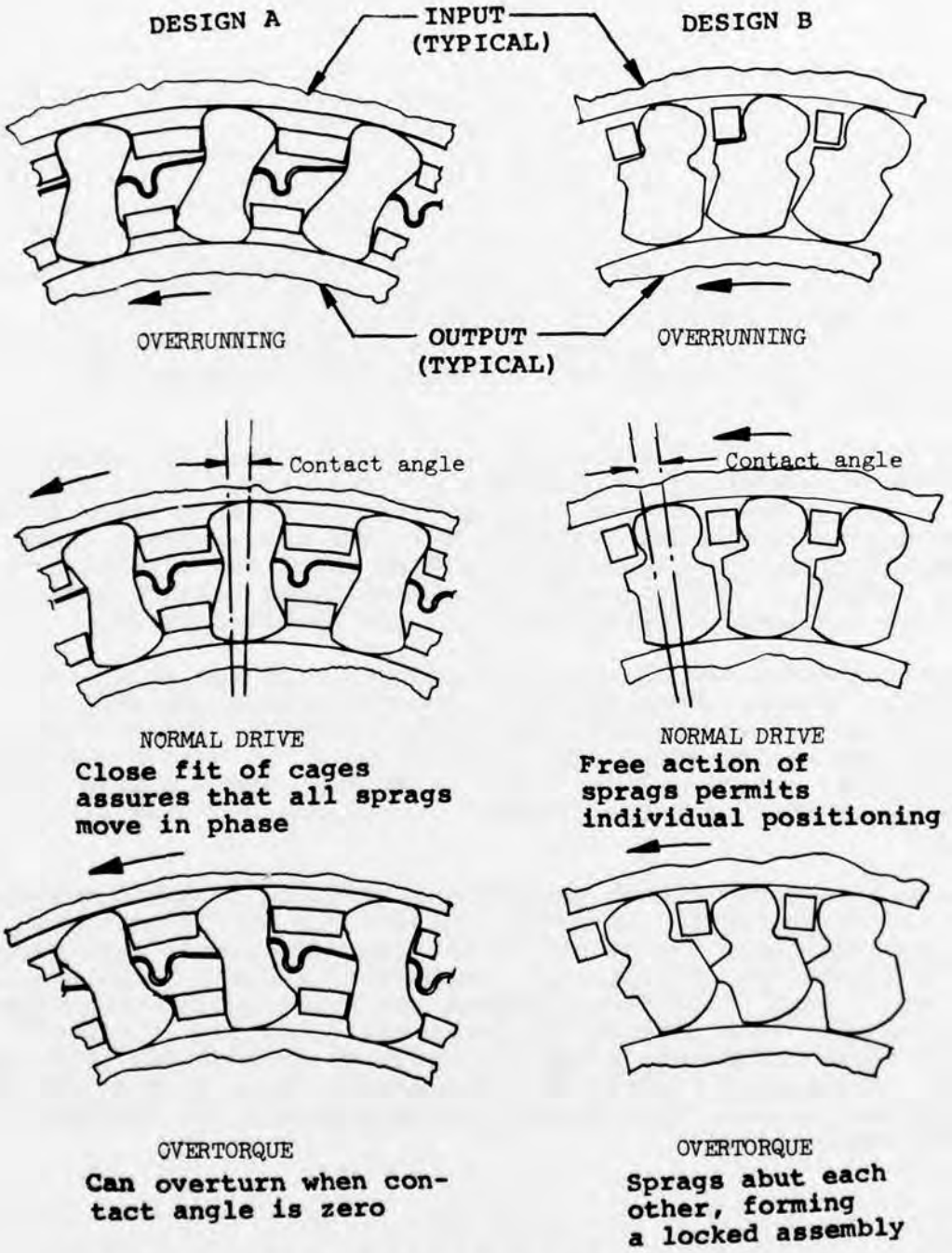

Figure 3. Principles of Operation of Two Sprag Overrunning Clutches.

"roll over" under high static torque conditions is a possible sprag failure mode for the type A design.

The candidate sprag clutch design is shown in Figure 4. Both types A and B fit into the same envelope provided by the outer shaft inside diameter, the inner shaft outside diameter, and the innermost oil dams. With the straddle-bearing arrangement shown between input and output shafts, bearing brinelling may occur because the bearings are not preloaded. However, the arrangement shown provides good support for the sprag unit and is preferred over a back-to-back mount on one side of the sprag unit, such as that used in the spring clutch design. Another key feature is the straddle mounting of the entire unit through the outer shaft. This arrangement provides good support for the clutch unit and minimizes concentricity problems.

For high-speed operation, the outer shaft assembly, without the oil dams, bearings, or inner shaft, is balanced as an assembly. This is the most critical component for unbalance since it has the most mass and the largest radii, and has hardware (nuts and bolts) in the flange areas all of which can unbalance the assembly. The oil dams are generally in balance because of the inherent concentricity of these machined parts.

Lubrication is fed to the innermost shaft of the sprag over-running clutch, where it then proceeds through the shaft to lubricate the sprags and the clutch bearings. The oil dams force the entire sprag area to flood with oil when the outer housing is rotating. The diameter of the dams are less than the inner shaft outside diameter by between .005 and .015 inch.

The entire sprag clutch assembly is isolated from the remainder of the drive train. The unit contains its own support bearings, which react only the weight of the unit since only pure torque is transmitted. This is the recommended design practice. It is not a good practice to combine the sprag clutch with other units, such as a gear on the outer shaft, because the loads from these components often influence the structural integrity and operation of the clutch. In general, this is true for all freewheel units. They should be isolated and not combined with other units.

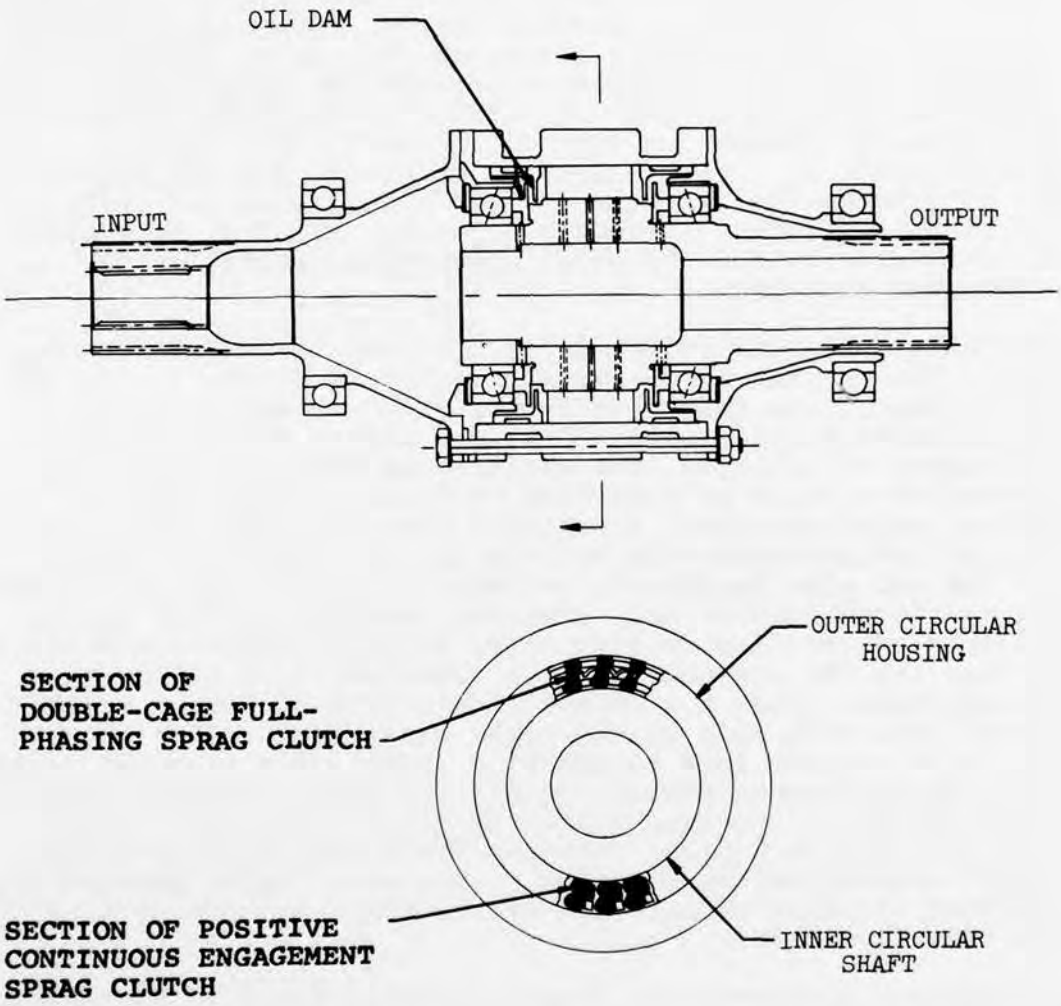

Figure 4. Sprag Overrunning Clutch.

RAMP-ROLLER CLUTCH

The ramp-roller clutch and its design derivatives is one of the oldest types of overrunning clutches known. Many patents for this type of clutch date from the 1800's. The ramp-roller clutch is commonly used in helicopter transmissions. Driving action is obtained by wedging a cylindrical roller between a cam-shaped member and a circular member. The cam member can be located on the inner or the outer portion of the unit. It is common automotive practice to broach the cam on the inside of the outer shaft of the ramp-roller overrunning clutch. This greatly reduces the cost of the unit. For aircraft applications, it is not practical to broach the cam because the tolerances are critical to keep the size of the unit small and because grinding is required. Also, the cost of a broach is not warranted for the usual production quantities of helicopter clutches.

The basic operating principle of the ramp-roller overrunning clutch can be seen in the cross section of Figure 5. In the design shown, the innermost member is a cam shaped as an equillateral polygon with "n" sides, where "n" is equal to the number of rollers. The rollers are positioned in relation to each other by a carrier or "cage" member that is spring loaded to impart a constant torque to the cage. This preload torque causes the rollers to touch the outer housing and cam and also forces the rollers to remain in contact under all operating conditions. When the input and output shafts are twisted relative to each other so as to wedge the rollers between the cam and housing, the freewheel unit is in the driving mode. When the opposite direction of torque is applied, the rollers will roll on the outer housing and slide on the cam, allowing the unit to overrun. Positive spring and plunger force is maintained throughout all operating modes by careful consideration of centrifugal loads and friction during the design of the mechanism. The cam shaft has circular-shaped relief grooves across the face of the cam. These grooves are provided for ease of assembly of the unit and have no other functional purpose.

The candidate ramp-roller clutch designed for 1500 horsepower and 20,000 rpm is depicted in Figure 6. The unit shown contains 14 equally spaced rollers. Generally, 12 or 14 rollers are employed as this is the maximum number that will fit into an equillateral polygon cam design with the normal ratio of roller diameter to cam diameter. More rollers can be designed into the unit if an undercut type of cam is used. The undercut cam design requires axial grinding as opposed to circumferential grinding of the equillateral polygon cam and is, therefore, not used since accuracy is sacrificed. The number of rollers should always be an even number to permit broaches to extend through diametrically opposed roller pockets in the cage.

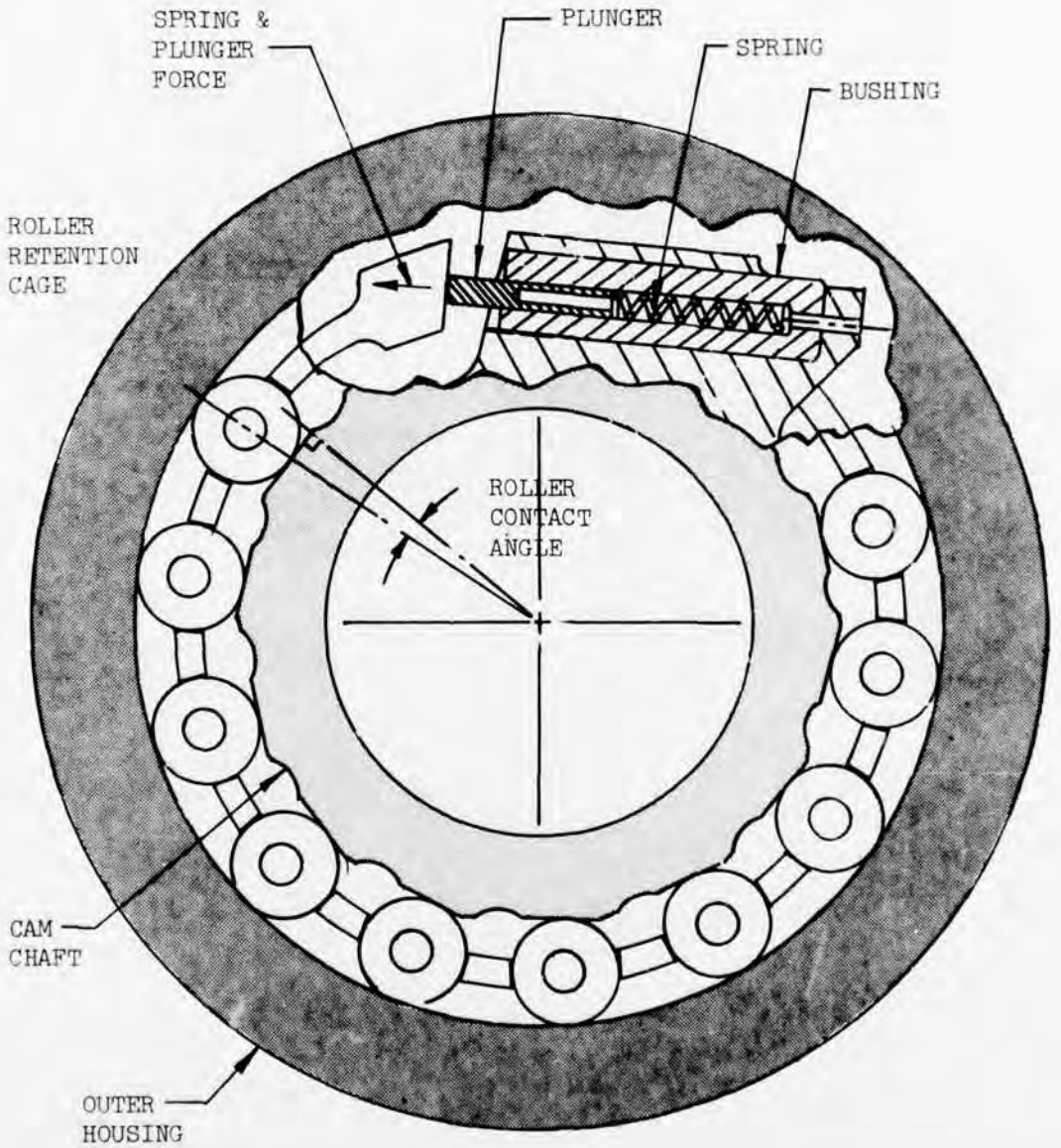

Figure 5. Cross Section of Ramp-Roller Overrunning Clutch.

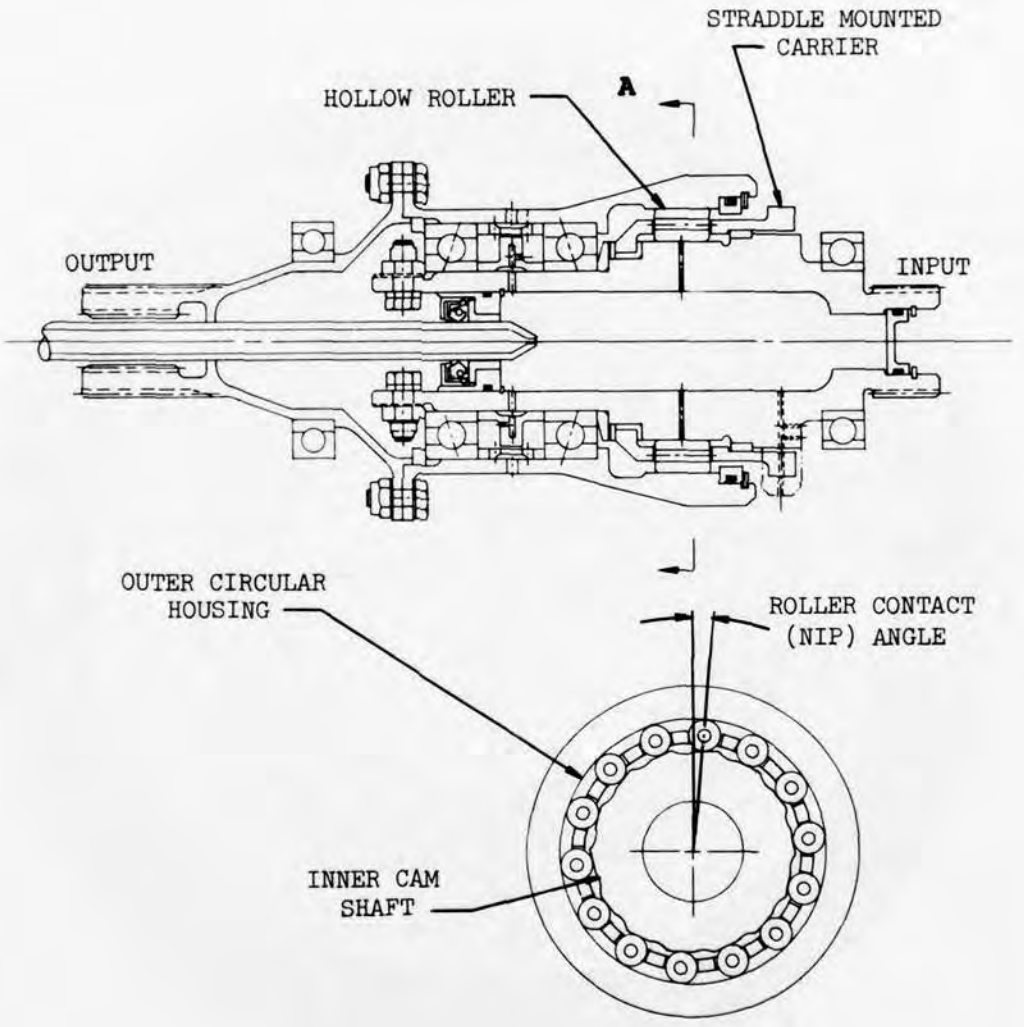

Figure 6. Ramp-Roller Overrunning Clutch.

The carrier of the ramp-roller clutch is straddle mounted. This is not done to provide rigidity to the carrier but rather to provide a trapped area into which oil must congregate and from which to pass through the gaps between the rollers and the carrier. Oil must pass over the rollers and lubricate the proper areas with this design.

Hollow rollers are used to reduce Hertizian contact stresses. Since Hertz stresses generally dictate the overall size of the ramp-roller clutch, hollow rollers in effect reduce the overall size of the unit. The rollers are crowned on the outside diameter to reduce end loading.

Overall support for the unit is provided through the preloaded back-to-back duplex bearing set. A better arrangement is to support the freewheel unit entirely on the outer shaft. This arrangement is, however, heavier and more expensive than the design shown and was, therefore, not used.

Lubrication is fed to the inside of the unit from a fixed jet. The sealed inner chamber will pressurize because of the restriction created by the exit jet passages being of less area than the inlet line. The pressurized lubrication feature is incorporated to reduce wear during full-speed overrunning. For a low-speed design (under 10,000 rpm), it is better to have the cam as the output member and lubricate by centrifugal action. For the high-speed freewheel unit, the centrifugal load of the rollers on the housing would be too high to permit the cam output design. During differential overrunning, the centrifugal effects on the roller come into play in the cam input design, but the sliding speed is reduced and approaches zero as the differential speed approaches the locked position. Thus, for a high-speed ramp-roller clutch, it is better to design with the cam as the input member and to use pressurized lubrication.

The roller contact angle, commonly referred to as the "nip" angle, is a critical ramp-roller clutch design parameter. Small contact angles increase stresses in the clutch components. Any wear of the cam, the roller, or the housing will increase the nip angle. When the tangent of one-half of the roller contact angle exceeds the coefficient of friction, the roller will be unable to sustain load and will "spit out". This will usually occur with a nip angle in the area of 10 to 12 degrees. Thus, a low nip angle creates high loads, while a high nip angle does not leave enough material for wear. A desirable nip angle is in the range from 4 to 6 degrees. This value leaves ample room for wear and also does not create excessive normal roller loads.

ACTUATED DOUBLE-CAGE RAMP-ROLLER CLUTCH

The actuated double-cage ramp-roller clutch operates on the principle of the conventional ramp-roller clutch except that, during overrunning, the rollers do not come into contact with the outer housing. A compound planetary control device automatically disengages the rollers during overrunning by the actuation of a secondary, outer-roller retention cage. A cross section of the design is shown in Figure 7.

As shown in section A-A of the figure, the outer roller carrier is piloted on the inner carrier and is free to rotate about it. The inner carrier in turn is piloted on the cam shaft and is free to rotate about it. The inner carrier is identical in design to the carrier of the conventional ramp-roller clutch. A constant torque is applied to the inner cage by a pin and spring mechanism, just as it is with the conventional design. The outer cage has roller slots with one side of each beveled. When the two cages are rotated, the bevel portion of the outer cage contacts the roller, the rollers are loaded as shown in Figure 8.

When the clutch is in the overrunning mode, the roller has imparted to it an inward force that holds the roller against the cam. If the roller is held against the cam near the zero-nip-angle area, there will be an approximately .005-inch gap between the roller and the outer housing. Thus, during overrunning, there will be no roller movement and hence no wear on the major clutch components, i.e., the cam, the rollers, the cages, or the housing.

To rotate the cages relative to each other during overrunning, a small planetary arrangement is used. This planetary control unit automatically disengages the rollers from the outer housing whenever the outer housing rotates faster than the cam input shaft. Whenever the input speed reaches the speed of the output, the control mechanism disengages the outer carrier and permits the freewheel unit to function as a conventional ramp-roller clutch.

The control mechanism consists of an epicyclic unit with a sun gear rigidly attached to the cam shaft, a pinion gear free to rotate about the nonreactive planet carrier, and a ring gear attached to the outer housing. The pinion gear contains an additional section that is called the pinion roller. The diameter of the pinion roller is approximately equal to the pitch diameter of the pinion gear. A sun roller, attached to the outer carrier, meshes with the pinion roller and is preloaded against it. If the diameter of the sun roller were exactly equal to the pitch diameter of the sun gear, the roller would follow exactly the motion of the gear; i.e., the

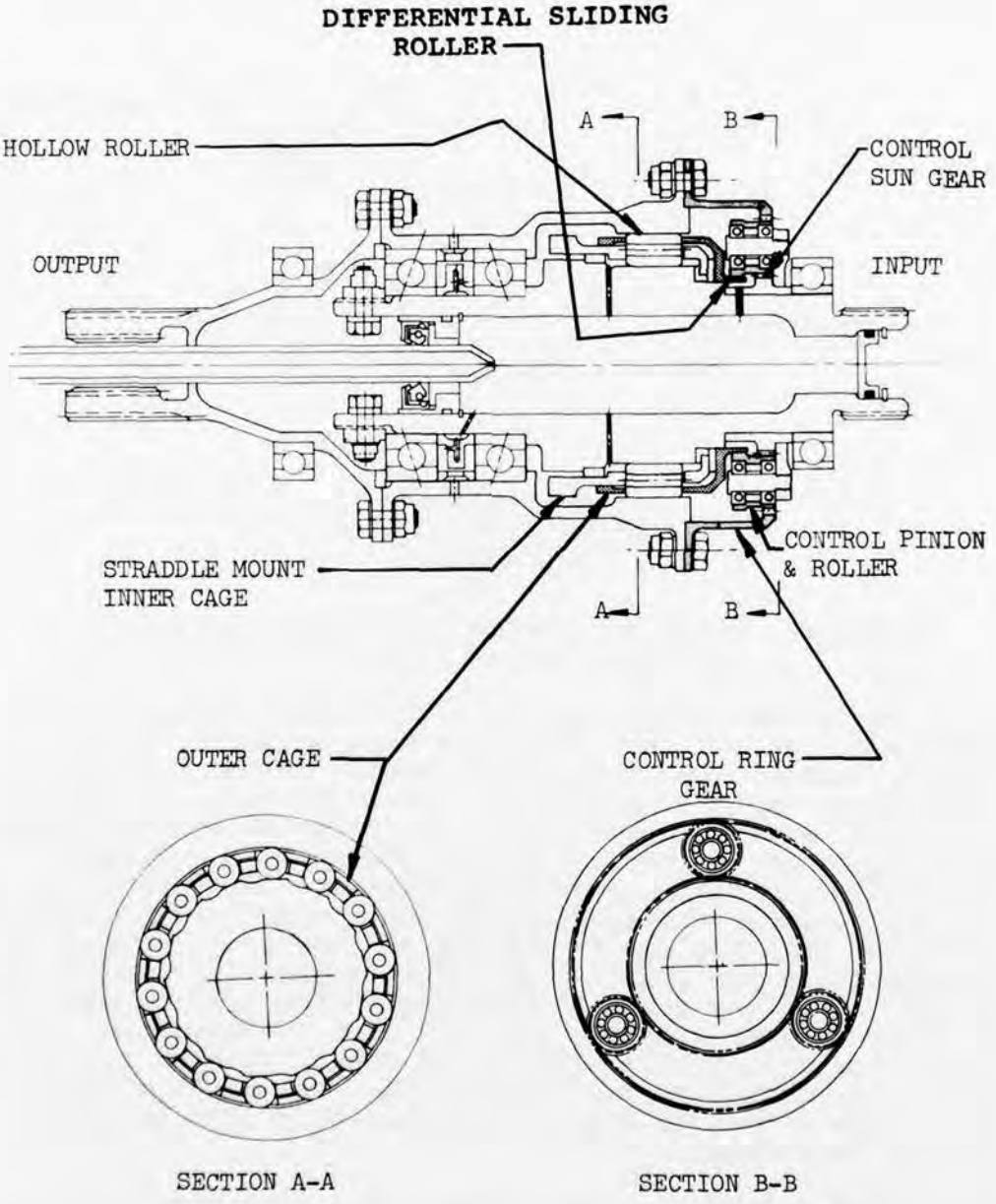

Figure 7. Actuated Double-Cage Ramp-Roller Overrunning Clutch.

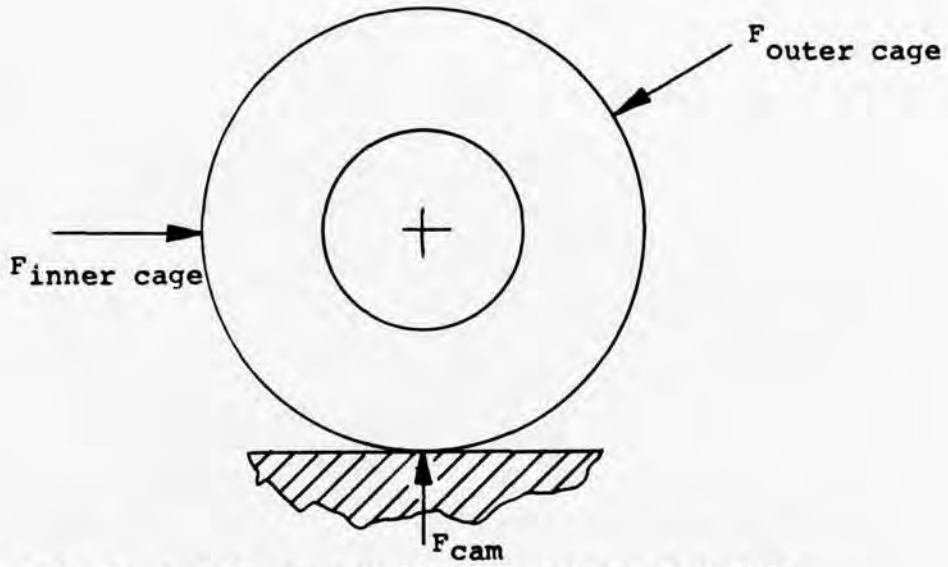

Figure 8. Loads on a Roller of Actuated Double-Cage Ramp-Roller Clutch.

outer cage would rotate exactly with the cam shaft. If the diameter of the sun control roller were slightly larger or slightly smaller than the pitch diameter of the sun gear, it would force the outer carrier to rotate relative to the cam at a small relative speed either clockwise or counterclockwise. For example, if the control pinion roller is one percent larger than the pinion-gear pitch diameter (approximately .616 inch versus .610 inch), the control sun roller will rotate at 158 rpm when the cam is stopped and the outer housing is rotating at 20,000 rpm. A back stop is provided on the inner carrier. When the outer carrier forces the rollers backward, the inner carrier will hit the back stop. Thereafter, the control sun roller will slip on the control pinion roller, but only at the relative speed of 158 rpm. The sliding velocity has therefore been reduced by a factor of 20,000 to 158 (a 126 to 1 reduction).

The control system described above has a high degree of redundancy because failure of any of the control components merely causes the clutch operation to revert to that of a conventional ramp-roller overrunning clutch. However, the design is complex and the added components increase cost.

BALL-BEARING-CARRIER RAMP-ROLLER CLUTCH

The ball-bearing-carrier ramp-roller clutch operates on the principle of the conventional ramp-roller overrunning clutch. The rollers of this design are individually mounted at each end by instrument ball bearings. When the clutch is driving, the drive load passes directly through the rollers and not through the bearings. A cross section of the design is shown in Figure 9.

The purpose of the ball bearings is illustrated in Figure 10. During overrunning, the rollers will be held in contact with the outer housing by the bearings, and the carrier will be rotated backwards by the action of oil on the outer housing impinging on the rollers. Since the bearings force the rollers into a position on a radial line about the center of rotation, the rollers will not contact the cam surface during overrunning. In this position, there is very little wear since the rollers roll on the outer housing with no other contact taking place.

Note that this design uses 10 rollers as opposed to the 14 rollers of the previous ramp-roller clutches. Moreover, the rollers are .500 inch diameter versus .375 inch in the conventional design, and the cam is smaller in cross section. The purpose of these changes is to reduce the rpm of the rollers about their own axes during full-speed overrun. In the conventional ramp-roller clutch with a 3-inch-diameter housing bore and a .375-inch-diameter roller, the rollers are rotating at 160,000 rpm about their own axes. With the 10 rollers at a smaller radius, the rollers are rotating at 120,000 rpm about their own axes during full-speed overrunning. The 120,000-rpm figure is equal to the maximum allowable rpm recommended by the manufacturer for the instrument bearings. The disadvantage with the larger rollers is the increased centrifugal loads during overrunning. In both the conventional and ball-bearing-carrier ramp-roller clutches, the rollers are designed for equal bending margins of safety under the maximum static loading. The roller stress is maximum on the inside hole directly under the load point.

The lubrication of the ball-bearing-carrier ramp-roller clutch follows the principles of the conventional clutch designs. Oil is fed to the innermost driveshaft where it is metered to the roller area. From the roller area the oil passes through the instrument bearings.

The mounting arrangement is similar to that of the sprag clutch. The outer member is supported at both ends, forming a rigid assembly. The input cam shaft is supported and is free to center itself through the rollers.

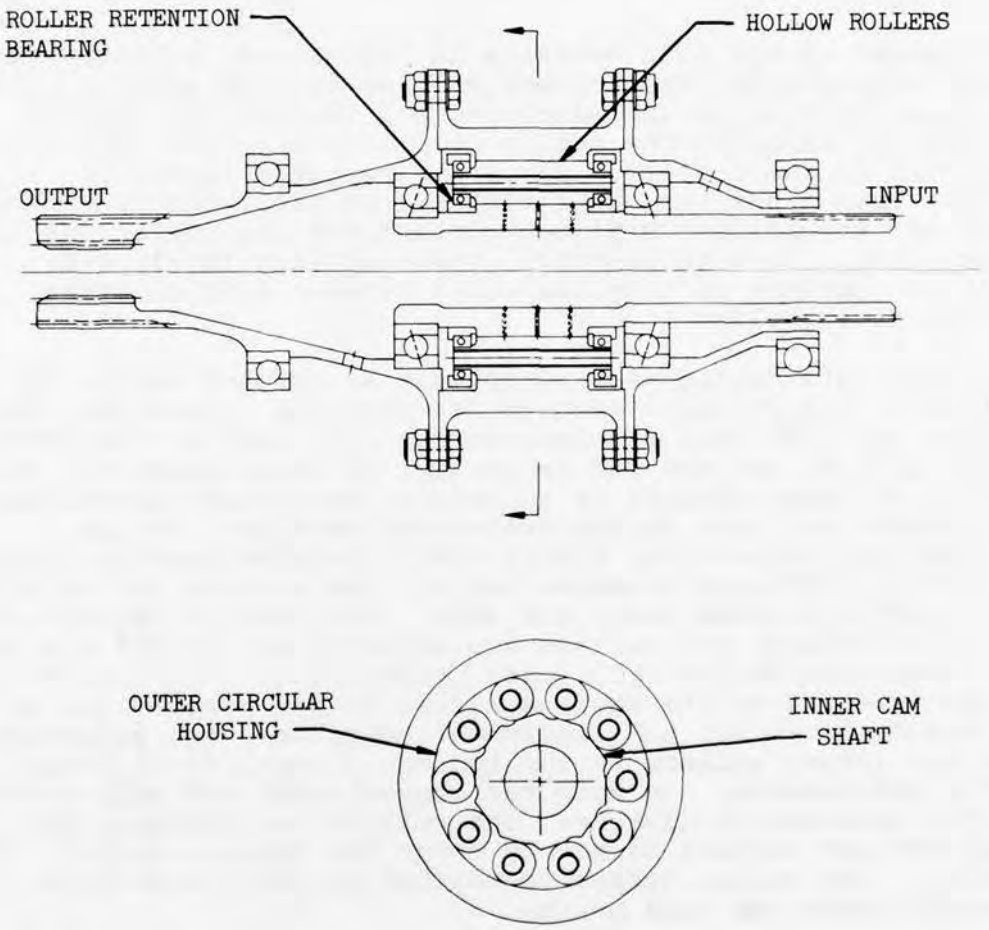

Figure 9. Ball-Bearing-Carrier Ramp-Roller Overrunning Clutch.

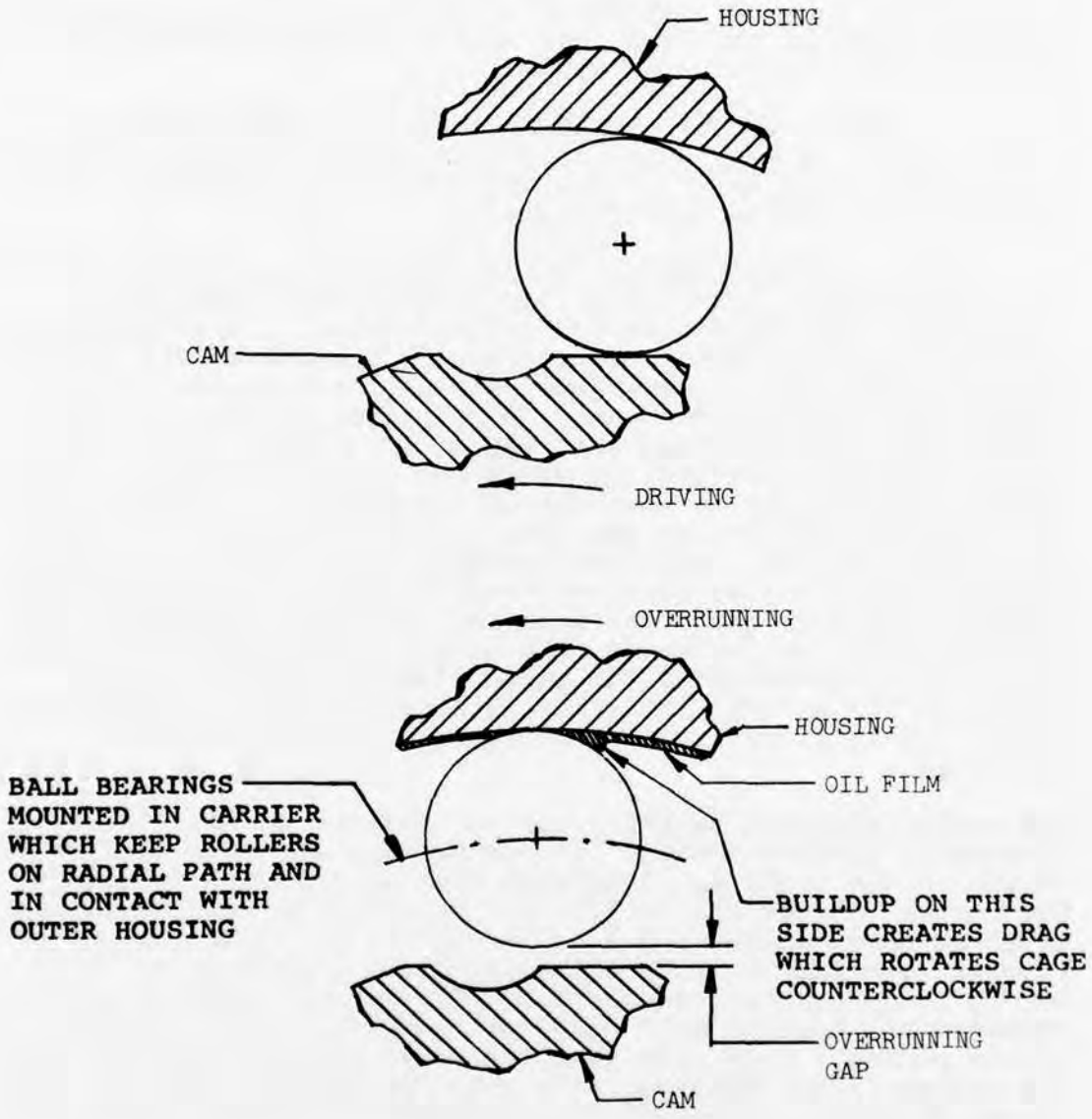

Figure 10. Position of Rollers During Overrunning, Ball-Bearing-Carrier Ramp-Roller Clutch.

ROLLER-GEAR RAMP-ROLLER CLUTCH

The final type of ramp-roller clutch to be considered has been termed the "roller-gear ramp-roller" overrunning clutch. The name comes from the similarity of the clutch roller to a roller-gear-drive type of pinion where a small spur gear is attached to each roller of the freewheel unit. The roller-gear ramp-roller clutch is shown in Figure 11.

The spur gear attached to each roller has a pitch diameter that is equal to the outside diameter of the rollers. Attached to the outer housing is a ring gear whose pitch diameter is equal to the housing bore diameter.

The roller-gear ramp-roller clutch operates on the same principle as does the conventional ramp-roller clutch previously described. The purpose of the geared-roller arrangement is to drive the rollers during overrunning. In a conventional ramp-roller clutch, the rollers theoretically roll on the outer housing and slide on the cam. In practice, sliding is reduced on the cam and introduced into the outer housing. From previous high-speed testing, it was shown that the rollers and the housing are subject to wear during overrunning. If the rollers were in pure rolling, as the theory indicates, the wear would be greatly reduced. With the internal ring gear driving the rollers of the roller-gear ramp-roller clutch, the rollers are forced to roll on the outer housing. Although sliding on the cam shaft will be increased, the wear rate at this point has been reduced by means of the pressurized lubrication system employed. Thus, with the roller-gear ramp-roller overrunning clutch, overall performance should be increased and wear decreased.

The roller and gear assembly can be designed and manufactured in several different ways. In one method, the gear is inertia-welded to the rollers. A through bolt may be employed since the torque between the rollers and the gear is very low. Electron-beam welding may also be employed. Figure 12 shows several alternate methods of manufacture. The best solution may be the recess action gearing. The pinion contains only addendum and has its root diameter above the pitch diameter of the pinion. Thus, the gear can be machined integrally with the roller. The internal drive gear contains no addendum and is all dedendum. Since it is a separate component, there are no manufacturing difficulties involved.

Note also that the roller-gear ramp-roller clutch utilizes 10 rollers as did the ball-bearing-carrier ramp-roller clutch. As in the ball-bearing-carrier overrunning clutch, the purpose of the fewer rollers (10 versus 14) is to reduce the rpm of the roller about its own center. Also, the gear teeth are

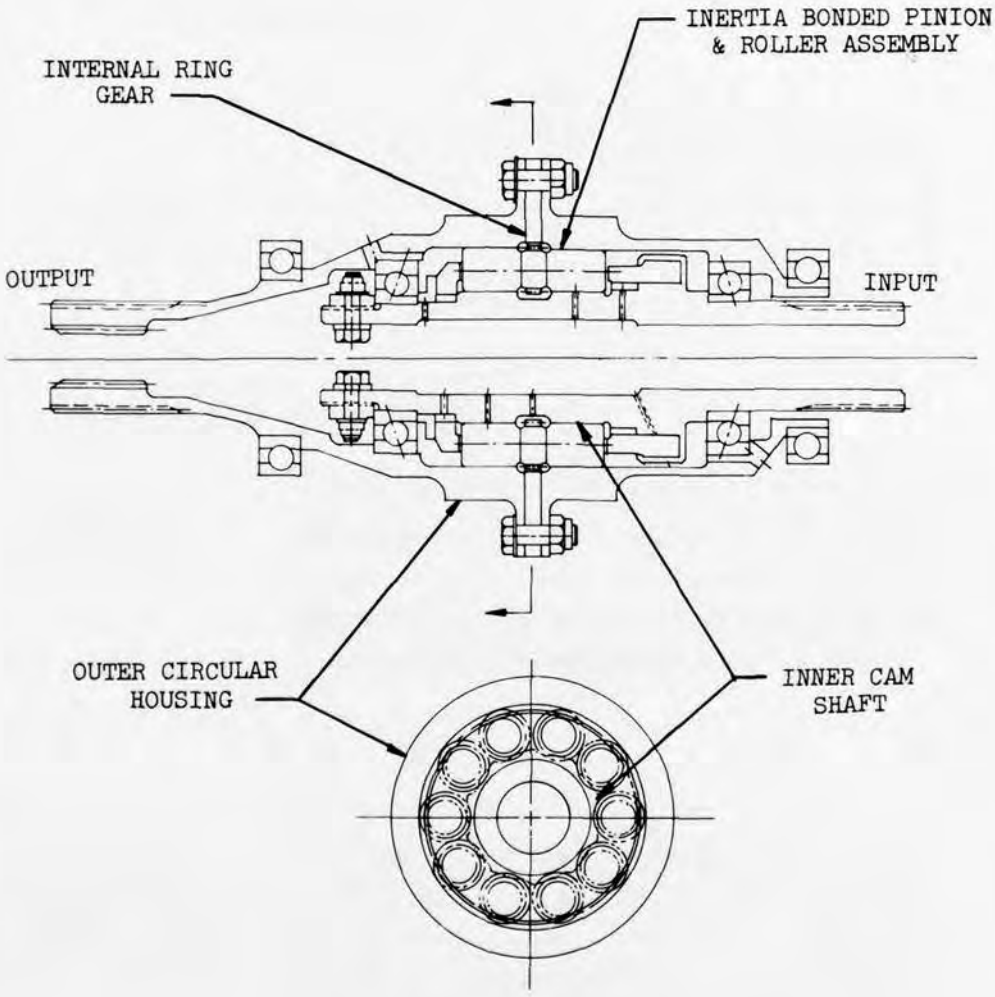

Figure 11. Roller-Gear Ramp-Roller Overrunning Clutch.

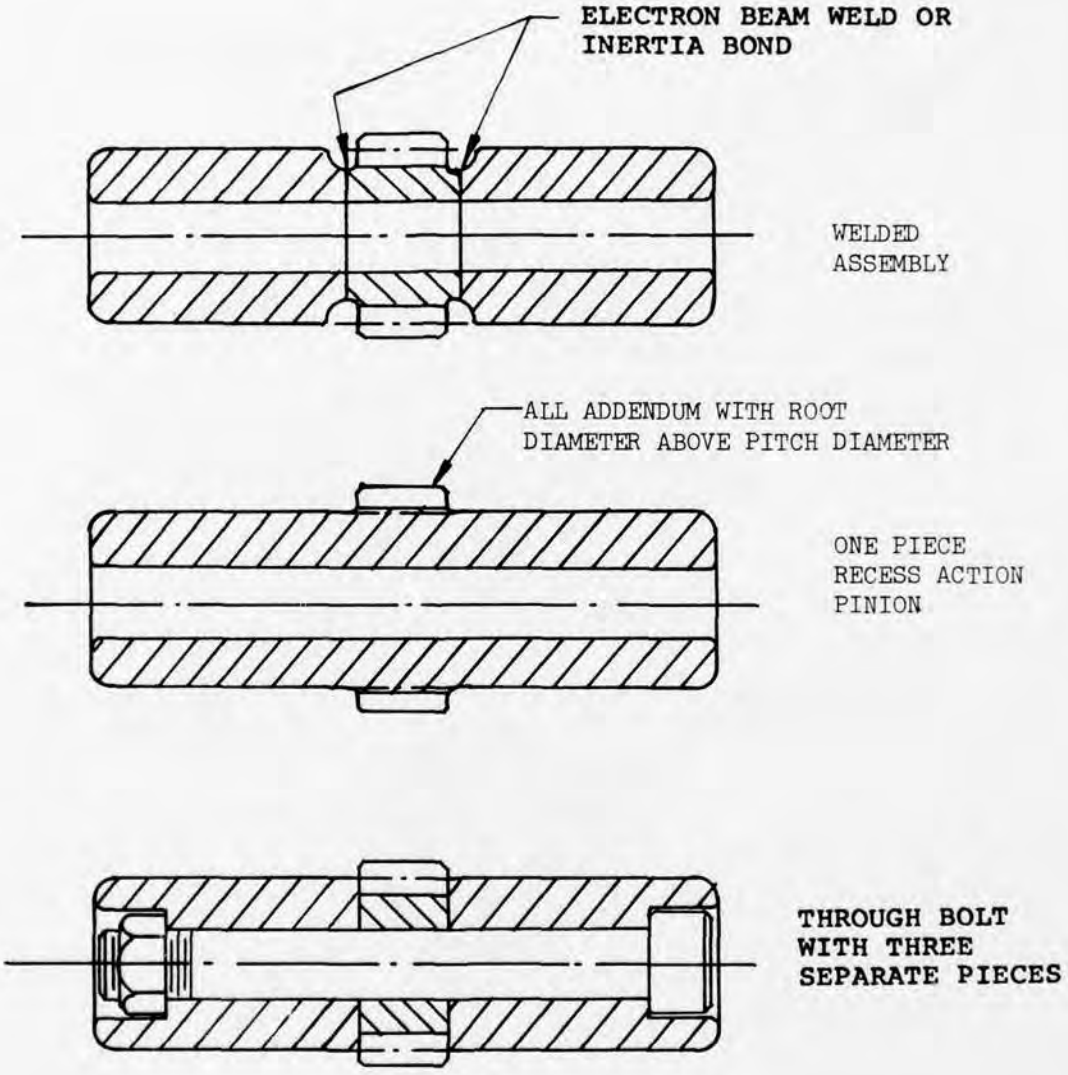

Figure 12. Alternate Designs of Roller and Gear Assembly.

stronger in the .5-inch-diameter gear than in a .375-inch-diameter gear for the same number of teeth because a thicker tooth can be used. The disadvantage of the larger diameter roller and gear assembly is that the centrifugally induced force becomes high at 20,000 rpm, having a value of 1010 pounds. This leads to increased wear in the form of higher pressure between the roller and housing.

Overall support for the roller-gear ramp-roller overrunning clutch is provided by two bearings attached to the output member. Two bearings located between the input and output shafts provide support for the input cam shaft.

In the event any of the components of the gear drive fail, such as the teeth or the weld in the roller and gear assembly, the operation of the unit will revert to that of a conventional ramp-roller clutch. Thus, almost any type of failure of the gear unit is fail-safe other than a failure that would jam the rollers.

Lubrication of the unit is by conventional means through metering ports on the innermost cam shaft. A thin film of oil is retained on the output shaft by proper location of the drain holes.

POSITIVE-ENGAGEMENT RATCHET CLUTCH

The positive-engagement ratchet overrunning clutch uses a curvic coupling as the torque carrying member. A control device consisting of a helical spline and a pawl and ratchet assembly automatically disengages the curvic coupling during overrunning. With the driving members disengaged, there are no rubbing parts other than the small pawls of the control ratchet. A cross-sectional view of the design is shown in Figure 13.

Once the two halves of the curvic coupling are engaged, the positive-engagement ratchet clutch drives directly through the curvic coupling, with no torque being transmitted by the control ratchet. One-half of the curvic coupling is attached to the internal member of a helical spline. The helix angle of the spline is arranged such that the thrust produced during the transmittal of torque overcomes the separating loads created by the curvic coupling. The faces of the coupling are held together by this axial thrust on the spline. The pawl and ratchet assembly aligns the teeth with the spaces of the mating curvic-coupling half during engagement.

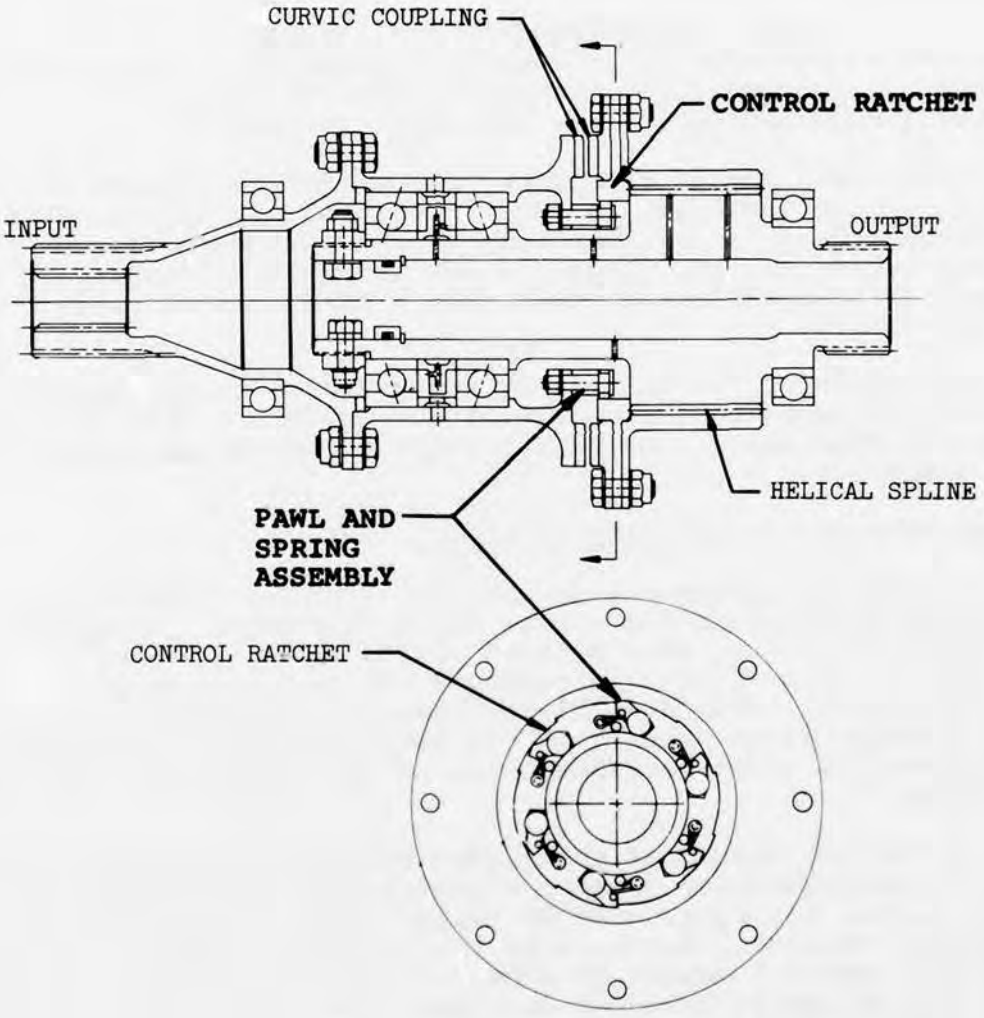

Figure 13. Positive-Engagement Ratchet Overrunning Clutch.

Whenever the input shaft tends to run slower than the output shaft, the reverse thrust created on the helical spline drives the movable curvic-coupling half out of engagement. When it travels the proper axial distance, it hits a stop whereupon further movement is prevented. Since the input shaft is still attempting to rotate slower than the output, the ratchets will overrun. The faces of the curvic coupling do not touch during overrunning, and the only rubbing parts are the small control ratchets.

When the input shaft attempts to drive faster than the output, one of the three pairs of pawls will engage the ratchet that locates the movable curvic coupling half into the proper position for engagement. After the pawl engages, the drive torque attempts to travel through the helical spline. This creates an axial load that advances the spline and curvic coupling into engagement. Once the two faces of the opposing curvic-coupling halves have "bottomed", all the torque passes through the curvic-coupling teeth.

The advantage with this arrangement is of course that the components that rub during overrunning, namely the pawls and the ratchet, can be designed very small and light. If the natural frequency of the pawls and springs is designed to be low, the pawl will be unable to respond to the forcing frequency of the ratchet, which is equal to the number of teeth times the rotational speed. If the pawl cannot respond to the ratchet frequency, it will simply remain motionless and "hydroplane" on the ratchet tips. There is very little wear of the pawl and ratchet assemblies under these conditions. There is, of course, no wear on the helical spline or the curvic coupling.

The movable curvic coupling, the ratchet, and the internal helical-spline members have been designed as separate components. This has been done only for ease of manufacture for the prototype hardware. For a production design, the three pieces could be combined into one, and the bolted connection could be eliminated.

Support of the positive-engagement ratchet overrunning clutch is provided by two ball bearings that straddle the input and the output shafts. With this type of design, the weight of the unit must be supported by the tandem back-to-back duplex bearings located between shafts. The preferred method is to support the freewheel unit entirely on the outer shaft. This support method was not employed in the design shown because the additional component required would be expensive to manufacture and would add considerable weight to the unit. Weight, cost, and reliability trade-offs should be conducted to determine the best mounting arrangement.

Lubricant is supplied to the innermost shaft, whereupon it is fed to the helical spline, the ratchet and pawl area, and the curvic coupling.

FACE-RATCHET CLUTCH

The face-ratchet overrunning clutch is a direct-drive clutch that uses a ratchet as the overrunning mechanism. Figure 14 depicts the general design configuration. This design has been used to a limited extent in a previous production helicopter.

Driving action is obtained directly through axially opposed cam members. A slightly negative rake angle on the driving faces locks the two members together during driving. Operation is similar to that of a jaw clutch.

During overrunning, a straight spline is provided that allows axial movement of one-half of the face cam. The side of the cam opposite to the drive side has a ramp that forces the ratchet faces apart during overrunning. A spring and pin mechanism loads the movable cam member against its mate to permit locking whenever the input speed attempts to exceed the output.

Load sharing between the faces of the mating ratchet members is obtained by holding close tolerances on the angular location of the driving faces. The faces would necessarily be case-carburized and ground.

At first glance, it may appear that the face-ratchet overrunning clutch is unsuitable for high-speed operation. Increased speed will increase the clashing of the faces. However, when considering the oscillating face cam member as a spring and mass system and considering the approximate weight of the moving member and the spring rates of the individual springs, it is seen that the natural frequency of the movable system can easily be designed to be as low as 400 cycles per minute. The forcing frequency during overrunning will always be much higher than this and is found by multiplying the number of ratchet teeth by the rpm. In operation, the mass and spring system will follow the forcing frequency at all differential speeds from zero up to its natural frequency.

At differential speeds higher than the natural frequency, the oscillating ratchet will be unable to follow the forcing cam and the tips of the ratchets will just be touching. With proper lubrication, a hydroplaning effect will result, and very low wear rates are expected. As the input shaft speed approaches the output shaft speed, the movable cam member will begin to follow the mating cam motion. At synchronous speed,

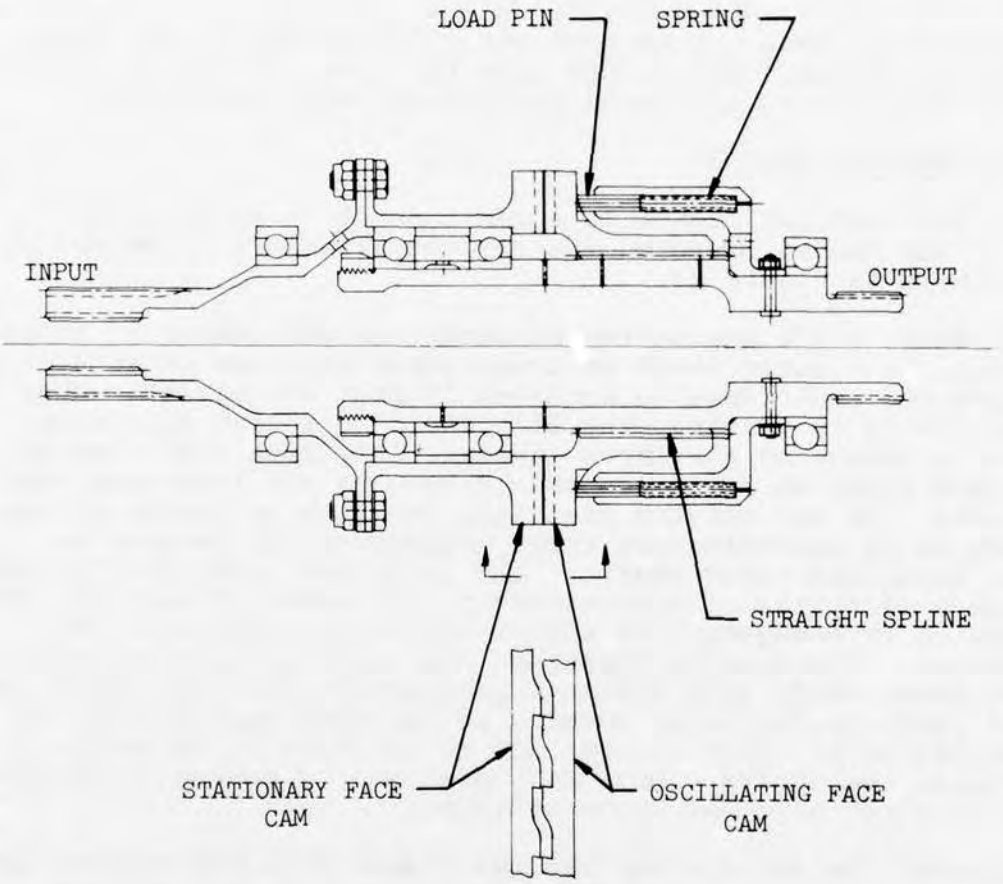

Figure 14. Face-Ratchet Overrunning Clutch.

the faces will engage and the unit is in the drive mode.

The support mounting of the face-ratchet overrunning clutch is through a tandem back-to-back bearing arrangement from the input shaft to the output shaft. As previously stated, the preferred support method is to support the outer shaft independently by separate support bearings at each end. This support method was not employed in the design shown because of the excessive cost and weight.

Lubrication does not present any difficulties in the face-ratchet clutch. Oil is fed from the innermost shaft through metering jets to all areas where metal wear can occur.

LINK-RATCHET CLUTCH

The link-ratchet clutch is a new concept in overrunning clutches and is based on the ratchet principle. The design is shown in Figure 15.

The inner shaft has on its extremity an odd number of ratchet teeth. The outer shaft is constructed with two pockets in which two centrifugally actuated "links" are placed. When the clutch is driving, the back end of one link will drop into a pocket of the inner ratchet. The link will then be in direct drive as it is compressed between the inner and outer shafts. In the driving position, the line of action of the link is at approximately three degrees to the tangent to the inner and outer shafts. The inner and outer shafts rotate with a clearance of approximately .010 inch. Since only one link is in engagement, a radial separating load will be created. The mounting bearings have enough clearance so that the inner shaft will displace because of the link radial load, and react on the outer housing on the side opposite to the engaged link. This removes all of the running clearance between the shafts. Once displaced and in contact, the unit is "locked" into the drive position.

Whenever the input shaft rotates slower than the output, the link becomes disengaged and freewheels over the ratchets. The centrifugal load attempts to drive the thin end of the link into the ratchet, but a wedge-shaped pocket gathers oil as it rotates and will not allow the link end to engage unless the relative velocity of the parts is low. The relative velocity approaches zero as the difference between the speeds of the input and output members approaches zero. When the unit is stopped, a small permanent magnet is used to assure engagement upon start-up. An alternate design uses a spring to tend to hold the thin end in engagement. Figure 16 shows the link, the hydroplane pocket and the magnet.

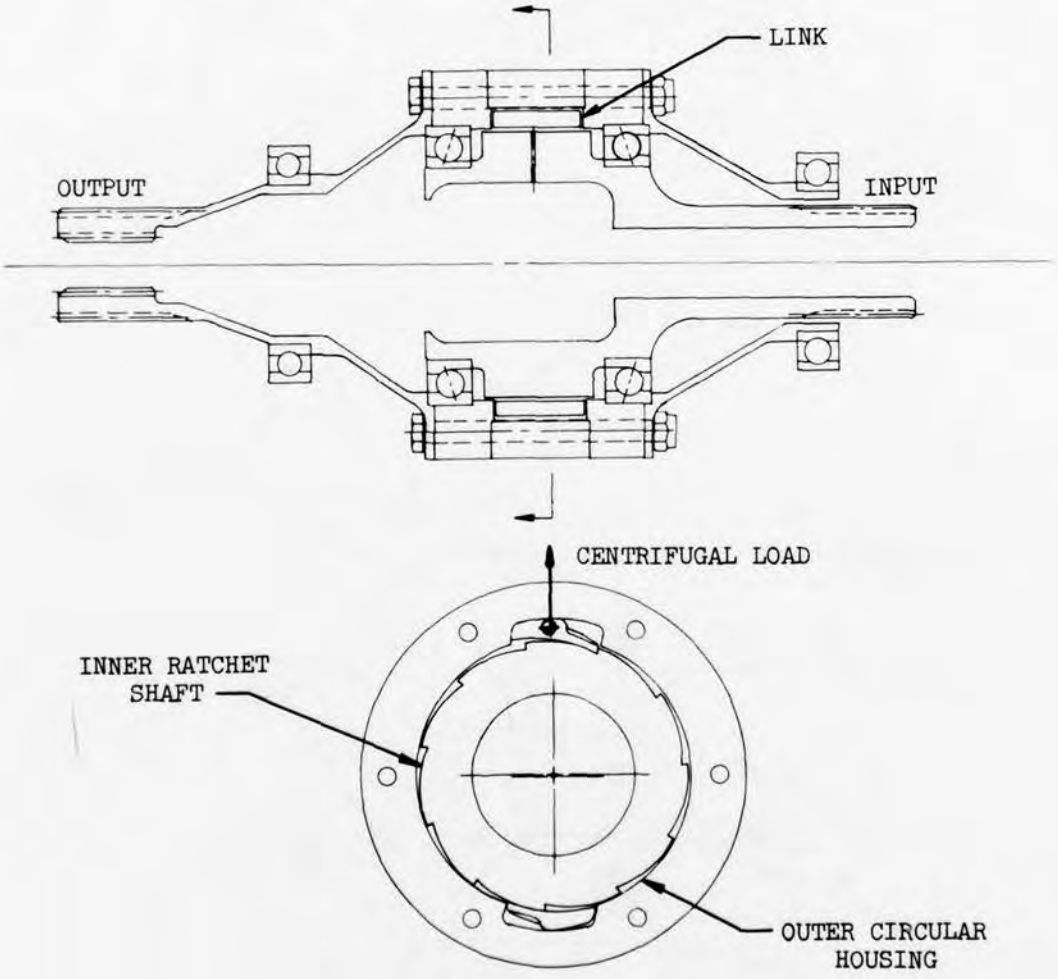

Figure 15. Link-Ratchet Overrunning Clutch.

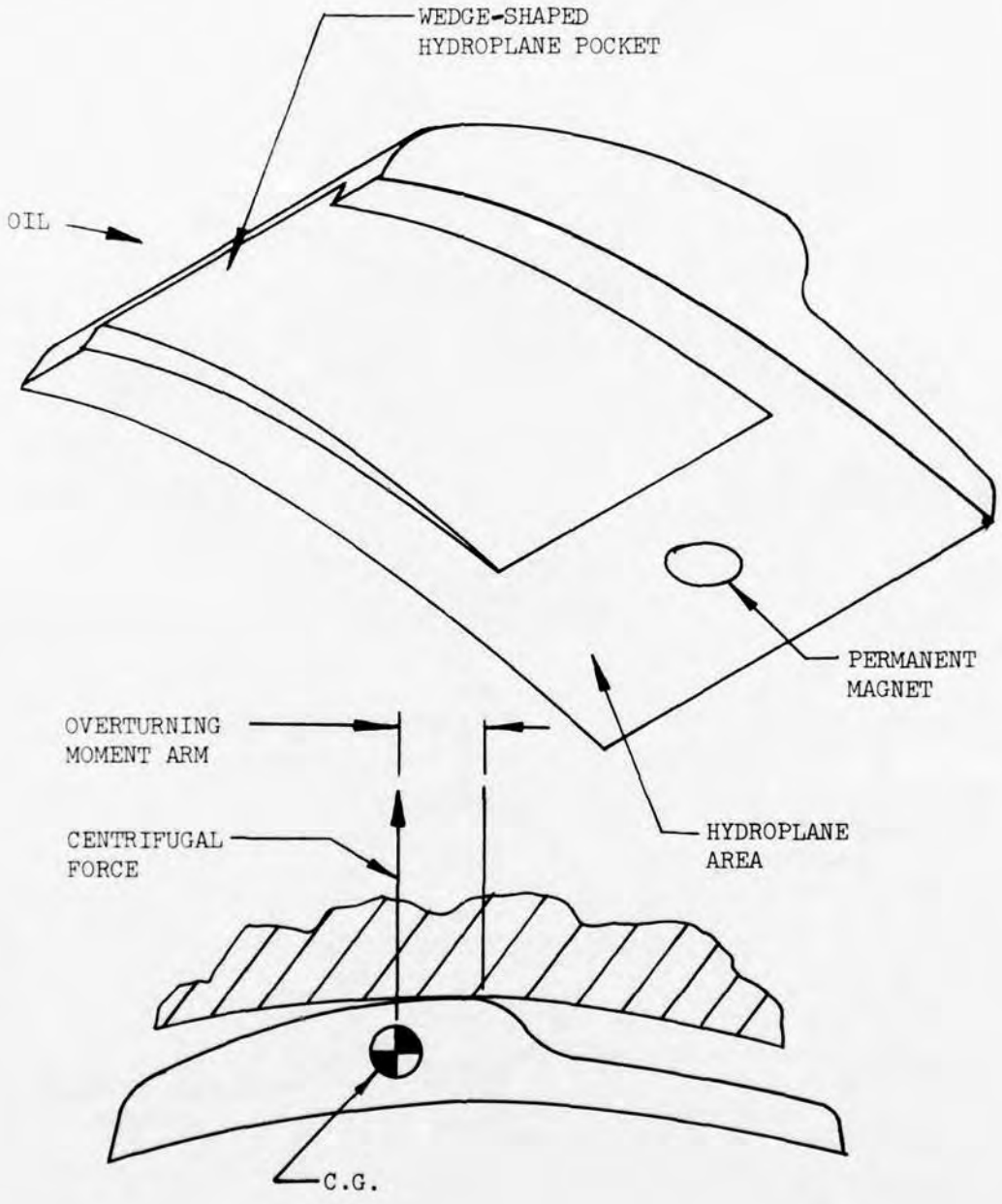

Figure 16. Isometric of Link, Link-Ratchet Clutch.

A major difference exists between the link-ratchet overrunning clutch and all other previous designs shown. In the link ratchet clutch, only one member is used to transmit the total load created by the torque. In the spring, the ramp-roller and the other types of clutches, multiple members are used to share the load. When multiple members are used, load sharing becomes a function of the accuracy of the location of the contacting members. With only one member in contact in the link-ratchet clutch, the need for great accuracy is eliminated.

When in the drive mode, the inner and outer shafts contact each other by displacing the amount required to remove the running clearance. In this position, the unit is inherently out of balance. The small radial displacement (approximately .010 inch) is not important at low speeds. However, it does become a dominant factor when speeds approach 20,000 rpm. Because of the inherent out of balance the link-ratchet overrunning clutch is not recommended at speeds above 12,000 rpm.

Having an odd number of ratchets on the inner shaft with two links permits only one link to engage at a time. This also provides a high degree of redundancy since one link may fail completely or all ratchets may fail except one. In the design shown, there are eleven ratchet faces on the inner shaft. Even with ten ratchets sheared off, the clutch will be operable.

EVALUATION OF DESIGNS

SELECTION MATRIX

Since it would be prohibitively expensive to fabricate and test samples of each of the ten candidate clutch designs, it was decided that only the three best clutches would be fabricated and tested. These were:

(1) Spring
(2) Sprag Design A
(3) Ramp Roller

The evaluation process used in determining the relative rankings of the clutches was a weighted factor method. In using this method, all relevant clutch performance criteria were determined and assigned percentages based on their relative importance, with the sum of these percentages equalling 100%. Each clutch was then evaluated for each of fourteen criteria and assigned a fraction of the percentage assigned to that criteria based on its ability to meet the criteria. The better a particular clutch met a performance criteria, the greater the fraction of the assigned percentage it received. For example, the assigned percentage for weight was 13%. The sprag design "A", the lightest of the clutches received 12.3%; the actuated double-cage ramp-roller clutch, the heaviest, received only 9.2%. The sum of the fourteen percentages for each clutch, i.e., the "figure of merit," was used to determine the relative ranking of each clutch. A "perfect" figure of merit is of course 100%.

This selection process, while subjective in nature, tends to preclude any bias in the evaluation of the clutches. First, breaking down the evaluation into fourteen separate and distinct criteria permits a thorough examination of each facet of overrunning clutch performance. Second, all evaluations were based on full-size layout drawings of the clutches, sized according to the speed and power required. Furthermore, all evaluations were based on commonly accepted engineering principles and practices.

The only area of the evaluation based solely on engineering judgment was the weighted percentages assigned to each of the evaluation criteria. To assess these, arbitrary values were first assigned to each of the fourteen categories. Comparisons of relative importance were then made among the criteria, and the values were adjusted accordingly. This comparative process was repeated until no further changes resulted. After this interaction, the final percent "weight" carried by each design parameter was established.

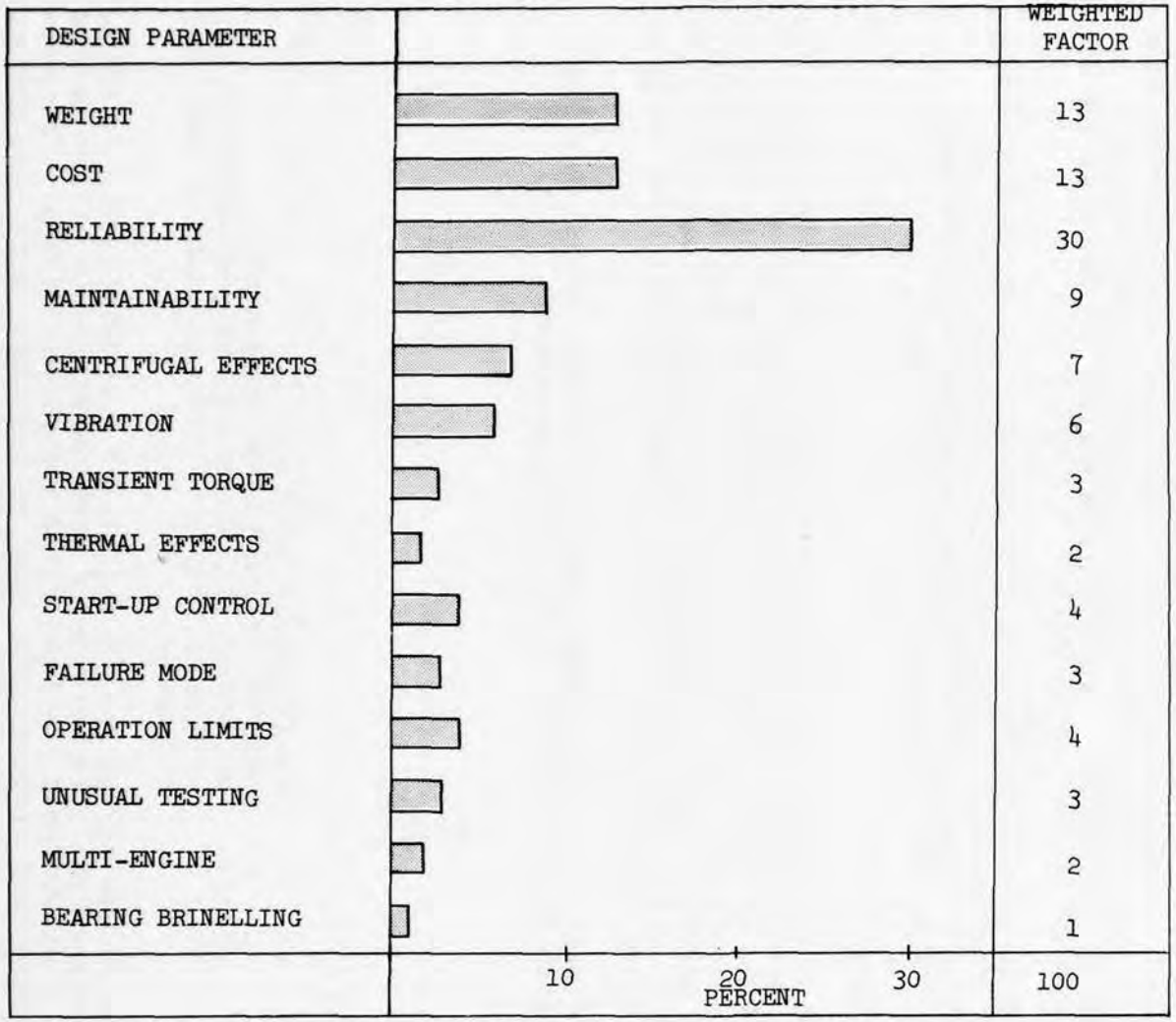

Figure 17. Overrunning Clutch Design Parameters and Weighting Factors.

To determine the variation in these percentages that might be expected due to the subjective judgment involved, a group of independent engineers, conversant in helicopter overrunning clutch operation, were asked to assign weighted percentages to the fourteen criteria based on their own judgment. They were given no information other than the fourteen categories. Surprisingly, their percentages varied by not more than three percent from those assigned by the Sikorsky engineering staff. A summary of the parameters and the weighted factors is presented in Figure 17.

The following sections of this report discuss in detail the fourteen criteria comprising the figure of merit, the rationale used in calculating the percentages for each criteria, and the ratings of the clutches.

WEIGHT

The first design parameter considered in the selection matrix is weight, which has a maximum value of 13 percent in the figure of merit. The weight parameter takes into consideration envelope size as well as weight. To make up the total of 13 percent, envelope size has been assigned a value of 4 percent, while the actual weight of the parts has been assigned a value of 9 percent.

The weight is calculated using a full-size layout for each clutch design and the following relationship:

$$W = \sum_{i=1}^{n} \rho i Vi + Wh \qquad (1)$$

where

W	=	total weight of clutch
ρi	=	density of individual components
Vi	=	volume of individual clutch components
Wh	=	weight of standard hardware, such as bearings and bolts.

The volume of the individual clutch components, Vi, as shown in Equation 1, is calculated from measurements of the layout of a clutch that has been sized for proper stress. The weight of standard hardware, Wh, such as bearings, nuts, and bolts, is found from catalogues and other standard sources.

The envelope of the clutch is also considered in the evaluation and has been included with weight because envelope volume relates directly to overall weight by the size of the housing that is required to hold the clutch. The larger the volume

of the clutch is, the larger the size of the housing is. In the evaluation of envelope volume, only the "active" portions of the clutch have been used. The active portions of the clutch include the envelope of the components that do the driving or overrunning. Support bearings, adaptor shafts, adaptor splines, etc., are not included in the active envelope. For simplicity, the envelope of the active components is assumed to be a solid cylinder of diameter, d, and length, ℓ. Table 1 summarizes the total weight, envelope dimensions, and volume for each of the 10 candidate clutch designs.

TABLE 1. WEIGHT AND ENVELOPE SUMMARY, CANDIDATE CLUTCH DESIGNS.

Name	Total Assy Weight-lb	Active Env Length - in.	Active Env Dia - in.	Volume $in.^3$
Spring	7.73	9.80	3.40	89.0
Sprag A	7.94	3.00	3.75	33.1
Sprag B	8.04	3.00	3.75	33.1
Ramp Roller	9.32	5.00	3.75	55.2
Actuated R R	10.34	5.25	4.75	93.0
Ball Brg R R	8.00	3.12	4.50	49.7
Roller Gear R R	9.10	4.90	4.50	77.9
Pos Eng Ratchet	8.90	5.00	4.70	86.7
Face Ratchet	9.09	5.00	4.00	62.8
Link Ratchet	9.07	2.60	4.40	39.5

Once the weight and volume are established, it remains to evaluate the overall weight ratings. For both the weight and envelope, the assumption is made that the lowest weight and the lowest envelope are approximately 90% of optimum, whereas the highest weight and envelope are approximately 50% of optimum. The optimum grades or ranks are of course 9% for weight and 4% for envelope. Thus, for weight, 9% will correspond to 7 pounds and 0% will correspond to 20 pounds. For envelope, 4% will correspond to 30 cubic inches and 0% will correspond to 200 cubic inches. These assumptions can be expressed mathematically as follows:

$$\%\ wgt = 13.846 - .692\ W \quad (2)$$

$$\%\ vol = 4.706 - .0235\ V \quad (3)$$

where

% wgt	-	% rating of 9% for weight
% vol	=	% rating of 4% for volume
W	=	weight of each clutch
V	=	volume of active clutch components

When substituting the values of weight and volume from Table 1 into Equations 2 and 3, the overall ranking is determined for "weight" in the selection matrix. These rankings are summarized in Figure 18. The higher the percent ranking for weights, the lower the weight and the smaller the envelope of the clutch are. Note that the overall ratings for weight fall within a narrow range of from 9.2% for the lowest (actuated double-cage ramp-roller clutch) to 12.3% for the highest (sprag design A). This is because the weights and volumes for the candidate designs are all within a narrow range of values since they have all been designed for the same conditions (1500 hp at 20,000 rpm).

COST

The cost parameter of the selection matrix also consists of 13% of the figure of merit. The costs have been divided into two parts consisting of recurring and nonrecurring. Recurring costs are the costs of the overrunning clutch unit in production and include the material and the labor required for manufacture. The nonrecurring costs are the costs to develop the clutch to the point where it is ready for production. These nonrecurring costs consist of the costs of engineering preliminary design, detail design, fabrication of prototype hardware, and qualification testing. Recurring costs are assumed to account for 9%, while nonrecurring are assumed to account for 4%.

Included in the evaluation of nonrecurring costs are the costs to design the freewheel unit. These costs consist of the costs of engineering hours for analysis of the freewheel unit, engineering design hours, and engineering hours to complete detail drawings. The engineering hours required for analysis depend on the complexity of the design. The double-cage actuated-ramp-roller clutch, for example, will require the most time for analysis since it is the most complex. Similarly, the detail design of the double-cage actuated-ramp-roller clutch will require more engineering time since there are more detail drawings to produce. Nonrecurring costs also include that for fabrication of prototype hardware. It is assumed

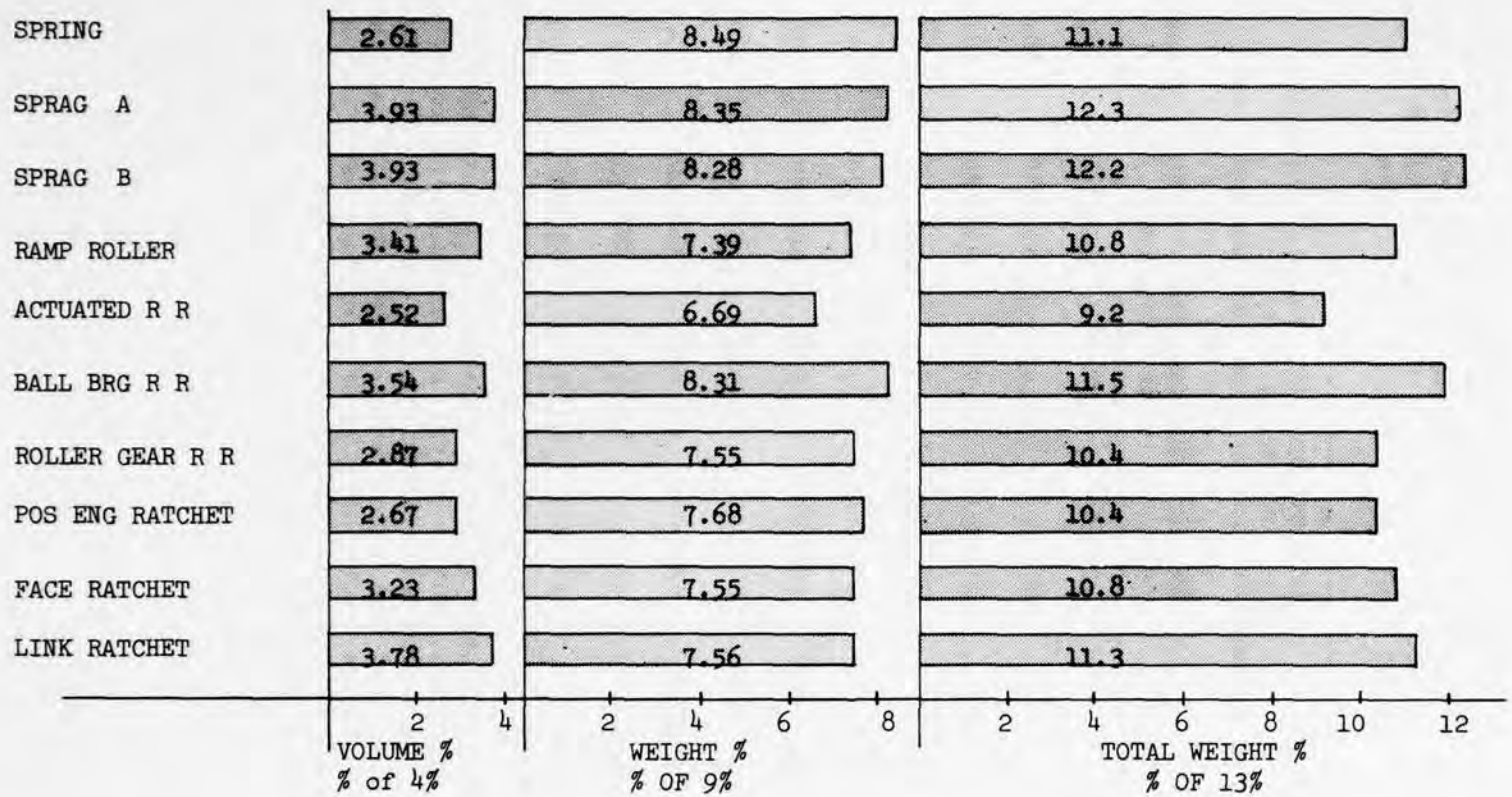

Figure 18. Summary of Percent Rankings for Weight and Envelope, Candidate Clutch Designs.

that three prototype clutches are required for initial testing to substantiate the operation of any new clutch design. The test cost, which is also included in nonrecurring costs, is assumed to be $35,000 for each design. Table 2 summarizes the nonrecurring costs of clutch development.

TABLE 2. COSTS TO DESIGN, FABRICATE, AND TEST PROTOTYPE CLUTCHES

	Engr Design Cost ($)	Prototype Hardware Cost ($)	Prototype Test Cost ($)	Total Nonrecurring Cost ($)
Spring	32,200	50,850	35,000	118,050
Sprag A	26,600	42,450	35,000	104,050
Sprag B	26,600	40,875	35,000	102,475
Ramp Roller	35,000	53,850	35,000	123,850
Actuated R R	54,600	55,125	35,000	144,725
Ball Bearing R R	23,800	41,925	35,000	100,725
Roller Gear R R	37,800	46,050	35,000	118,850
Pos Eng Ratchet	42,000	55,050	35,000	132,050
Face Ratchet	26,600	55,725	35,000	117,325
Link Ratchet	23,800	34,740	35,000	93,540

The recurring costs include the cost of standard hardware, such as bearings, nuts, bolts, rollers, and sprags, and the costs of the materials (forgings or bar stock) to fabricate the clutches and the labor hours required for machining and assembly. These costs have been computed assuming a production run of 100 pieces, which is common for helicopters. A summary is shown in Table 3.

TABLE 3. COSTS OF OVERRUNNING CLUTCHES IN PRODUCTION.				
	Hardware ($)	Material ($)	Labor @$25/hr Hours	Total $ Recurring
Spring	80	200	390	10,030
Sprag A	130	150	330	8,530
Sprag B	380	125	320	8,505
Ramp Roller	80	200	420	10,780
Actuated R R	110	250	430	11,110
Ball Brg R R	224	100	330	8,574
Roller Gear R R	80	100	360	9,180
Pos Eng Ratchet	80	225	430	11,055
Face Ratchet	80	200	430	11,030
Link Ratchet	80	80	270	6,910

Figure 19 summarizes the total of recurring and nonrecurring costs. The ratings for recurring costs based on 9% and nonrecurring costs based on 4% are calculated using a linear relationship. For nonrecurring costs, $90,000 is assumed to have a rating of 4%, while $200,000 is assumed to have a rating of 0%. For recurring costs, $6,000 is assigned 9% while $20,000 is assigned 0%. The above conditions are expressed mathematically by the following formulas

$$\%\ \text{nonrecur} = 7.272 - .00003636\ (\$\ \text{nonrecur}) \quad (4)$$

$$\%\ \text{recur} = 12.8571 - .0006428\ (\$\ \text{recur}) \quad (5)$$

where

% nonrecur	=	% of 4% for nonrecurring costs
% recur	=	% of 9% for recurring costs
$ nonrecur	=	total nonrecurring costs (Table 2)
$ recur	=	total recurring costs(Table 3)

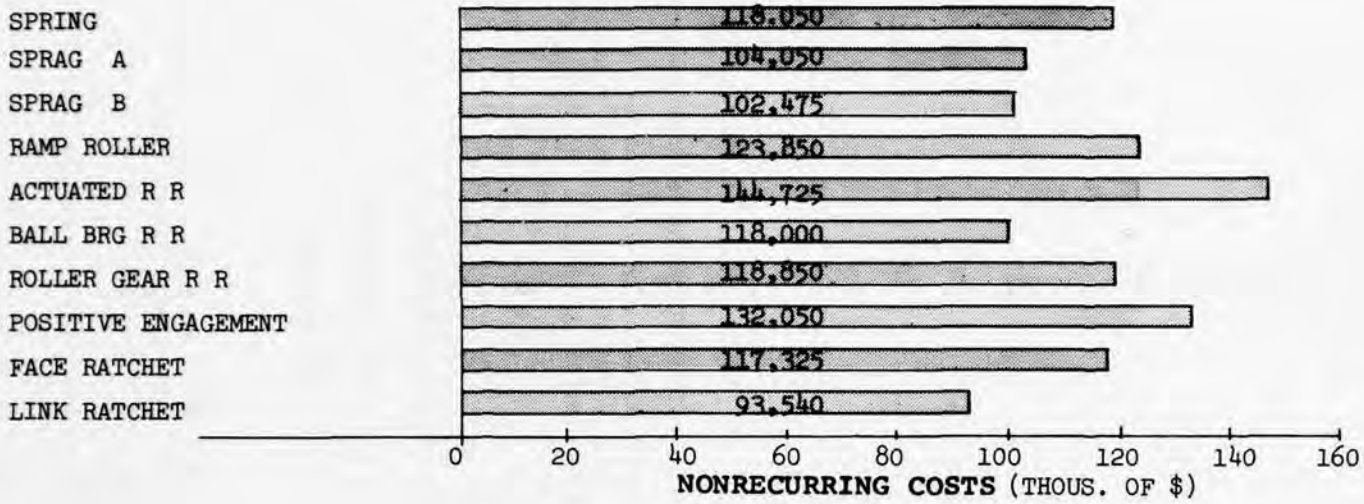

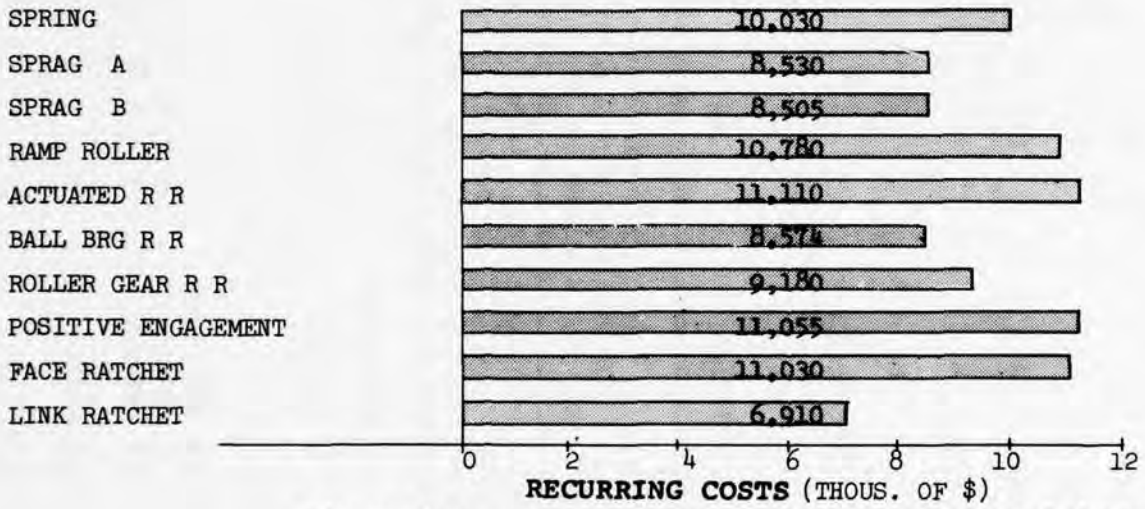

Figure 19. Total Costs of Overrunning Clutches.

High ratings for percent recurring and nonrecurring costs indicate a lower-cost design. The highest overall cost rating was achieved by the link ratchet clutch owing to its overall simplicity. Sprag clutches also had high ratings for cost. The actuated double-cage ramp-roller clutch has the lowest cost rating. The final evaluation is summarized in Table 4.

TABLE 4. EVALUATION OF THE COSTS OF OVERRUNNING CLUTCHES.

Name	Nonrecurring Costs Portion of 4%	Recurring Costs Portion of 9%	Total Costs Portion of 13%
Spring	2.98	6.41	9.4
Sprag A	3.49	7.37	10.9
Sprag B	3.49	7.55	11.0
Ramp Roller	2.77	5.93	8.9
Actuated R R	2.01	5.72	7.7
Ball Bearing R R	3.61	7.35	10.9
Roller Gear R R	2.95	6.96	9.9
Pos Eng Ratchet	2.47	5.75	8.2
Face Ratchet	3.00	5.77	8.8
Link Ratchet	3.89	8.42	12.3

RELIABILITY

The reliability parameter of the selection matrix carries the most weight, having an assigned value of 30%, and is, therefore, the most important factor in overrunning clutches designed for helicopters. To fully evaluate reliability in overrunning clutches, five reliability parameters are considered:

(1)	Number of Parts	5%
(2)	Fail-Safety	8%
(3)	Overrunning Wear	9%
(4)	Driving Fracture	3%
(5)	Confidence Factor	5%
		30%

Figure 20 shows graphically the relative magnitudes of the factors making up the reliability parameter.

The first parameter included in reliability is the number of parts. In the evaluation of the number of parts, a ball bearing is considered a single part, whereas the 14 rollers of the ramp-roller clutch are considered 14 individual parts, the 20 sprags of sprag design B are considered to be 20 parts, etc. Although, in itself, the number of parts comprising a component assembly is not a direct measure of reliability, experience has shown that a definite relationship exists. In general, the higher the number of parts is, the greater the chance of failure is, as shown by the relationship for the overall reliability of an assembly:

$$\frac{1}{R} = \sum_{i=1}^{n} \frac{1}{Ri} \qquad (6)$$

where

R = overall system assembly reliability
Ri = individual component reliability
n = number of parts

Hence, the greater the number of parts is, the lower the overall reliability will be, assuming no change in the individual component reliabilities.

In the ten candidate clutch designs examined, the number of parts varied considerably from a minimum of 10 parts in the link-ratchet clutch to a maximum of 55 parts, found in both the positive-engagement ratchet and the actuated double-cage ramp-roller clutches. The number of parts are shown in Figure 21 for each of the 10 candidate clutch designs.

In arriving at the actual percent ratings for the number of parts, a linear relationship was used where the clutch with the lowest number of parts was assumed to be approximately 90% of optimum, while the clutches with the greatest number of parts were assumed to be 50% of optimum. This leads to the relationship that 9 parts correspond to 5% while 110 parts correspond to 0%. Expressed mathematically

$$\%\ \text{no. parts} = 5.445 - .0495n \qquad (7)$$

where

% no. parts = percent rating of 5% for number of parts
n = number of active clutch parts (Figure 21)

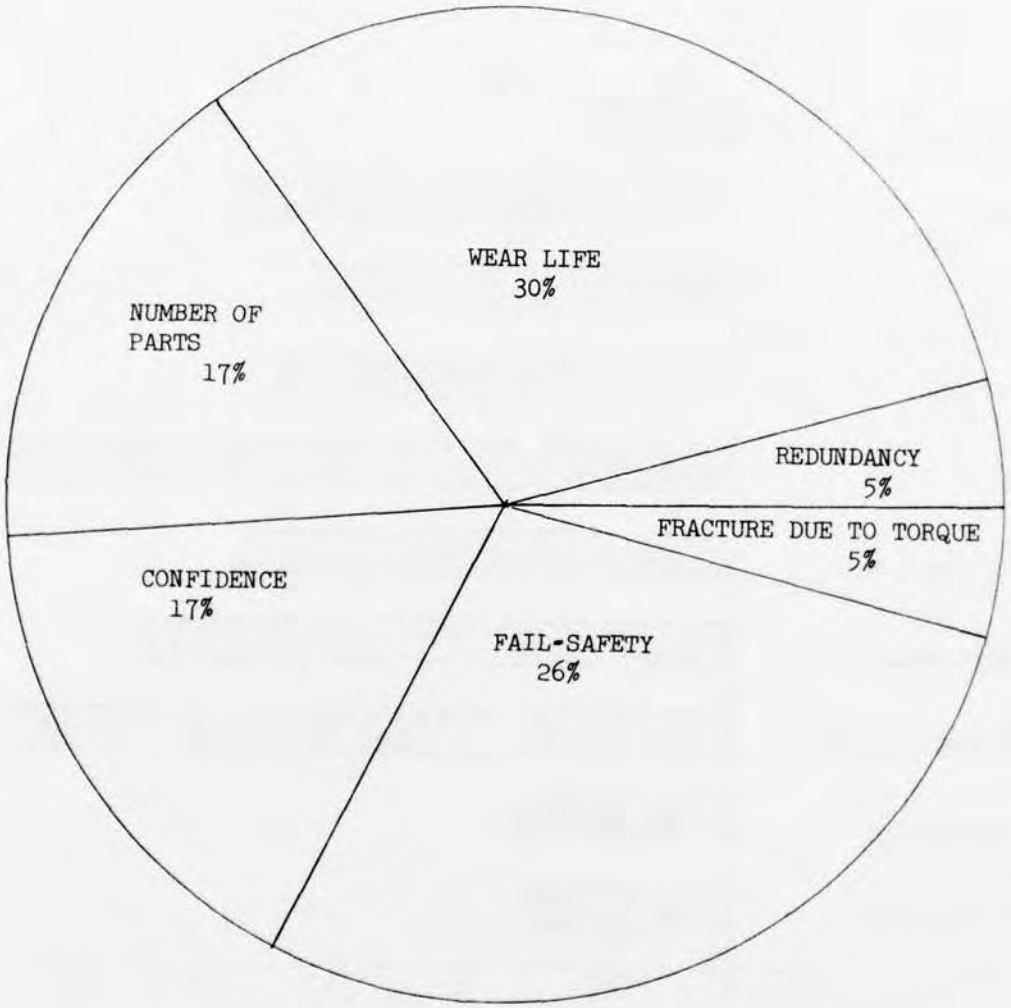

Total Reliability Rating = 30%

Figure 20. Percentage Contribution of Overrunning-Clutch Reliability Factors.

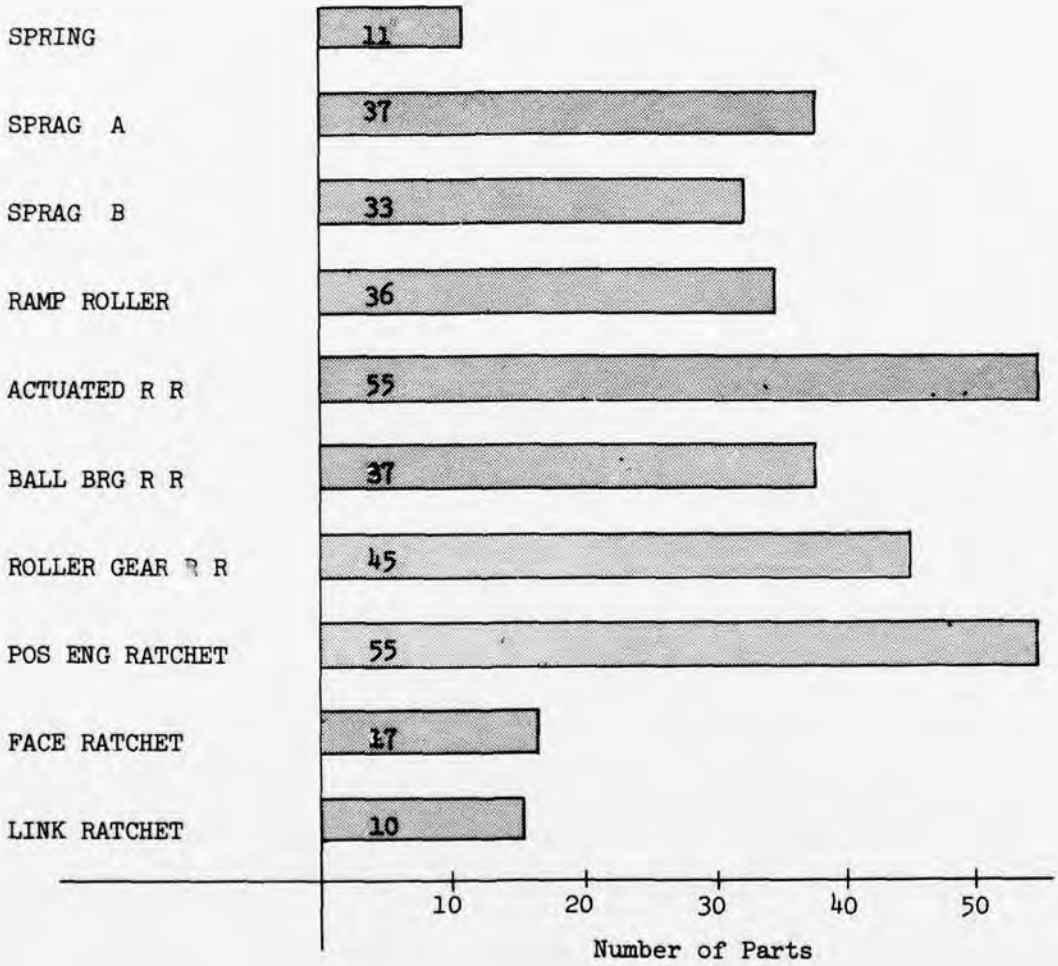

Figure 21. Number of Parts in Candidate Clutch Designs.

The second reliability rating factor is fail-safety, which has been assigned a value of 8%. To evaluate fail-safety, the assumption is made that the overrunning clutch has malfunctioned in its most common failure mode. The resultant effect is then analyzed. Five different severities of failure are assumed. The least severe type of malfunction occurs when the clutch is capable of driving, and in fact does drive, but is unable to engage after shutdown and startup for the next mission. Although this could be harmful to engines in that it permits the engine to overspeed, it is not catastrophic, since it will occur on the ground during startup. The next order of failure in the ranking of severity is a clutch malfunction where the input and the output members of the clutch slip relative to each other and are unable to carry full load, but do drive when the load is lowered to a sufficient level. This type of malfunction may occur during a period of heavy hover when the freewheel unit is transmitting high torque loads. The next most severe malfunction occurs when the freewheel unit jams and is unable to freewheel but can still drive. The problem here is that this particular malfunction is usually not detected until the clutch is supposed to be in the freewheeling mode, such as during an engine failure or an emergency engine shutdown. Since the clutch is locked, it cannot freewheel and the transmission drives the free turbine portion of the engine. On a typical helicopter this procedure requires so much energy that the aircraft sink rate becomes dangerously high. The fourth most severe type of freewheel unit malfunction is the clean break wherein the clutch cannot transmit any torque. This condition may occur during periods of high torque transmittal and can cause the loss of an aircraft. The most severe failure assumed is the complete disintegration of the clutch where loose parts may cause secondary damage to nearby transmission components.

Each of the ten candidate clutch designs was examined and the most likely failure mode determined by engineering judgment and experience with similar designs. The most likely failure mode, the resultant effect on aircraft performance, and the assumed rating as a percentage of 8% are listed in Table 5.

The third item in the reliability rating of the selection matrix is overrunning wear, which is assigned a value of 9%. Overrunning wear is probably the most common reliability problem in a helicopter overrunning clutch. During overrunning there must be two or more rubbing surfaces in any type of mechanical freewheel unit. These surfaces are subject to wear that can eventually lead to various clutch malfunctions depending on the type of design.

TABLE 5. FAIL-SAFETY RATINGS FOR CANDIDATE OVERRUNNING CLUTCH DESIGNS.

Name	Most Likely Failure Mode	Resultant Effect on Aircraft	Fail-Safety Rating 8% Max
Spring	Wear of spring and housing	Slippage - able to freewheel	4.0
Sparg A	Sprag rollover	Loss of drive - no secondary damage	2.0
Sprag B	Wear of sprag, housing, and shaft	Slippage - able to freewheel	4.0
Ramp Roller	Wear of rollers, housing, and cam	Spit-out of rollers or slippage	4.0
Actuated R R	Wear of actuation mechanism, rollers, and cam	Spit-out of rollers or slippage	4.0
Ball Brg R R	Wear of rollers, cam, and housing	Spit-out of rollers or slippage	4.0
Roller Gear R R	Wear of rollers, cam, and housing	Spit-out of rollers or slippage	4.0
Pos Eng Ratchet	Fracture of engaging mechanism	Loss of drive; possible secondary damage	0.5
Face Ratchet	Fracture of ratchet	Loss of drive; possible secondary damage	0.5
Link Ratchet	Brinelling of ratchet faces	Loss of drive, clean break	2.0

To evaluate the overrunning wear of the ten candidate clutch designs, the mean times between failures (MTBF) due to wear were calculated. Where available, wear rates determined from tests were used in the MTBF calculations. This data was adjusted for the speed and load requirements of this program, since wear is dependent on the product of rubbing velocity and pressure (load). Where test data was unavailable, conservative engineering estimates based on experience were made for the wear rates. In all cases, the allowable wear is the wear that would necessitate rework or replacement, but would still permit the proper operation of the clutch.

The formula for calculating the MTBF for each clutch is

$$MTBF_i = \frac{Wa}{Wm} \frac{35\ t}{\left[\frac{rpm}{rpmt}\right]^2} \tag{8}$$

$$MTBF_c = \frac{1}{\sum_{i=1}^{n} \frac{1}{MTBF_i}} \tag{9}$$

where

$MTBF_c$	=	mean time between failures of clutch assembly
$MTBF_i$	=	total flight hours to reach allowable wear for individual clutch components
Wa	=	allowable wear for component
Wm	=	measured wear from test or conservative estimate
t	=	test time during which wear, Wm, was measured
35	=	factor for flight hours per overrunning hour
$\left[\frac{rpm}{rpmt}\right]^2$	=	correction factor for speed
rpm	=	rpm of clutch (20,000)
rpmt	=	test rpm at which wear, Wm, was measured

Wear rate data is available on the spring clutch from Reference 2 on both type A and type B sprag clutches, from Reference 3, and on the ramp-roller clutch from Reference 4. The positive-engagement ratchet clutch was tested in Reference 5, but no wear data was taken. Wear-rate data from ramp roller tests is also applicable to the actuated ramp-roller, the ball-bearing-carrier ramp-roller, and the roller-gear ramp-roller clutches by applying appropriate factors to correct for pressure and velocity (PV).

Table 6 summarizes the results of the wear-life calculations, while Figure 22 displays the final clutch MTBR's graphically. Note that the ratchet-type clutches generally have long lives. This is because the allowable wear of the ratchet clutch members is much greater than those for other types of clutches. Note also that the wear lives of several of the ramp-roller clutches are short. This is mainly due to high roller centrifugal loads, which cause wear especially in the ball-bearing carrier and roller-gear types of ramp-roller clutches.

The wear lives of the overrunning clutches cannot be expressed linearly. A clutch with a 2000-hour wear life is not 20% as reliable as a clutch with a 10,000-hour wear life, but rather, it is almost as good. This is because of the relatively low usage of a typical helicopter where the retirement life may not reach 10,000 hours. A relationship has been assumed which expresses wear life as a percent of 9%:

$$\%\ \text{wear} = \sqrt{81 - \left[9 - \frac{L}{1000}\right]^2} \qquad (10)$$

where

% wear = % rating of 9% for wear
L = wear MTBR (Figure 22).

(2) Lynwander, P., Meyer, A. G., Chachakis, S., SPRING OVERRIDING AIRCRAFT CLUTCH, Avco Lycoming Division, USAAMRDL Technical Report 73-17, Eustis Directorate, U.S. Army Air Mobility Research and Development Laboratory, Fort Eustis, Virginia, May 1973, AD 766309.

(3) Lynwander, P., Meyer, A. G., Chachakis, S., SPRAG OVERRIDING AIRCRAFT CLUTCH, Avco Lycoming Division, USAAMRDL Technical Report 72-49, Eustis Directorate, U.S. Army Air Mobility Research and Development Laboratory, Fort Eustis, Virginia, July 1972, AD 747807.

(4) Kish, Jules G., AIRCRAFT CLUTCH ASSEMBLIES, RAMP ROLLER, Sikorsky Aircraft, USAAMRDL Technical Report 72-31, Eustis Directorate, U. S. Army Air Mobility Research and Development Laboratory, Fort Eustis, Virginia, July 1972, AD 747816.

(5) Wirth, Charles J., POSITIVE ENGAGEMENT CLUTCH, Kaman Aerospace Corporation, USAAMRDL Technical Report 73-96, Eustis Directorate, U. S. Army Air Mobility Research and Development Laboratory, Fort Eustis, Virginia, December 1973, AD 775835.

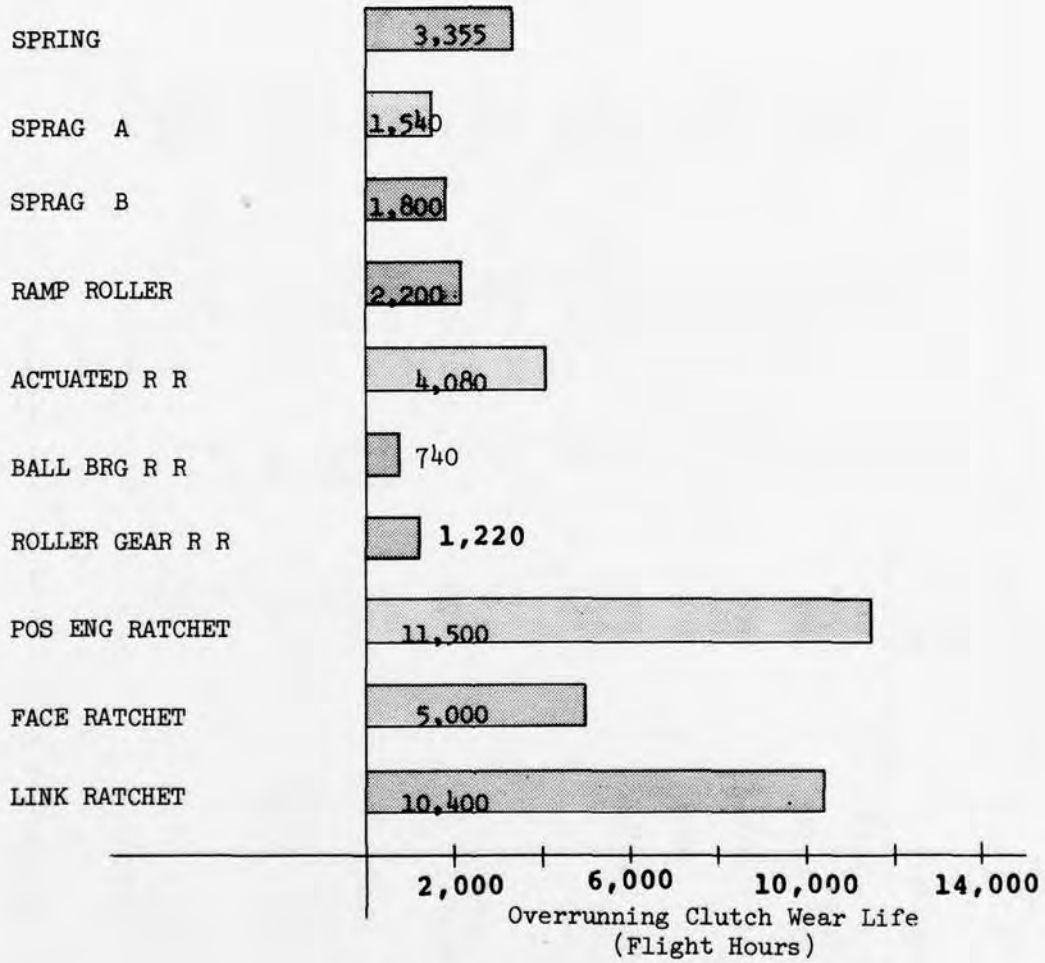

Figure 22. Overrunning Clutch Wear Life.

TABLE 6. WEAR LIFE, CANDIDATE CLUTCH DESIGNS

Clutch	Component	Allow Wear (in.)	Test (hr)	Meas Wear (in.)	Component Clutch $MTBR_i$	MTBR
Spring	Input Shaft	.001	30	.0000	∞	3355
	Spring	.004	30	.0022	3355	
	Output Shaft	.001	30	.0000	∞	
Sprag A	Input Shaft	.001	5	.0000	∞	1540
	Sprags	.010	5	.002	1540	
	Output Shaft	.003	5	.0000	∞	
Sprag B	Input Shaft	.001	5	.0000	∞	1800
	Sprags	.010	5	.0017 (1)	1800	
	Output	.003	5	.0000	∞	
Ramp Roller	Cam	.005	5	.0000	∞	2200
	Rollers	.010	5	.0012 (2)	2560	
	Housing	.005	5	.001	15,360	
Actuated R R	Cam	.005	100	.0000	∞	4080
	Rollers	.010	100	.0000	∞	
	Housing	.005	100	.0000	∞	
	Control Roller	.001	100	.001 (3)	6140	
	Control Ring	.002	100	.001 (3)	12,280	
Ball Brg R R	Cam	.005	5	.0000	∞	740
	Rollers	.010	5	.0021 (4)	1460	
	Housing	.005	5	.0000	∞	
	Bearings	N.A.	N.A.	N.A.	1500	

TABLE 6. (Continued)

Clutch	Component	Allow Wear (in.)	Test (hr)	Meas Wear (in.)	Component $MTBR_i$	Clutch MTBR
Roller Gear R R	Cam	.005	5	.0000 (5)	∞	1220
	Rollers	.010	5	.0024 (5)	1280	
	Housing	.005	5	.0000 (6)	∞	
	Ring Gear	.020	5	.0001 (6)	61,500	
	Pinion Gear	.020	5	.0001	61,500	
Pos Eng Ratchet	Input Shaft	.020	50	.0001 (7)	615,000	11,500
	Moveable Spline	.020	50	.0001 (7)	615,000	
	Ratchet	.020	50	.003 (7)	20,500	
	Pawl	.030	50	.003 (7)	30,700	
	Spring	.010	50	.0001 (7)	307,000	
	Curv Cplg(mov)	.020	50	.0001 (7)	615,000	
	Curv Cplg(fixed)	.020	50	.0001 (7)	615,000	
Face Ratchet	Input Shaft	.020	50	.0001 (7)	615,000	5000
	Mov Face (spline)	.020	50	.0001 (7)	615,000	
	Mov Face (ratchet)	.020	50	.004 (7)	15,630	
	Pin (4)	.010	50	.002 (7)	15,630	
	Spring (4)	.010	50	.0001 (7)	307,000	
	Fix Ratchet	.020	50	.004 (7)	15,630	
Link Ratchet	Input Shaft	.020	50	.003 (7)	20,500	10,400
	Link	.020	50	.003 (7)	20,500	
	Outer Housing	.005	50	.000	∞	

Note (1) Adjusted for 4400 test rpm and 50% differential speed.
(2) Excessive wear caused by tungsten carbide, assumed 50% of actual measured.
(3) Conservative assumption for 100 test hours.
(4) Adjusted to 776-lb roller from 256-lb roller centrifugal force for conventional ramp roller.
(5) Adjusted to 1010-lb roller from 256-lb roller centrifugal force for conventional ramp roller.
(6) Conservative estimate of gear wear in 5 hours.
(7) Conservative estimate - no data available.

In equation 10, any life of 9000 hours or greater will have the full 9% rating while lower percents will be calculated for wear lives of less than 9000 hours.

The next evaluation parameter for clutch reliability is driving fracture, which carries a weight of 3%. Driving fracture is divided into redundancy of torque path (1.5%) and ultimate torque capacity (1.5%). The redundancy of torque path considers a clutch's ability to drive in the event of a fracture of one or more clutch components. If one examines the link-ratchet clutch, it is seen that this design is highly redundant. One link can be lost and all but one of the ratchets may be fractured and the clutch will still operate. The ramp-roller type of clutch also has a degree of redundancy in that the loss of any roller can be compensated for by the remaining rollers. One pin and spring assembly is also redundant since there are two assemblies per clutch. The spring clutch also has a degree of redundancy in that the drive can be accomplished through friction even in the event of a spring fracture. The actuated ramp-roller clutch can lose its entire control mechanism without detriment to safe operation, since the clutch will act as a conventional ramp roller. The positive-engagement ratchet clutch has six pawl assemblies for redundancy. The resultant ratings for drive-fracture redundancy reflect the relative degree of redundancy in the candidate clutch designs. The highest ranking were the actuated ramp roller, the positive-engagement ratchet, and the link ratchet.

The second part of reliability in driving fracture deals with the static torque capacities of the clutch designs. Assuming the design engineer uses proper methods of stress calculation and if all clutches are designed to the same factors of safety, they will all fracture at the same load. Hence, static torque capacity is merely a matter of proper sizing for stress and cannot be different for different designs. Therefore, each clutch has been given the maximum rating of 1.5% for this parameter.

The last factor to be considered in reliability is the confidence factor, which has a maximum value of 5%. The confidence factor is a measure of previous history of usage of the particular design. The sprag clutch of type A, for example, has been used in almost every helicopter from the earliest designs to the present and, hence, must be considered to have the full 5% rank for confidence. Similarly, a high degree of experience and field history is available on the conventional ramp-roller clutch, which must also be considered to have a rank of 5%. The type B sprag clutch also has a high degree of experience but not to the extent the type A design has, and therefore it has a lower ranking. The spring clutch has not been used in production but has performed exceptionally during

previous tests and is considered to have a high degree of confidence, as does the positive-engagement ratchet. The face-ratchet clutch has been used in helicopters but only to a small extent. There is some confidence in this design but not to the extent of the above-mentioned clutches. The actuated double-cage ramp-roller, the ball-bearing-carrier ramp-roller, the roller-gear ramp-roller, and the link-ratchet designs are all concepts that are newly developed and have never been tested.

The summary of the ratings for all reliability factors of the selection matrix is presented in Table 7.

MAINTAINABILITY

The maintainability parameter of the overrunning clutch selection matrix is assigned a maximum value of 9%. Maintainability is measured in maintenance man-hours per flight hour (MMH/FH) and is evaluated for each candidate clutch design by determining the maintenance hours required to replace the clutch assembly in the field and then by dividing these hours by the clutch life (including scheduled and nonscheduled removals). The higher the maintainability rating is, the lower the maintenance requirement is. The maintenance man-hours required for one replacement includes hours to remove the unit from the aircraft, the time required to overhaul the unit, and the man-hours required to reinstall the unit on the aircraft. The time needed to overhaul a freewheel unit includes the time needed to disassemble, inspect, repair and reassemble the unit, and the cost of replacing parts. The cost of replacement parts has been assumed to be 10% of the cost of the clutch in production (see the Cost chapter) and is converted to maintenance man-hours by dividing by the hourly rate (25 dollars per hour assumed). This is the largest single factor in the cost of an overhaul, as shown in Table 8, which summarizes the maintenance man-hours required for one clutch replacement.

TABLE 7. RELIABILITY FACTOR RATINGS

Name	No. of Parts 5% Max	Fail-Safety 8% Max	Wear Life 9% Max	Fracture Due to Torque 1.5% Max	Redundancy of Fracture 1.5% Max	Confidence Factor 5% Max	Reliability 30% Max
Spring	4.90	4.00	7.00	1.50	1.25	4.00	22.7
Sprag A	3.61	2.00	5.03	1.50	1.25	5.00	18.4
Sprag B	3.81	4.00	5.40	1.50	1.25	4.50	20.5
Ramp Roller	3.66	4.00	5.89	1.50	1.25	4.00	21.3
Actuated R R	2.72	4.00	7.54	1.50	1.35	0.00	17.1
Ball Brg R R	3.61	4.00	3.57	1.50	1.25	0.00	13.9
Roller Gear R R	3.22	4.00	4.52	1.50	1.25	0.00	14.5
Pos Eng Ratchet	2.72	0.50	9.00	1.50	1.35	3.00	18.1
Face Ratchet	4.60	0.50	8.06	1.50	1.25	1.00	16.4
Link Ratchet	4.95	2.00	9.00	1.50	1.50	0.00	19.0

TABLE 8. MMH REQUIRED FOR CLUTCH REPLACEMENT ON AIRCRAFT

Name	Removal MMH	Disassembly MMH	Inspection MMH	Overhaul Repair MMH	Overhaul Parts $ in MMH	Assembly MMH	MMH Assembly on A/C	MMH to Replace 1 Unit
Spring	.3	1.7	2.0	2.1	40.1	3.4	.7	50.3
Sprag A	.3	1.7	2.0	2.1	34.1	3.4	.7	44.3
Sprag B	.3	1.7	2.0	2.1	33.0	3.4	.7	43.2
Ramp Roller	.3	2.4	2.0	2.9	43.1	4.8	.7	56.2
Actuated R R	.3	3.6	3.0	4.4	44.4	7.2	.7	63.6
Ball Brg R R	.3	2.4	2.0	2.9	34.3	4.8	.7	47.4
Roller Gear R R	.3	2.4	2.5	2.9	36.7	4.8	.7	50.3
Pos Eng Ratchet	.3	3.6	3.0	4.4	44.2	7.2	.7	63.4
Face Ratchet	.3	2.0	2.0	2.4	44.1	4.0	.7	55.5
Link Ratchet	.3	1.7	2.0	2.1	27.6	3.4	.7	37.8

In Table 8 the maintenance time required for clutch removal has been assumed to be the same for all designs, .3 hour. Similarly, the MMHS for assembly on the aircraft are assumed to be the same for all clutches, .7 hour. The assembly time is greater than the disassembly time because care is required in the alignment of parts during assembly. Similarly, the reassembly of the clutch during overhaul is longer than the disassembly time.

To determine clutch life, the following formula is used

$$MTBR = MTBUR \left[1 - e^{-TBO/MTBUR} \right] \quad (11)$$

where

MTBR = mean time between removals for scheduled and unscheduled reasons
MTBUR= mean time between unscheduled removals
TBO = time between overhauls.

If the assumption is made that the TBO is equal to the MTBUR, Equation 11 reduces to

$$MTBR = .63\ MTBUR \quad (12)$$

Equation 12 is used to determine the mean time between removals for each clutch. The mean time between unscheduled removals is assumed to be the overrunning clutch's wear life as determined in the "Reliability" section of this report. The MMH/FH of a unit is then determined by dividing the maintenance man-hours required for replacing the unit by the MTBR of the unit.

A linear distribution of rating points is assumed and a MMH/FH of .001 as the equivalent of the highest achievable rank of 9% and a MMH/FH of .25 as the lowest achievable rank of 0%. These assumptions are expressed mathematically by

$$\%\ MAIN = 9.036 - 36.145\ (MMH/FH) \quad (13)$$

where

% MAIN = portion of 9% for maintainability

Table 9 summarizes the MMH/FH while Figure 23 summarizes the rankings for the ten candidate clutch designs.

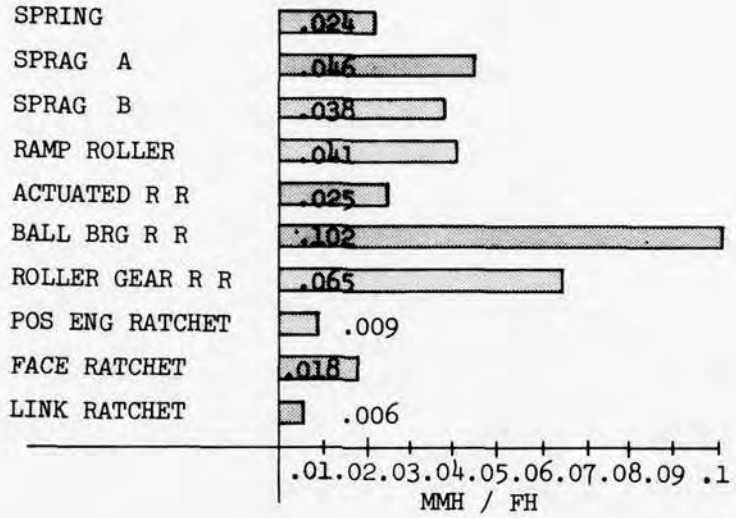

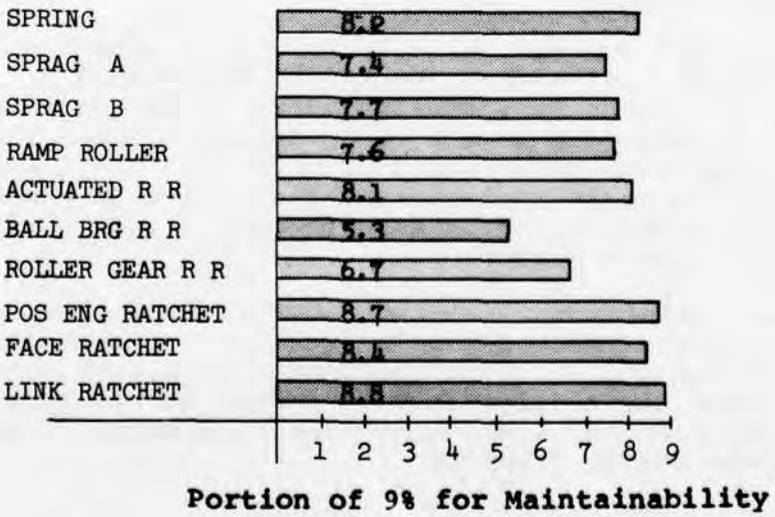

Figure 23. Maintainability Ranking.

TABLE 9. OVERRUNNING CLUTCH MAINTAINABILITY

	Wear Life MTBUR	Flight Hours MTBR	MMH for 1 Overhaul	MMH/FH
Spring	3350	2110	50.3	.024
Sprag A	1540	970	44.3	.046
Sprag B	1800	1140	43.2	.038
Ramp Roller	2200	1340	56.2	.041
Actuated R R	4080	2570	63.6	.025
Ball Brg R R	740	470	47.4	.102
Roller Gear R R	1220	770	50.3	.065
Pos Eng Ratchet	11,500	7250	63.4	.009
Face Ratchet	5000	3150	55.5	.018
Link Ratchet	10,400	6550	37.8	.006

CENTRIFUGAL EFFECTS

The ratings for centrifugal effects on the candidate overrunning clutch designs have been assigned a maximum value of 7%. This 7% rating is subdivided into 2% for wear due to centrifugal force and 5% for engagement problems arising from or associated with centrifugal effects. Although wear from centrifugal force is an important parameter, it has been assigned only 2% because it is also considered under the reliability design parameters.

Centrifugal effects in high-speed overrunning clutches may become the predominant design criterion. Care in design can reduce centrifugal loads on components by sizing the units as small as possible consistent with proper stress levels. The centrifugal force of a spinning mass at distance r from the axis of rotation is given by

$$Fc = M r \omega^2 \qquad (14)$$

where

Fc	=	centrifugal force
M	=	mass
r	=	radius
ω	=	angular velocity - rad/sec

The largest factor in Equation 14 is the angular velocity, which is a function of the square of the overrunning speed. Thus, for the 20,000-rpm overrunning speed of the candidate designs, centrifugally induced forces can cause high loads on rotating components.

However, some designs have inherently lower centrifugally induced loads. In the spring clutch, for example, centrifugal force induced in the spring will cause the spring to expand radially. This is a design problem from the standpoint of premature engagement. However, it is not a design problem from the standpoint of the spring subjecting the housing to high loads: the spring reacts outward loads within itself. In the face-type clutches, such as the positive engagement ratchet and the face ratchet, the driving mechanism, i.e., the curvic coupling and the face ratchet, are not in themselves affected by centrifugal force. The control mechanisms of these two clutches are subject to centrifugal loads, and in the face ratchet clutch, centrifugal force on the pin is a problem if the pin cannot overcome the friction force created from the centrifugal load and is unable to work against the face ratchet at high speeds. A summary of the centrifugal loads on the candidate clutch components is presented in Figure 24.

Note that high loads are induced in the rollers of the ball-bearing-carrier ramp-roller clutch and in the roller-gear ramp-roller clutch. These clutches are designed with 10 rollers versus 14 rollers in the conventional ramp-roller clutch because they need more cross-sectional area, for bearings in the ball-bearing carrier and for the pinion in the roller-gear type. Note also that the link-ratchet clutch has a high centrifugal load on the link. However, this is not as serious a problem as in the other types because the link pivots about a fulcrum point that counterbalances the majority of the centrifugal load. Only the overturning moment due to the effect of the center of gravity of the link creates loads on the housing and ratchet. The ratings for wear and engagement problems associated with centrifugal force are summarized in Table 10.

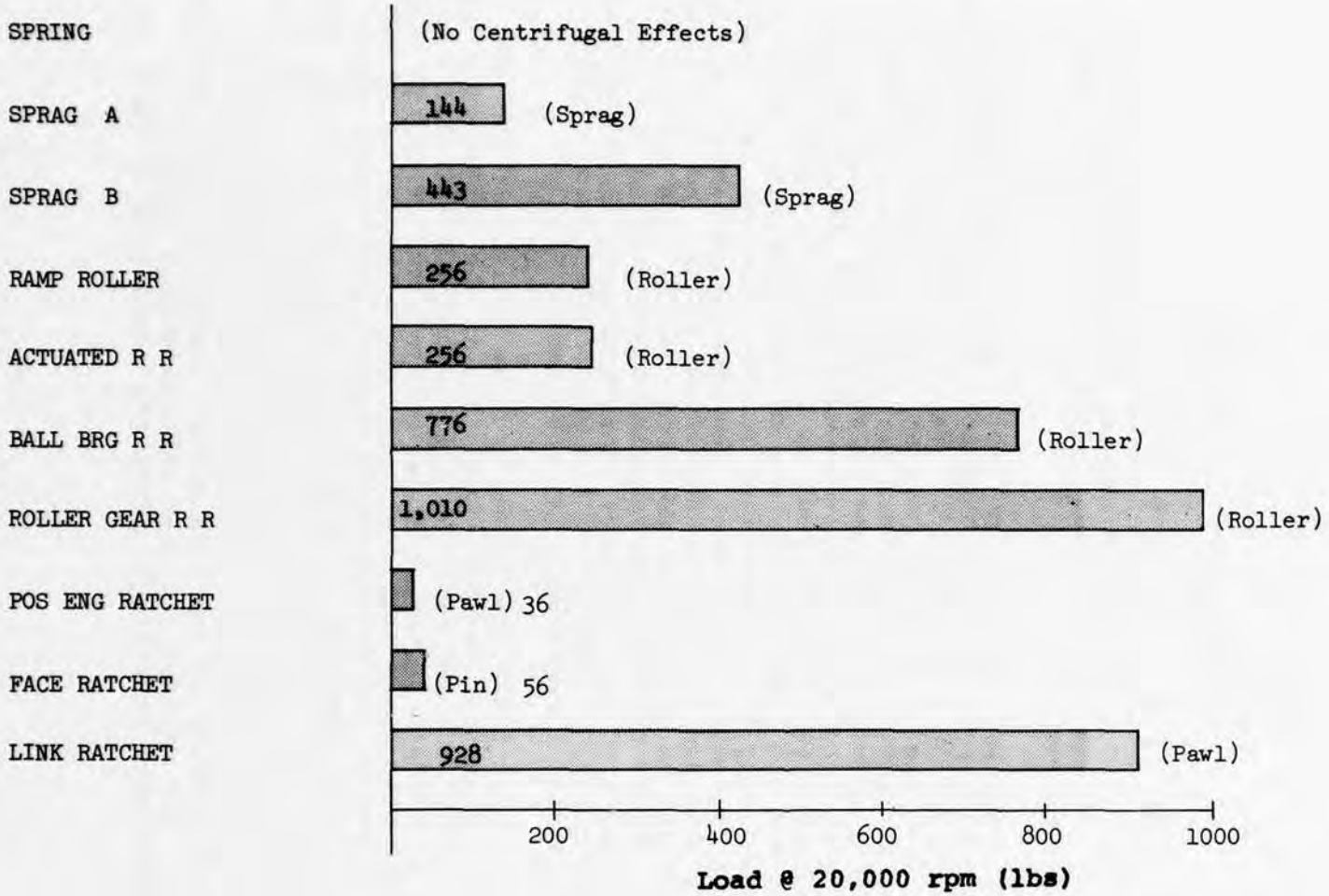

Figure 24. Centrifugal Load on Overrunning Clutch Components.

TABLE 10. CENTRIFUGAL EFFECTS SELECTION MATRIX RATINGS

Name	Wear Rating - 2%	Engagement Rating - 5%	Total Centrifugal Force Rating - 7%
Spring	2.0	5.0	7.0
Sprag A	1.8	5.0	6.8
Sprag B	1.5	*1.0	2.5
Ramp Roller	1.5	5.0	6.5
Actuated R R	2.0	5.0	7.0
Ball Brg R R	0.5	0.5	1.0
Roller Gear R R	0.5	0.5	1.0
Pos Eng Ratchet	1.8	5.0	6.8
Face Ratchet	1.8	0.0	1.8
Link Ratchet	1.5	3.0	4.5

*Based on previous testing.

VIBRATION

The vibration parameter of the selection matrix is assigned a maximum value of 6% and is subdivided into lateral and torsional vibration, where each has a rating of 3%.

Lateral vibration refers to shaft "wipping" modes. To determine the critical speeds of the candidate clutch designs, Sikorsky computer program #E009, "Shaft Critical Speeds," was used. This program computes the critical speeds of a shaft with uniform and lumped weights on "n" supports with various boundary conditions. The method of solution is based on the Mykelstad numerical tabular method where the internal shears, moments, slopes, and deflections are calculated from the lumped masses, the physical geometry, and an estimate of the critical speed of the system. Iterations are made until the shaft conditions for kinetic and potential energies are balanced.

The first step in calculating the critical lateral bending frequencies of the candidate clutch design was to create a mathematical model of each clutch. Each model consisted of a series of shafts having stiffnesses but no masses connecting a series of discrete lumped masses. It was only necessary to enter the outside diameter and the inside diameter for each clutch component since the program calculated the mass and stiffness properties required. Any extraneous masses and rotary inertias not accounted for, such as nuts and bolts, were added to the program inputs. Bearing supports were modeled with both pitching and lateral spring rates. No damping was included in the analysis.

The computer calculations of the natural bending frequencies of the candidate clutch designs showed that the frequencies were very high for all designs. The general configuration of an overrunning clutch is such that the average cross-sectional moment of inertia is high compared to the distance between supports. This results in high bending stiffness for most clutch designs, which leads to high natural frequencies.

It is desirable to design the clutch so that the first natural frequency of vibration is greater than 120% of the operating speed. The lowest frequency calculated was 34,000 rpm for the link ratchet, which is well above the minimum design criteria. The lateral vibration modes obtained, even though high, were not bending modes but rather rigid body modes. The first bending critical frequencies are all higher than the rigid body modes calculated. The results are summarized in Table 11.

TABLE 11. SUMMARY OF NATURAL FREQUENCY (RIGID BODY) MODES

Clutch	First Mode (rpm)	Second Mode (rpm)
		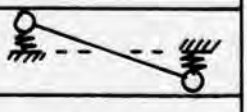
Spring	---	66,000
Sprag A	---	91,000
Sprag B	---	91,000
Ramp Roller	---	64,000
Actuated R R	---	60,000
Ball Brg R R	39,000	131,000
Roller Gear R R	---	105,000
Pos Eng Ratchet	---	88,000
Face Ratchet	---	60,000
Link Ratchet	34,000	160,000

The torsional vibration factor of each clutch is dependent on the clutch's effect on the overall drive system. The helicopter drive train can be modeled as a series of rotary inertias connected by torsional springs as shown in Figure 25. The freewheel unit is assumed to be placed between the engine and the transmission input, as shown in the figure. In this position, the clutch's effects on the drive train in terms of inertia and spring rate become reduced as shown by the example that follows.

The overall system spring rate for two springs in series is given by

$$\frac{1}{Ke} = \frac{1}{K1} + \frac{1}{K2} \qquad (15)$$

where

Ke = equivalent system spring rate
K1,K2= spring rates of clutch and transmission

When determining the spring rate of the main transmission, the total angle of twist is referred to the input and then divided into the input torque. Thus, the components near the output of the transmission, such as the main rotor shaft, have large effects on the spring rate when reflected to the freewheel unit since the spring rate is reflected by speed squared. Even though the main rotor shaft may twist only a fraction of a degree at full torque, the twist at the input is multiplied by the reduction ratio. For a typical helicopter with 20,000 rpm input, the output is usually in the order of 250 rpm. Thus, the reduction ratio is approximately 80 to 1. Small angles of twist at the output are magnified by this reduction ratio. The resultant effect is that the typical main transmission has a relatively low spring rate when referred to the input shaft. For a typical medium-size helicopter with 20,000 rpm and 1500 hp at the inputs, the main transmission spring rate is in the order of 73 inch-pounds/degree. If the spring rate of the overrunning clutch is known, an equivalent spring rate for the main transmission including the overrunning clutch can be calculated using Equation 15.

The torsional spring rates of the various clutches are found from previous test data or by calculating from the layouts of the candidate designs. A summary is presented in Table 12.

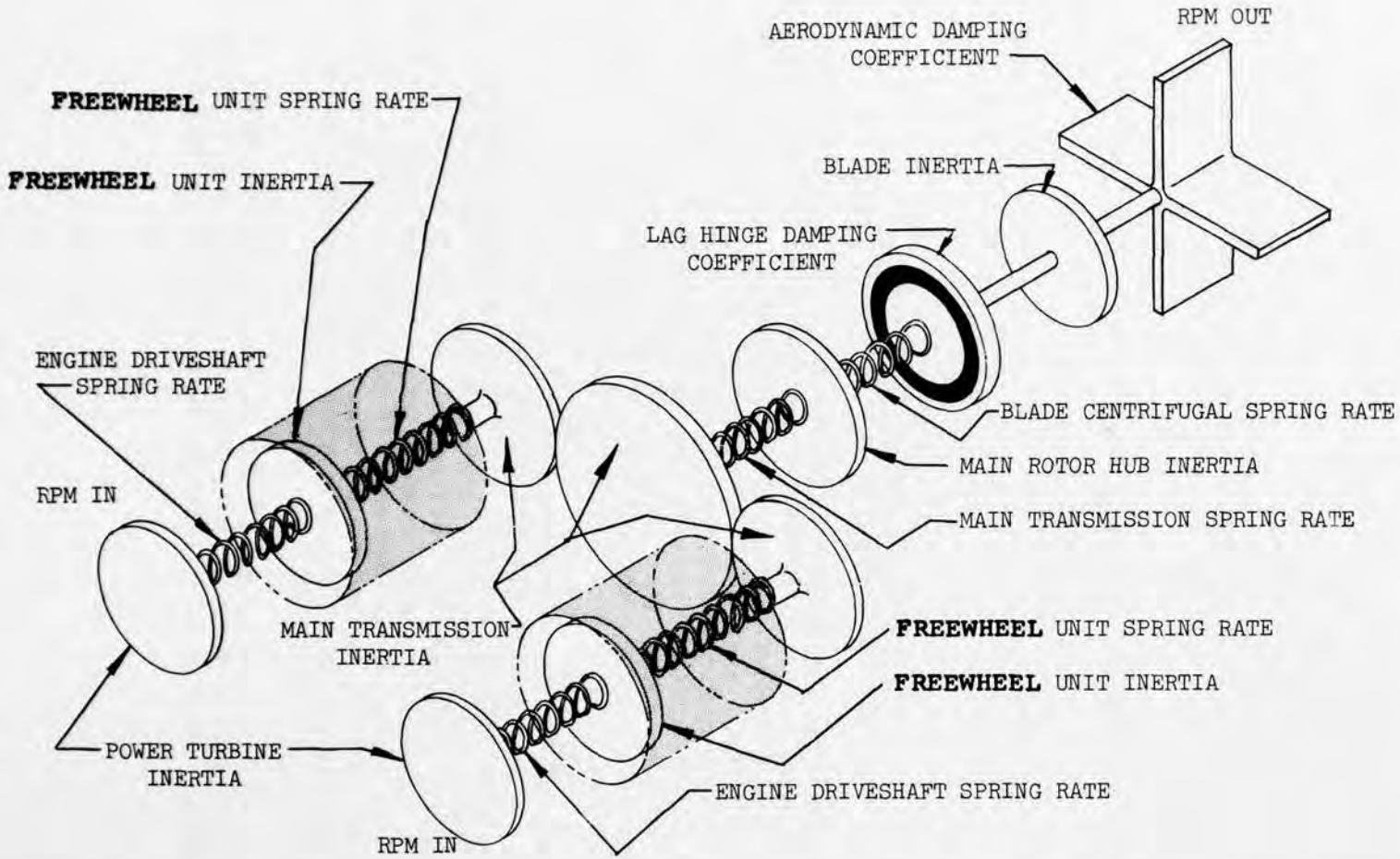

Figure 25. Drive System Simulation Neglecting the Effect of the Tail System.

TABLE 12. OVERRUNNING CLUTCH SPRING RATES AND EQUIVALENT TRANSMISSION SPRING RATES

Name	Clutch Spring Rate - in.-lb/deg	Transmission Equivalent Spring Rate - in.-lb/deg	$\frac{Wl}{Wn} = \sqrt{\frac{Kl}{Kn}}$
Baseline		73.0	1.000
Spring	645	65.6	.948
Sprag A	1750	70.0	.979
Sprag B	1380	69.3	.974
Ramp Roller	2250	70.7	.984
Actuated R R	2250	70.7	.984
Ball Brg R R	1970	70.4	.982
Roller Gear R R	2090	70.5	.983
Pos Eng Ratchet	12,600	72.6	.997
Face Ratchet	16,500	72.7	.998
Link Ratchet	8000	72.3	.995

In Table 12, the last column indicates the ratio of the natural frequency of the transmission with the clutch installed to the natural frequency without the clutch. This number represents the percent reduction in each system's natural frequency due to the addition of the overrunning clutch to the input shaft. This percent ratio is a square root function of the spring rate ratio. Note that the effect of the overrunning clutch on the transmission's natural frequency is generally very small.

The ratings for vibration for the candidate are calculated using the second lateral frequency modes for lateral bending and using the percent reductions in transmission natural frequencies for torsional vibration ratings.

For lateral bending, a frequency of 160,000 cycles per minute or above is given a ranking of 3%, while a lateral bending frequency of 60,000 cycles per minute is assigned a 2% rating. This relationship is expressed as

$$\% V_{lat} = 1.4 + \omega_n/100{,}000 \qquad (16)$$

where

$\% V_{lat}$ = percent rating of 3% for lateral bending
ω_n = second mode lateral bending natural frequency

For torsional frequency, a percent reduction in transmission natural torsional frequency of 1.000 represents a rating of 3%, while a percent of .900 represents a 0% rating.

This is expressed by

$$\% V_{tors} = 30 X - 27 \qquad (17)$$

where

$\% V_{tors}$ = percent ratings of 3% for torsional vibration
X = ratio of the transmission's natural frequency with clutch to the transmission's natural frequency without clutch

The final candidate ratings for vibration are shown in Figure 26.

TRANSIENT TORQUE

The transient torque ratings of the candidate freewheel unit designs carry a maximum rating of 3% in the selection matrix. This parameter rates the clutches' capability for transmitting high static torques for short durations. Generally, transmission components are designed statically to a static load factor of 2 or 2.25 times the maximum engine torque capability and in addition must have a factor of safety of 1.5 applied to the load factor. With these static factors applied, the freewheel unit must withstand transient torques of up to 3.375 times the normal torque (in this case 3570 inch-pounds is equivalent to 20,000 rpm at 1500 hp). Previously obtained test data on the spring, sprag, and ramp-roller clutches has shown that this static requirement is easily met since all clutches were tested to four times the dynamic capacity without failure. In any freewheel unit design, static capability is merely a matter of proper sizing for stress. Therefore, all of the candidate designs have been assigned the maximum value in the selection matrix for transient torque capability.

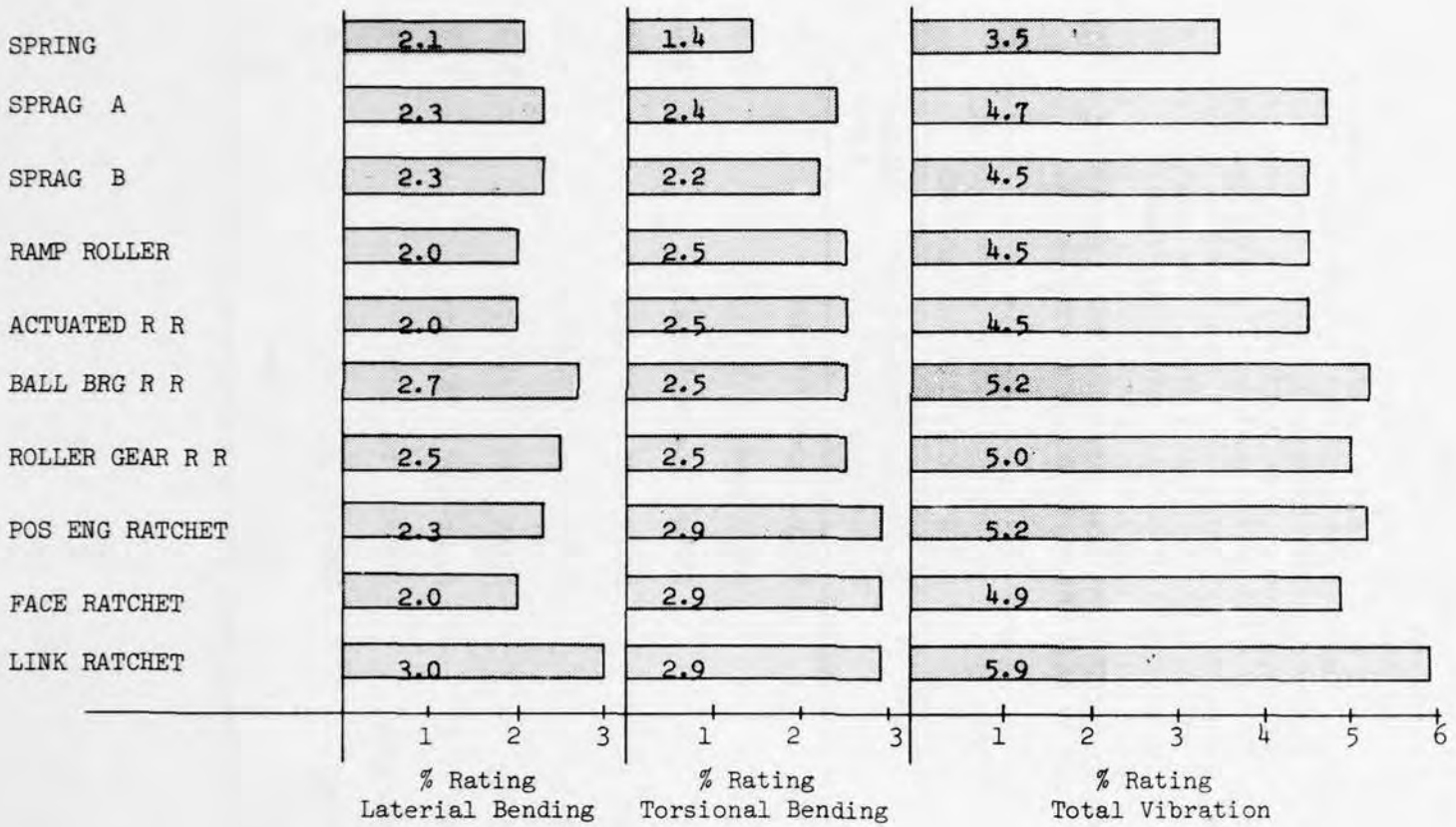

Figure 26. Selection Matrix Rating for Overrunning Clutch Vibration.

Another way to evaluate transient torque is to examine the effect of a transient overload condition. In the case of the spring clutch and the design B sprag clutch, the input and output shaft members will slip suddenly in relation to each other. However, both units will be operational once the transient is removed. The design A sprag design will "flop-over" and be inoperative. The ramp-roller types of clutches will usually "spit out" their rollers, which can result in fracture of their roller carrier. The ratchet types of clutches will shear the driving faces. In evaluating the transient characteristics of the candidate designs, the resultant effect of a static overload failure was examined and engineering judgment exercised. The resultant ratings as portions of 3 percent are shown in Table 13.

TABLE 13. TRANSIENT OVERTORQUE RATINGS, CANDIDATE CLUTCH DESIGNS

Name	Resultant Effect of Transient Overload	Rating as a Portion of 3%
Spring	Slip, operational	3.0
Sprag A	Flop-over, failure	2.8
Sprag B	Slip, operational	3.0
Ramp Roller	Spit out, failure	2.8
Actuated R R	Spit out, failure	2.8
Ball Brg R R	Spit out, failure	2.8
Roller Gear R R	Spit out, failure	2.8
Pos Eng Ratchet	Shear, failure	2.8
Face Ratchet	Shear, failure	2.8
Link Ratchet	Shear, failure	2.8

THERMAL EFFECTS

The next performance parameter to be considered in evaluating the ten candidate overrunning clutches is the effects of extreme temperatures on clutch operation. This parameter was given a total weight of 2%: 0.5% for high-temperature effects and 1.5% for low-temperature effects.

Thermal expansion was the only factor considered in evaluating the clutches' performances at extremely high temperatures. Examination of each of the clutch designs revealed that, assuming proper dimensional control during manufacture, high temperatures would have no detrimental effects on the operation of any of the clutches. Therefore, each clutch was given the maximum rating of 0.5% for high-temperature operation.

For low-temperature operation, consideration was given to the effect of increased oil viscosity on clutch performance particularly on start up in addition to the resulting dimensional changes. A marked increase in oil viscosity could prove particularly troublesome for those clutches that depend on the movement of small parts for proper operation. The more viscous oil could slow considerably, or even stop, the movement of these small parts. For example, the actuated double-cage ramp-roller clutch received the worst rating for low-temperature operation. At extremely low temperatures, the spring pin could hang up, preventing correct engagement. This problem is common to all ramp-roller designs. In addition, one of the small control components, such as the control cage, control rollers, bearings, or gears, could fail to function properly. The ball-bearing ramp-roller clutch has the potential problem of one of the small bearings hanging up, thereby preventing the roller from rolling. The face-ratchet clutch received the same low rating as the ball-bearing ramp-roller clutch. While much simpler than the ball-bearing ramp-roller clutch, it depends on the proper functioning of the pin and spring assembly to ensure engagement. It was judged that this component was vulnerable to "sticking" during extremely cold weather, and thus, it received a low rating. Both sprag clutches received the same rating because of the possibility of the sprag engagement springs hanging up. The spring, positive engagement ratchet, and link ratchet all received the maximum rating of 1.50%, since it was judged that low temperatures would have minimumal effects on their proper operation.

A summary of thermal-effect ratings of the ten clutches appears in Table 14.

TABLE 14. SUMMARY OF THERMAL EFFECTS RATINGS			
Clutch	High Temperature Rating	Low Temperature Rating	Rating 2% Max
Spring	.5	1.50	2.00
Sprag Design A	.5	.75	1.25
Sprag Design B	.5	.75	1.25
Ramp Roller	.5	.75	1.25
Actuated R R	.5	.15	.65
Ball Bearing R R	.5	.60	1.10
Roller Gear R R	.5	.60	1.10
Pos Eng Ratchet	.5	1.50	2.00
Face Ratchet	.5	.15	.65
Link Ratchet	.5	1.50	2.00

START-UP CONTROL

The next criterion on which the ten clutch designs were rated was start-up control, which was given a maximum weight of 4%. This parameter serves as a measure of a clutch's ability to provide positive engagement upon engine start-up. This factor was also divided into two parts: engagement shock load factor and positive drive factor. The engagement shock load factor was given a weight of 1% and was dependent on the maximum angular travel of the clutch prior to engagement. The greater the possible angular travel, the lower the rating. The engagement shock load factor was determined by the following formula:

$$F_{s2} = 1 - \frac{X}{90} \qquad (18)$$

where

F_{s2} = engagement shock load factor
X = maximum angular travel before engagement - deg

With angles of travel greater than 90 degrees prior to engagement, the engagement shock load factor is assumed to be zero. The sprag and conventional ramp-roller clutches scored highest in this category since the maximum angular travel was 1 degree or less for these clutches. The spring clutch received a zero rating since it could possibly go through approximately 90 degrees before engagement.

The positive drive factor, which received a 3% weight, was a measure of the degree of positive drive of a clutch. Ratchet clutches, which do not depend on friction to drive, were given the maximum rating of 3%. Friction-drive clutches, such as the spring, sprag, and ramp-roller clutches, were given a rating of 2.25%. The ball-bearing-carrier clutch, which is the least positive drive of the clutches, received a rating of only .75%. The start-up control ratings of the ten clutches are summarized in Table 15.

TABLE 15. SUMMARY OF START-UP CONTROL RATINGS

Clutch	Max Δ Before Engage	Engagement Shock Load Factor Portion of 1%	Positive Engagement Factor Portion of 3%	Overall Rating Portion of 4%
Spring	90°	0	2.25	2.3
Sprag A	1°	.99	2.25	3.2
Sprag B	1°	.99	2.25	3.2
Ramp Roller	1°	.99	2.25	3.2
Actuated R R	15°	.83	2.25	3.1
Ball Brg R R	15°	.83	.75	1.6
Roller Gear R R	1°	.99	2.25	3.2
Pos Eng Ratchet	39°	.57	3.00	3.6
Face Ratchet	22.5°	.75	3.00	3.8
Link Ratchet	16°	.82	3.00	3.8

FAILURE MODES

Another criterion on which the overrunning clutches were evaluated was the probable result of various failure modes. This category, which received a total weight of 3%, was divided into three factors: overrunning wear failure, failure due to loss of lubrication, and failure due to over torque. Each of these three factors received a weight of 1%.

The overrunning wear failure mode was based on the number of parts susceptible to wear and a technical assessment of the effect of this wear on proper clutch operation. Table 16 summarizes the rating for the ten candidate clutches for overrunning failure modes.

TABLE 16. OVERRUNNING FAILURE MODE RATINGS

Clutch	Items Subject to Wear	Resultant Failure	Rating %
Spring *	Spring, Housing	Failure to engage	.80
Sprag A	Sprags, Housing	Rollover	.75
Sprag B	Sprags, Housing	Rollover	.75
Ramp Roller	Rollers, Cams, Housing Cage	Spit out	.70
Actuated R R	Control Roller, Control Ring	Clutch will operate as standard ramp roller	1.00
Ball Brg R R	Bearings, Roller, Housing	Spit out	.70
Roller Gear R R	Gears, Roller, Housing Cage, Cam	Spit out	.65
Pos Eng Ratchet**	Ratchet, Pawl, Spline	Failure to engage	.90
Face Ratchet**	Input and Output Ratchets, Spline, Spring	Failure to engage	.90
Link Ratchet**	Ratchet, Link	Failure to engage	.90

* Low wear from previous test experience.
** Wear in hydroplane is minimal.

The loss-of-lubrication failure mode factor was determined to be exactly the same for each clutch as the overrunning wear failure mode factor. While failure due to loss of lubrication would occur much more quickly, the relative behavior of the clutches would be the same as for overrunning wear; thus, the ratings are the same.

The over-torque failure rating was based on the ability of the clutch to drive after sustaining such a failure. If a clutch could still drive after over-torque failure, it was given the full 1%. If it could not, it was given 0. Table 17 summarizes the total failure-mode ratings for the ten candidates.

TABLE 17. TOTAL FAILURE MODE RATINGS

Clutch	Wear Failure Rating	Loss of Lubrication Rating	Over Torque Failure Rating	Overall Rating
Spring	.80	.80	1.00	2.6
Sprag A	.75	.75	0	1.5
Sprag B	.75	.75	1.00	2.5
Ramp Roller	.70	.70	1.00	2.4
Actuated R R	1.00	1.00	1.00	3.0
Ball Brg R R	.70	.70	1.00	2.4
Roller Gear R R	.65	.65	1.00	2.3
Pos Eng Ratchet	.90	.90	0	1.8
Face Ratchet	.90	.90	0	1.8
Link Ratchet	.90	.90	1.00	2.8

LIMITS OF OPERATION

The limits of operation factor was given a total weight of 4%, 1% for each of the following categories: torque, lubrication, speed, and temperature. This parameter was used as a measure of the clutch's ability to maintain proper operation of the extreme limits that could be incurred in a helicopter environment.

The torque limit was assumed to be that which would be encountered in an HLH application at the engine speed of approximately 12,000 rpm and a torque of 100,000 in.-lb. It was found that any of the ten clutches, if properly designed, could easily withstand this torque. Therefore, each design was given the maximum of 1% in this category.

Each clutch was also given 1% in the lubrication limit category. For this parameter, a rating of less than 1% would have been given only if a clutch had an extraordinary lubrication requirement, e.g., a significantly increased flow requirement, significantly more parts requiring lubrication, or a special lubrication system design requirement. None of the clutches under consideration presented any of these problems and, therefore, were all given the maximum rating.

The next limit on which the clutches were rated was speed. The limit chosen for the basis of this rating was 35,000 rpm, the maximum anticipated speed for future STAGG (Small Turbine Advanced Gas Generator) derived engines. Engineering judgment and previous test experience were used to determine the maximum practical speed at which a specific clutch design might be expected to operate. The spring, actuated ramp-roller, positive-engagement ratchet, and face ratchet designs were all judged to be practical designs for 35,000-rpm applications. The two sprag clutches and the other ramp-roller clutches were judged to be practical only to 20,000 rpm based on previous test experience. Beyond this speed, the centrifugal forces on the small actuating parts are detrimental to proper clutch operation. The link ratchet was judged to have a speed limitation of only 12,000 rpm. This clutch by its design is necessarily imbalanced by the offset between inner and outer shafts and, therefore, would not be able to operate at the higher speeds. The ratings for this category were determined by the following formula:

$$\text{Limit Speed Rating} = \frac{\text{Limit Speed}}{35{,}000} \qquad (19)$$

The limits that were considered in the temperature rating were -65°F minimum to 550°F maximum. A maximum rating of .5% was assigned for each limit. The maximum temperature is that temperature at which advanced technology gearboxes may be expected to operate. This temperature exceeds the carburizing limit of 450°F. Therefore, all clutches were given the identical rating of .41% (450/550 x 1/2). The spring, positive-engagement ratchet and link-ratchet clutches were judged to be suitable for the low-temperature limit of -65°F. All other clutches were judged to be suitable for operation to -65°F, but with some possible problems because of the possibility of small parts "hanging up". The final ratings for temperature were calculated using .41% for high temperature and .50% for low temperature for the spring, positive-engagement ratchet, and link ratchet. All other clutches received .30% for low-temperature operation. The ratings for torque limit, lubrication limit, speed limit, and temperature limit are summarized in Table 18.

TABLE 18. CLUTCH OPERATIONAL LIMIT RATINGS

Clutch	Torque Limit Rating Portion of 1%	Lubrication Limit Rating Portion of 1%	Speed Limit Rating Portion of 1%	Temperature Limit Rating Portion of 1%	Overall Limit Rating Portion of 4%
Spring	1.0	1.0	1.0	.91	3.9
Sprag A	1.0	1.0	.57	.71	3.3
Sprag B	1.0	1.0	.57	.71	3.3
Ramp Roller	1.0	1.0	.57	.71	3.3
Actuated R R	1.0	1.0	1.0	.71	3.7
Ball Brg R R	1.0	1.0	.57	.71	3.3
Roller Gear R R	1.0	1.0	.57	.71	3.3
Pos Eng Ratchet	1.0	1.0	1.0	.91	3.9
Face Ratchet	1.0	1.0	1.0	.71	3.7
Link Ratchet	1.0	1.0	.34	.91	3.3

UNUSUAL TEST REQUIREMENTS

Unusual test requirements carry a rating of 3% maximum in the selection matrix. The ratings in this criteria, as the title implies, were dependent on whether or not any special tests would be required during this program to fully evaluate the clutch design. Only three designs would have required special testing: the positive-engagement ratchet, the face ratchet and the link ratchet. All of these tests would concern the determination of the vibration characteristics of the pawl when freewheeling. In order to properly design these ratchet clutches, the spring rate should be such that the pawl hydroplanes when freewheeling. To determine the proper spring rate is difficult by analysis. Therefore, tests would have to be performed where pawls with various spring rates would be observed during freewheeling. This could be accomplished by visual observation using a strobe light at various speeds. Since this type of test would be neither difficult nor expensive, the ratchet clutches were all given a rating of 2% for this criterion. All other clutches received the full 3%.

MULTI-ENGINE OPERATION

Clutches that are used in helicopters with more than one engine must be able to withstand much longer periods of overrunning than clutches on single-engine helicopters. The multi-engine helicopter freewheel unit will overrun whenever one engine is inoperative. This can occur during start-up if there is no rotor brake on the aircraft or during emergency engine shutdown. The ratings in the selection matrix for multi-engine operation are based on the clutches' abilities to overrun at differential speeds. The maximum rating is 2%. The ratings have been based on the values given for overrunning wear failure in the Failure Modes section and are twice the amounts shown for 1% in Table 16.

BEARING BRINELLING

This criterion measures a clutch's susceptibility to bearing brinelling. This condition can occur only if the bearings cannot be preloaded or if the bearings must support the weight of the clutch through the bearings. Clutches in which the bearings cannot be preloaded are both sprag clutches, the ball-bearing-carrier ramp-roller clutch, and the link-ratchet clutch. These clutches all received a rating of 0.3% of the maximum 1%. Clutches that must react the weight of the unit through the bearings are the ramp roller, the actuated ramp roller, the positive-engagement ratchet, the face ratchet, and the roller-gear ramp roller. Since this condition is more likely to cause brinelling than the unpreloaded case, these clutches were assigned a rating of 0.7%. The spring clutch, in which neither condition is present, received the full 1%.

FINAL DESIGN SELECTION

The design selection matrix with the complete ratings for each of the ten candidate clutches is shown in Table 19. The last column, labeled the "Figure of Merit", contains the overall ratings for the clutches. From the figure of merit it can be seen that the clutches, ranked in descending order of rating, are as follows:

1. Spring
2. Link Ratchet
3. Ramp Roller
4. Sprag Design A
5. Sprag Design B
6. Positive-Engagement Ratchet
7. Actuated Double-Cage Ramp Roller
8. Face Ratchet
9. Roller-Gear Ramp Roller
10. Ball-Bearing-Carrier Ramp Roller

It had been decided that three designs would be selected for fabrication and testing. The three designs selected were the spring, the ramp-roller, and the sprag design A clutches. The link ratchet, although placing second in overall rating, was not selected as one of the final three designs. This design, unlike any of the other designs, has never been fabricated or tested and has an inherent imbalance when locked that makes it unsuitable for speeds exceeding 12,000 rpm, whereas testing will be conducted at 20,000 rpm. On the basis of these considerations, the sprag design A was selected instead of the link ratchet for fabrication and testing.

While the spring clutch, on the basis of the figure of merit, was clearly superior to the other clutches, the same cannot be said of the two other designs selected for fabrication and test. The ramp-roller, both sprag, and the positive-engagement ratchet clutches all placed within 2 percentage points of each other in the figure of merit. All of these clutches are good candidates for helicopter freewheel units. It was decided that, in addition to the spring clutch, it would be advisable to fabricate and test the sprag and ramp roller designs since these clutches are the most commonly used in the helicopter industry. The high ratings received by the link-ratchet clutch certainly make it a candidate for future investigation. The positive-engagement ratchet clutch also warrants further development.

TABLE 19. OVERRUNNING CLUTCH DESIGN SELECTION MATRIX

	WEIGHT	COST	RELIABILITY	MAINTAINABILITY	CENTRIFUGAL EFFECTS	VIBRATION	TRANSIENT TORQUE	THERMAL EFFECTS	START-UP CONTROL	FAILURE MODES	OPERATION LIMITS	UNUSUAL TESTING	MULTI-ENGINE	BEARING BRINELLING	FIGURE OF MERIT
1. Spring	11.1	9.4	22.7	8.2	7.0	3.5	3.0	2.0	2.3	2.6	3.9	3.0	1.6	1.0	81.3
2. Sprag A	12.3	10.9	18.4	7.4	6.8	4.7	2.8	1.3	3.2	1.5	3.3	3.0	1.5	0.3	77.4
3. Sprag B	12.2	11.0	20.5	7.7	2.5	4.5	3.0	1.3	3.2	2.5	3.3	3.0	1.5	0.3	76.5
4. Ramp Roller	10.8	8.9	21.3	7.6	6.5	4.5	2.8	1.3	3.2	2.4	3.3	3.0	1.4	0.7	77.7
5. Actuated R R	9.2	7.7	17.1	8.1	7.0	4.5	2.8	.7	3.1	3.0	3.7	3.0	2.0	0.7	72.6
6. Ball Brg R R	11.9	10.9	13.9	5.3	1.0	5.2	2.8	1.1	1.6	2.4	3.3	3.0	1.4	0.3	64.1
7. Roller Gear R R	10.4	9.9	14.5	6.7	1.0	5.0	2.8	1.1	3.2	2.3	3.3	3.0	1.3	0.7	65.2
8. Pos Eng Ratchet	10.4	8.2	18.1	8.7	6.8	5.2	2.8	2.0	3.6	1.8	3.9	2.0	1.8	0.7	76.0
9. Face Ratchet	10.8	8.8	16.4	8.4	1.8	4.9	2.8	.7	3.8	1.8	3.7	2.0	1.8	0.7	68.4
10. Link Ratchet	11.3	12.3	19.0	8.8	4.5	5.9	2.8	2.0	3.8	2.8	3.3	2.0	1.8	0.3	80.6
Percent of 100%	13	13	30	9	7	6	3	2	4	3	4	3	2	1	100

DETAIL DESIGN

The overrunning clutches used in this program were designed for the following conditions

Speed	20,000 rpm
Endurance design power	1500 hp
Static design power	3000 hp
Minimum oil inlet temperature	195°F
Maximum oil inlet pressure	100 psig
Lubricant	MIL-L-7808

For interchangeability with the test equipment, each clutch was designed with the same input and output splines and with the same overall length. The clutch support-bearing mountings were slightly different but adapter housings were fabricated for each design that were easily changed so that only one basic clutch support and one torque path were required to test all three designs.

SPRING CLUTCH

The spring clutch configuration used in this program is shown in Figure 27. Although a different configuration arbor was used during some of the tests, the final design is as shown, with the slotted bronze spacer on the overrunning end of the clutch. Figure 28 is a photograph of the clutch hardware prior to test, while Figure 29 shows the spring clutch's major assemblies.

Torque is fed to the input side of the spring clutch at 20,000 rpm. The input housing bore must transfer the input torque to the spring, building up gradually from the teaser coils to the center coil, where all the torque passes out of the input housing. Although the spring does not rotate relative to the input housing, the bore is hardened in a high-heat treatment (Rc 54 min) as a precautionary measure. The input housing of the spring clutch also pilots and retains the spring arbor.

The output housing of the spring clutch transfers torque in a mirror image of the input housing. From the spring's center coil, the torque gradually decreases to the teaser coils. At the teaser coils, all of the torque has been transferred from the spring to the output housing. The major requirement of the output housing is to have a hard wear surface because it is here that the spring's teaser coils rub and slide during

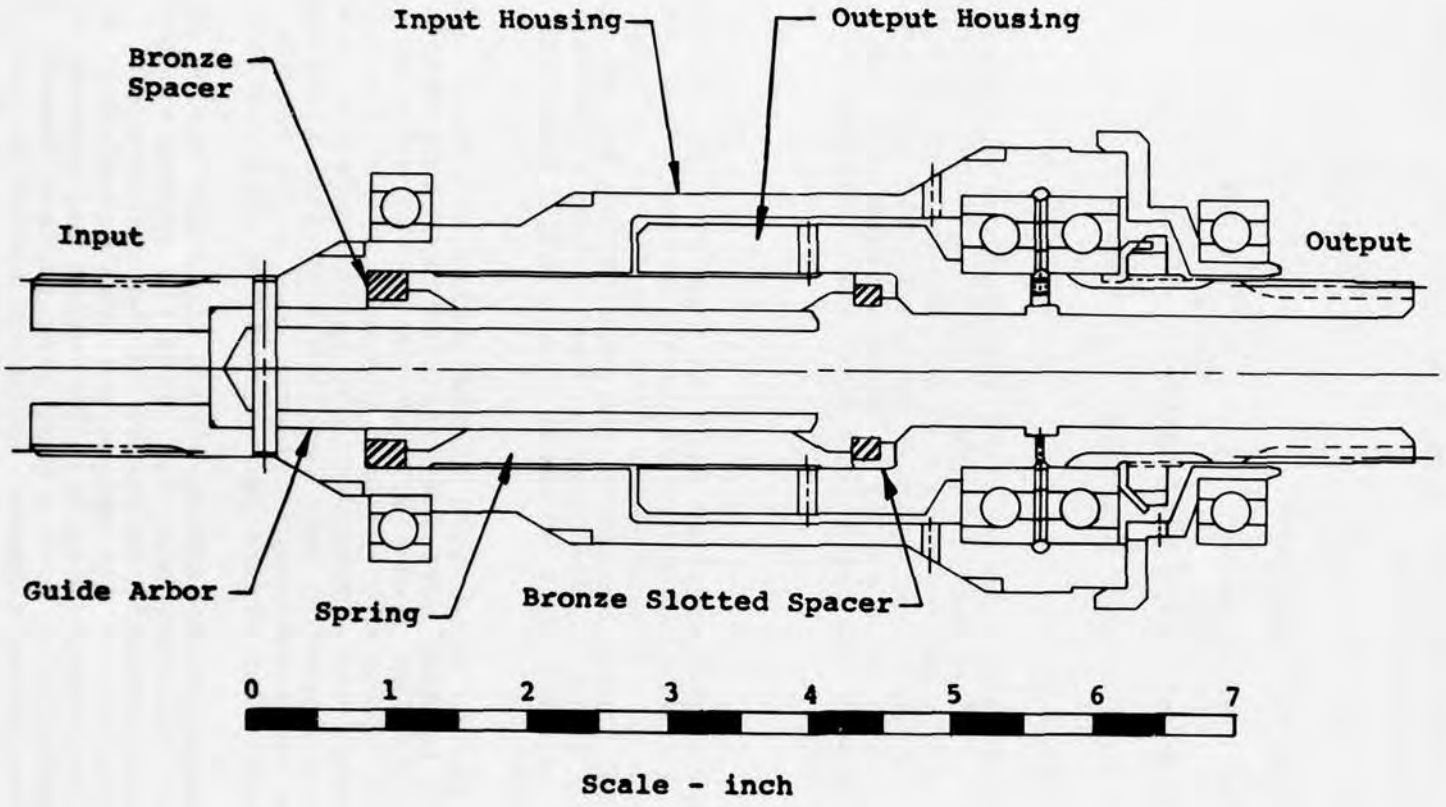

Figure 27. Spring Clutch Design, Cross Section.

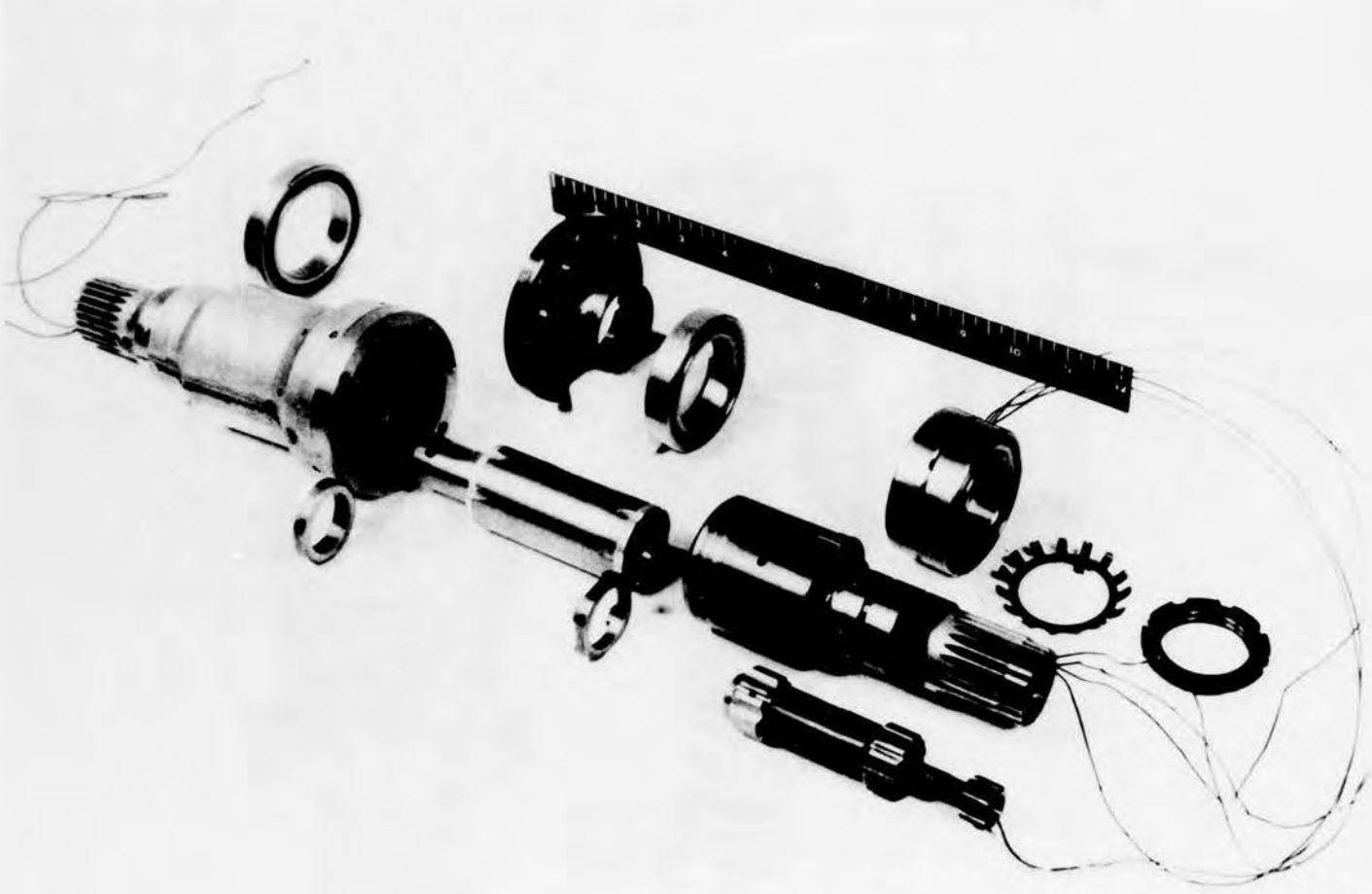

Figure 28. Spring Clutch Components.

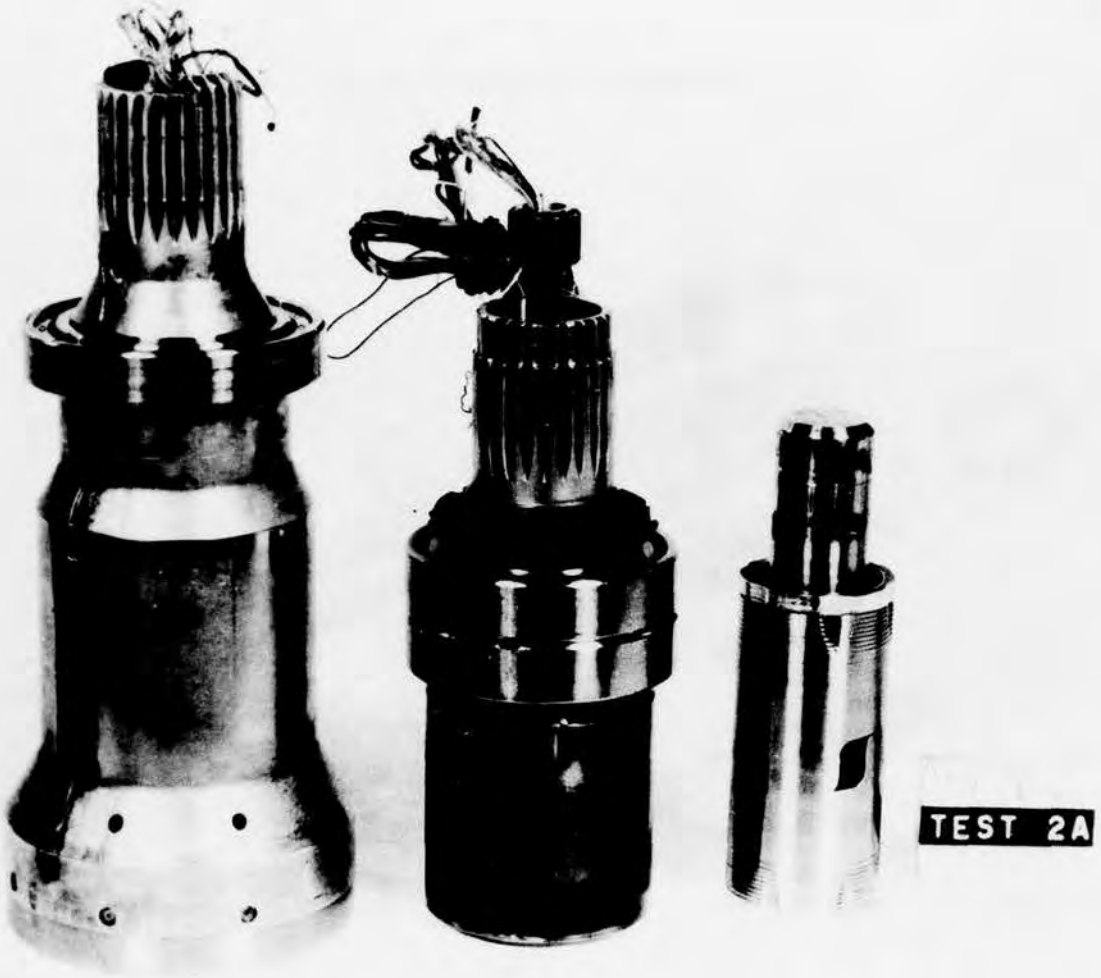

Figure 29. Spring Clutch Subassemblies.

overrunning. Overrunning wear on the output housing bore is reduced because the bore is hardened in a high-heat treatment (Rc 54 min).

Both the input and the output housings of the spring clutch are structurally designed to withstand the hoop tensions created by the pressure exerted by the spring on the bores of the housings as the spring expands during torque application. Low-cycle fatigue, ground-air-ground (GAG) is considered during the design phase.

The key to the operation of the spring clutch is the spring itself. Vacuum-melt H-11 tool steel, through-hardened to Rockwell C-54 to 56, was used as the spring material for this program. In the configuration used in the Task I tests, the teaser coils were silver plated as a wear barrier. The silver plating proved to be a nuisance as it continually chipped and peeled, creating loose pieces that then scored the output housing bore and spring O.D. During the Task II tests, the spring's teaser coils were not silver plated. A spring without plating proved to be the better of the two configurations and is recommended for future designs.

The spring is held in the input housing by the spring guide arbor. At rest, there is an interference of .0025 to .0050 inch between the spring I.D. and guide arbor O.D. When the input housing is rotating, centrifugal forces are induced in the spring coils and as the spring expands outward, the interference fit of the spring and arbor decreases. The spring is designed to be free from the arbor at full operating speed (20,000 rpm). Tests conducted during the program showed that the spring was free from the arbor at approximately 15,000 rpm.

A complete description of the spring clutch and a structural analysis are presented in Reference 1.

SPRAG CLUTCH

The sprag clutch configuration used in this program is presented in Figure 30. This configuration was used throughout all testing on the program. A photograph of the individual hardware components is shown in Figure 31. Figure 32 shows the assembled sprag clutch.

The two-row sprag unit contains drag bands and clips that impart a torque through the sprag-unit cages to the sprags so as to keep them in contact with the inner and outer races. These drag devices also inhibit relative rotation between the sprag unit and the outer (input) shaft by means of a frictional

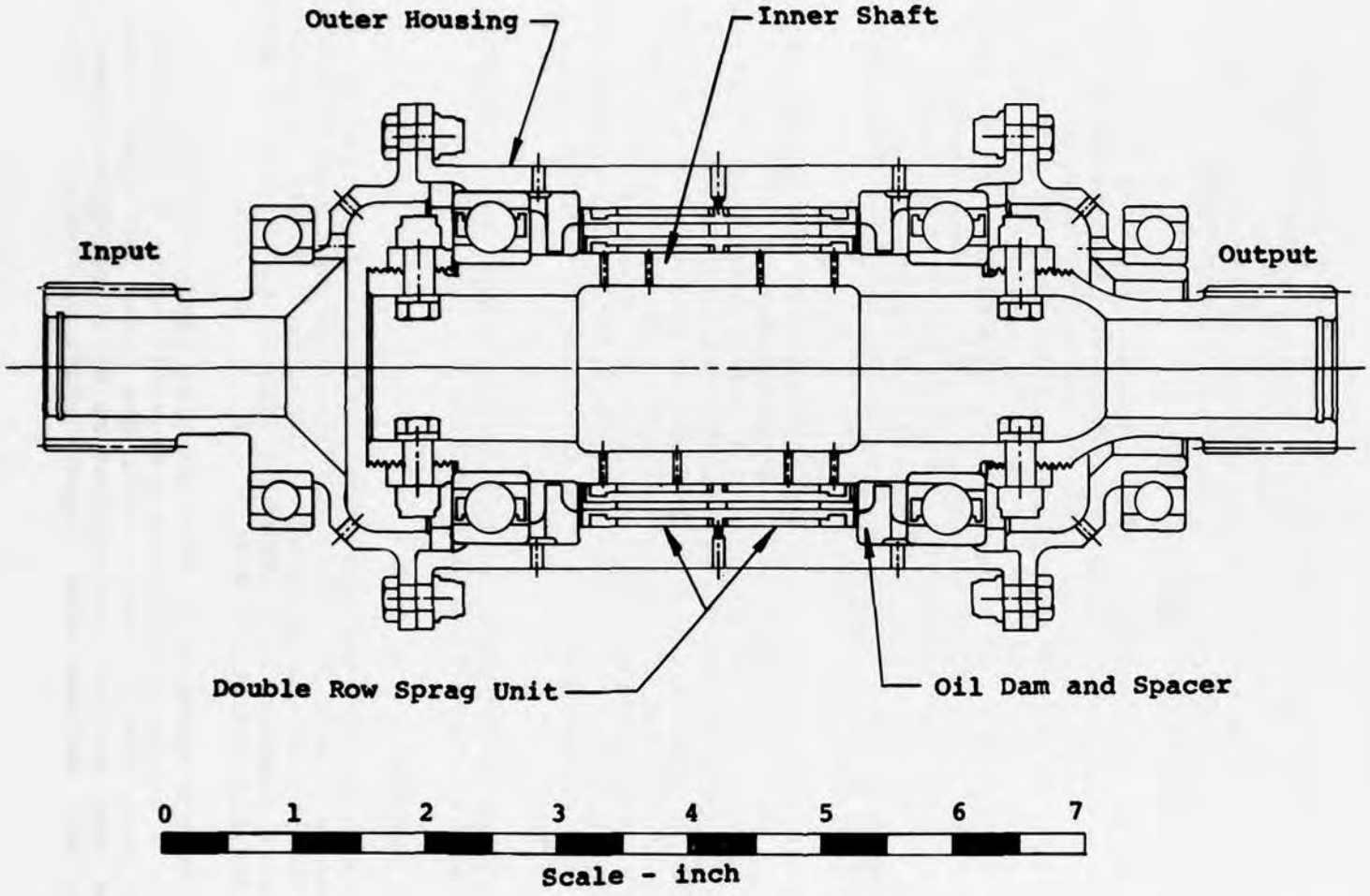

Figure 30. Sprag Clutch Design, Cross Section.

Figure 31. Sprag Clutch Components.

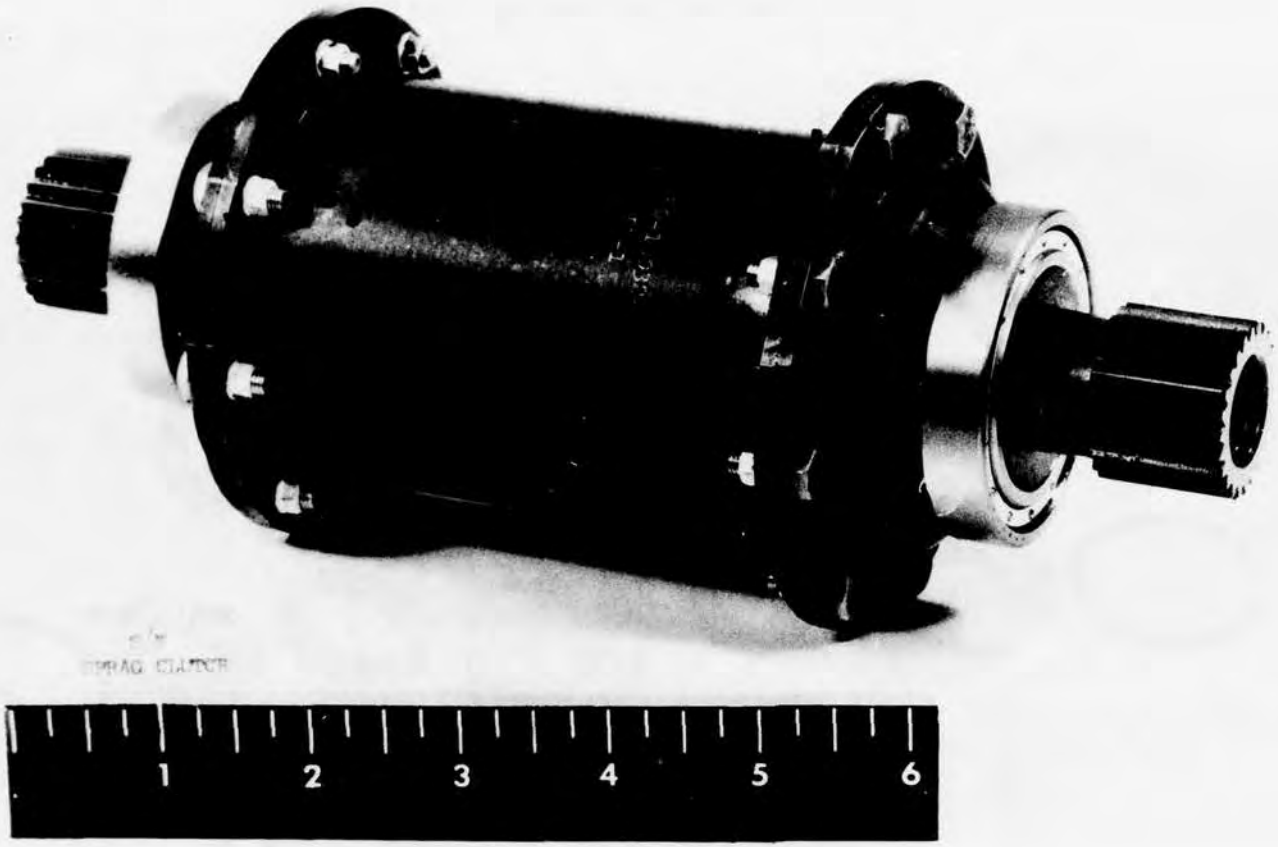

Figure 32. Sprag Clutch.

drag torque that exceeds the frictional torque created during overrunning on the inner race. During overrunning, relative motion occurs only on the inner race where the velocity is lower and also centrifugal effects on the sprags are reduced (sprags are stationary during full-speed overrunning).

The outer housing is designed to withstand the hoop tensions created by the loads acting perpendicular to the sprag contact points during torque application. Since these loads also produce high Hertzian stresses between the sprags and the housing, the outer housing must have a hardened surface. Generally, the sprag clutch's outer housing is manufactured from a case-carburized steel, such as AMS 6260 (SAE 9310), heat-treated to Rockwell C-58 to 64 case hardness with a core hardness of Rockwell C-30 to 45.

The inner shaft of the sprag clutch provides a wear surface for the clutch during overrunning. The inner shaft is designed to react the compressive stresses produced by the loads acting perpendicular to the inner cam surface whenever torque is applied. Low-cycle (GAG) stresses are considered in the design of both the inner shaft and the outer housing.

The lubricant for the sprag unit is fed to the center of the output shaft. Since this shaft is always rotating, centrifugal force causes the lubricant to flow outward to the sprag area and the outer race. A dam arrangement, located on each side of the sprag unit, is used on the outer shaft. The diameter of the inner lip of each of the dams is smaller than the diameter of the inner race; thus, when the outer race rotates, the entire sprag area between the races is flooded with oil, assuring that a film of oil exists between the sprags and the inner race.

The sprag unit itself is comprised of two cages, the sprags, and various friction strips and bands. The sprags are manufactured from bearing tool steel SAE HTB-2, M50, or AMS 6490. The nitriding diffusion process is used to increase the sprag's surface hardness to Rockwell C77, forming a hard wear surface. The cages generally used in aircraft sprag units and those used in this program are fabricated from bar or tube stock, such as SAE 4340 steel with broached pockets. This type of cage design is superior to the deep-draw, flat-steel type, which is often used in commercial applications.

Because of the specialized nature of the fabrication and design process of the sprag unit itself, it is usually cost-effective to purchase these items from companies who specialize in their design and manufacture rather than attempting to fabricate them in-house.

A complete description of the sprag clutch used in this program, as well as a detailed structural analysis, can be found in Reference 1.

RAMP-ROLLER CLUTCH

The ramp-roller clutch configuration used in this program is shown in Figure 33. The individual components are shown in Figure 34, while the assembled clutch is shown in Figure 35.

The input member for the high-speed ramp-roller clutch of this program was the cam shaft. For high-speed roller clutches, the cam should be the input to reduce centrifugal effects on the rollers since the cam and rollers will be at rest during full-speed overrun. The function of the cam shaft is to transmit torque from the input spline to the cam flats, whereupon the rollers transfer the load to the outer housing. For purposes of load sharing in the ramp-roller clutch, the geometry of the cam shaft must be very closely controlled during manufacture. Generally, the dimension across the flats is held to $\pm$.0005 inch with tight control of angular tolerance from one flat to the next. The cam of an aircraft ramp-roller clutch is manufactured as an equillateral polygon with N sides, N being equal to the number of rollers.

Commercial units have been designed with undercut flats; however, tolerance control is difficult since grinding must be done in the axial direction as opposed to the tangential across-the-flat grinding of the aircraft-type cam design.

The function of the cage of the ramp-roller clutch is to hold all the rollers in alignment during overrunning and to keep the rollers in contact with the outer housing and the cam flats. In aircraft clutches, this is accomplished with a pin and spring mechanism that applies a load to the carrier in the tangential direction. A pin in a closely fitting hole is used with a compression spring so that the spring is totally enclosed in the pin and spring hole. Centrifugal forces on the spring will not create distortions, such as might be present were the spring free to translate. Care must be taken in the design of the pin and spring mechanism to insure that the total pin load will not become excessive or, in the opposite case, will not decrease or even become zero under the influence of centrifugal force.

The outer housing of the ramp-roller clutch transmits the roller loads through the housing and out of the clutch. The housing is designed to withstand the hoop tensions created by the normal component of the roller loads during torque transmittal. Low-cycle fatigue (GAG) stresses are considered.

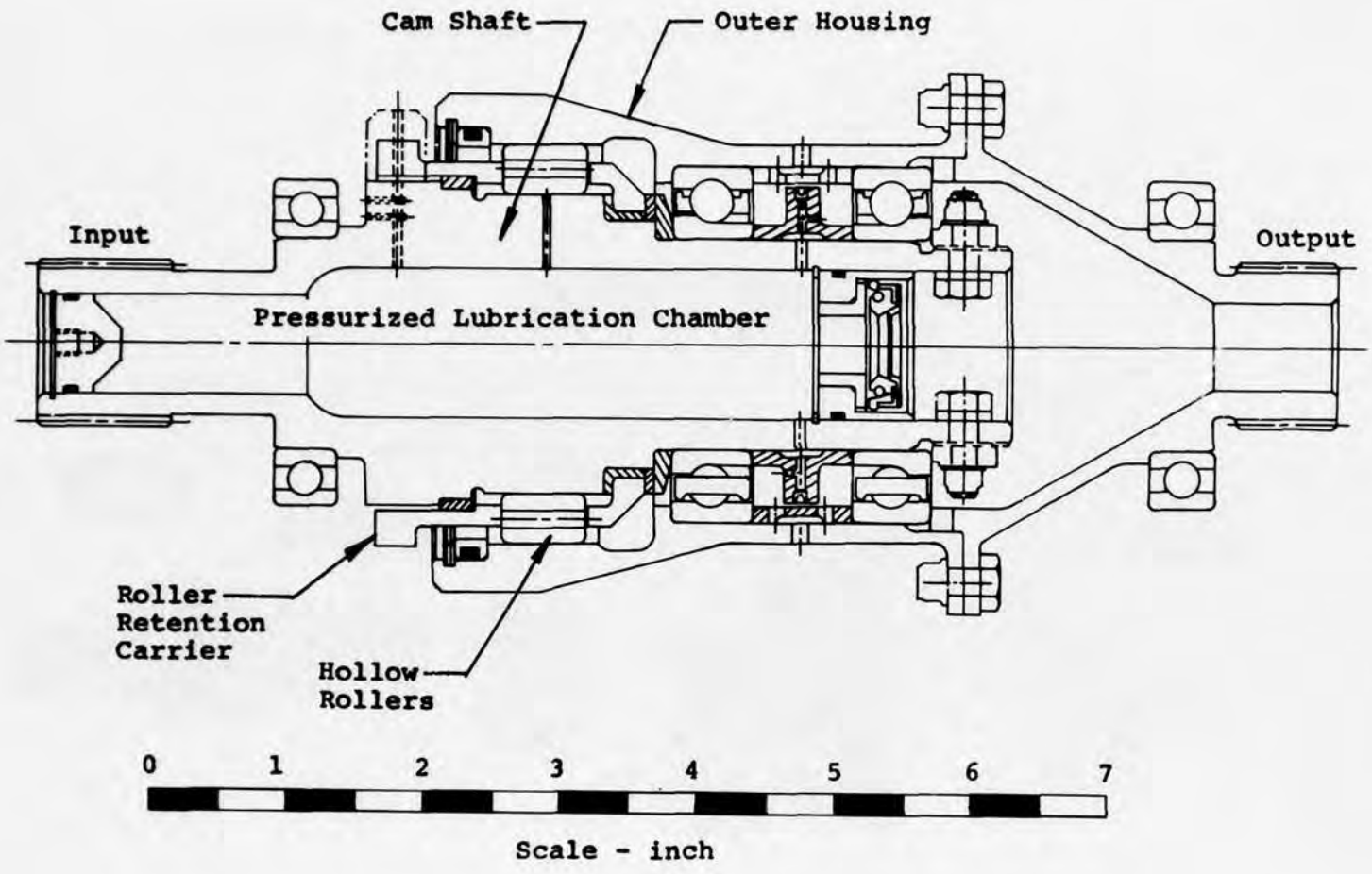

Figure 33. Ramp-Roller Clutch Design, Cross Section.

Figure 34. Ramp Roller Clutch Components.

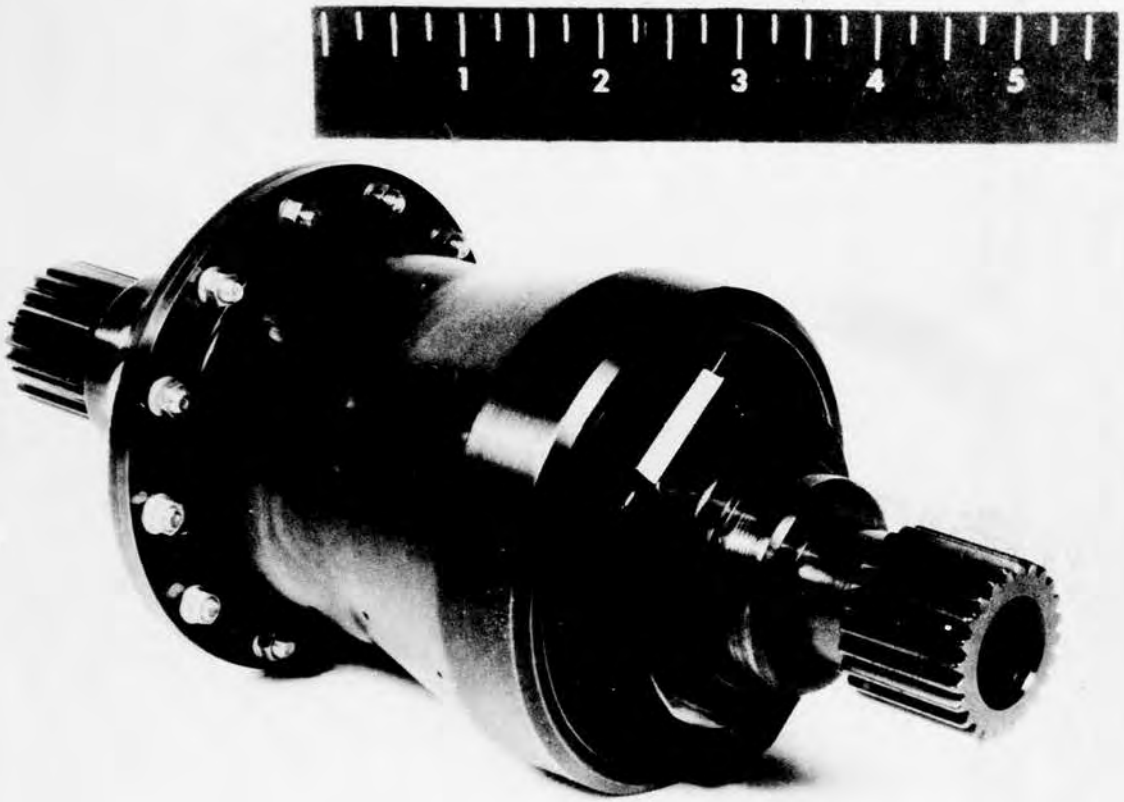

Figure 35. Ramp Roller Clutch.

Both the cam and the outer housing must withstand the sliding, rolling, and scuffing of the rollers during overrun. A very hard, smooth surface is therefore required to keep wear to a minimum. The roller clutch is also usually designed for Hertz stress between the rollers and the outer housing and between the rollers and the cam flats. The high Hertz stresses produced also require a hard surface. For these reasons, the outer housing and the cam shaft are generally manufactured from SAE 9310 case-carburized steels and are heat-treated to Rockwell C58 minimum case hardness with a very deep case depth (.050 min).

A complete description of the ramp-roller clutch design as well as a detailed structural analysis can be found in Reference 1.

TEST FACILITY

OVERRUN

The twin steam-turbine test facility used in this program was successfully used in Contract DAAJ02-71-C-0028, Sprag Overriding Aircraft Clutch (see Reference 3) and in Contract DAAJ02-71-C-0035, Spring Overriding Aircraft Clutch (see Reference 2). Figure 36 is a cross-sectional layout showing the major components of the overrun facility. The facility employs two independently controlled 100-horsepower, 30,000-rpm steam-turbine prime movers with speed-increasing gearboxes at the turbine outputs. The first turbine drives the clutch input shaft, while the second drives the clutch output shaft. A pad is provided on each speed increaser to accommodate slip-ring assemblies that transmit data from the rotating shafts. The turbines are mounted on a movable bed and can be adjusted in the axial direction. The rig is designed so that, after the initial assembly, the clutch test cartridge may be removed without disturbing either of the support test stands. This arrangement assures consistent alignment after disassembly and reassembly for each test clutch and rapid turnaround between tests. The test rig installation is shown in Figure 37.

STATIC

The test rig installation shown in Figure 38 was used for both the cyclic fatigue and static overload tests. The facility employs an electrohydraulic, servo-controlled, rotary actuator system for loading. Test frequency for cyclic loading is 10 cycles per second using sine-wave excitation. Torque is applied through an adapter spline bolted to the clutch input shaft. The load is reacted through a torque sensor that is bolted to an adapter and splined to the clutch output shaft. Torque readouts are observed with an oscilloscope, a digital voltmeter, and a load amplitude measurement system. The clutch is precisely aligned by applying torque through the system and making the necessary adjustments until the readings of the strain gages located about the test clutch outer housing are in balance.

A listing of government-furnished equipment is presented in Table 20.

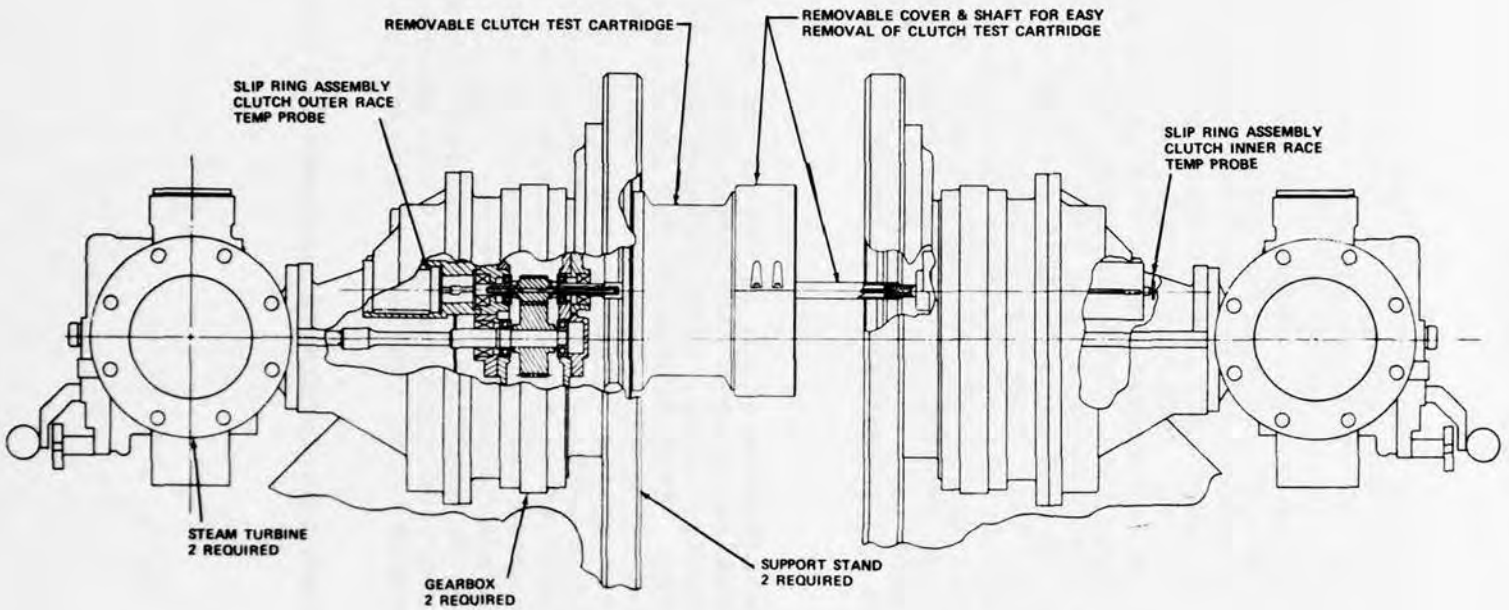

Figure 36. Steam Turbine Test Rig Arrangement, Overrunning Facility.

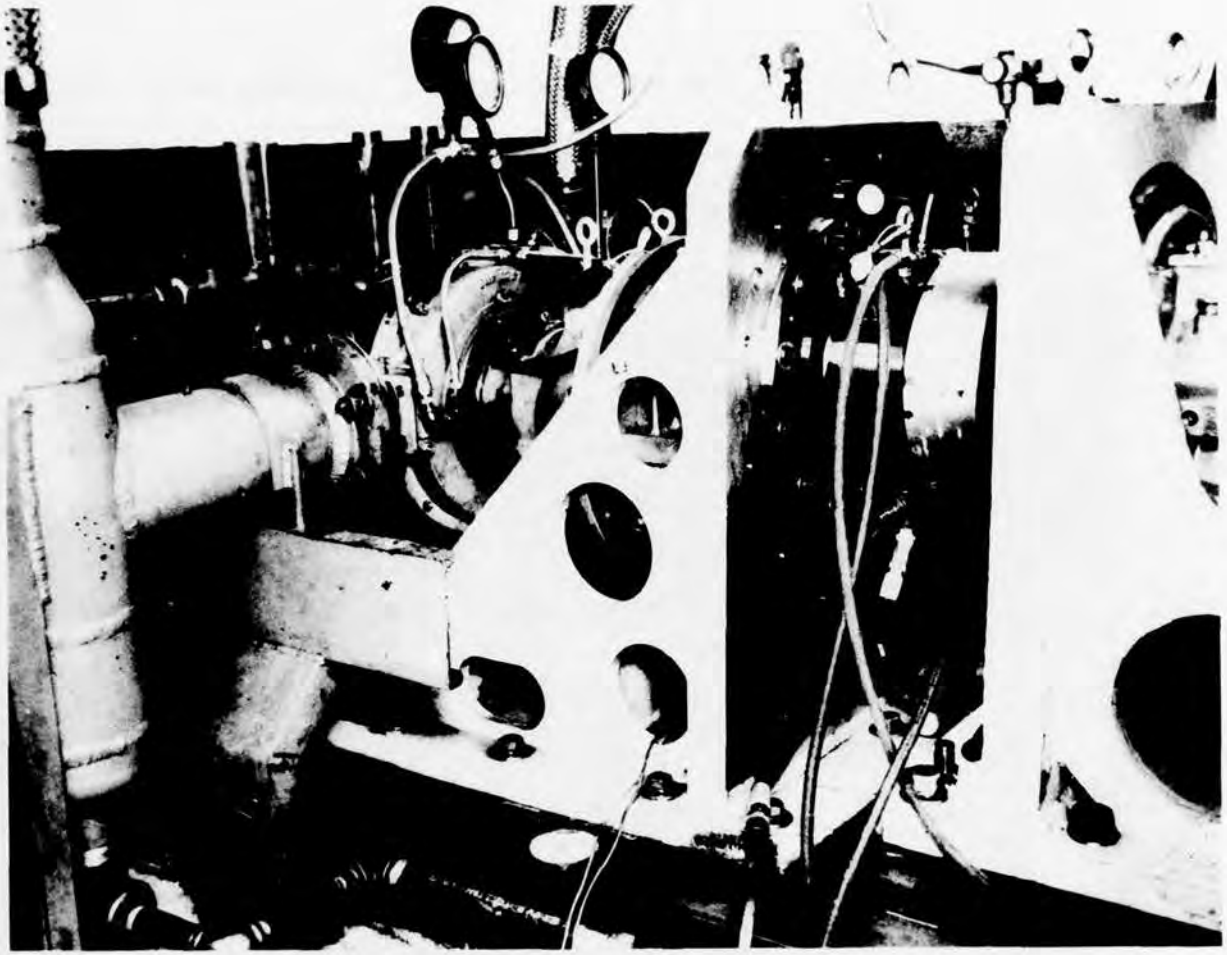

Figure 37. Steam Turbine Test Rig Installation.

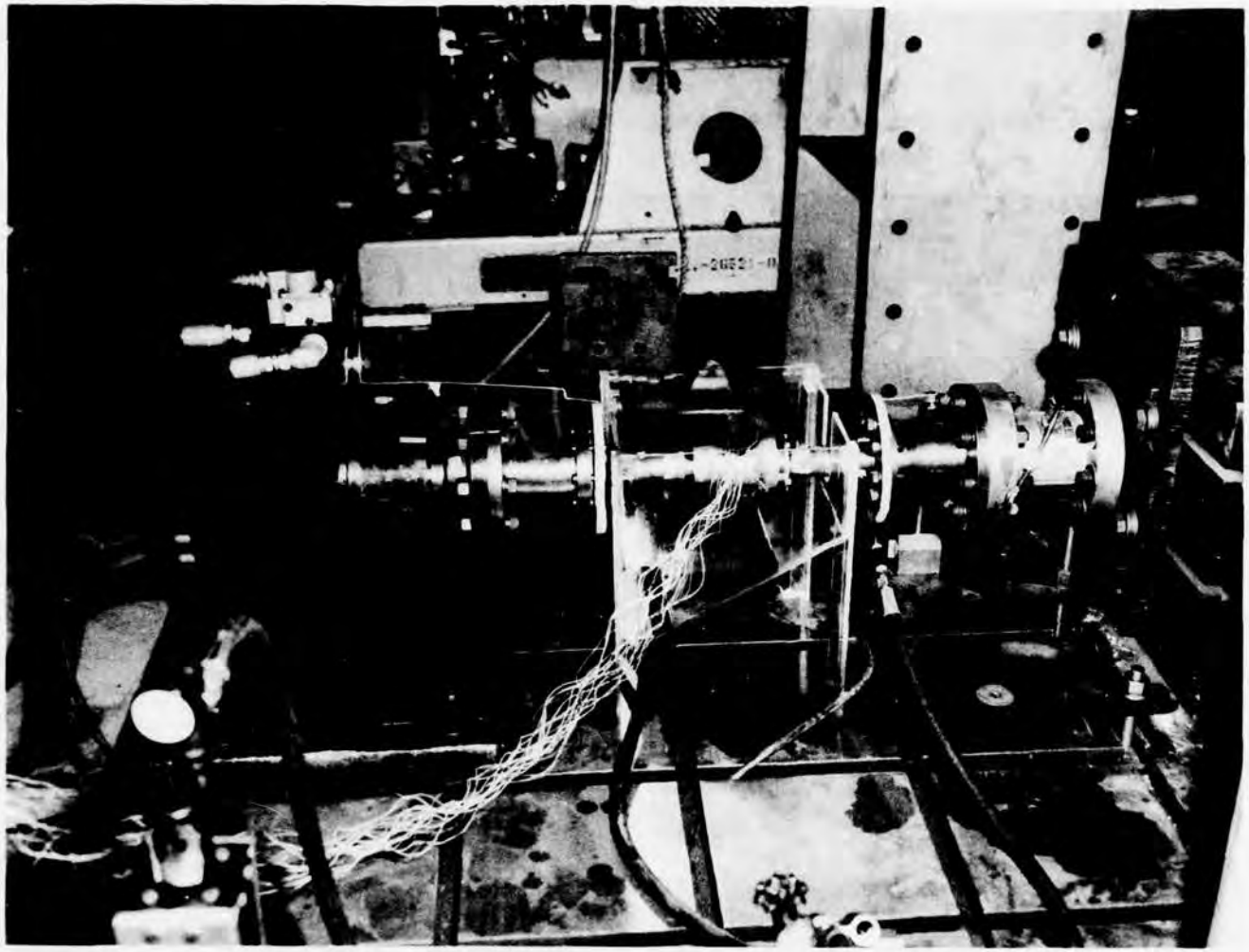

Figure 38. Test Facility for Cyclic Load and Static Testing.

TABLE 20. GOVERNMENT-FURNISHED TEST EQUIPMENT		
STE No.	Description	Quantity
1058-9	Barber-Stockwell Steam Turbine	1
1059-9	Barber-Stockwell Steam Turbine	1
1058-53	Walters Gearboxes	2
1158	Clutch Test Rig	1
1076	MTS Actuator and Lebow Torque Transducer	1

TURBINE

The test rig shown in Figure 39 is used for dynamic load, environmental, and dynamic cyclic fatigue testing. This facility uses a T53 gas-turbine engine to drive the clutch. The clutch output shaft is splined to a flywheel and a waterbrake in series. The flywheel-waterbrake combination is designed to simulate helicopter inertia and load-absorption characteristics.

The T53 model gas turbine is a high-speed engine capable of 1500 horsepower at 20,000 rpm output speed. The waterbrake is a standard Model 1800, which incorporates its own torquemeter. Clutch turnaround is accomplished by removing the flywheel and the waterbrake assemblies as a unit from the support stand. The test clutch cartridge can then be removed. This arrangement minimizes the need for realignment between clutch cartridge replacements. The assembled test rig is shown in Figure 40.

The flywheel of the turbine facility was designed with a moment of inertia of 5373 pound-inch^2. This inertia simulates the UTTAS's blades, rotor head, and transmission system reflected to the engine speed by the ratio squared. Thus, the turbine facility not only simulates the power and the torque transmission of the freewheel unit, but also simulates the helicopter drive train inertia as felt by the clutch. The turbine facility has the capability of testing the overrunning clutch in ground operation, such as start up, full-speed overrun, differential-speed overrun, high-speed engagements and disengagements, high-temperature environment, low-temperature environment, and cyclic torsional loading, as well as flight load simulation up to the full clutch rating.

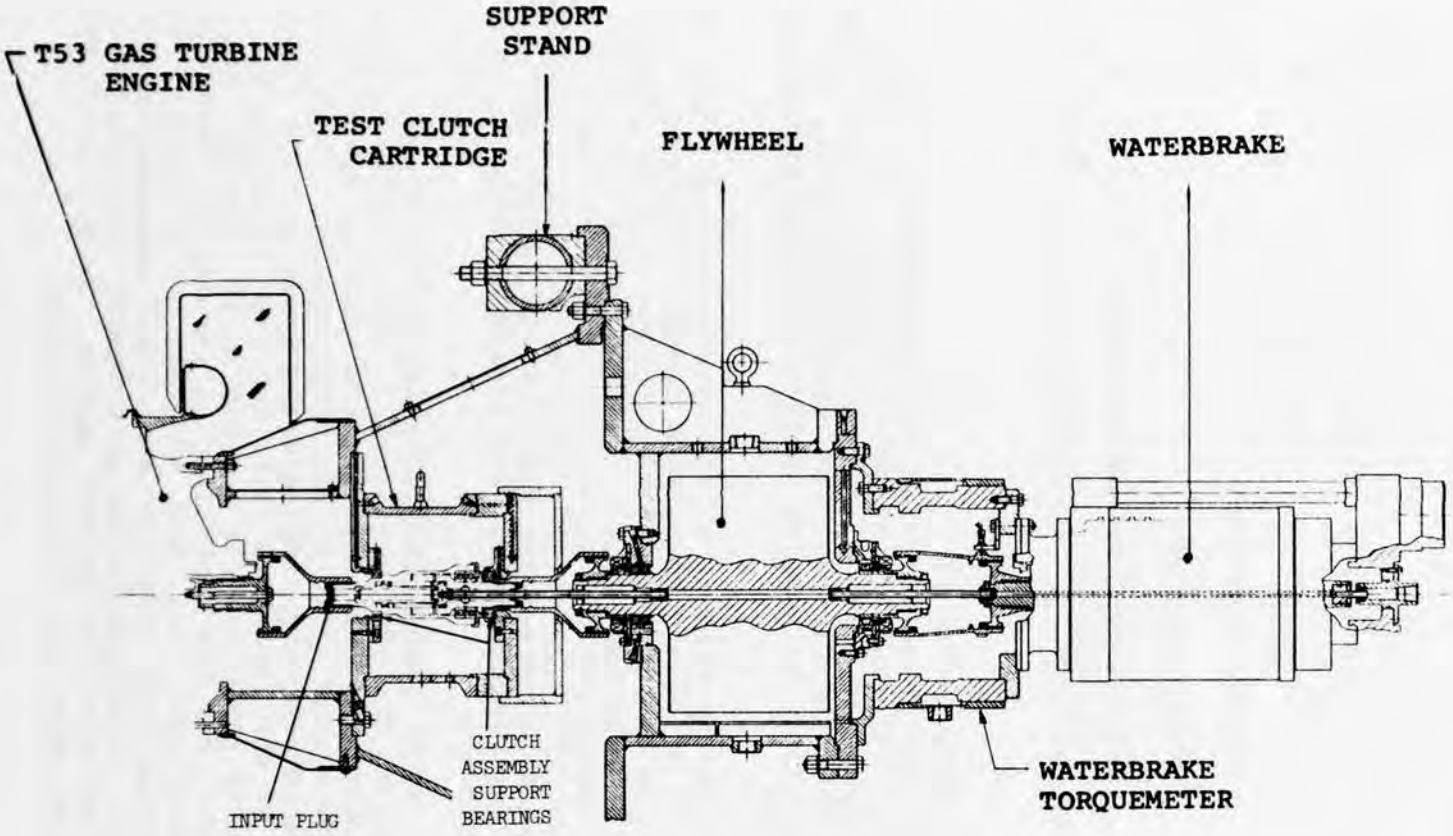

Figure 39. Power Turbine Test Rig Arrangement.

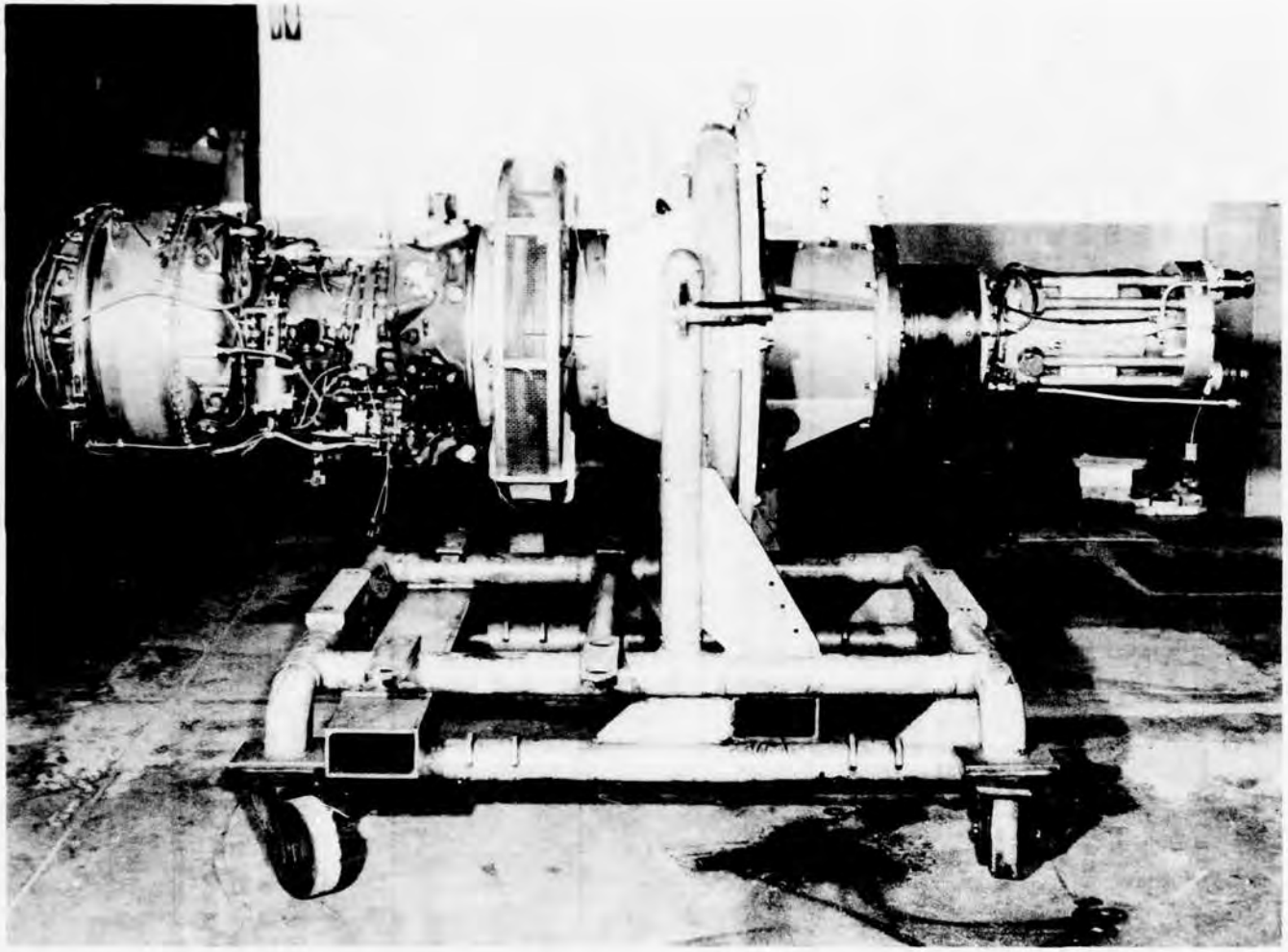

Figure 40. Power Turbine Test Rig Assembly.

FACILITY LUBRICATION

The oil used for this program was MIL-L-7808 with a maximum inlet pressure of 100 psig. Temperature of the oil was kept between 190°F and 210°F except for the environmental tests, where oil sump temperatures were 300°F and 0°F, and the static load tests, where oil was at room temperature. An optimum oil flow rate of 0.8 gpm established during the overrun (no-load) tests was selected for each of the clutch candidates as the 100% design flow. This flow rate was used throughout the program except for the static overload test where the clutch cartridges were wetted during assembly. The 0.8-gpm flow rate was for oil entering the clutch cartridge, which for all designs was through the inner race. Centrifugal force or pressure then distributed the oil to lubricate the working clutch components and clutch support bearings. For all test rigs, the designed distribution of the oil flow within the clutch was as shown in Table 21.

TABLE 21. FLOW TO TEST CLUTCHES

Clutch Type	% Oil Distribution* Working Components (Sprags, Spring and Rollers)	Clutch Support Bearings
Sprag	100	100**
Spring	75	25
Roller	83	17

Notes:

* 100% = 0.8 gpm.

** All of the oil lubricates the sprags first and then goes on to lubricate the clutch support bearings.

The oil flow path for the spring clutch used in the overrunning facility is shown in Figure 41. Oil enters the clutch cartridge from the output side where two small-diameter oil holes meter the flow between and through the back-to-back bearings. Lubrication and cooling paths at the energizing-coil end of the spring are provided by reliefs in the face and the outside diameter of the output spacer and by grooves in the end coils of the spring. The oil exits through holes in the output and input shafts. The arbor has a blind hole at the input end, and the torquemeter shaft coupling has strain gage and temperature sensing wires running through it at the output end, which prevents oil from escaping. This configuration was used for most of the Task I testing of the spring clutch.

The final configuration of the spring clutch, shown in Figure 42, was used for the last part of Task I and all of Task II testing. In Figure 42, holes in the transfer tube at the output end of the arbor meter oil to the duplex bearings and the spring. During overrunning, the input shaft, which contains the oil transfer tube, is not rotating so the oil is forced to flow under pressure. Once it leaves the metering holes, centrifugal force due to the output shaft's rotation causes the oil to flow through the spring and back-to-back bearings.

The lubrication schematic for the steam turbine test rig is shown in Figure 43. Oil was introduced from the input side of the clutch because the existing slip-ring equipment for measuring drag torque was coupled to the output side of the clutch. The wire exits from holes in the torquemeter shaft adapter, which also acts as a plug to prevent oil from escaping. For each configuration, oil enters the clutch from the input side, where O-rings prevent leakage past the input spline couplings.

In the sprag clutch, Figure 44, oil enters the output shaft where it is retained by the centrifugal dam at one end and at the torquemeter shaft adapter at the other end. Holes in the output shaft allow the oil, which is subject to centrifugal force, to enter the clutch chamber, where it is captured by the oil dams. Small drain holes in the outer race allow a metered amount of oil to escape, providing a continuous turnaround of oil in the chamber to dissipate heat. This arrangement also reduces sludge buildup. Scavenge ports, located in the outer race, drain some of the remaining oil, which escapes past the dams. The remainder of the oil lubricates the clutch support bearings. Therefore, the total amount of oil entering the clutch cartridge, 0.8 gpm, goes directly to lubricate the sprags.

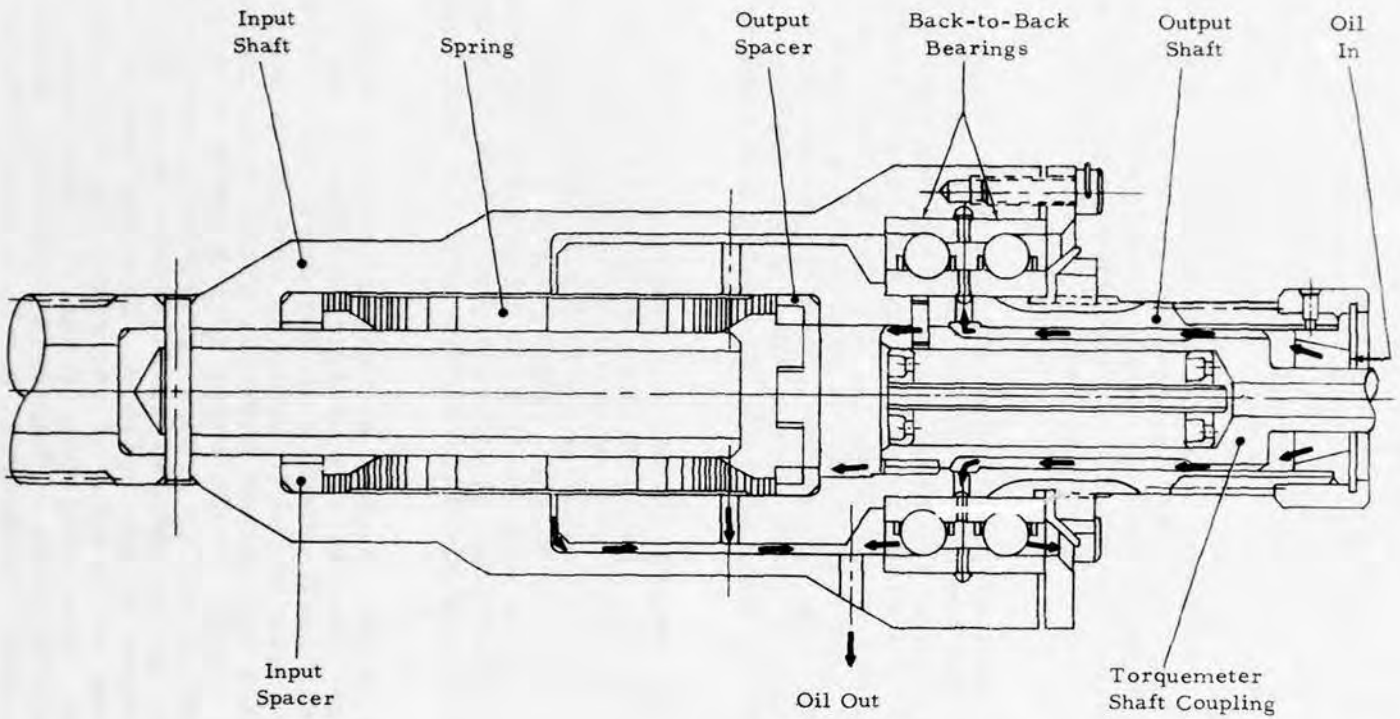

Figure 41. Initial Oil Flow Path Configuration in the Spring Clutch When Used on the Steam Turbine Test Rig.

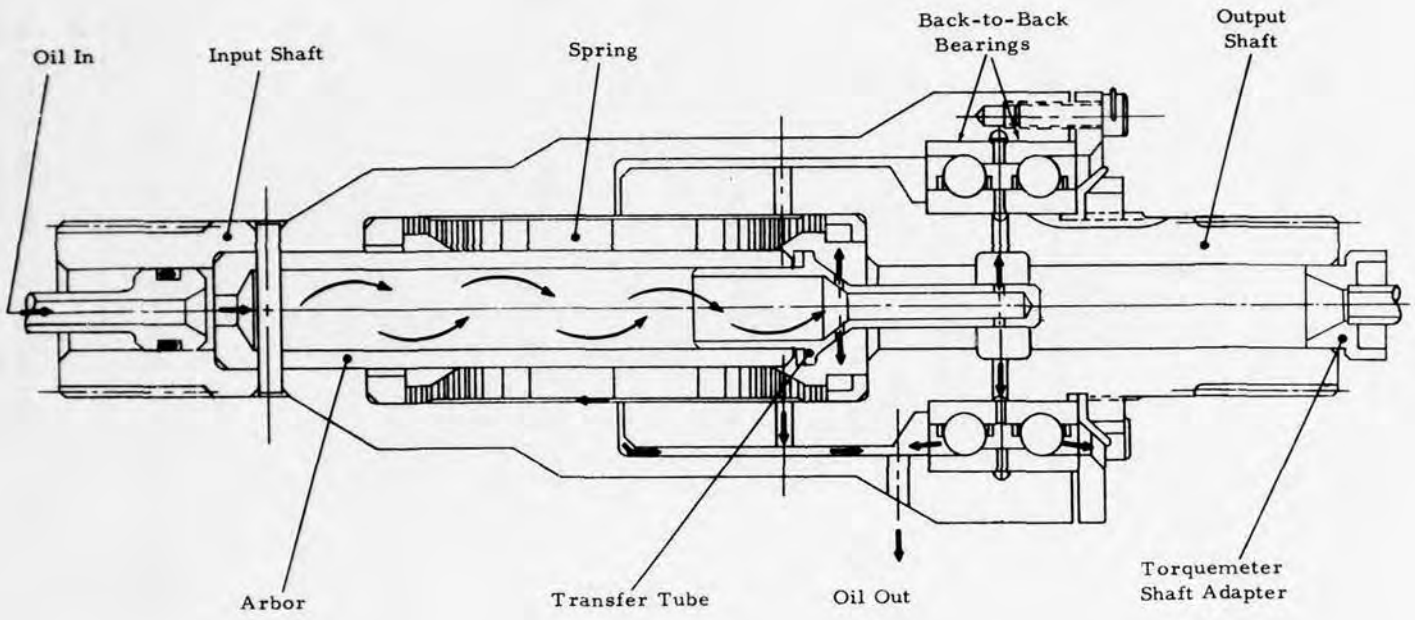

Figure 42. Final Configuration of the Spring Clutch's Oil Flow Path When Used With the Steam Turbine Test Rig.

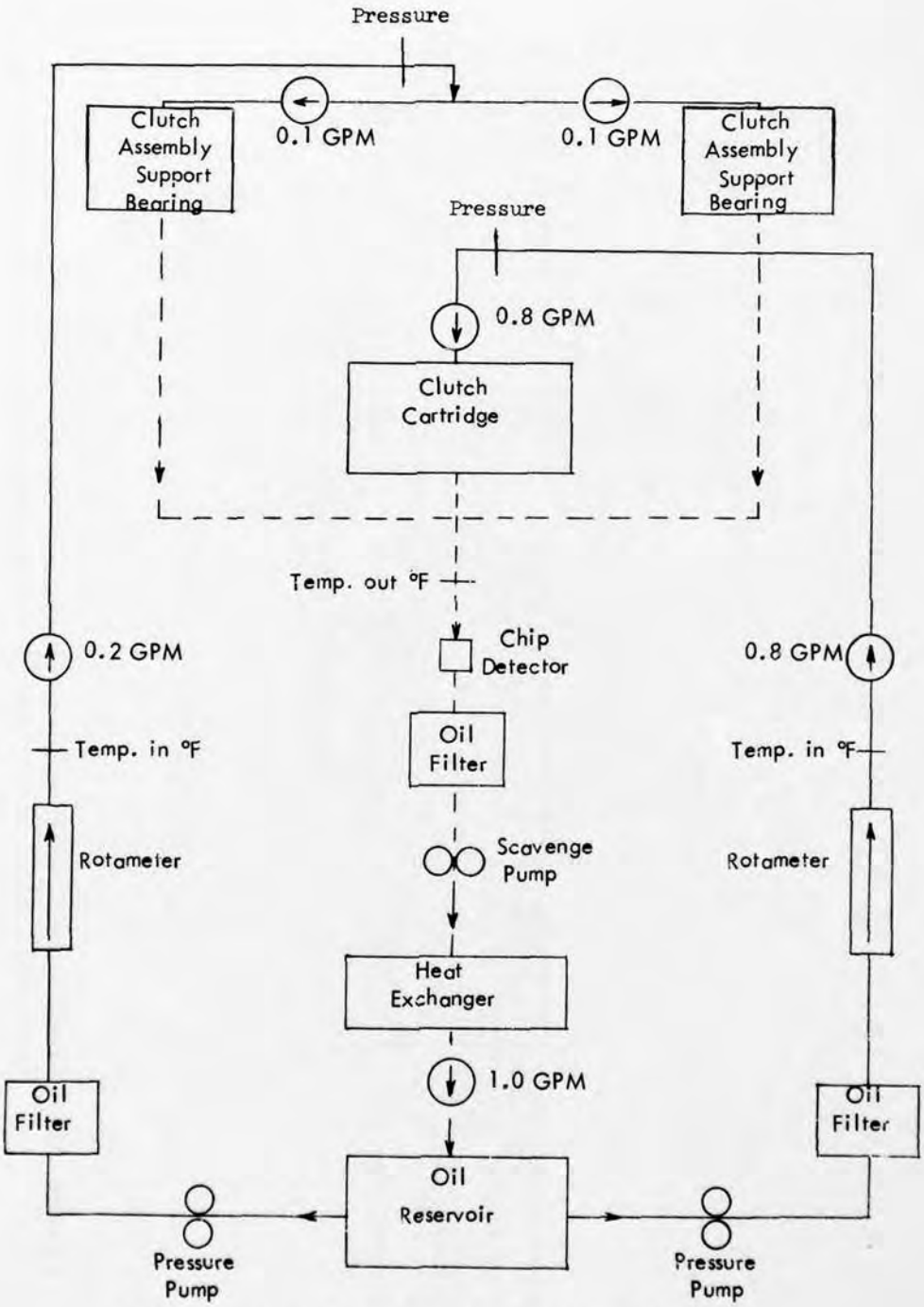

Figure 43. Lubrication Schematic for the Steam Turbine Test Rig.

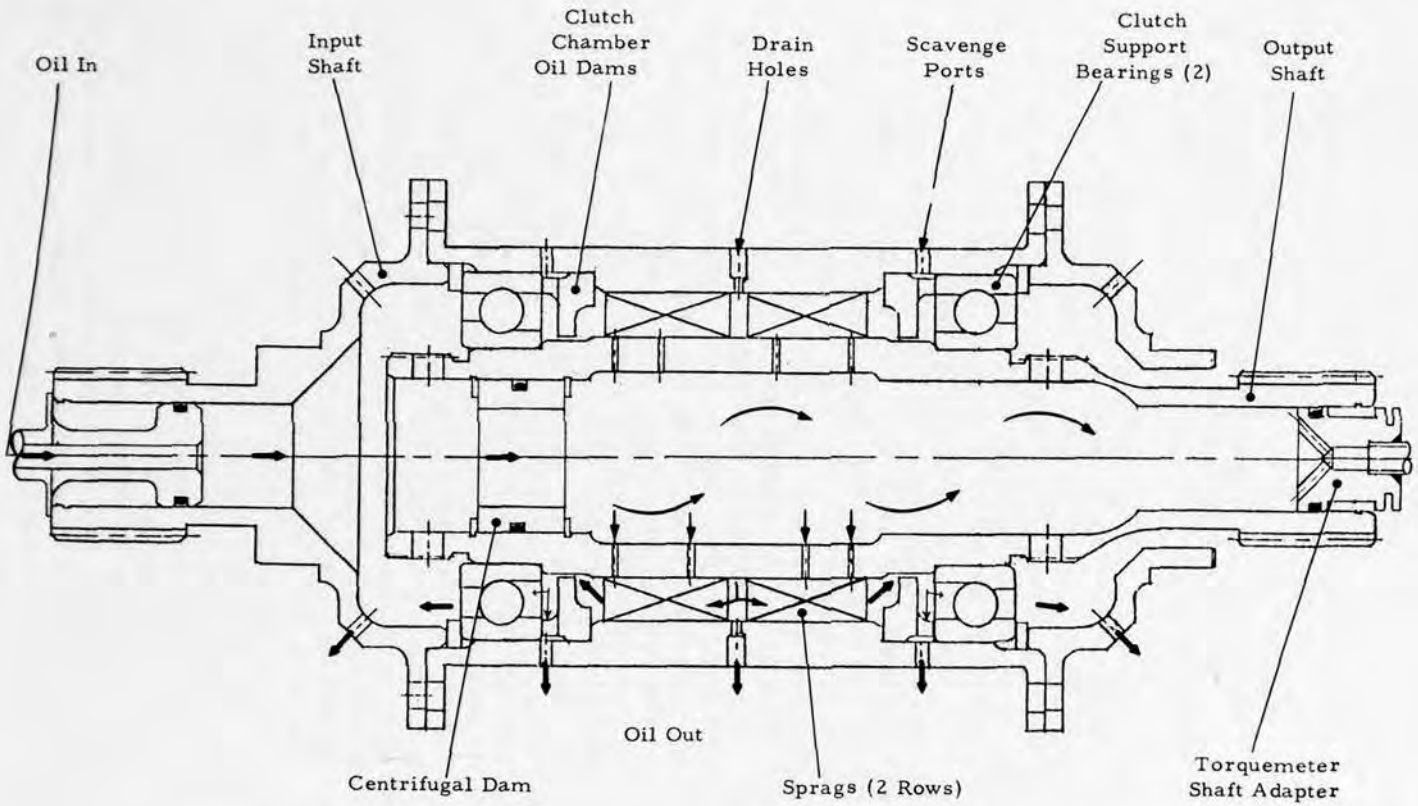

Figure 44. The Oil Flow Path in the Sprag Clutch When Used With the Steam Turbine Test Rig.

The lubrication path for the ramp-roller clutch is shown in Figure 45. The oil plug provides for chamber pressurization since the input shaft is stationary during overrunning. Holes in the input shaft allow the oil to leave the pressurized chamber, lubricating the rollers and clutch bearings. The oil dam maintains a film of oil at the interface of the rollers with the output shaft. Oil is metered to the clutch bearings by jets in the matched set of spacers located between the bearings. Oil exits from the input side of the clutch cartridge and through holes in the output shaft assembly.

The lubrication schematic for the power turbine test facility is depicted in Figure 46. A pressurized manifold is used to distribute oil through trunk lines to the flywheel bearings, the coupling shaft splines, the clutch cartridge, and the clutch assembly support bearings. The gas turbine engine is coupled to the input side of the rig as shown. This arrangement dictated that the flow of oil in the lubrication system had to be from output to input. Oil enters the rig at the open end of the waterbrake and follows a path along the centerline of the test rig through the waterbrake and the flywheel and into the clutch housing. The oil is metered along the way to lubricate the input and the output flywheel spline couplings. By design, oil enters each of the three clutch cartridges at 1.43 gpm through the oil transfer tube, as shown in Figures 47 through 49 for the spring, sprag, and ramp-roller clutches, respectively. This tube transfers oil to the clutches in the same manner as described for the steam turbine test rig at the rate of 0.8 gpm. A hole at the left end of each tube also provides oil to lubricate the engine to clutch-cartridge spline-coupling shafts. The input plugs in Figures 47 through 49 act as bumpers to provide axial positioning of the spline shafts and direct oil to lubricate the spline couplings. The centrifugal dams in Figures 47 and 48 serve to keep oil flowing to the coupling splines and prevent it from flowing back into the clutch. In Figure 49, the dam is closed off at the left end. Some of the oil flows through the metering holes to lubricate the spline couplings, while the remainder flows over the dam to lubricate the rollers. In Figure 47, the oil transfer tube is supported solely in the output shaft. In Figure 48, the tube is again supported in the output shaft by the manifold supports. In Figure 49, however, the tube must be supported by both the input and the output shafts. The tube is semifixed at the right end so that it will rotate at the same speed as the output shaft. At the left end, the tube is supported by a bearing and seal arrangement that provides for uniform rotation during the differential mode of operation when the input and the output shafts are rotating at different speeds.

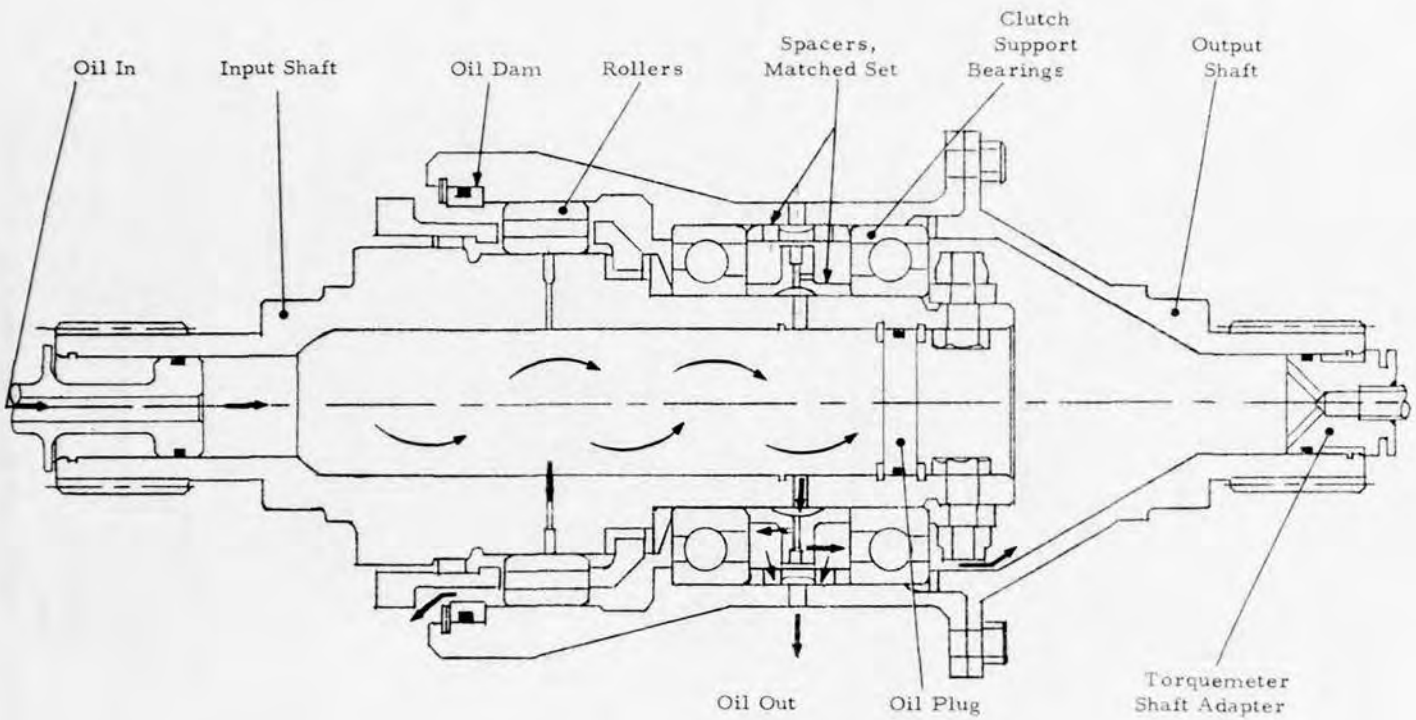

Figure 45. Oil Flow Path of the Ramp-Roller Clutch When Used With the Steam Turbine Test Rig.

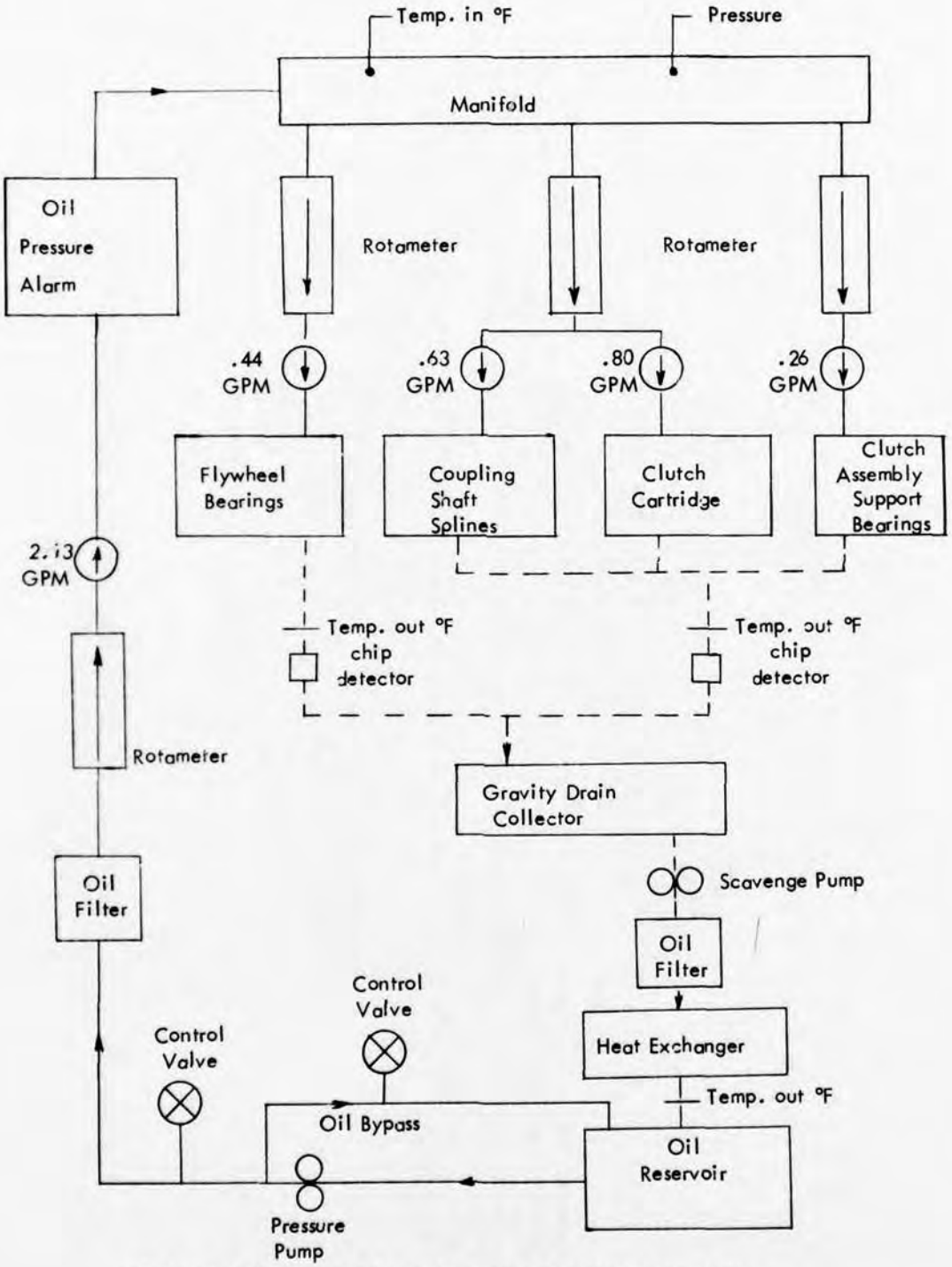

Figure 46. Lubrication Schematic of the Power Turbine Test Rig.

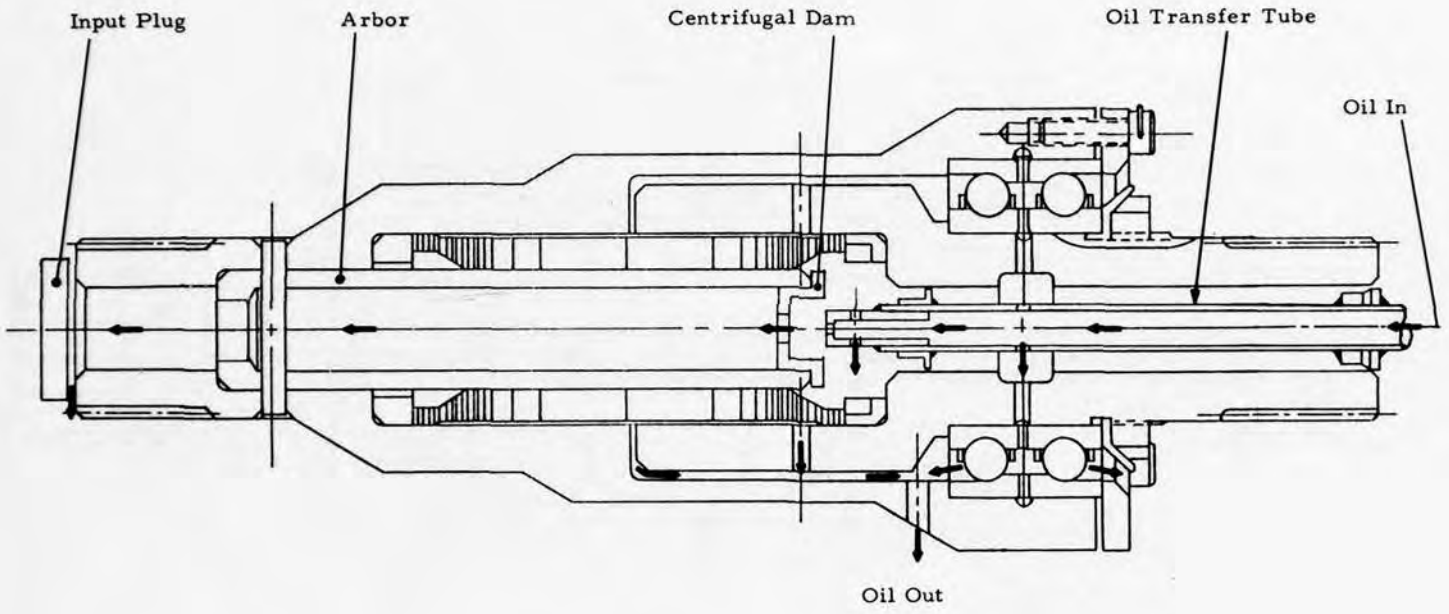

Figure 47. Oil Flow Path in the Spring Clutch When Used With the Power Turbine Test Rig.

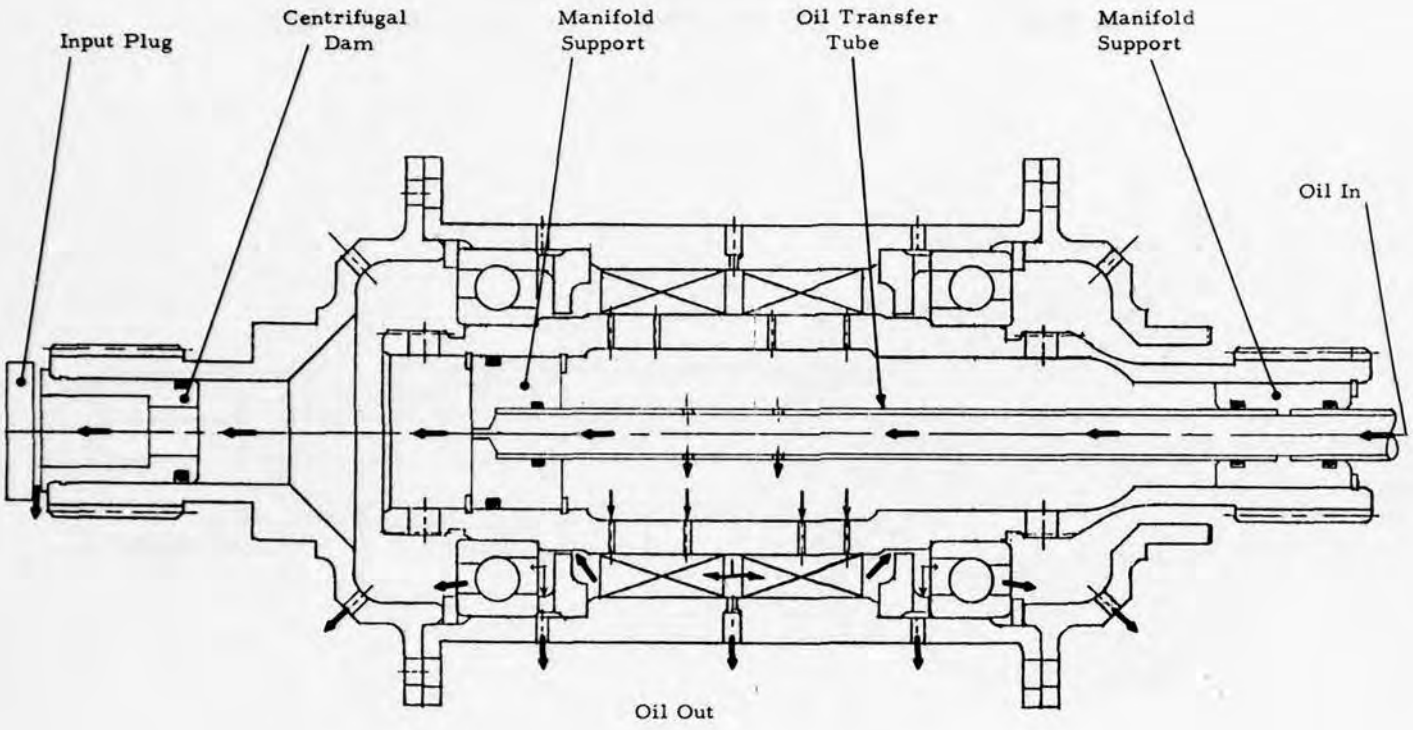

Figure 48. Oil Flow Path in the Sprag Clutch When Used With the Power Turbine Test Rig.

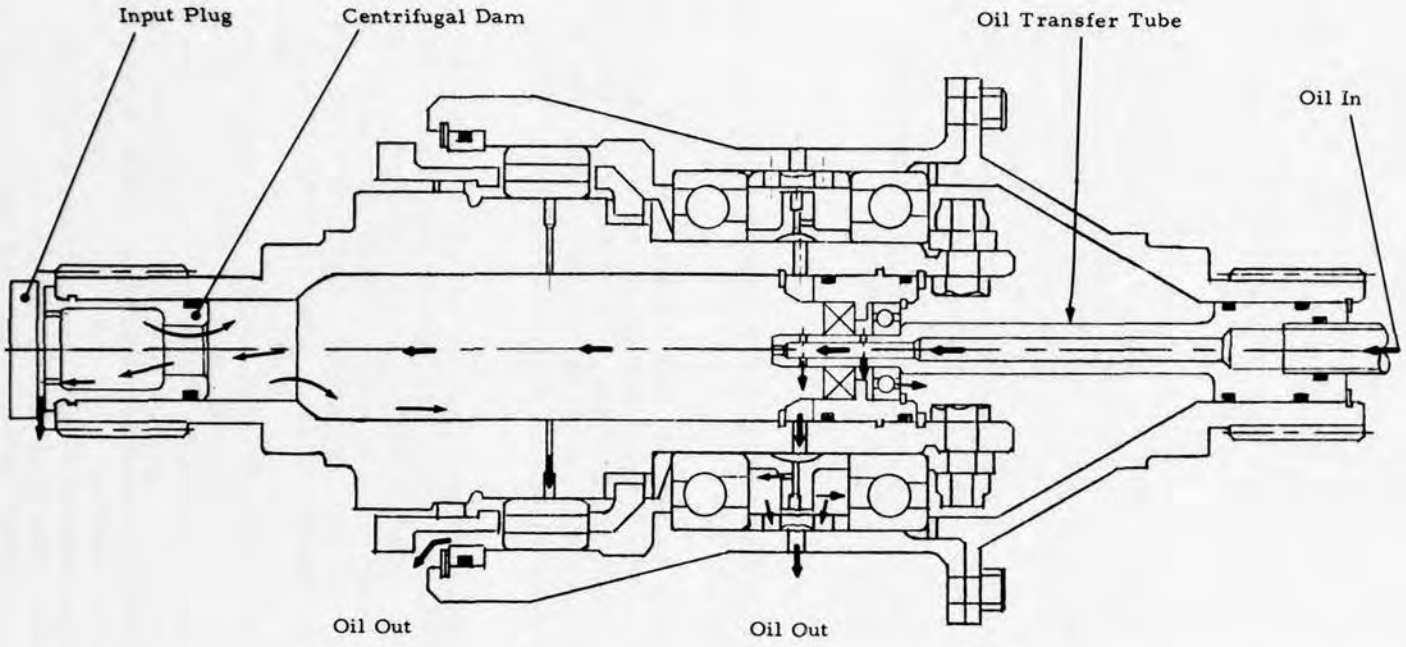

Figure 49. Oil Flow Path in the Ramp-Roller Clutch When Used With the Power Turbine Test Rig.

The lubrication schematic for the static test facility is shown in Figure 50. Standard hydraulic equipment, such as a rotameter, a pressure gage, and control valves, are used to monitor and control the system. The arrangement circulates the room temperature oil at a rate of 0.8 gpm in a closed-loop circuit. The facility had provisions for detecting metal chips and filtering the oil. A malfunction in the MTS unit, such as a change in torque or an indication of a metal chip, would unload the system and stop the test.

The oil flow path for a typical installation is shown in Figure 51. Oil enters the rig through the oil transfer tube located inside the output shaft, which is sealed with an O-ring to prevent leakage. The other end of the shaft is sealed with an oil plug. The pressurized oil flows outward through holes in the output shaft to lubricate the clutch. The clutch assembly is completely enclosed between input and output adapters by a plastic casing, as shown in Figure 38. The oil collects in the bottom of the casing where it is recirculated through the rig by the pressure pump. All three clutches are lubricated in this manner.

INSTRUMENTATION

The measurements taken during the tests of this program are summarized in Table 22.

Speed measurements taken on the steam turbine (overrunning) facility were recorded from magnetic pickups mounted directly onto the steam turbine shafts. In the power turbine stand, input speed measurements were monitored from the engine tachometer pad, while output speed was measured directly from the waterbrake.

Temperature measurements were taken with thermocouples mounted at various positions. The oil reservoir temperature was also monitored in the power turbine test facility. During static cyclic-load testing on the static test facility, oil temperature monitoring was not required, and the test was conducted with oil at room temperature. During overrunning, the highest temperature for each clutch occurs in the area where the sliding is maximum between the shaft and the clutch component. For all clutches, this point is on the output shaft since this is the shaft that is always rotating during freewheeling. In the spring clutch, the tip of the thermocouple pickup was set .030 inch from the output shaft surface where the teaser coils ride during overrun. In the sprag clutch, the thermocouple wires were embedded in the output shaft and were located .030 inch from the inner shaft O.D. (clutch race) in the overrunning sliding area. In the ramp-roller clutch, the

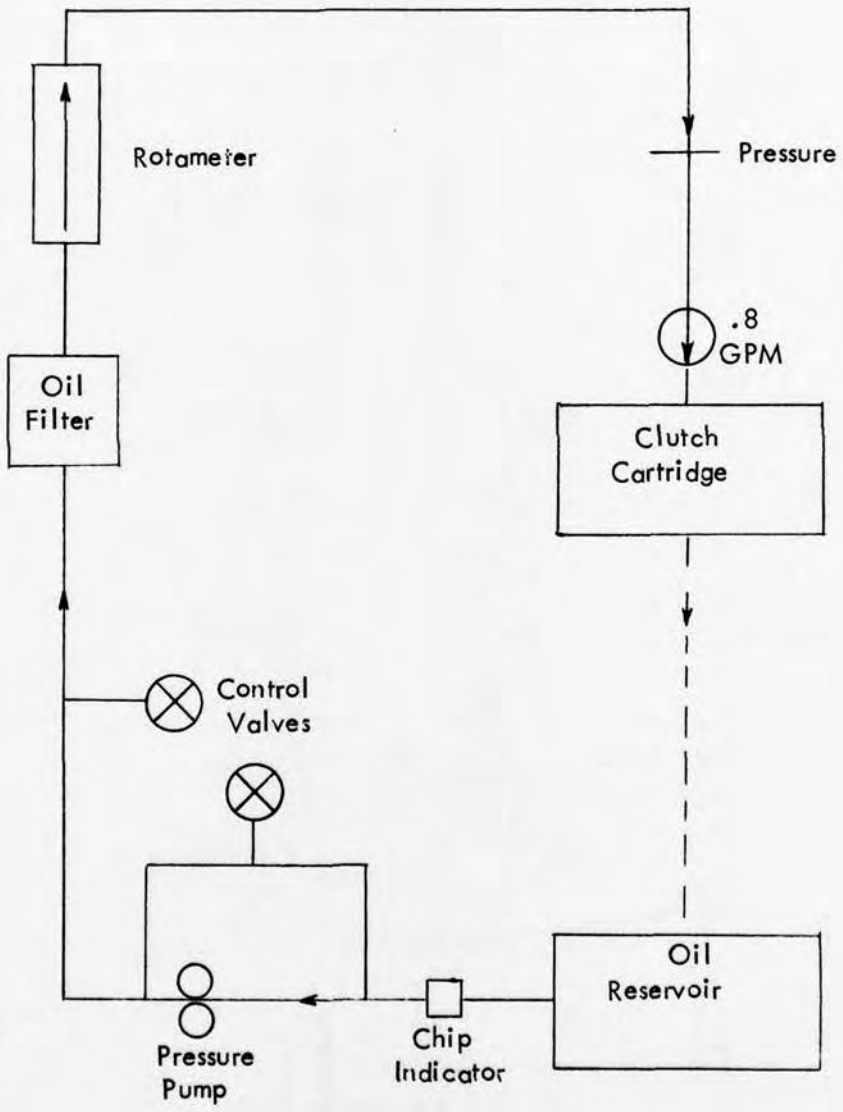

Figure 50. Lubrication Schematic of the Cyclic Load Test Rig.

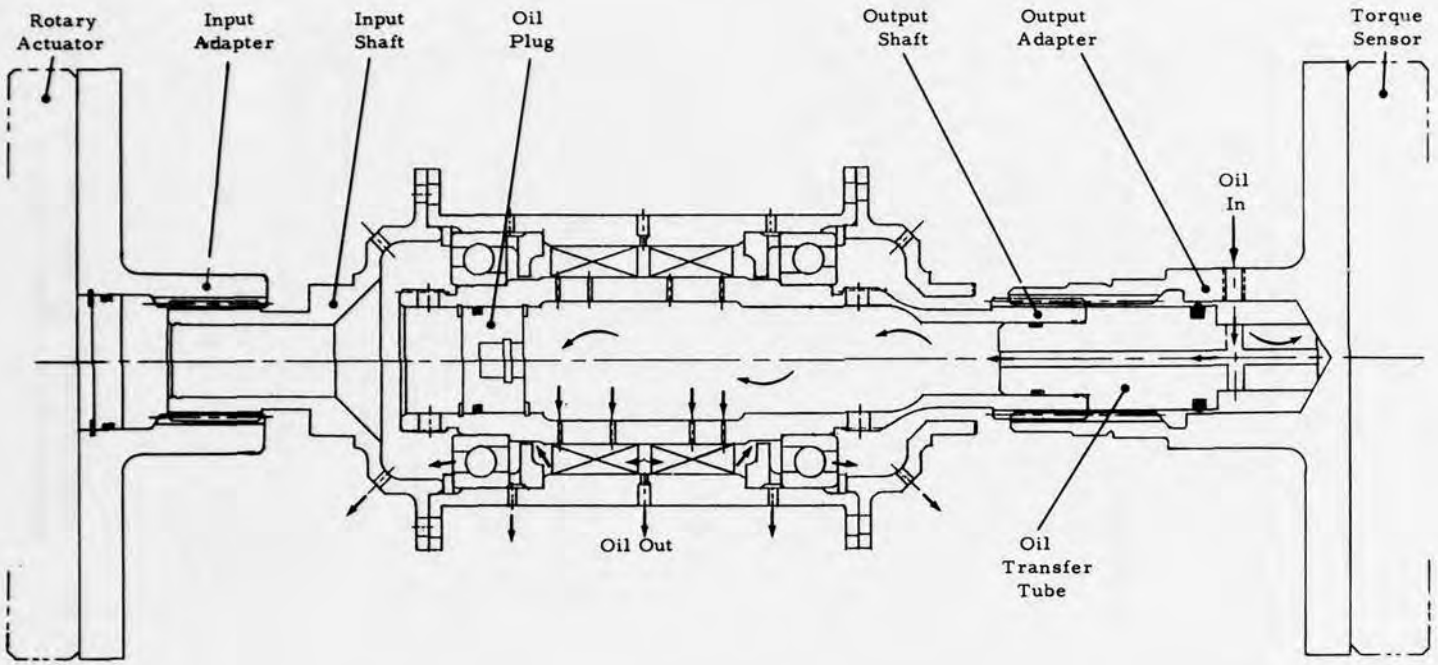

Figure 51. Oil Flow Path of the Sprag Clutch When Used With the Cyclic Load Test Rig.

TABLE 22. INSTRUMENTATION SUMMARY

Recorded Parameter	Monitoring Equipment	Steam Turbine		Power Turbine		Cyclic Load	
		Where Monitored	Means of Record	Where Monitored	Means of Record	Cyclic	O'Load
Speed(rpm) in & out	Magnetic Pickup	Both Turbines	Digit Counter	Tach Waterbrake	Digit Counter	N/A	N/A
Temp (^{O}F) oil in & out	Thermo-couple	Input, Output	Brown Record	Input, Output, Reservoir	Digit Readout	Room Temp	Room Temp
Clutch Out Shaft	Thermo-couple	Inner & Outer Race	Slip Ring Brown Record	-	-	N/A	N/A
Clutch Brgs	Thermo-couple	Position 1,2,3,4	Brown Record	Position 1,4	Digit Readout	-	-
Oil Press in (psi)	Gage	Input	Gage	Input	Digit Readout	Gage	N/A
Oil Flow in (PPH)	Flowmeter	Input	Rotameter	Input	Cox Element	Rotameter	Wetted
Torque (in.-lb)	Strain Gage	Output Shaft	Strain Recorder	Pwr Turb Shaft/ Water-brake	Electric T-meter/ Strain Recorder	Load Cell	Load Cell

thermocouple wires were located .075 inch from the outer housing's inner bore directly over the roller rolling area.

The temperatures of the clutch assembly support-bearing outer races were monitored during both the steam turbine overrunning tests and the power turbine dynamic load tests. The inner clutch support bearing temperatures were monitored in the steam turbine overrunning tests only. Thermocouples were affixed in two places, 180 degrees apart, touching the bearing raceways. The raceways monitored were on the output shaft of each clutch, which corresponds to the inner bearing race for the sprag and the spring clutches, and the outer race for the roller clutch.

Oil pressure and flow were monitored by pressure gages and flowmeters during all tests. The locations are indicated in the lubrication schematics of Figures 43, 46, and 50.

For the initial spring clutch overrunning testing of Task I, the drag torque measurements were taken with a strain-gaged shaft, as shown in Figures 49 and 52. For all other overrunning testing, the torquemeter arrangement shown in Figure 53 was used for measuring drag torque. Strain gages located on the fingers of the shaft, as shown in Figure 54, were used to measure clutch overrunning drag torque. Figure 55 shows a heavier-section shaft that was used later in the test program.

In the power turbine test facility, clutch output torque was measured by the waterbrake torquemeter, which uses a strain gage measurement of the reaction torque on the housing of the waterbrake.

Clutch input torque was measured from the engine's power turbine by an electric torquemeter that uses the magnetostrictive principle. The response of the torquemeter is 0.01 second; i.e., the electrical signal will indicate torque correct to within ± 2 percent not more than 0.01 second after a step change in torque. Both torquemeters were connected to a Sanborn Recorder for monitoring of torque.

In the static test facility, torque load was applied to a bolted adapter splined to the clutch's input side. The torque load was reacted through a torque sensor (load cell) bolted to another adapter and splined to the clutch's output side. Torque readout was observed using an oscilloscope, a digital voltmeter, and a load-amplitude measurement system.

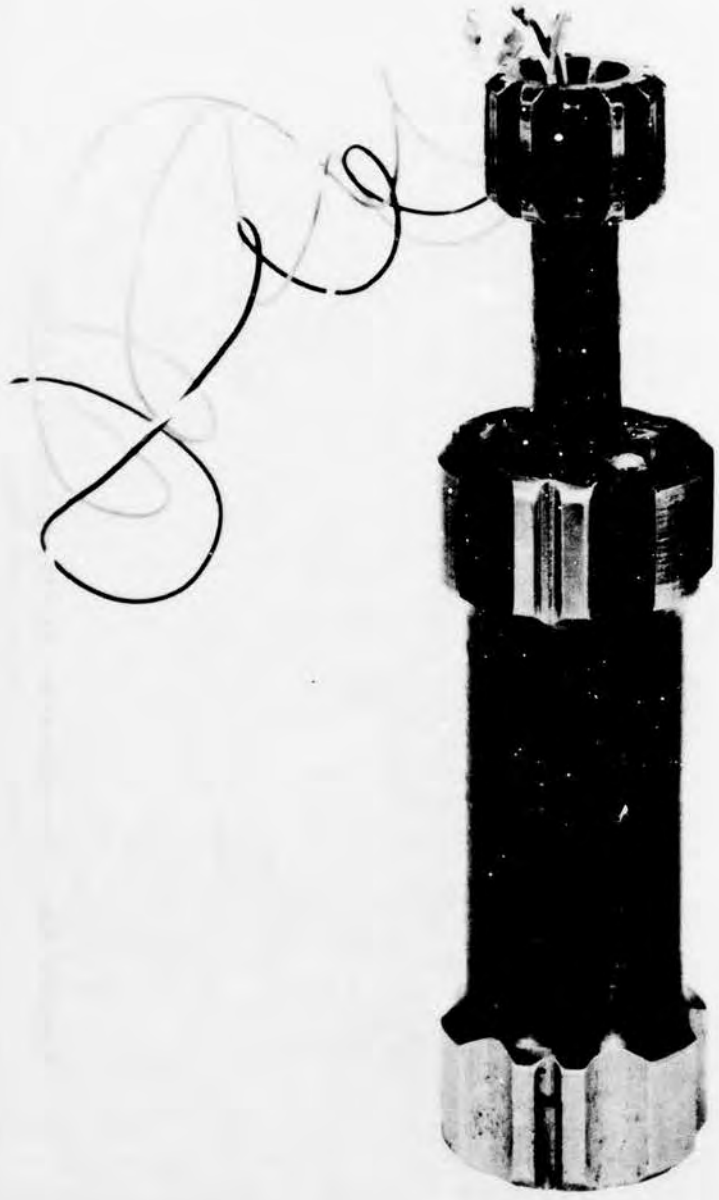

Figure 52. Torquemeter Used in Task I Testing of the Spring Clutch.

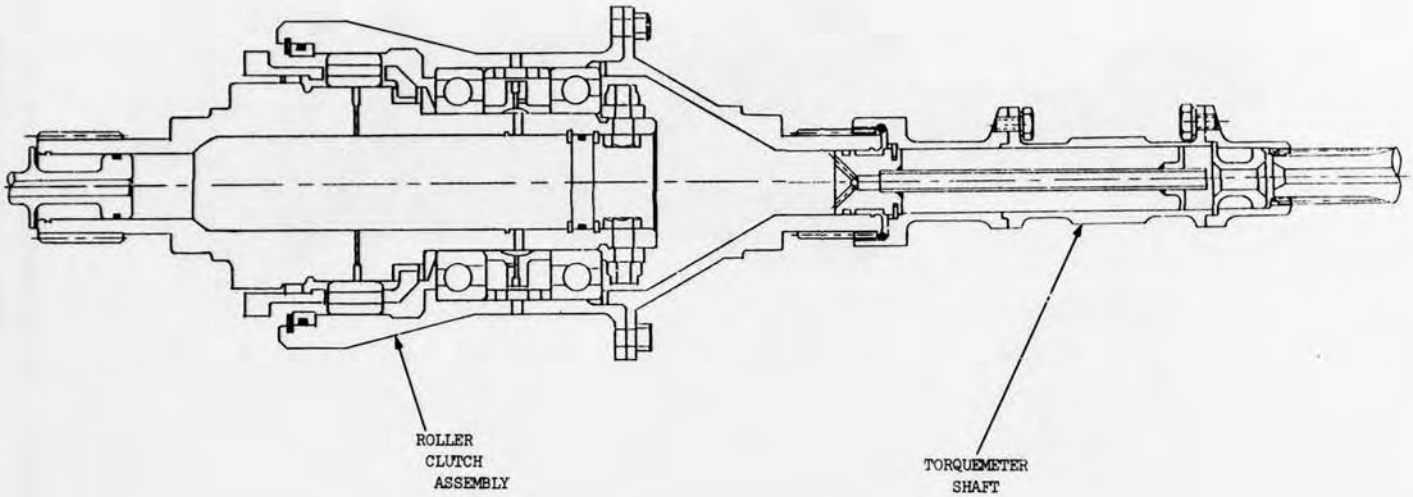

Figure 53. Torquemeter Shaft Assembly in the Steam Turbine Test Rig.

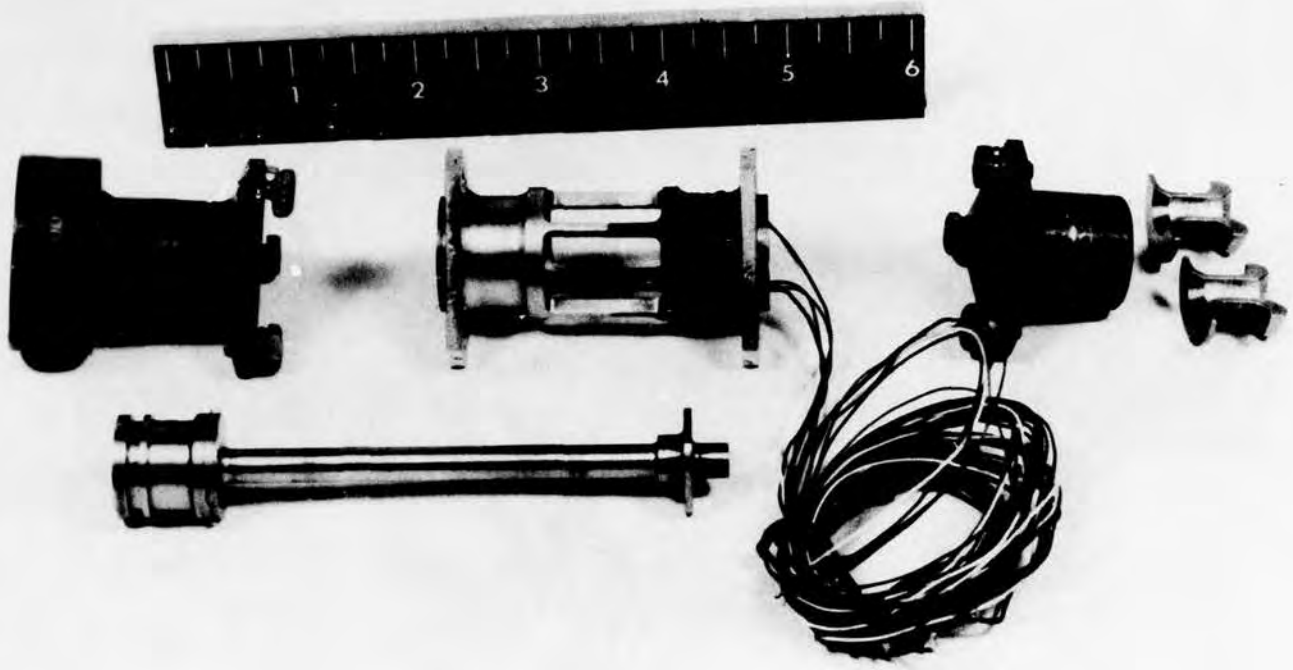

Figure 54. Details of the Torquemeter Used in the Steam Turbine Test Rig.

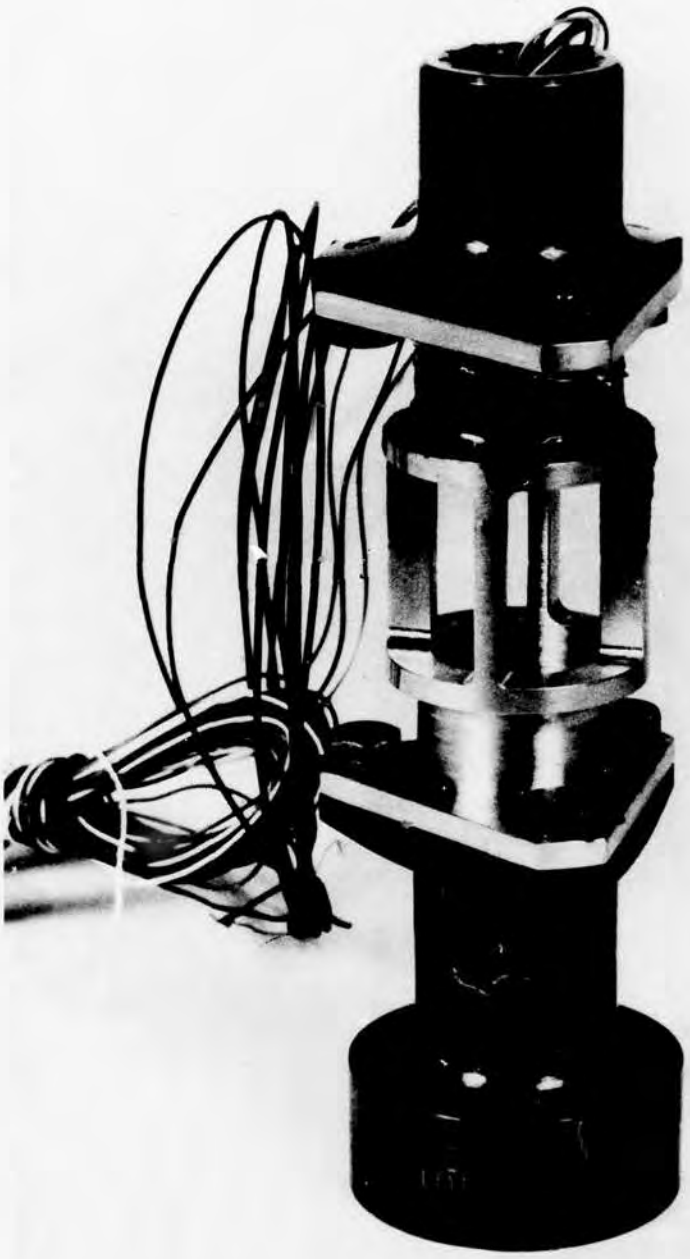

Figure 55. Torquemeter Shaft Assembly Used in the Heavy Duty Turbine Test Rig.

To monitor vibration levels through the test, accelerometers were mounted on the clutch housing at the 12 and 3 o'clock positions. These pickups were used to monitor radial displacement and velocity, and used 1-117 type vibration meters. On the power turbine test rig, vibration was monitored on the flywheel in two places and on the waterbrake in one place. Both axial and radial vibrations were monitored on the engine in two places by a C.E.C. model 128 unit.

Magnetic, quick-disconnect chip detectors were located in the scavenge oil lines of all test rigs (see lubrication schematics.) A model 350 Sanborn recorder was used on the power turbine test rig for monitoring of key parameters. Each engagement of the power turbine endurance tests was numbered, and for the total test of 150 cycles, there were 750 engagements.

Prior to testing, all clutch components were completely dimensionally inspected. The inspection equipment included an Indi-Ron for measuring roundness and a proficorder for measuring surface texture. Measurements were also taken following each test run in order to determine component deterioration during operation.

TEST PROCEDURES

During the test phase of this program, certain precautions were taken with each type of clutch during assembly and disassembly. These precautions consisted mainly of reassembling the test hardware components into the exact locations and positions that they occupied prior to disassembly. By care in marking assembly positions, the test hardware remained in an essentially undisturbed state throughout all phases of testing.

The spring of the spring clutch was always placed on its arbor with the same end towards the input. The spring clutch's bearing inner and outer races were marked so that they could be assembled into exactly the same positions for each test.

On the sprag clutch, each individual sprag was numbered and assembled into a correspondingly numbered slot in the sprag retention cage. Thus, throughout all tests, the sprags never changed positions relative to one another. The input housing, the sprag outer housing and the adapter housing were bolted together and balanced as a unit. The fastener hardware and the sprag clutch's inner duplex bearings were also marked.

On the ramp-roller clutch, the roller retention cage was marked so that the lugs would not be switched 180 degrees. Each roller and its corresponding roller slot was individually numbered, and the clutch bearing races were labeled. As with the sprag clutch, the fastener hardware used to join the outer housing to its support housing was match-marked.

These precautions were required during the test program so that measurements of wear, which were taken after each disassembly, would be consistent. Also, as the test hardware "wears in", machining tolerances and other irregularities are removed from the hardware (high spots worn off, etc.). However, only by assembling the part into exactly the same positions after each test was this "wear in" of hardware maintained.

RETESTING

Retesting during the Task I phase of the program was conducted at any time the clutches experienced a problem and the design was changed. Depending on the nature of the problem encountered, either the test was repeated in its entirety or the test was repeated to the point that proved whether or not the problem had been solved. The purpose of the redesign and retesting effort was to prepare the three clutch designs for the Task II test effort, which included the majority of the endurance testing of the program.

TASK I

The purpose of the Task I tests was to subject each clutch to full-speed and differential-speed overrunning, and dynamic engagement and full-load tests. These developmental type tests were designed to quickly determine the clutch's ability to function satisfactorily in the high-speed environment for which they were designed. These development tests were the proving ground for the longer duration Task II endurance tests that were to follow.

Full-Speed Overrun

The Task I full-speed overrunning test was conducted on the overrunning facility. One of each of the three clutch designs was tested in the full-speed overrun condition, and the following procedure was the same for all designs. During full-speed overrun, the input shaft is fixed (zero speed) and the output shaft is at 100% speed, which was 20,000 rpm for this test program.

The initial full-speed overrun test of Task I consisted of 5 hours of full-speed overrunning with 200% oil flow. During all full-speed overrun tests, the oil inlet temperature was maintained between 195°F and 215°F.

The test rig was instrumented to monitor the following parameters during the 200% oil-flow test:

- Clutch input and output shaft speeds
- Oil temperature in and out of test clutch
- Clutch input or output shaft temperature
- Clutch inner- or outer-bearing race temperature
- Clutch input or output shaft temperature
- Oil pressure into test clutch
- Oil flow rate into test clutch
- Clutch drag torque
- Test clutch vibration (displacement and velocity)
- Chip detection

The above raw data was recorded every 15 minutes. At the completion of the 5-hour run at 200% oil flow, the clutch was disassembled and inspected.

A second 5-hour full-speed overrun test was then conducted on each clutch at 100% design flow. The same data was recorded as in the 200% flow test.

At the conclusion of the 100% flow test, an oil flow data test was conducted. During this test, the above measurements were recorded for each condition of operation after temperatures had stabilized. Full-speed overrun tests were conducted at all permutations of the following speeds and flows:

- Speed of output (input fixed) 20,000, 15,000, 10,000, 5000 rpm
- Flow rate 200%, 150%, 100%, 75%, 50%

The purpose of the oil flow test was to obtain data in all conditions of operation.

Differential-Speed Overrun

Task I differential-speed overrunning tests were conducted on the overrunning facility. The same clutches that were used in the full-speed overrun tests were used in the differential-speed overrun tests, and the following procedure was employed on all designs. Differential-speed overrunning occurs when the output speed is higher than the input speed and the input speed is greater than zero. For the differential-speed tests of Task I, the output speed was 20,000 rpm and the input speeds were 50%, 67%, and 75% of the output (10,000, 13,400, and 15,000 rpm). These differential speeds represent typical values that may be expected in twin-engine helicopter operation.

The oil flow used for the Task I differential-speed tests was the 100% design flow condition. During all differential-speed overrun tests, the oil inlet temperature was maintained between 195°F and 215°F. The first test was conducted at 50% differential speed, with input at 10,000 rpm and output at 20,000 rpm. The test duration was 3 hours. During the 3 - hour 50% differential-speed test, the following parameters were monitored and data was recorded every 15 minutes:

- Clutch input and output shaft speeds
- Oil temperatures in and out of test clutch
- Clutch input or output shaft temperature
- Clutch inner- or outer-bearing race temperature
- Oil pressure into test clutch
- Oil flow rate into test clutch
- Clutch drag torque
- Test clutch vibration (displacement and velocity)
- Chip detection

The above procedure was repeated for additional three-hour runs at 67 and 75% differential speeds for a total of three runs of three hours each and a grand total of nine hours per clutch. At the conclusion of nine hours of differential-speed operation, each test clutch was disassembled and inspected.

Dynamic Load

Task I dynamic load testing was conducted on the turbine test facility. The same clutches used in the overrunning tests were used in the turbine dynamic-load tests.

Each of the three clutch designs was subjected to testing in the turbine test facility, which simulated ground operations and takeoff of the helicopter. Three test cycles were conducted on each clutch with each cycle consisting of the following:

a. Start turbine and accelerate to 100% speed under the simulated inertia and drag torque of a flat-pitch rotor (approximately 400 hp).

b. Operate turbine with clutch engaged for 5 minutes.

c. Reduce engine speed to ground idle, permitting the flywheel to overrun and the test clutch to disengage.

d. Increase turbine speed to 100% to engage clutch.

e. Repeat steps c and d for a total of five disengagements and five engagements.

f. Increase drive to 100% of the design condition (1500 hp, 20,000 rpm) to simulate takeoff.

g. Shut turbine down.

During the turbine testing, the following parameters were recorded:

- Clutch input and output shaft speed
- Oil temperature in and out of test clutch
- Oil pressure into test clutch
- Oil flow rate into test clutch
- Turbine power (capable of recording transient response)

RETEST

Whenever any design changes or modifications to the clutch hardware were made, the clutch was subjected to a retest to determine if the design change was functioning properly. These design changes and retests are described in the "TASK I TEST RESULTS" section of this report.

TASK II

Full-Speed Overrun

The Task II full-speed overrunning tests were conducted on the same facility as the Task I testing. However, the Task II tests were for much longer time periods.

Overrunning tests were conducted on each clutch of the three clutch designs with the output speed at 100% (20,000 rpm) and the input shaft fixed (zero speed). The flow was 100% of design oil flow. The oil inlet temperature was maintained between 195°F and 215°F. Each clutch then underwent two 25-hour tests. Two 25-hour disassemblies and inspections were conducted for each of the three clutch candidates. The following parameters were recorded every 15 minutes:

- Clutch input and output shaft speeds
- Oil temperatures in and out of test clutch
- Clutch input or output shaft temperature
- Clutch inner- or outer-bearing race temperature
- Oil pressure into test clutch
- Oil flow rate into test clutch
- Clutch drag torque
- Test clutch vibration (displacement and velocity)
- Chip detection

Differential-Speed Overrun

The Task II differential-speed overrunning tests were conducted on the overrun facility and were similar to the Task I differential-speed tests but for longer periods of time. The clutches that were used in the full-speed overrun tests were used in the differential-speed tests. The clutch output speed was adjusted to 100% (20,000 rpm) and the input speed was adjusted to 50% (10,000 rpm). The clutches were operated in this condition for 5 hours, then the input speed was adjusted to 67% (13,400 rpm). After 5 hours of operation in 67% differential overrun, the input speed was adjusted to 75% (15,000 rpm), and operation was continued for another 5 hours. Thus, the full cycle consisted of 15 hours with 5 hours each in 50%, 67%, and 75% differential-speed operation. During this test, the following parameters were recorded every 15 minutes:

- Clutch input and output shaft speed
- Oil temperature in and out of the test clutch
- Clutch input or output shaft temperature
- Clutch inner- or outer-bearing race temperature
- Oil pressure into test clutch
- Oil flow rate into test clutch
- Clutch drag torque
- Test clutch vibration (displacement and velocity)
- Chip detection

Upon completion of the 15-hour test cycle, the test clutch was disassembled and inspected. A second 15-hour test cycle was then conducted, identical in test conditions to the first 15-hour cycle, for a total test time of 30 hours of differential-speed overrunning per clutch.

Dynamic Load

The Task II dynamic-load turbine tests were conducted on the turbine test facility. The same clutches used in the overrunning tests were subjected to the turbine-test cycles, with each cycle consisting of the following:

a. Start turbine to engage clutch and accelerate to 100% speed under the simulated inertia and drag torque of a flat-pitch rotor (400 hp).

b. Operate turbine with clutch engaged for 5 minutes.

c. Reduce engine speed to ground idle, permitting the flywheel to overrun and the test clutch to disengage.

d. Increase turbine speed to 100% to engage clutch.

e. Repeat steps c and d for a total of five disengagements and five engagements.

f. Increase drive to 100% of design condition (1500 hp, 20,000 rpm) to simulate takeoff. Operate for 1 minute.

g. Reduce drive torque to 400 hp to simulate flat-pitch rotor.

h. Operate turbine with clutch engaged for 5 minutes.

i. Disengage and engage clutch five times using engine speed control and flywheel as in steps c and d above.

j. Increase drive to 100% of design condition (1500 hp, 20,000 rpm) to simulate takeoff. Operate for 1 minute.

k. Shut turbine down.

Each dynamic load test cycle as outlined in steps a through k above consisted of 1 start-up, 10 dynamic engagements, 10 dynamic disengagements, 2 runs at full power, and 1 shut down. This cycle was repeated 75 times for each clutch which simulated a total of 75 start-ups, 750 dynamic engagements and disengagements, 150 takeoffs, and 75 shut downs.

The following parameters were monitored and recorded during the Task II dynamic-load tests:

- Oil flow rate
- Temperature of oil in and out
- Oil inlet pressure
- Clutch input and output shaft speed
- Turbine power (capable of recording transient response)

Environmental

Environmental testing of Task II consisted of testing with high- and low-temperature oil using the same clutches as were used for the dynamic-load tests. The tests were conducted on the turbine test facility.

Cold-Oil Test

Each clutch of the three clutch designs was subjected to cold-temperature tests in the turbine test facility conducted according to the following procedure:

a. Operate clutch in normal manner to obtain residual oil.

b. Shut down turbine engine.

c. Turn valve that supplies oil to clutch to the off position.

d. Cool clutch housing to -40°F and clutch oil supply to 0°F.

e. Start engine at simulated flat-pitch rotor (approximately 400 hp) and operate at ground idle (approximately 10,000 rpm) for 5 minutes. During this period, there will be no oil to the clutch.

f. After 5 minutes of operation at the condition specified in step e, open valve allowing oil to flow to clutch from clutch oil supply.

g. Increase turbine speed to 100% (20,000 rpm).

h. Reduce turbine speed to ground idle, disengaging clutch.

i. Increase turbine speed to 100% (20,000 rpm) to re-engage clutch.

j. Repeat steps h and i for a total of five disengagements and five engagements.

k. Increase torque to 100% (1500 hp) to simulate takeoff. Operate for 1 minute.

l. Stop turbine.

Repeat steps c through l for a total of ten cold-start cycles. Record the following data:

- Oil flow rate
- Temperature of oil in and out
- Oil inlet pressure
- rpm in and out
- Turbine power (capable of measuring transient response)

At the conclusion of the cold-oil test, the clutches were disassembled and inspected.

Hot-Oil Test

The hot-oil test was conducted with the oil supply to the clutches preheated to 300°F. The procedure and the data taken were identical to those in the Task I dynamic-load test except that only ten cycles of testing were completed, for a total of 50 engagements and disengagements per clutch. At the conclusion of the hot-oil test, the clutches were disassembled and inspected.

Dynamic Cyclic

The dynamic cyclic tests were conducted on each of the three clutch designs using the turbine test facility. The clutches that were used in the previous tests were again used for the dynamic cyclic tests.

The turbine fuel control was rigged with a valve driven by a motor and cam device. The cam was driven at one revolution per second that opened and closed the fuel control at that rate. The high and low limits of the fuel control were set to provide 100% and 90% torque, respectively. Thus, in operation, the fuel control regulated the turbine to operate at 95% $\pm$5% or 1425 hp $\pm$75 hp. Each clutch was tested in this condition for 3 hours at 1 cycle per second for a total of 10,800 cycles.

The following parameters were recorded during this test:

- Oil flow rate
- Temperature of oil in and out
- Oil inlet pressure
- Input and output rpm
- Turbine power (capable of measuring transient response)

At the conclusion of the dynamic cyclic test, the clutches were disassembled and inspected.

Static Cyclic

Static cyclic testing was conducted on each of the three clutch designs in the static test facility.

With the output held stationary, a torque was applied in the engagement direction of 9450 $\pm$ 1000 inch-pounds for 10 million cycles. At the completion of the static cyclic torque test, the clutches were disassembled and inspected. The following data was recorded throughout the test:

- Torque
- Angular displacement
- Outer shaft radial deflection

Static Overload

A new (unused) clutch of each design was subjected to a static overload test in the static test facility. Holding the output stationary, torque was applied in the engagement direction and increased in 500 inch-pound increments to 400% of the design torque (18,900 inch-pounds) or until failure. At the completion of the test, each clutch was disassembled and inspected. The following data was recorded at the 500-inch-pound increments:

- Torque
- Angular displacement
- outer shaft radial deflection

TEST RESULTS

TASK I TEST RESULTS

Full-Speed Overrun Test Results

The purpose of the full-speed overrunning test of Task I was to determine the proper flow of oil for each clutch and to serve as a breaking in period for the more rigorous testing later on. The full-speed overrunning test of Task I was also used to uncover problems associated with overrunning. The overrunning testing consisted of two tests on each clutch of the three clutch designs. In the first test, each clutch was operated with the input fixed and the output rotating at 20,000 rpm for 5 hours with 200% oil-flow conditions. After disassembly and inspection, a second test of 5 hours duration was conducted at 100% flow conditions. During these tests, measurements were taken at flows of 200%, 150%, 100%, 75% and 50% so that comparative curves could be drawn.

The first full-speed overrunning test was conducted with the spring clutch. The oil flow to the clutch was adjusted to 700 ± 35 pounds per hour (1.6 gpm), with a 175±10-pound-per-hour (.20-gpm) flow to the support bearings. Various speed rundown tests were conducted where the output speed was varied from 20,000 rpm to 5000 rpm in 5000-rpm increments, and test measurements were taken with the flow at the conditions of Table 23.

TABLE 23. TEST CLUTCH OIL FLOW CONDITIONS

% Flow	Flow to Clutch		Flow to Support Bearings	
	lb/hr	gpm	lb/hr	gpm
200	700±35	1.60±.08	175±10	.40±.02
150	525±20	1.20±.05	130±10	.30±.02
100	350±20	.80±.05	90±10	.20±.02
75	260±15	.60±.03	65±10	.15±.02
50	175±10	.40±.02	45±10	.10±.01

At the conclusion of the spring clutch's speed rundown test, a 5-hour full-speed overrun test was conducted with the flow at the 200% design condition of 1.6 gpm. Disassembly and inspection after this test showed slight indications of wear on the teaser coils. A small amount of wear was also present on the end face of the spring and on the corresponding section of the bronze washer that separates the spring from the output-housing end face. The condition of these parts after the first 5-hour run can be seen in Figure 56.

Figure 56. End View of Spring and Bronze Bushing at Completion of 5 Hours of Full-Speed Overrunning, Task I.

The spring clutch was reassembled, and a second 5-hour full-speed overrun test was conducted at the 100% design flow condition of .80 gpm. At the conclusion of this 5-hour test, the spring clutch parts were examined, and although no distress signals were evident during the test, the parts were found to have some signs of deterioration. Figure 57 shows the condition of the spring teaser coils, which show areas of missing plating. The plating is silver and was applied to the teaser coils as a wear barrier for overrunning. The plating that had chipped then proceeded to flow with the oil in an attempt to exit from the clutch. During this process, the center section of the spring along with several areas of the bore of the output housing sustained scoring marks as shown in Figure 58. The chipping was considered a minor problem, and it was decided to clean the parts and continue testing.

The sprag clutch was the second unit to be subjected to the full-speed overrun test. The first sprag overrun test consisted of 200% and 150% oil flow, taking data at 20,000 rpm, 15,000 rpm, 10,000 rpm, and 5000 rpm. The sprag clutch was then tested for 5 hours at full-speed overrun with the input fixed (zero speed) and the output rotating at 20,000 rpm. During this test, the flow was set to 200% (1.6 gpm).

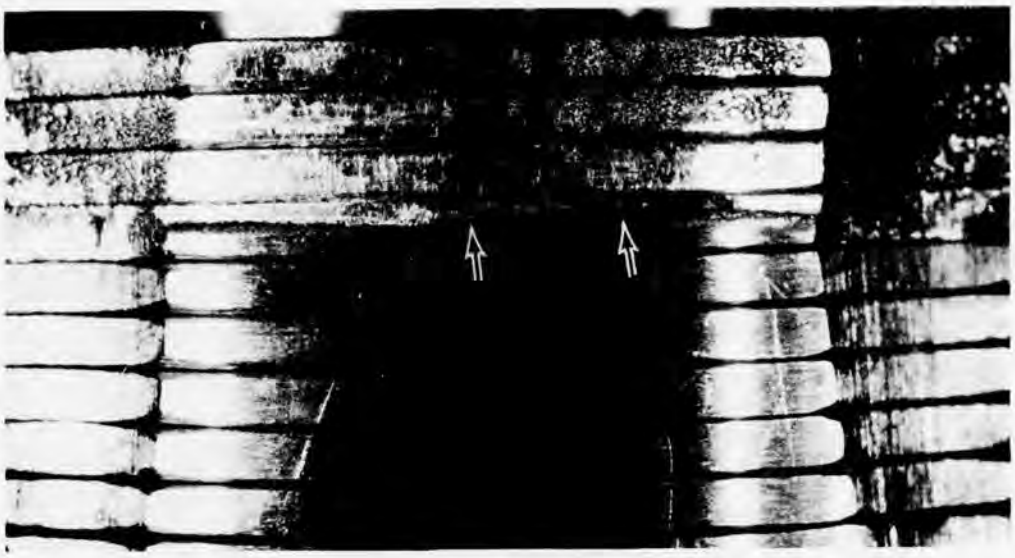

Figure 57. Spring Teaser Coils on Overrunning End After Full-Speed Overrunning Test, Task I.

The sprag clutch's 100% flow condition was established as .80 gpm and was the same as the spring clutch's flow, as shown in Table 23. At the conclusion of the 5-hour test run, the sprag clutch was disassembled and inspected. It was found that the wear on the sprags was higher than was to be expected for so short a duration of overrunning. Figure 59 is a photograph of sprag numbers 1, 7, 19, and 31, which were chosen at random and represent an average wear condition. The average band width of the wear was in the order of .015 inch. Also evident was wear on the inner shaft and the drag strips of the sprag unit, as shown by the photographs of Figure 60. The outer shaft also shown in Figure 60 displayed sprag-contact-area marks, which were of negligible depth.

Although the wear was appreciable, it was decided to continue with the same hardware in the second 5-hour full-speed overrun test at 100% oil flow (.80 gpm). As the sprag was being run up for test, it was noted that the temperature of the inner race in the overrunning area was about 280°F while the oil temperature was 195°F. This condition was noted at 75% full-speed overrun. It was decided that this temperature rise (85°F) was excessive, and the test was terminated after approximately 45 minutes of operation at 75% full-speed overrun. A possible cause of high temperature can often be insufficient oil for cooling. A close inspection of the components showed that a possible source of oil leakage could be through the holes used to lock the bearing nut (part number

Figure 58. Spring Clutch Outer Ousing Bore After Full-Speed Overrunning Test, Task I.

Sprag #1

Sprag #7

Sprag #19

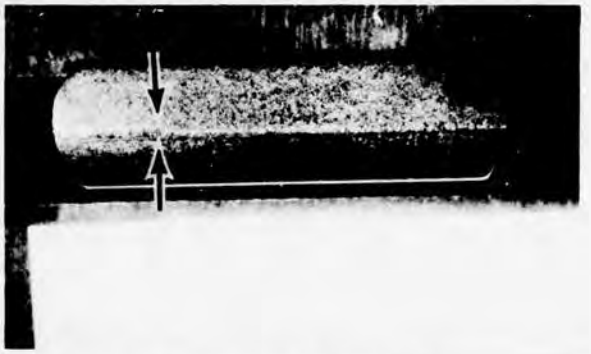

Sprag #31

Figure 59. Random Sprag Wear After 5 Hours of Full-Speed Overrunning, Task I.

Inner
Race
(Output Shaft)

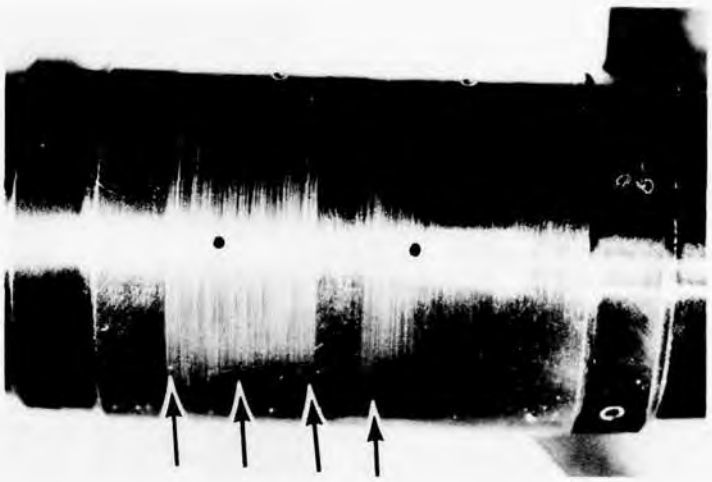

Sprag
Retainer

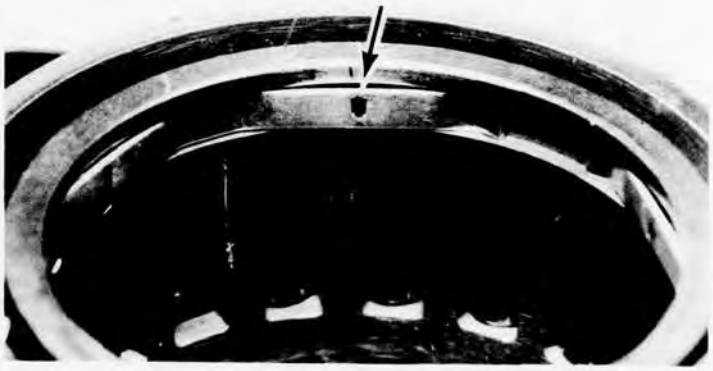

Outer
Race
(Input Shaft)

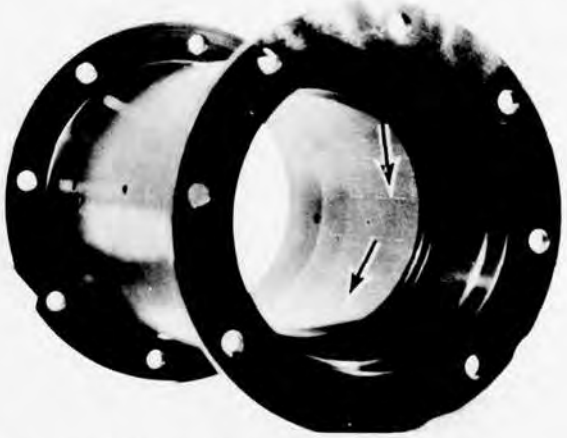

Figure 60. Sprag Clutch Components After 5 Hours of Full-Speed Overrunning, Task I.

38350-10012-101) to the inner shaft (part number 38350-10033-101). The lock nut contains six equally spaced radial holes, while the shaft has eight holes. Thus, for every 15 degrees of rotation of the nut, there will be two holes 180 degrees apart that align between the nut and the shaft. These holes are used in conjunction with two sets of nuts, bolts, and radius washers to lock the nut. However, when the nut is locked, substantial portions of the .234-inch-diameter holes will overlap one another, thereby forming escape paths for the clutch lubrication, as shown in Figure 61.

This problem was overcome by plugging the six unused holes in the shaft with silicone-rubber adhesive sealant. In operation, centrifugal force acts on the silicone sealant, tending to force the plug of rubber outward. However, the nut forms a natural trap, which holds the plugs in. The small overlapping areas were thus sealed. This rework procedure was considered a redesign, and all testing done to this point was discarded. The inner shaft O.D. was reworked by grinding the sprag overrun area from 1.7501 to 1.7489 inches diameter with a 9-rms finish. This reworked area was .0008 inch under the drawing low limit of 1.7497 inches diameter. In effect, this increases the sprag gripping angles, lowers sprag normal loads, and reduces stresses. However, the remaining material allowance for wear is, of course, reduced. The reworked shaft is shown in Figure 62.

After reworking the sprag clutch's inner shaft O.D., plugging the holes with silicone rubber, and replacing the entire sprag unit with a new sprag unit, testing was restarted at the beginning. This time, the entire speed rundown and the five-hour full-speed overrun at 100% flow tests were conducted without incident. The sprag inner-shaft race temperature was in the order of 212°F at the 100% flow of .8 gpm, whereas prior to blocking the holes in the shaft, the inner race temperature in the same flow condition was in the area of 280°F. Thus, a substantial improvement was obtained. Sprag wear was substantially reduced, as shown in Figure 63. The condition of the outer shaft's bore can be seen in Figure 64. New contact areas had been formed because the angular position of the sprag unit is changed after each assembly. Normally, the sprag unit will not change position with respect to the outer housing because the drag bands restrict relative rotation. The depth of the marks is negligible and cannot be measured (less than .00005 inch). Figure 65 shows the condition of the inner shaft overrunning area. The tangential score marks seen are caused by the sprag sliding over the shaft during overrunning. The depth of these marks measured .0002 inch to .00035 inch maximum on one side of the unit to zero 180 degrees away. The conditions of sprag number 1 after 5 hours and after 10 hours are shown in Figure 66.

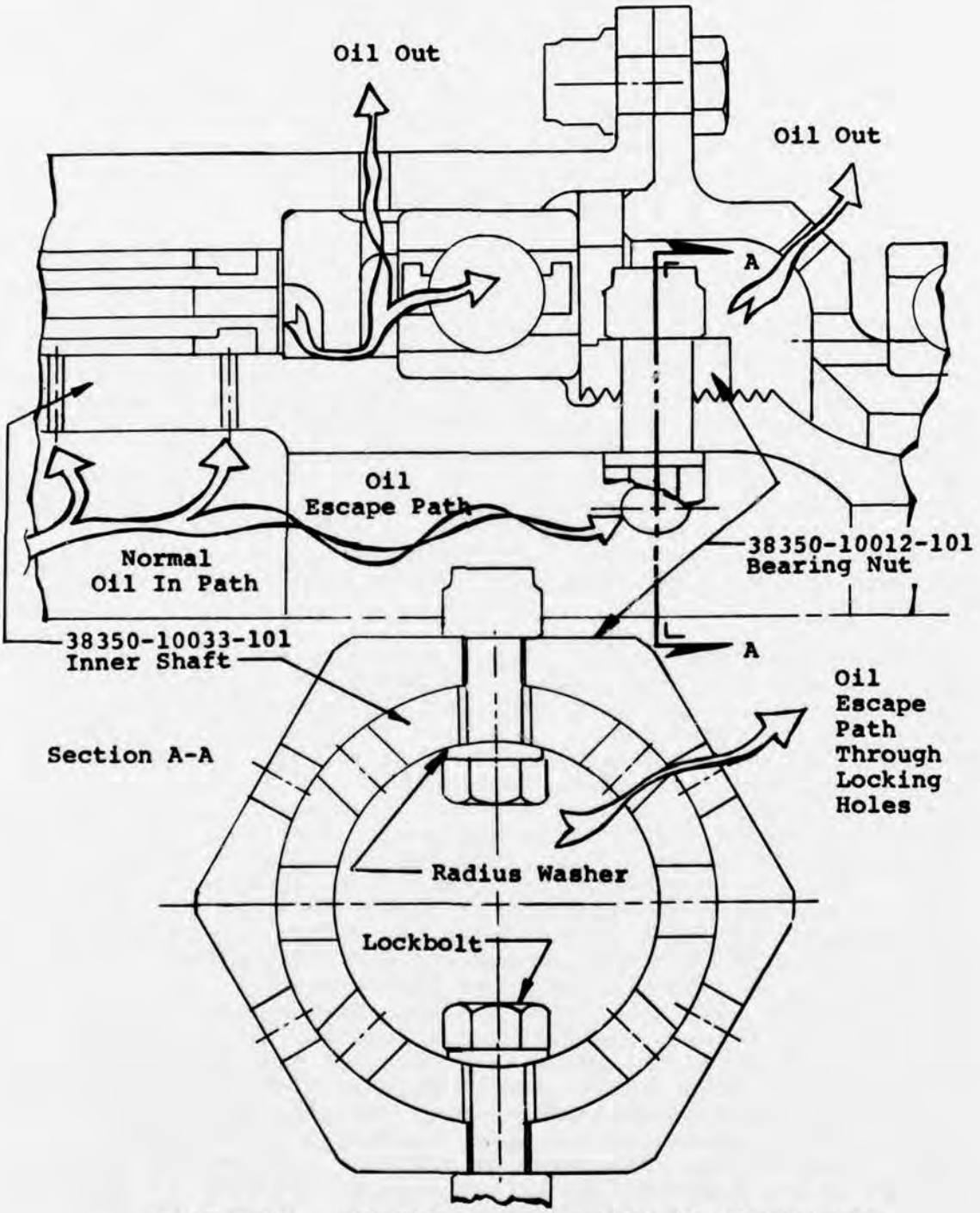

Figure 61. Lubricant Escape Path in First Sprag Clutch Design Found During Task I.

Figure 62. Reworked Sprag Clutch Inner Shaft With Plugged Holes.

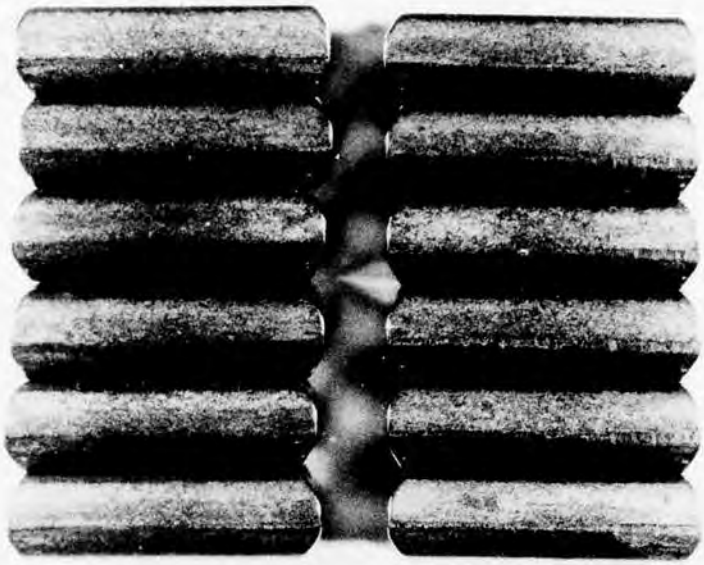

Figure 63. End View of Randomly Selected Sprags Showing Wear Incurred During Full-Speed Overrunning Test, Task I.

Figure 64. Sprag Clutch Outer Shaft Bore After Full-Speed Overrunning Test, Task I.

Figure 65. Sprag Clutch Inner Shaft After Full-Speed Overrunning Test, Task I.

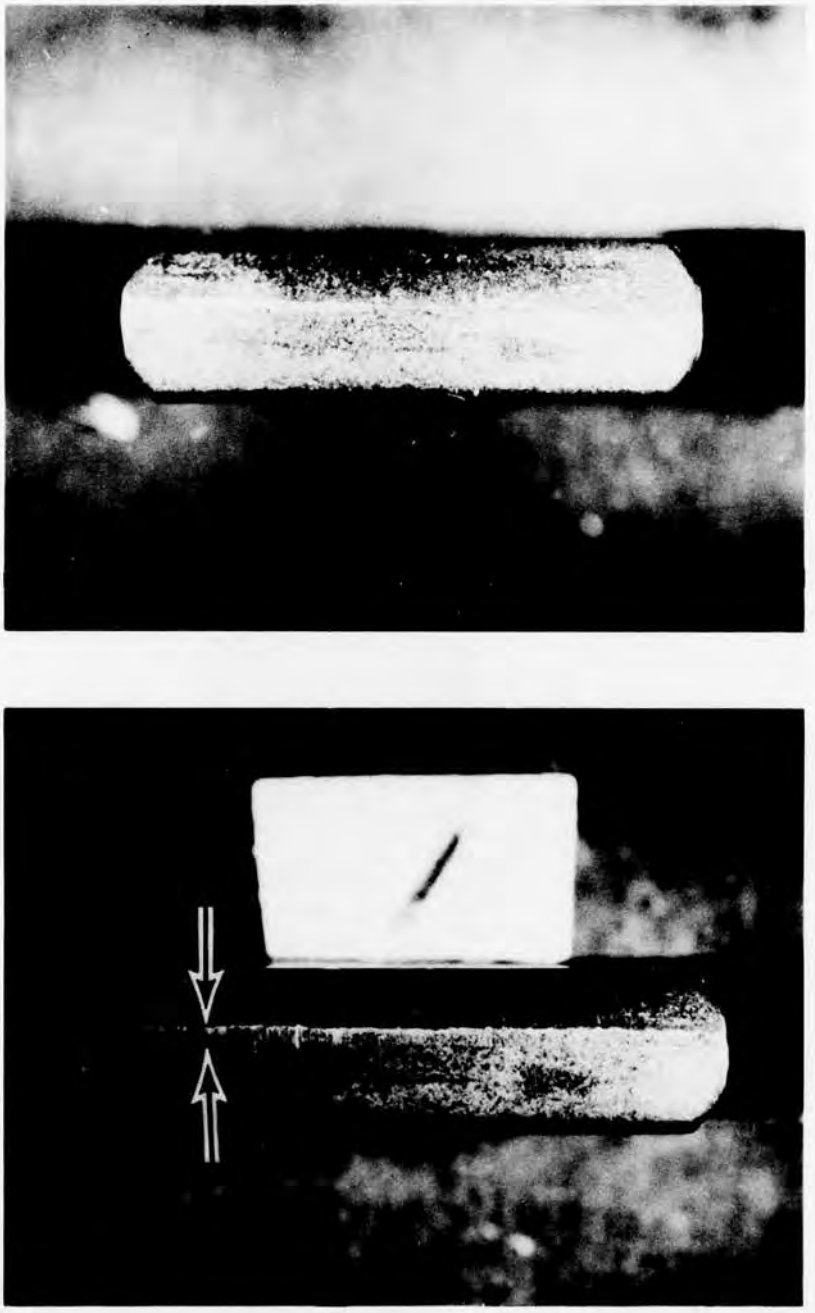

Figure 66. Number 1 Sprag After 5 Hours (Above) and After 10 Hours (Below) of Full-Speed Overrunning, Task I.

The ramp-roller clutch was the final clutch to be tested in the full-speed overrunning mode. After approximately 30 minutes of full-speed overrunning with the input fixed and the output rotating at 20,000 rpm, the nichrome tape holding the thermocouple wires to the outer housing was thrown off by centrifugal force. The wires were re-instrumented and the testing was restarted. The first test consisted of speed rundowns at 200% flow and at 150% flow with speeds of 20,000, 15,000, 10,000, and 5000 rpm. The 100% flow condition for the ramp-roller clutch was established as .80 gpm, which is identical to the spring and sprag clutch flows shown in Table 23. After the speed rundown test, the ramp-roller clutch was tested at full-speed overrun with 200% flow (1.6 gpm) for 5 hours. After the test, the clutch was disassembled and inspected. Figure 67 shows the condition of the outer housing's inner bore after 5 hours of testing.

Figure 67. Ramp-Roller Clutch, Outer Housing Roller Contact Area After 5 Hours Full-Speed Overrunning, Task I.

Figure 68 shows a typical roller and a typical front edge of a slot in the roller-retention cage, while Figure 69 is a photograph of the cam shaft. The cam shaft flats show no evidence of wear of any kind.

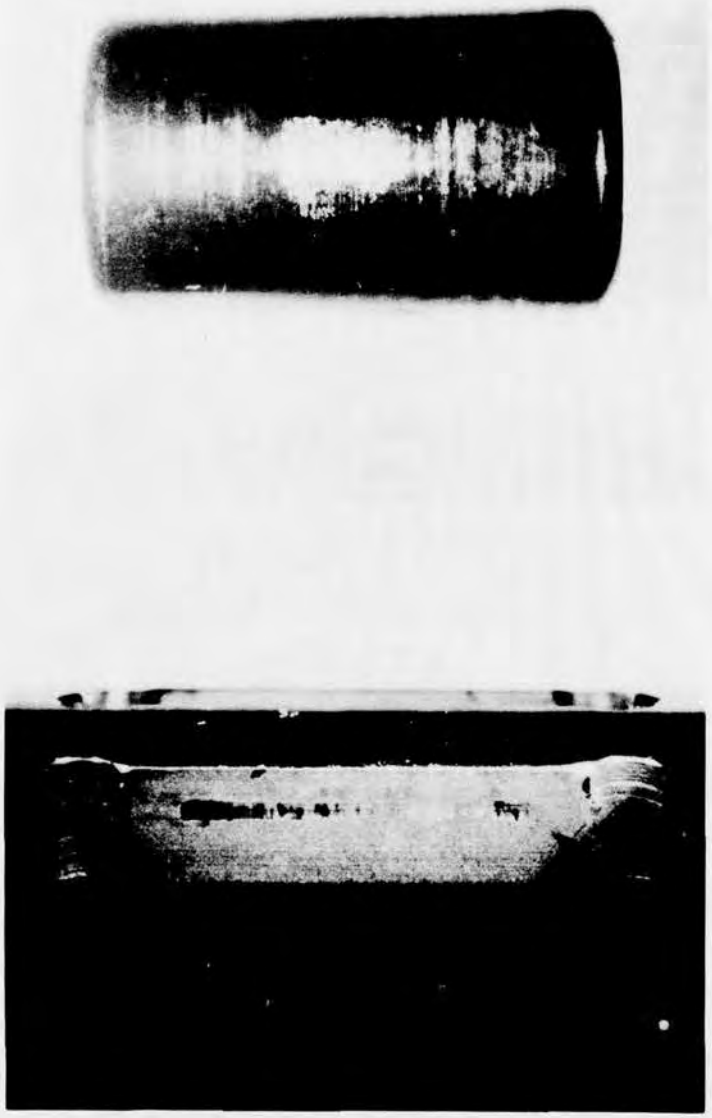

Figure 68. Typical Roller and Roller Slot in Cage After 5 Hours of Full-Speed Overrunning, Task I.

Figure 69. Ramp-Roller Clutch Cam Shaft After 5 Hours of Full-Speed Overrunning Test, Task I.

The second 5-hour full-speed overrun test of the ramp-roller clutch with 100% oil flow rate was then conducted. At this time, speed rundown tests were also conducted at 100%, 75% and 50% flow to obtain data. Disassembly and inspection of the hardware showed further evidence of wear but to a small degree. A disturbing fact was the rough nature of the surface finish developing on the rollers, as shown in two typical rollers of Figure 70. The diameters of all 14 rollers were measured and found to be .3749 inch, which is identical to the initial starting diameter of the new rollers, showing that the depth of wear was negligible. The outer housing bore, the cam shaft, and a typical roller slot are depicted in Figure 71.

The ramp-roller clutch test completed the full-speed overrunning testing of Task I. The clutch's drag torque in full-speed overrunning is measured with a strain-gage torquemeter shaft splined to the output shaft. Drag measurements, therefore, included the clutch's inner to outer support bearings as well as the drag of the clutch's overrunning member. In the spring clutch, overrunning drag occurs between the teaser coils of the spring and the output housing. In the sprag clutch, the ribbon spring rotates the sprags, causing them to touch both the inner and outer sprag raceways. This wedging action creates a frictional restraint during overrunning that, when combined with the innermost support bearing drag, gives the total overrunning drag for the sprag clutch. Ramp-roller clutch drag is created by the pin and spring assembly load, which imparts a torque to the roller retention cage in a direction that tends to wedge the rollers between the cam shaft and the outer housing. This wedging action creates frictional drag that, when combined with the inner support bearing drag, gives the total drag for the ramp-roller clutch.

The drag torques of all three clutch designs were measured during the full-speed overrunning tests as functions of output shaft speed (with input fixed) and as functions of lubricant flows from 50% to 200%. Figures 72 through 74 show drag torque versus flow for various full-speed overrunning rpm's for the spring, sprag, and ramp-roller clutches, respectively. Figures 75 through 78 show the same data plotted with all three clutches on each curve for 20,000 rpm, 15,000 rpm, 10,000 rpm, and 5000 rpm, respectively. Note that in all instances the sprag clutch had the highest values of drag, while the ramp-roller clutch was second and the spring clutch was the lowest. As would be expected, the ramp-roller and sprag clutch drags increase with increasing flow. The spring clutch, however, displays a relatively flat curve of drag torque versus flow for all conditions of operation and is almost insensitive to quantity of flow, perhaps because the exit path for the lubricant is less restricted.

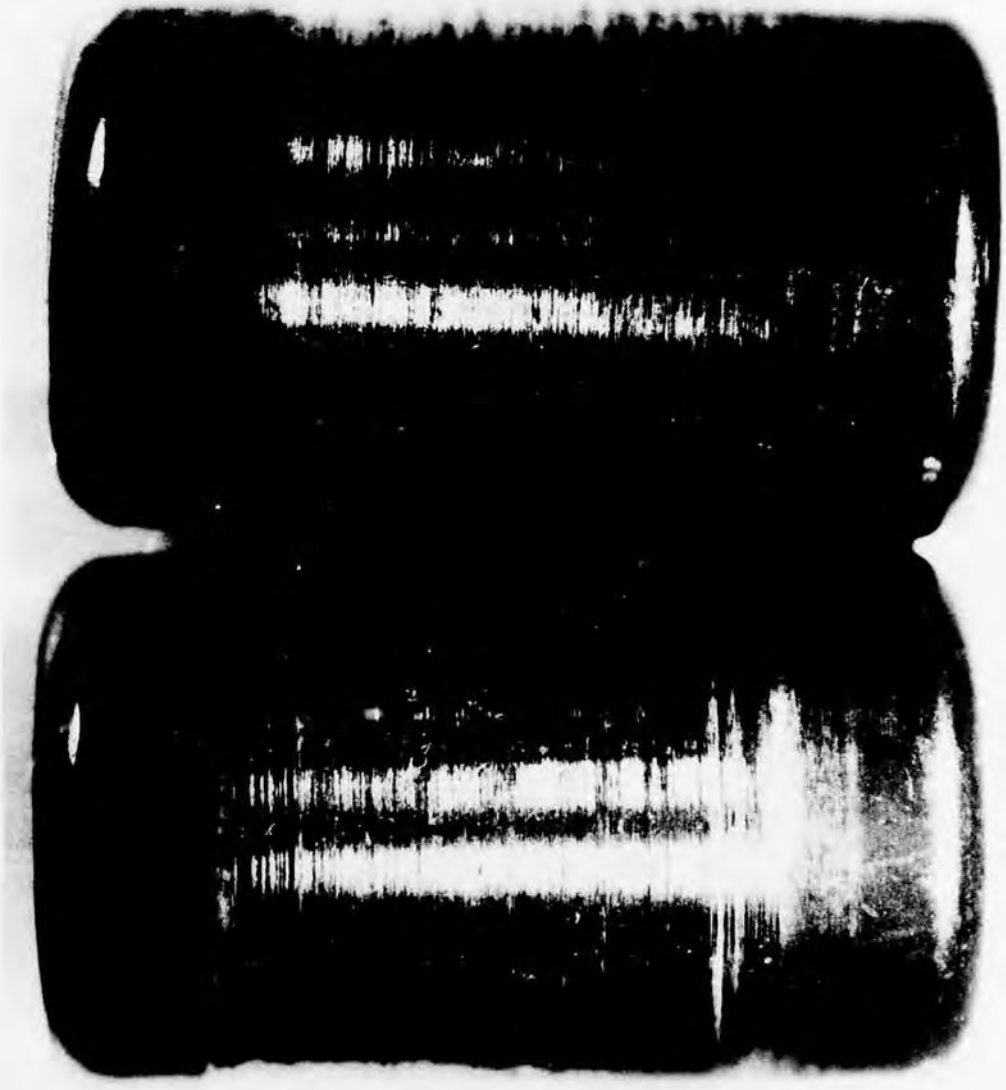

Figure 70. Typical Roller at Completion of Full-Speed Overrunning Test, Task I.

Outer Housing Bore

Cam Shaft

Roller Slot, Drive Side

Figure 71. Ramp-Roller Clutch: Outer Housing Bore, Cam Shaft, and Typical Roller Slot at Completion of Full-Speed Overrunning Test, Task I.

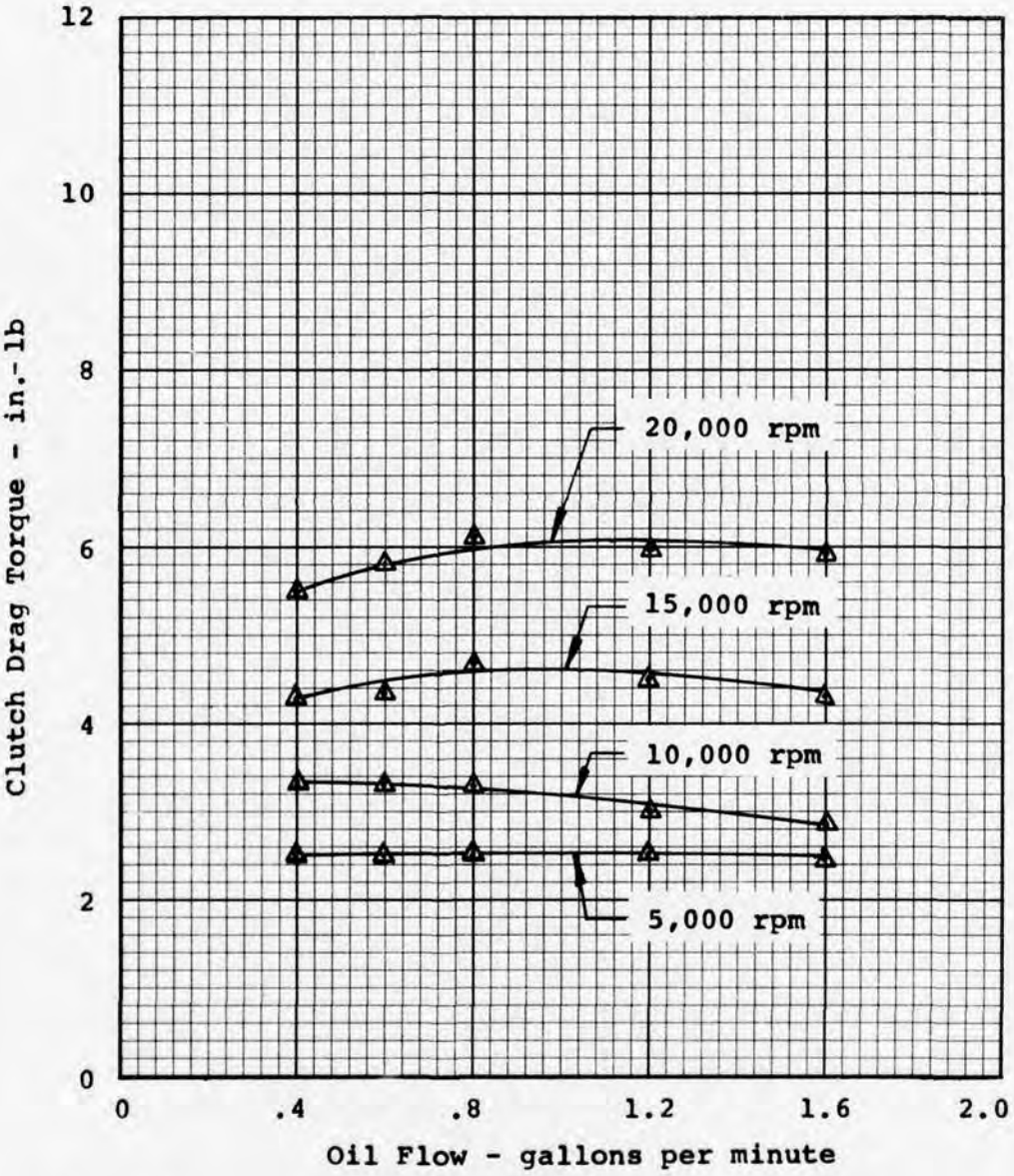

Figure 72. Drag Torque Versus Oil Flow at Various Full-Speed Overrunning Speeds (Input Fixed), Spring Clutch.

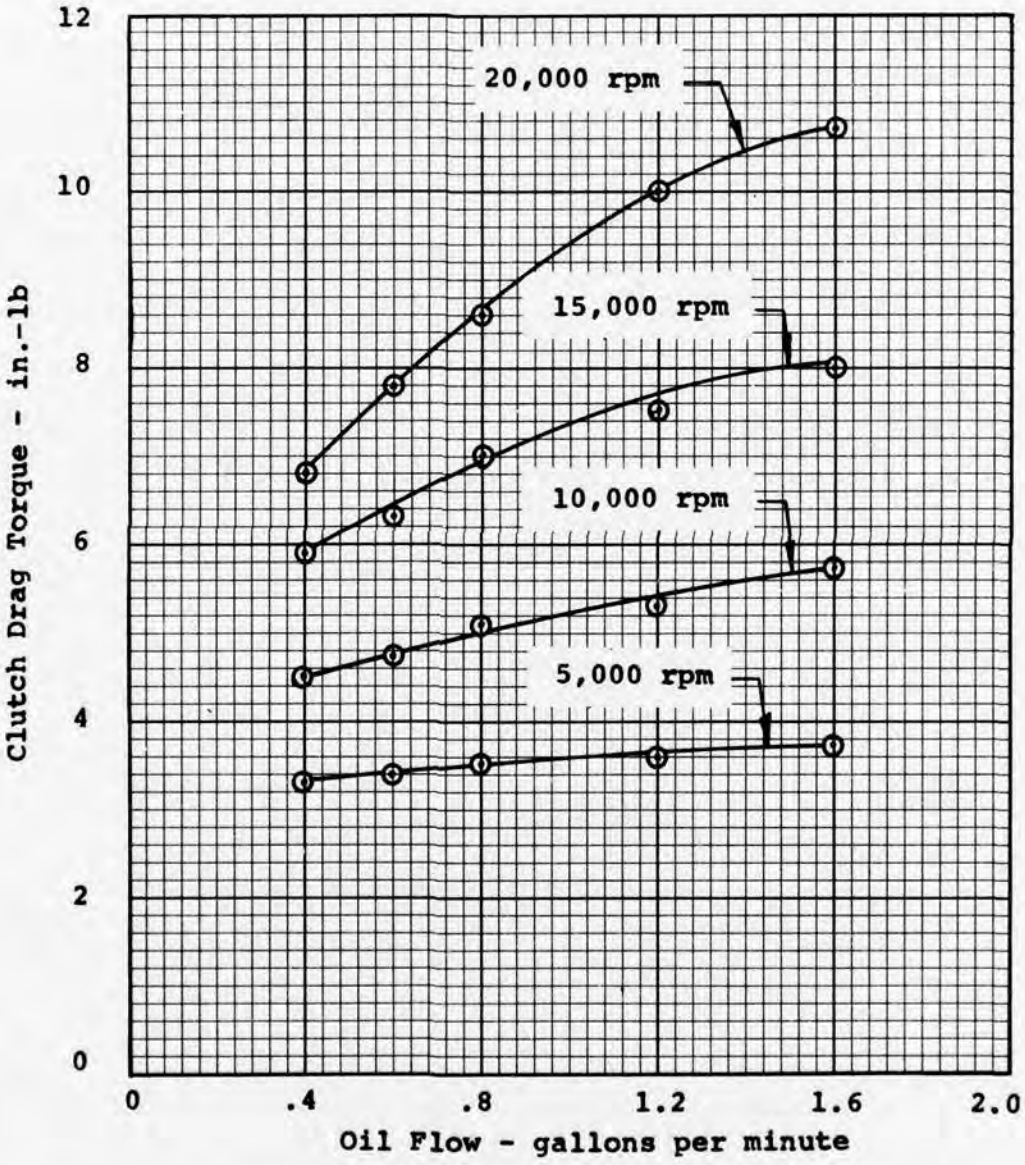

Figure 73. Drag Torque Versus Oil Flow at Various Full-Speed Overrunning Speeds (Input Fixed), Sprag Clutch.

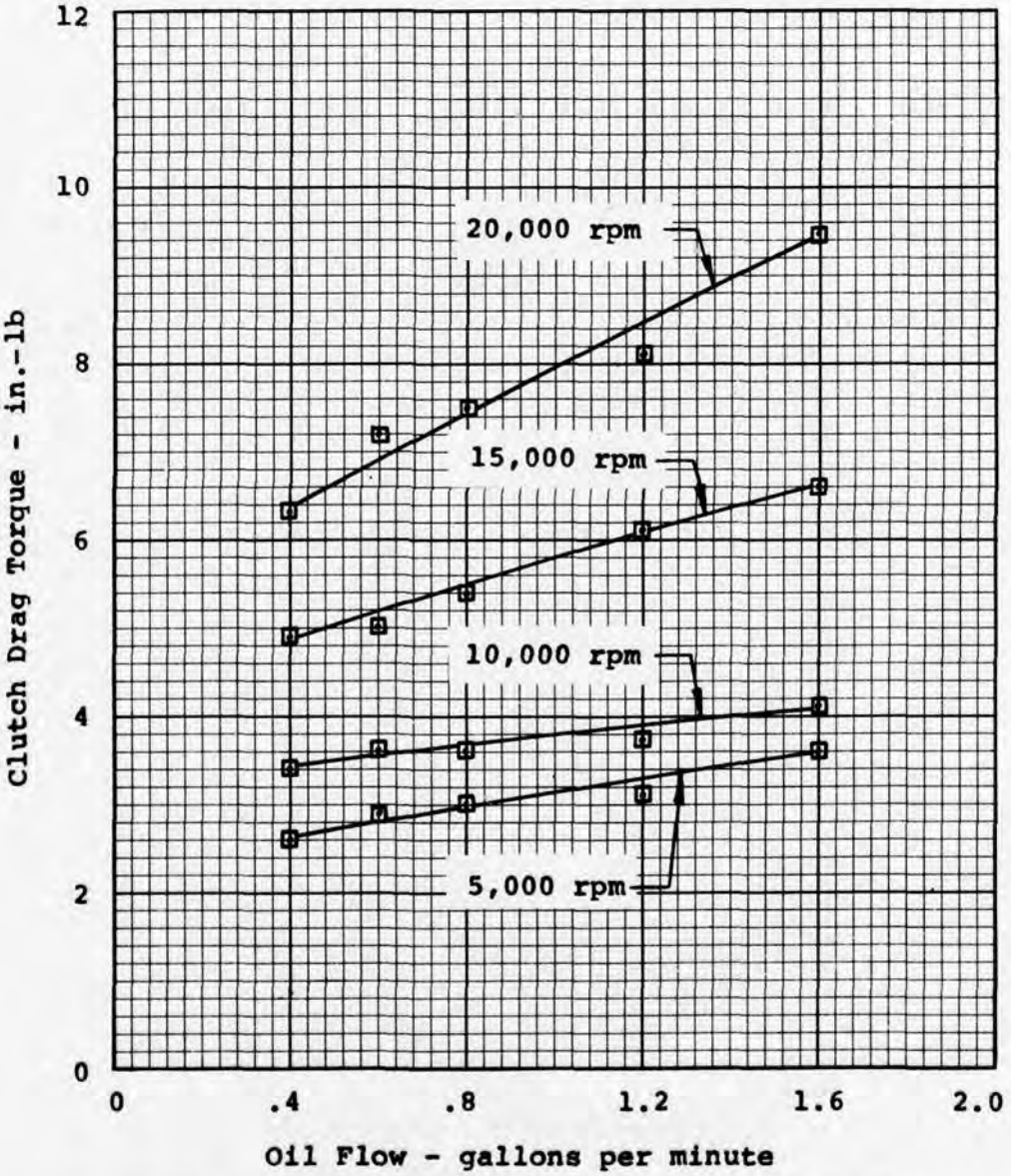

Figure 74. Drag Torque Versus Oil Flow at Various Full-Speed Overrunning Speeds (Input Fixed), Roller Clutch.

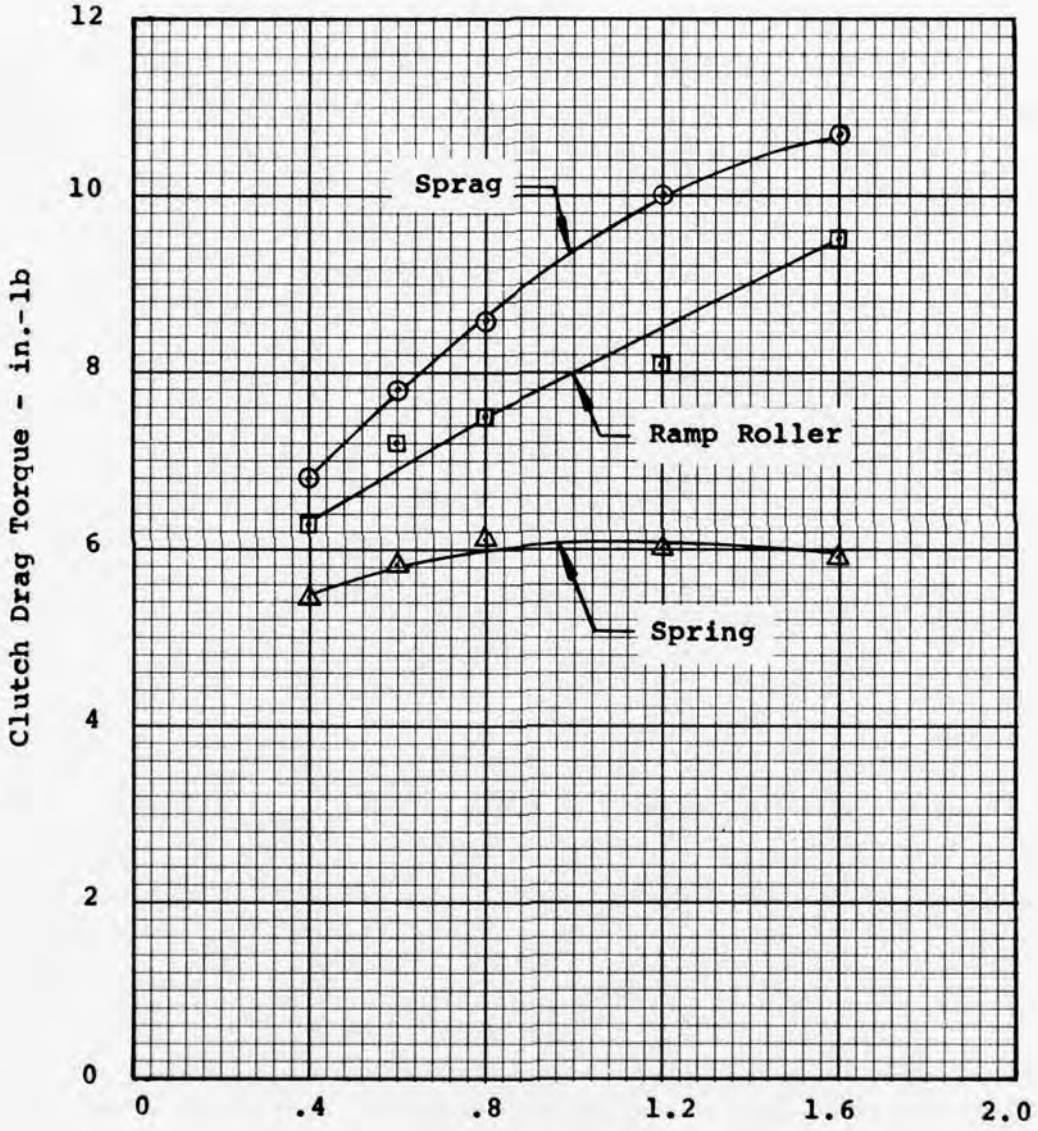

Figure 75. Drag Torque Versus Flow at 20,000-rpm Full-Speed Overrun for Spring, Sprag, and Ramp-Roller Clutches.

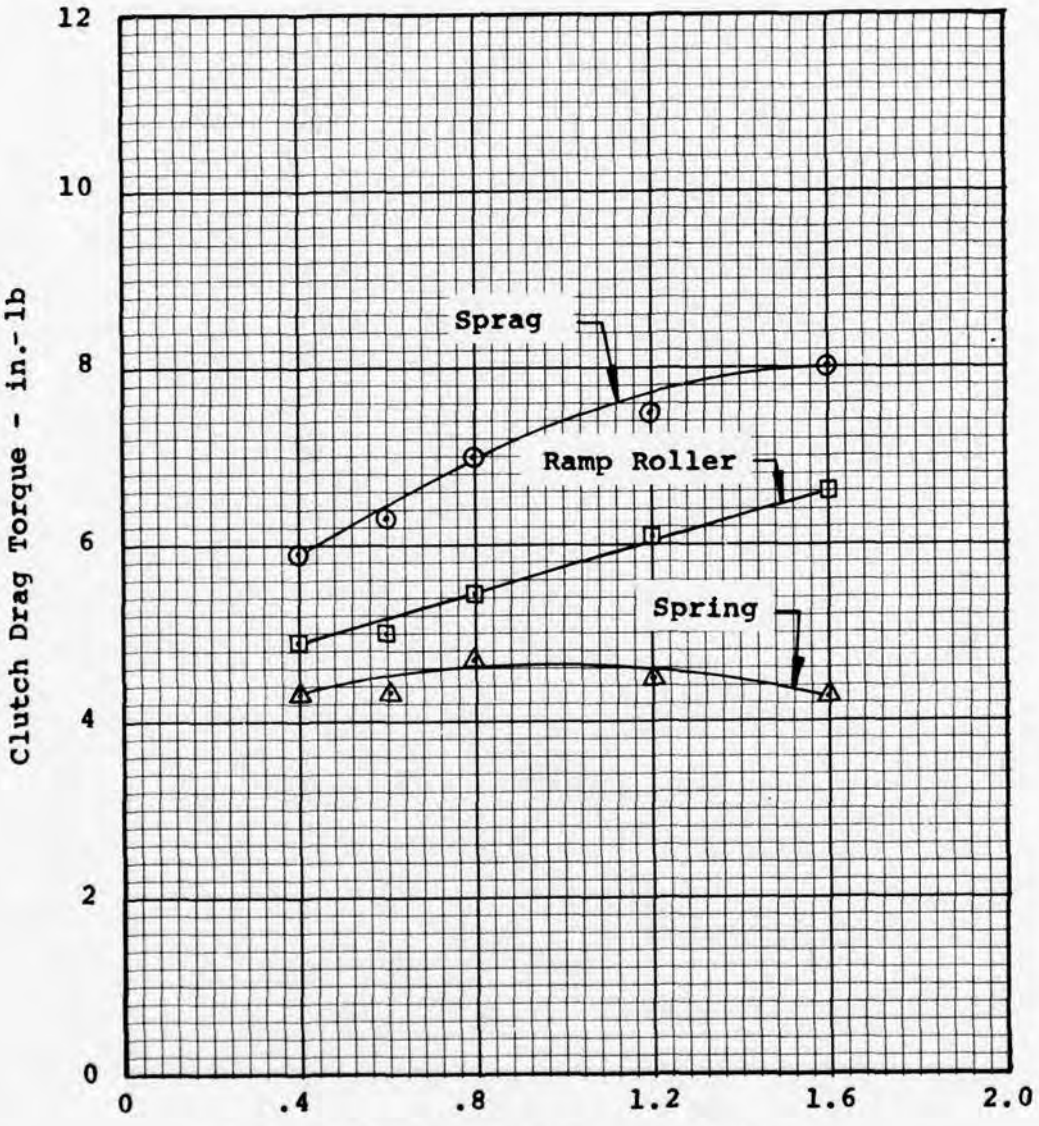

Figure 76. Drag Torque Versus Flow at 15,000-rpm Full-Speed Overrun for Spring, Sprag, and Ramp-Roller Clutches.

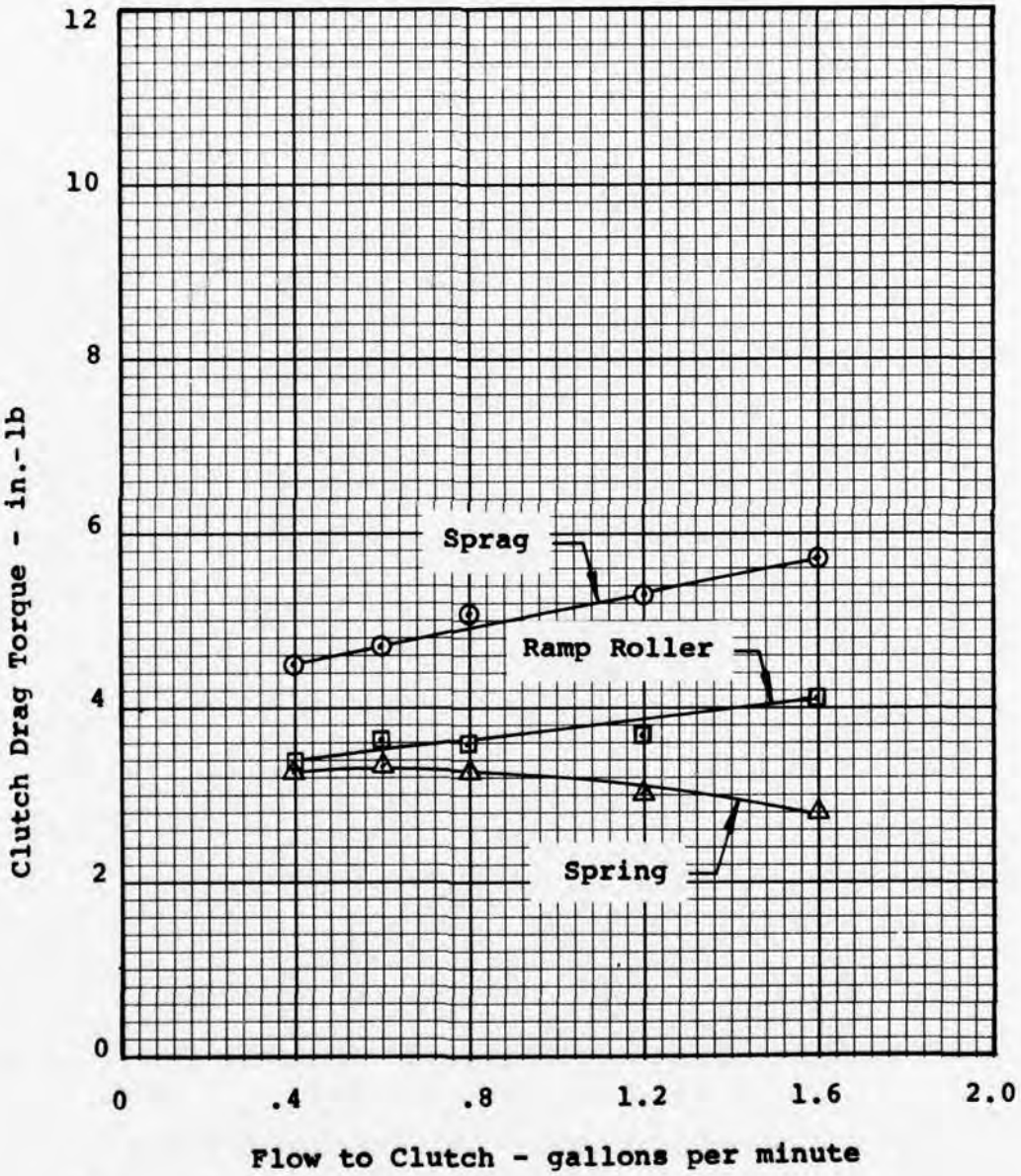

Figure 77. Drag Torque Versus Flow at 10,000-rpm Full-Speed Overrun for Spring, Sprag, and Ramp-Roller Clutches.

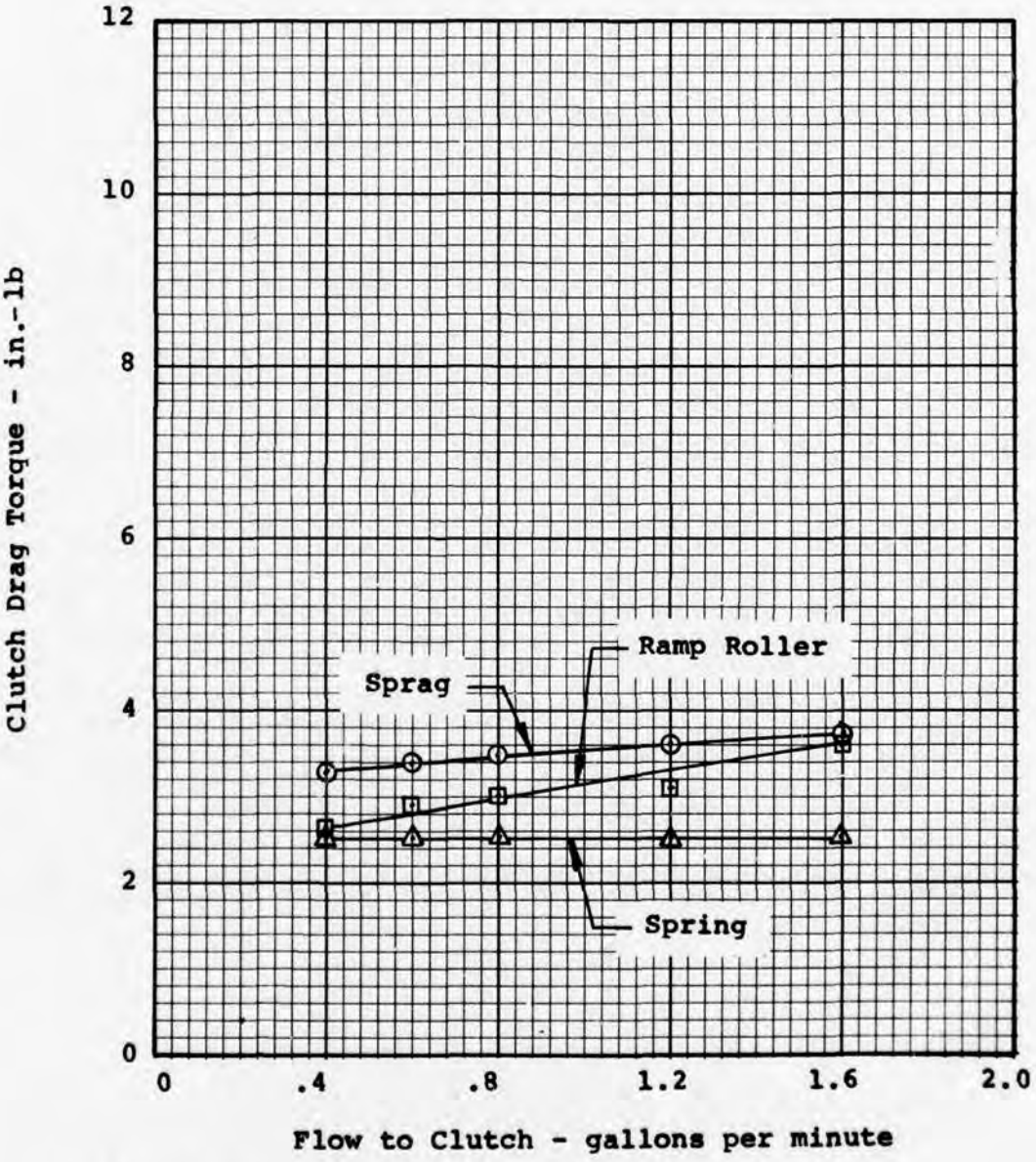

Figure 78. Drag Torque Versus Flow at 5000-rpm Full-Speed Overrun for Spring, Sprag, and Ramp-Roller Clutches.

Clutch race temperature versus flow for each clutch during full-speed overrun at 20,000 rpm is shown in Figure 79. The clutch race temperature for each type of clutch was measured at a point near the area of the race where the overrunning sliding or rolling occurs. In the spring clutch, this area was on the output housing's inner bore in line with the overrunning teaser coils. In the sprag clutch, the clutch race temperature was measured in the inner shaft directly beneath the sprag rubbing area, while in the ramp-roller clutch, the clutch race temperature was measured in the outer housing just over the roller rolling area. All race temperature measurements were made on the output housings of the clutches. At the chosen 100% flow condition of .8 gpm for each clutch, the clutch race temperature varied between approximately 215°F to 225°F. With the oil input at 205°F, this represents a temperature rise of between 10°F and 15°F. This is a desirable temperature rise in a helicopter overrunning clutch. With too little oil, the temperature rise will be excessive, while with too much oil, the parts will not be allowed to heat up. The 10°F- to 15°F-temperature rise was the basis for choosing .8 gpm as the 100% flow condition.

Figure 80 is a plot of clutch bearing temperature versus flow for all three clutches. The rise in bearing temperature with increased flow experienced by the roller clutch is probably from churning, whereas this condition did not occur in the sprag and spring clutches. Note that the bearing temperature of the spring clutch at 1.6 gpm is below the 205°F input oil temperature. Heat was being dissipated by conduction, convection, and radiation at a higher rate than it was being generated so that the oil was being cooled. Of course, this condition does not imply that no oil is needed for the spring clutch's bearings, for certainly lubrication is required whereas in this case cooling was not required. This unusual condition occurred because heat was being added to the oil supply to keep the oil inlet temperature between 195°F and 210°F.

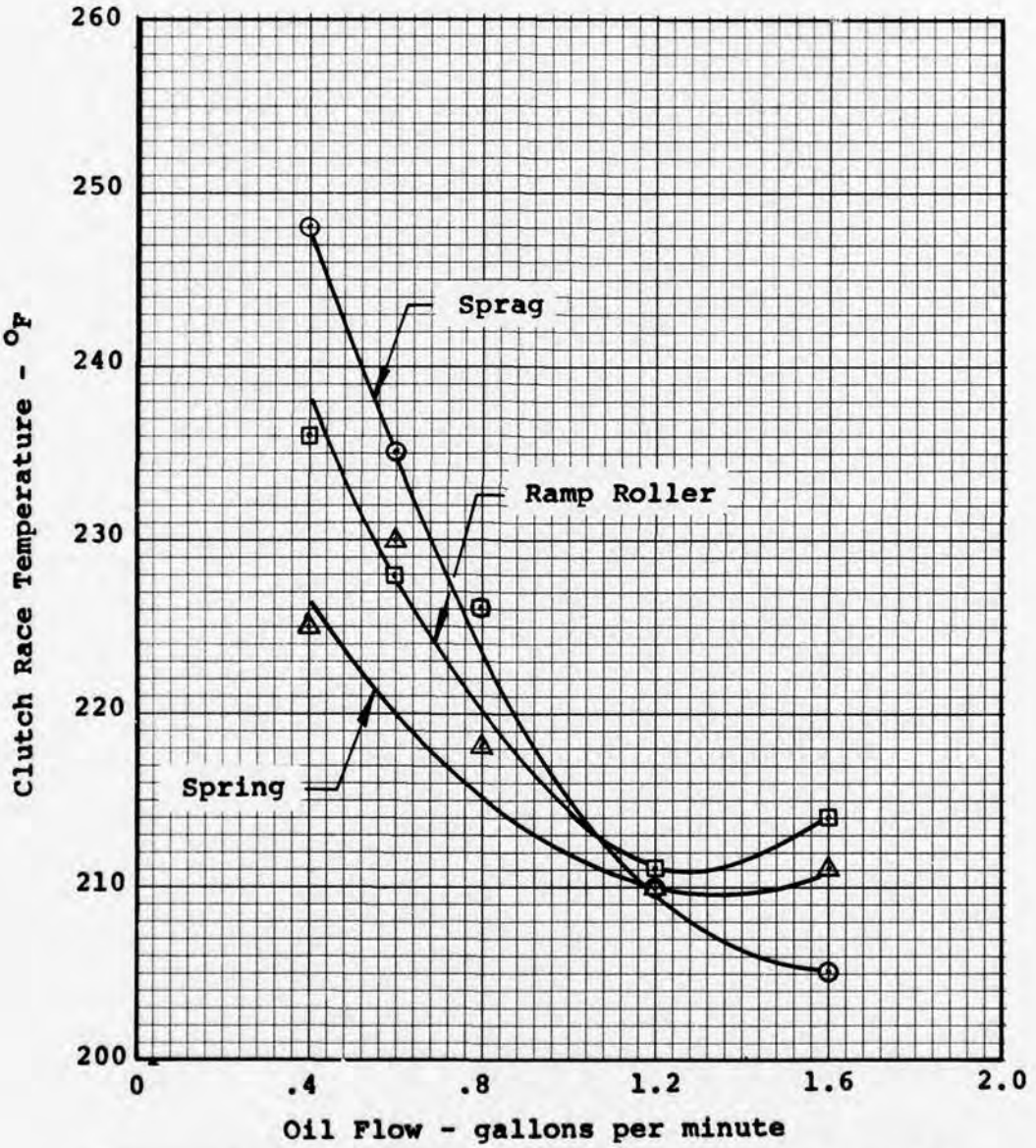

Figure 79. Clutch Race Temperature Versus Flow at Full-Speed Overrun for Spring, Sprag, and Ramp-Roller Clutches.

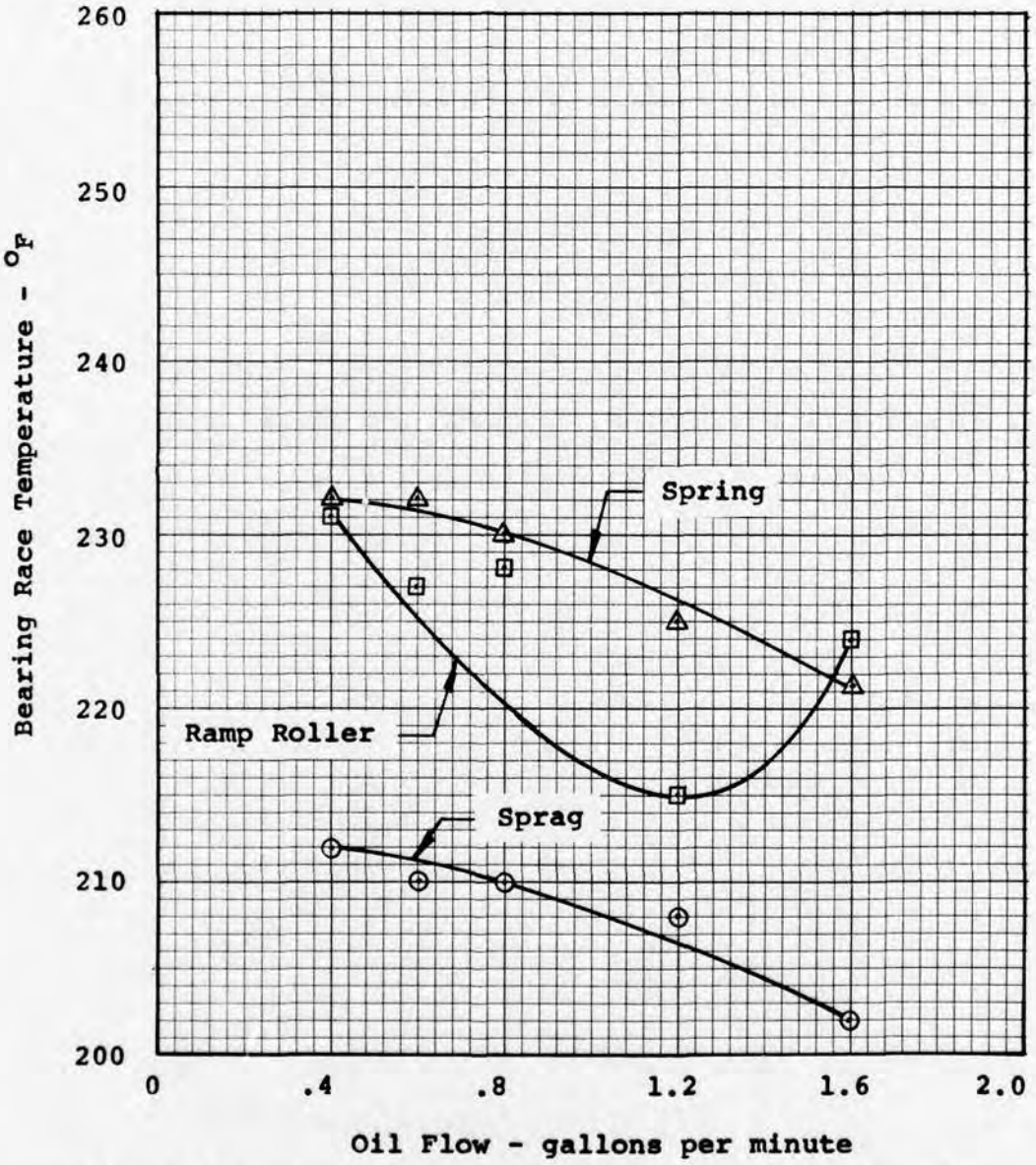

Figure 80. Bearing Race Temperature Versus Flow at Full-Speed Overrun for Spring, Sprag, and Ramp-Roller Clutches.

Differential-Speed Overrun Test Results

The purpose of the differential-speed overrunning test of Task I was to check out each clutch in the overrunning condition under the influence of centrifugal force on critical clutch elements, such as the spring coils of the spring clutch, the sprags of the sprag clutch, or the rollers of the ramp-roller clutch. Differential-speed overrunning is defined as overrunning clutch operation wherein both the input and output shafts are rotating. Since it is an overrunning test, the input is, of course, rotating at a slower speed than the output. The most common differential-speed overrunning that takes place in a helicopter transmission occurs when the transmission is rotated at full-speed by one engine and the other engine is at ground idle. This produces a situation where the freewheel unit on the engine that is at ground idle will have its input rotating at ground idle while the output rotates at full speed. In the overrunning tests conducted during Task I, the output shaft was rotating at 20,000 rpm and the tests were conducted with the input shaft at 50% (10,000 rpm), 67% (13,400 rpm) and 75% (15,000 rpm) of the output.

Differential-speed overrunning is a much more severe environment for wear of clutch rubbing surfaces than full-speed overrunning. In high-speed clutches, centrifugal forces produced on even the smallest rotating clutch elements can reach magnitudes that are greater than the forces produced during normal clutch operation under a torque load.

Task I differential-speed overrunning tests on each clutch consisted of a total of 9 hours of operation with 3 hours at the 50% condition, 3 hours at the 67% condition, and 3 hours at the 75% condition. At the conclusion of the 9-hour test run, each clutch was disassembled and inspected. The flow condition used was the 100% flow established during the full-speed overrunning tests: .8 gpm for each clutch.

The first clutch to be tested in the Task I differential-speed test was the spring clutch. The spring clutch was operated for 3 hours at 50% differential-speed overrun. At the completion of the 3-hour test, a speed rundown test was attempted wherein the input speed was varied from 15,000 to 5000 rpm to obtain drag torque data. During the speed rundown test when the clutch input speed was increased to approximately 15,000 rpm, the clutch had an inadvertent "engagement." The word engagement is in quotation marks because, with the input speed at 15,000 rpm and the output speed at 20,000 rpm, the clutch cannot truly "engage." What happened is that the clutch drag suddenly increased to the

point where the steam turbine driving the input and the steam turbine driving the output on the overrunning test facility could not overcome the torque differential across the clutch (from input to output), and hence, the turbines reached an equilibrium speed at approximately 17,000 rpm. In a helicopter transmission, this type of "false engagement" would not occur because the loads and inertias involved are much greater than in the steam turbine overrunning test stand.

Disassembly and inspection showed that some of the silver plating had chipped off the teaser coils of the clutch. These loose pieces of silver, in attempting to flow out of the clutch through the oil, had wedged between the output housing bore and spring outside diameter, causing the momentary increase in drag. Another factor that may have contributed to the false engagement was the drag on the end face of the teaser coils. Figure 81 shows the condition of the teaser coils after the test, while Figure 82 shows the output housing bore with some additional score marks to those incurred during the full-speed overrun test.

It was decided at this point that the ends of the spring should be replated and reground before testing continued.

With the replated spring installed, the differential-speed overrunning test of Task I was continued. In attempting to continue testing, the overrunning facility did not have the torque needed to disengage the input from the output to permit overrun. Disassembly revealed excess metal buildup on the spring O.D., causing excessive drag between the spring and the inside diameter of the output shaft. The components were cleaned and another attempt at operation ended with the same results. After examining the hardware, it was found that by loosening the preload between the clutch's inner support duplex bearings, the drag torque was considerably reduced and the "jamming" effect eliminated. Instead of the nominal 100-pound preload on the inner duplex bearings, the bearings were set at approximately .001 inch end play.

After assembly and resumption of testing, the spring clutch was once again able to disengage and operate in a normal manner. Three hours of testing at 67% differential-speed were completed. However, when the input speed was increased to 75% (15,000 rpm), the "false engagement" problem again reappeared. It was decided to complete the last 3-hour run at a somewhat reduced speed, and the test was completed at 72% differential (14,400 rpm). The condition of the spring at the completion of this test can be seen in Figure 83. As seen in the photographs, the new silver plating had again begun chipping. The problem may have been one of quality control. The spring of the spring clutch is a difficult

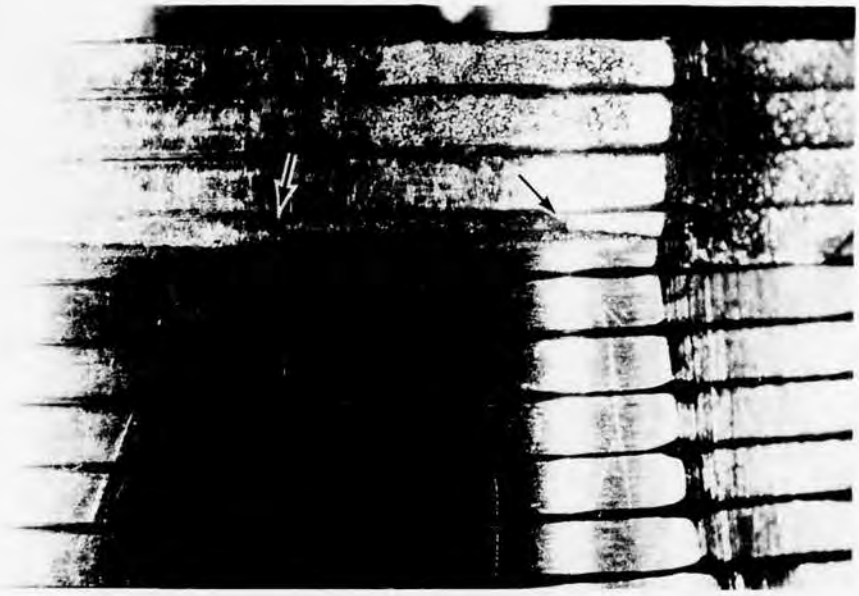

Figure 81. Spring Teaser Coils After 3 Hours of Differential-Speed Overrunning, Task I.

Figure 82. Spring Clutch Output Housing After 3 Hours of Differential-Speed Overrunning, Task I.

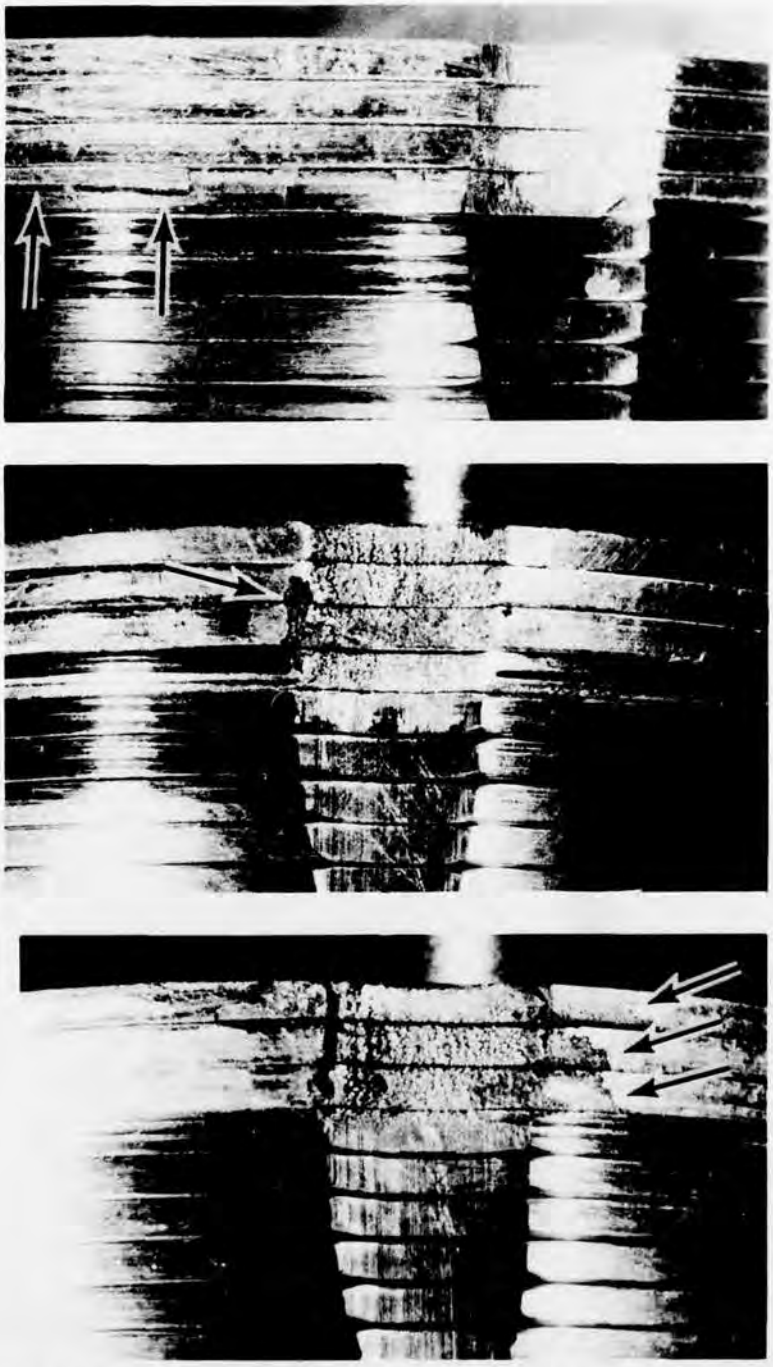

Figure 83. Spring Teaser Coils After Differential Speed Overrunning Test, Task I.

component to plate. Note the "bubbling" effect in the spring's teaser coil lubrication slots. This is an indication of poor plating quality. The effect of the silver-plating chipping was that in general the output housing sustained the greatest damage in the form of score marks on the inner bore, whereas the spring outside diameter was relatively free from scoring, as seen in Figure 84.

A new spring clutch was assembled and tested to determine if the false engagement problem was associated with only one clutch or would repeat on all clutches. The new clutch was operated in differential-speed conditions, and the false engagement occurred again with the new clutch at approximately the 75% differential-speed overrun condition. The components shown in Figure 85, namely the spring teaser coils and bronze bushings, were then coated with blueing and assembled again. The purpose of this test was to determine what areas of the spring and surrounding hardware were rubbing and creating the drag that was causing the false engagements. After a short run-in period, the spring clutch components were disassembled and inspected. Figure 86 shows the mating surfaces of two bronze bushings and the end of the spring with one of the bushings. Clearly, the scoring marks and removed blueing from the parts show that, although approximately .06-inch axial assembly clearance existed between the spring and the bushings, some degree of rubbing had occurred.

Examination of the problem of spring axial rubbing led to an alternate design for the spring clutch. The original design is at the top of Figure 87. In the original design, the arbor is attached to the input. Since the spring at rest has an interference fit with the arbor, the spring will remain in the same angular relationship to its arbor during overrunning, i.e., the spring will rotate with the input side of the clutch. During full-speed overrunning, the spring is at rest and rubbing takes place only on the teaser coils in contact with the output housing. During differential-speed overrunning, the spring rotates at the same speed as the input housing, with rubbing again taking place only on the teaser coils in contact with the output housing. A slotted spacer, guided on its outside diameter, is positioned between the end of the spring and the output housing. This spacer permits oil to pass through it to the spring's teaser coils and also acts as a sacrificial rubbing area for the spring during overrun. Relative motion is present between the overrunning end of the spring and this spacer. Therefore, if the spring touches the spacer in the axial direction during overrunning, drag is created.

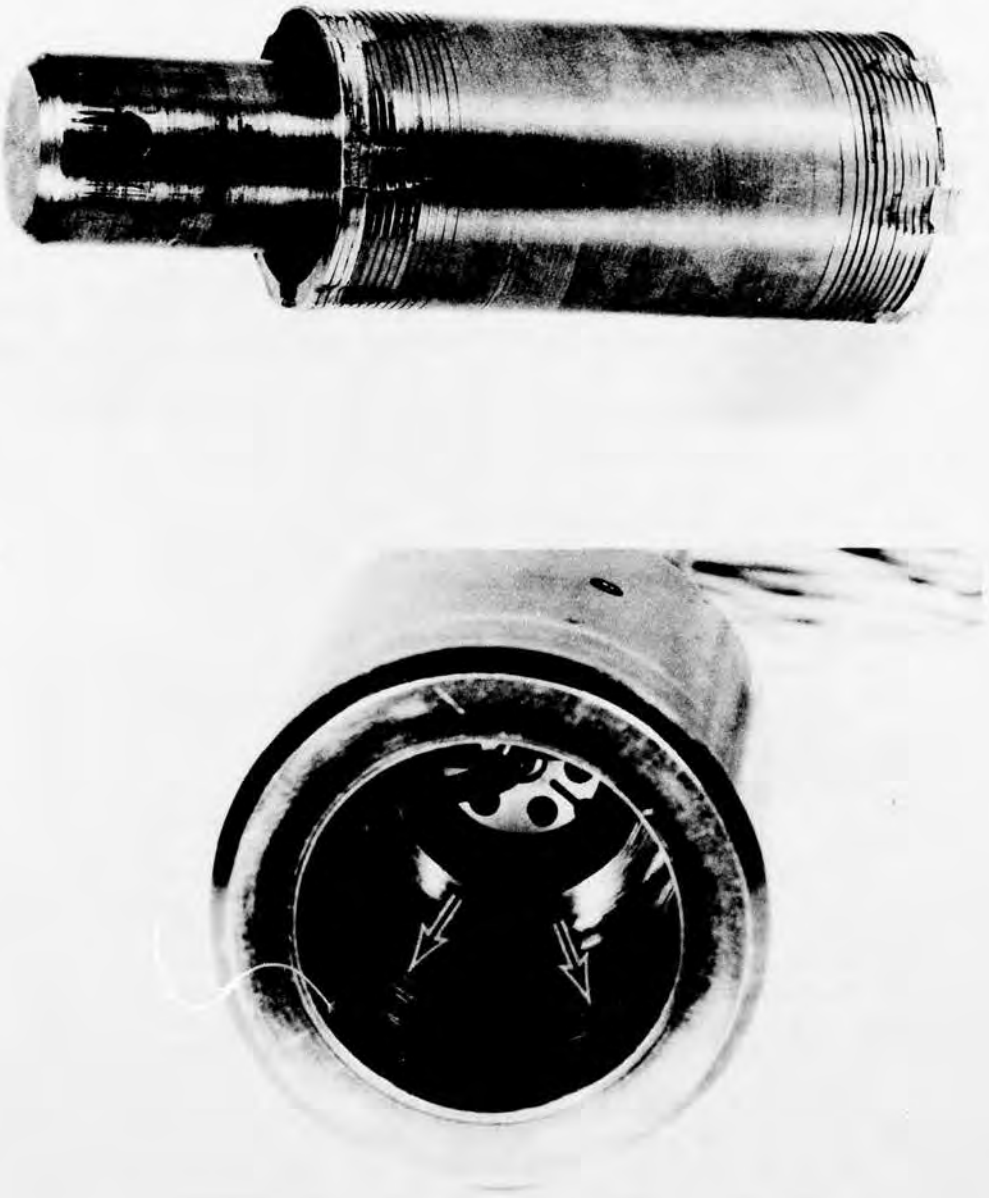

Figure 84. Spring and Output Housing After Differential-Speed Overrunning Test, Task I.

Figure 85. Spring and Spacers.

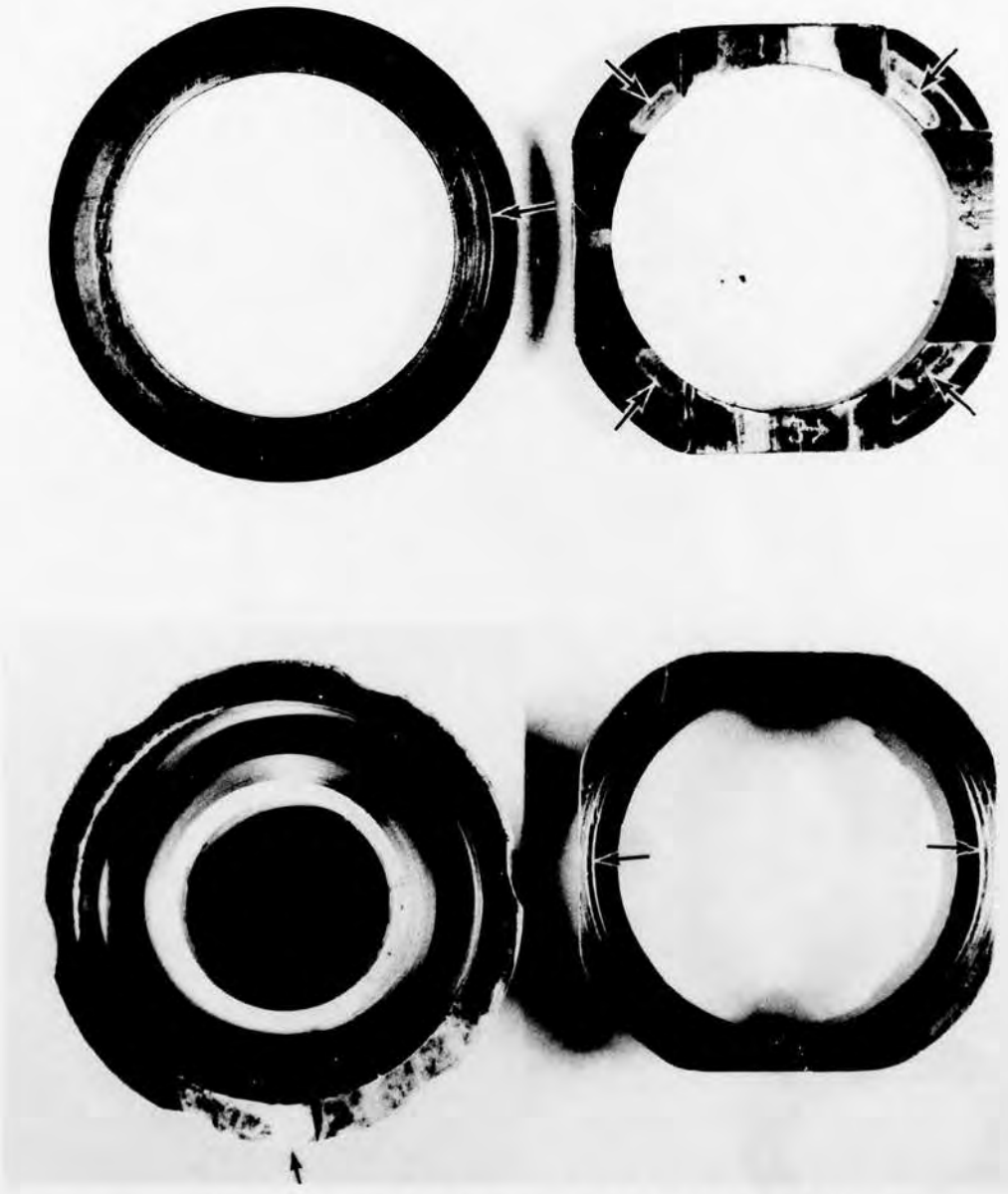

Figure 86. Spring and Spacers, End View.

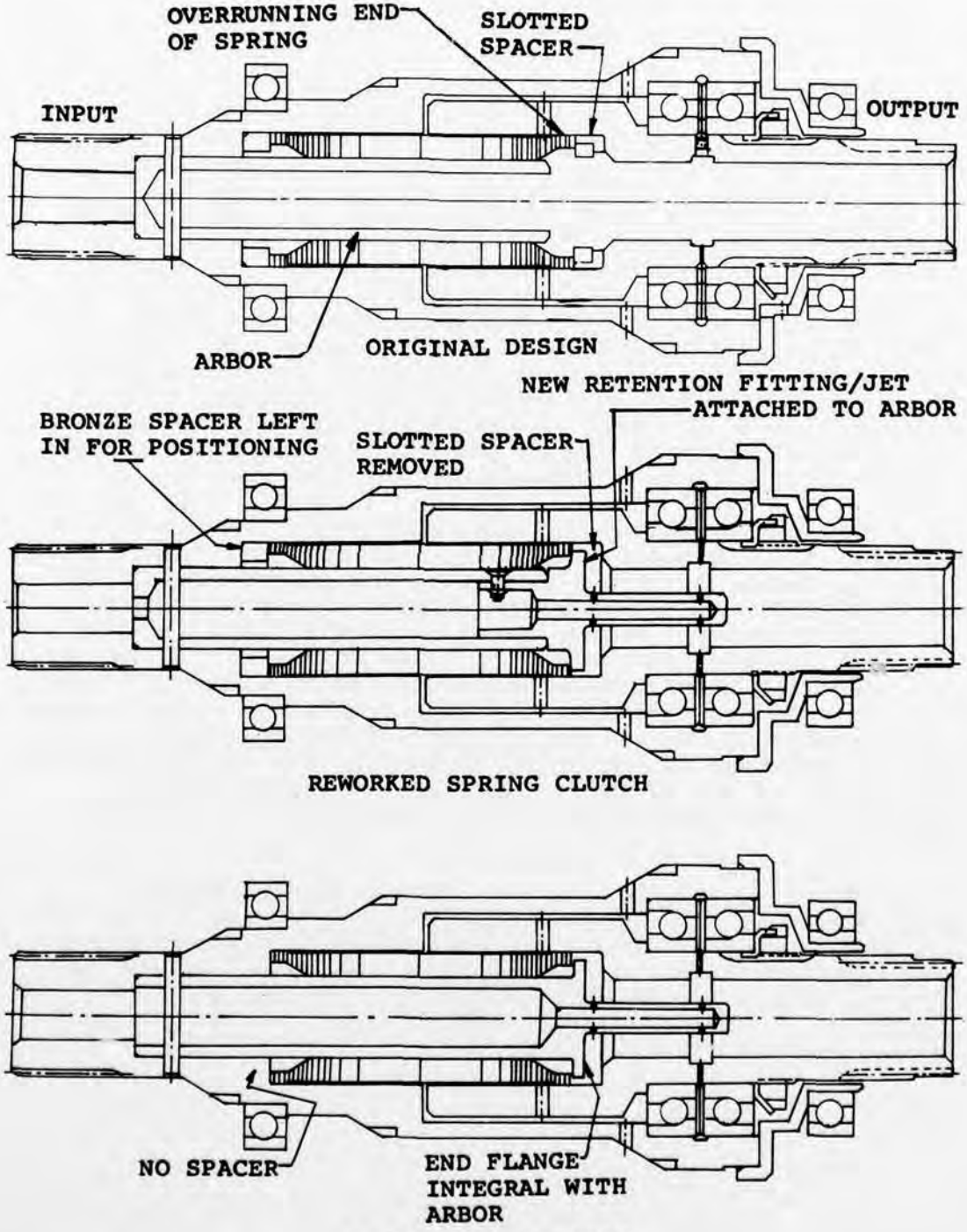

Figure 87. Spring Clutch Redesign With Flanged Arbor.

The object of the redesigned spring arbors shown in the center and the lower parts of Figure 87 is to eliminate the rubbing between the end of the spring and the adjacent bushing. This is accomplished with a flange on the spring arbor, as shown in Figure 87. The flange on the arbor restrains the spring axially and, most importantly, does not permit any relative motion between the end face of the spring and the output housing except on the outside diameter of the teaser coils. The center design of Figure 87 shows the modified clutch tested in this program. The flanged arbor was a reworked version of the original spring arbor. The modification consisted of drilling a lubrication hole on the input side of the clutch and riveting the flanged piece to the arbor. The design shown at the bottom of Figure 87 shows the flange and arbor as a single piece as it might be made in a production model. It was felt that with the elimination of the friction on the end faces of the spring and the bushings the spring clutch drag torque would be reduced and the false engagement problem would be reduced or eliminated.

The redesigned spring clutch was fabricated, assembled, and tested in the overrunning facility. At all input shaft speeds during differential-speed operation, the drag torque of the flanged-arbor spring clutch was reduced to approximately one-half of that of the bronze-spacer-design spring clutch. No difficulty was experienced in operation up to 82% (16,400 rpm) of output when a false engagement again occurred. However, this test showed that the spring with the flanged arbor was the superior design for reducing clutch drag, and it was decided that this design would be used in all further testing. The spring and the arbor are shown in Figure 88 as they appeared at the conclusion of the retest with the flanged arbor.

It was discovered later that the flanged-arbor design was inferior to the bronze-spacer design for cyclic load carrying capability, and since load carrying was considered more important than overrunning drag, the redesign with the flanged arbor was discarded in favor of the original configuration. This is fully discussed under the TASK II TEST RESULTS section of this report.

Figure 88. Spring and Flanged Arbor of Redesigned Spring Clutch.

The false-engagement problem was eventually traced to another source. Figure 89 shows score marks located on the spring's outside diameter and near the central section of the spring. These marks are attributed to differential motion between the spring and output housing. The question then arises as to why the spring O.D. should score whereas the spring teaser coils, which have higher rubbing pressure, do not score. The answer lies in the lubricant flow path. As the input shaft speed increases, the centrifugal force acting on the spring causes the spring to expand outward. At the speed where the false engagement occurs, the center coils rub the output housing bore and, because there is no lubrication to this section of the spring, the O.D. scores. Figure 90 shows that the lubricant can escape prior to reaching the sections of the spring that scored. In fact, when the spring expands onto the output housing bore, the spring forms a seal that will not permit lubricant to pass to the center coils. Figure 90 also illustrates a solution using slots in the output housing bore to channel oil to the center spring coils (see Reference 1 for a more detailed discussion of spring clutch lubrication.

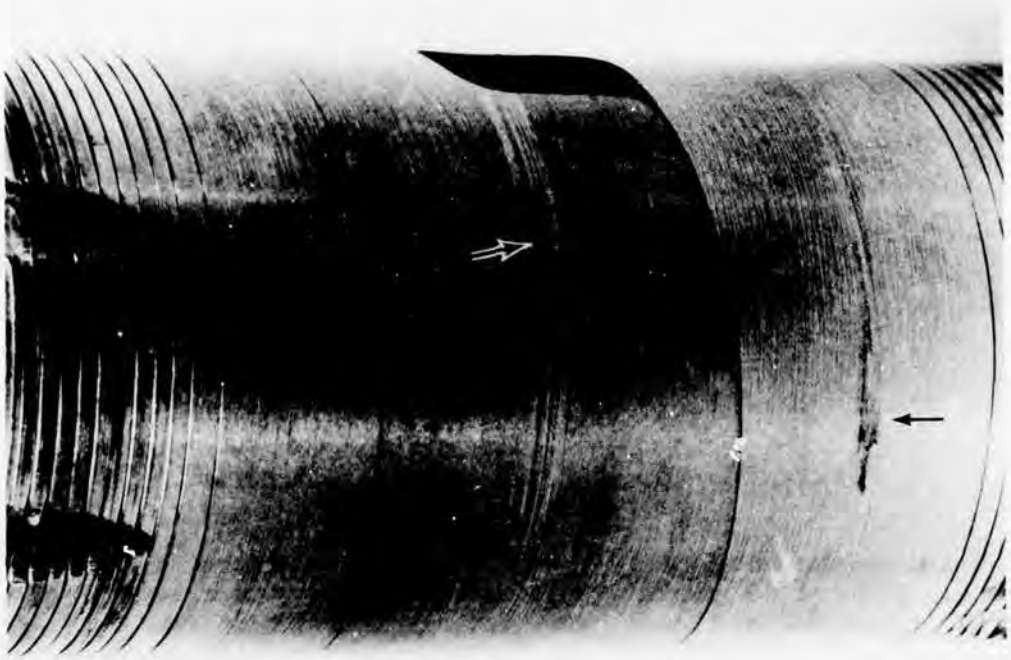

Figure 89. Spring Showing Score Marks From Contact With Output Housing.

Reworking the test hardware to add slots to the output housing bore was not feasible since the housing was hardened. Moreover, the test schedule did not permit the manufacture of new output housings so it was decided to continue testing with the same parts.

It should be pointed out that although the problem of the false engagement was consistent during the Task I differential-speed overrun tests, it was not considered a serious drawback. In a helicopter transmission and also in the dynamic turbine test stand of this program, the inertias involved are so large that any additional drag created by the spring rubbing on its O.D. would be negligible and would in no way affect the operation of the clutch in both the overrunning and the driving modes. The spring and the housing would become scored, of course, but the spring could function in this manner for many millions of cycles before any problems would be encountered.

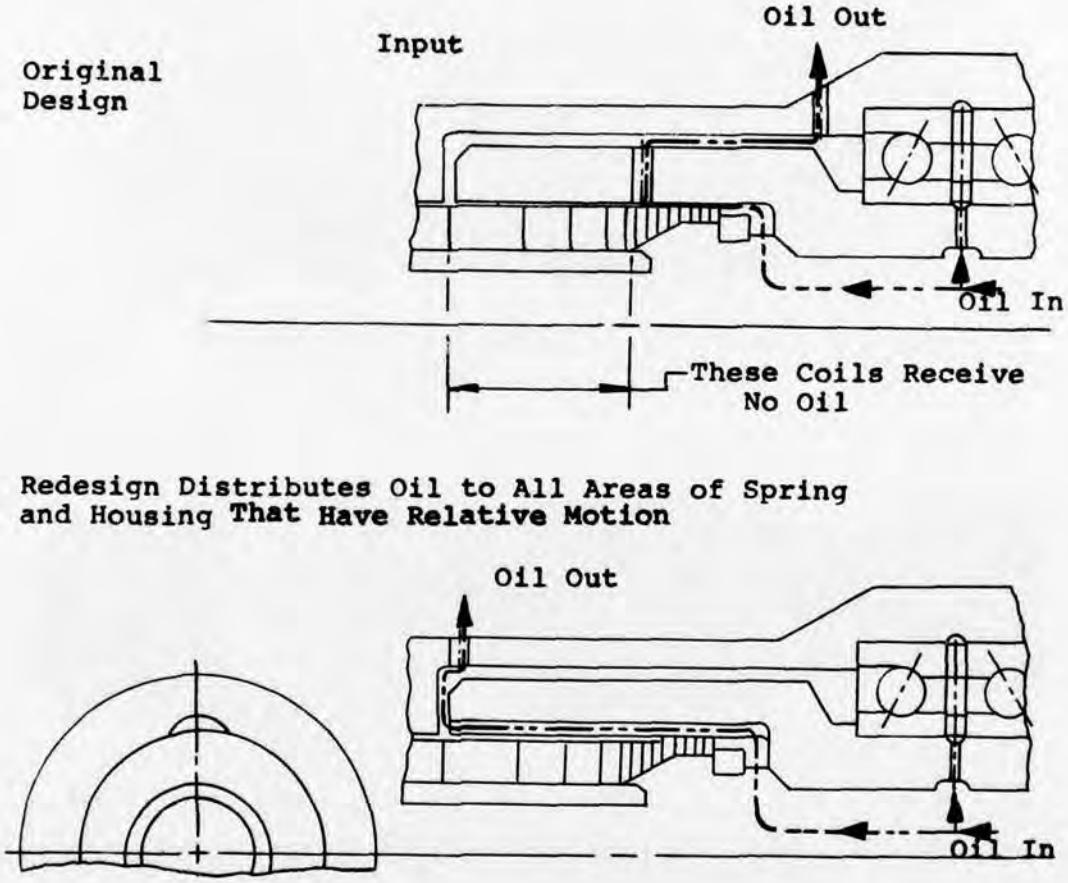

Figure 90. Spring Clutch Lubricant Flow Paths.

The second clutch to be tested in the Task I differential-speed overrunning test was the sprag clutch. At the 100% flow condition of .8 gpm for the sprag clutch, differential overrunning tests were conducted for 3 hours at each of the three differential overrunning conditions: 50, 67, and 75% (10,000, 13,400 and 15,000 rpm input speeds and a 20,000 rpm output speed). This test of the sprag clutch was run without incident. Figures 91, 92, and 93 show the conditions of the outer race, the inner shaft, and a typical sprag, respectively, at the conclusion of the test. The marks on the outer race at the sprag contact points were of negligible depth. The inner shaft had sustained race wear in the form of tangential

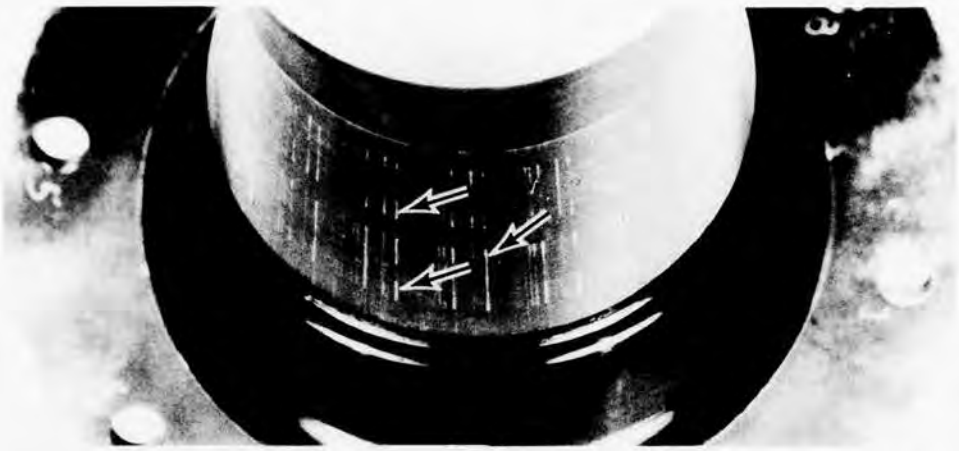

Figure 91. Sprag Clutch Outer Race After Differential-Speed Overrunning Test, Task I.

Figure 92. Sprag Clutch Inner Shaft After Differential-Speed Overrunning Test, Task I.

Figure 93. Typical Sprag Clutch Sprag After Differential-Speed Overrunning Test, Task I.

score marks to a depth of .0002 inch, which is well within the permissible wear of approximately .001 inch for that unit. The typical sprag shown had an average bandwidth of wear of approximately .015 inch, which, when converted to depth of wear, is less than .0002 inch.

The ramp-roller clutch was then subjected to the Task I differential-speed overrun test. Lubricant was fed to the clutch at .8 gpm (100% flow condition) for 3 hours at each of the three differential overrunning conditions: 50, 67, and 75% (10,000, 13,400, and 15,000 rpm input speeds and a 20,000-rpm output speed). At the start of the 75% overrun test, the ramp-roller clutch experienced a momentary torque increase, creating a false engagement similar to that experienced by the spring clutch in the full-speed overrun tests. As a result of this torque increase, the torquemeter shaft strain-gage bridge yielded permanently. Calculations showed that the yield strength of this shaft was approximately 18 inch-pounds of torque.

The 75% differential-speed overrun test on the ramp-roller clutch was continued with the input speed at 14,400 rpm (72%) in lieu of 15,000 rpm (75%), and the remaining test time was completed. After the test, the ramp-roller clutch was disassembled and inspected.

The most notable outcome of the differential-speed test was found on the cam shaft, as shown in Figure 94. For proper operation of a ramp-roller clutch in the overrunning mode, the overrunning wear area should be confined to a small bandwidth on the cam flat in the area where the roller contacts the cam flat. A small bandwidth of wear indicates that the rollers are in intimate contact with the outer housing and cam and have remained in contact for most of the test. Close inspection of the cam flats shown in Figure 94 shows that the bandwidth of wear on the flats is not in a concentrated line but extends from the start of the roller undercut pocket to the normal position, approximately one-third of the way up the flat. This wide bandwidth of contact indicates that the rollers along with the roller retention carrier were "chattering"; i.e., they were not in intimate contact with the outer housing and the cam flat but were oscillating back and forth, forcing the spring and plunger assembly away from its proper operating position. Further evidence of overrunning in several different positions is seen in the photograph of the leading edge of the retention cage roller pocket in Figure 95. Figure 96 shows the outer housing bore. The flake-like particles are the result of a mixture of hot oil and fine metal from the rollers and the carrier which tend to gather in that area of the outer housing (oil drain is from the opposite side of rollers).

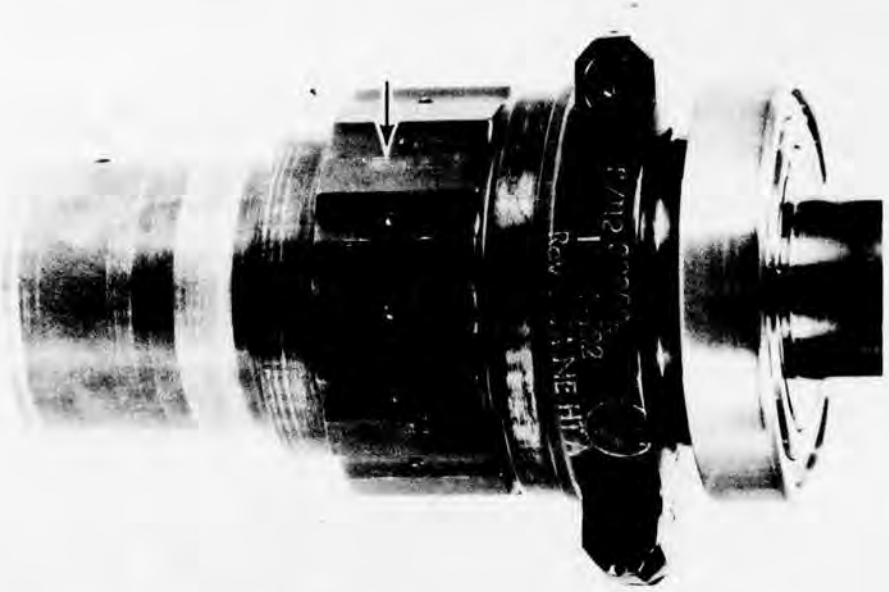

Figure 94. Ramp-Roller Clutch Cam Shaft After Differential-Speed Overrunning Test, Task I.

Another peculiar type of wear that occurred during the overrunning testing was wear on the roller end faces. This wear was confined to only three rollers, which were adjacent to one another. The worst roller is shown in Figure 97, while the retention cage is shown in Figure 98. The indicated slots show the signs of contact on the end roller faces. Slot number 4 also has some signs of wear, but to a much lesser extent.

The rollers were worn to an average depth of approximately .0005 inch on the diameter. It was decided at this time to try to correct the roller "chattering" by using a heavier spring in the spring and pin assembly. A heavier spring would apply a larger load to the pin and spring assembly, which in turn would aid in keeping the rollers in contact with the outer housing and cam shaft. The original spring, which was .016-inch-diameter wire, had a force of 1.5 pounds in the installed (overrunning no-load) position; whereas, the new spring, which was .018-inch-diameter wire, had a force of 2.1 pounds in the overrunning position. The roller-retention cage and rollers were also replaced with new components, and a differential-speed retest was conducted.

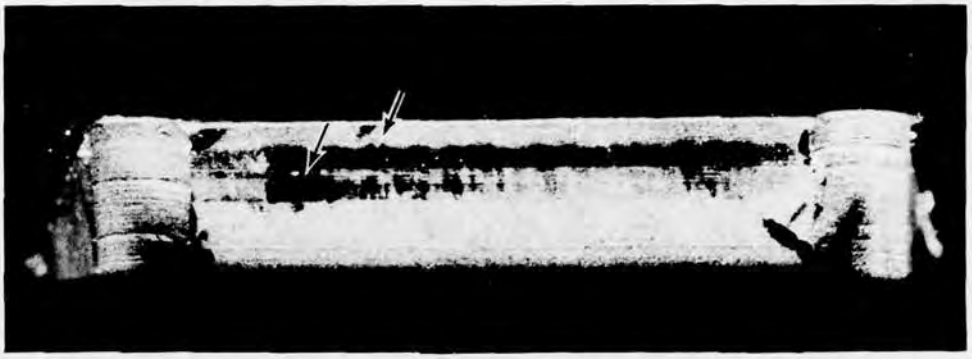

Figure 95. Roller Pocket of Roller Retention Carrier After Differential-Speed Overrunning Test, Task I.

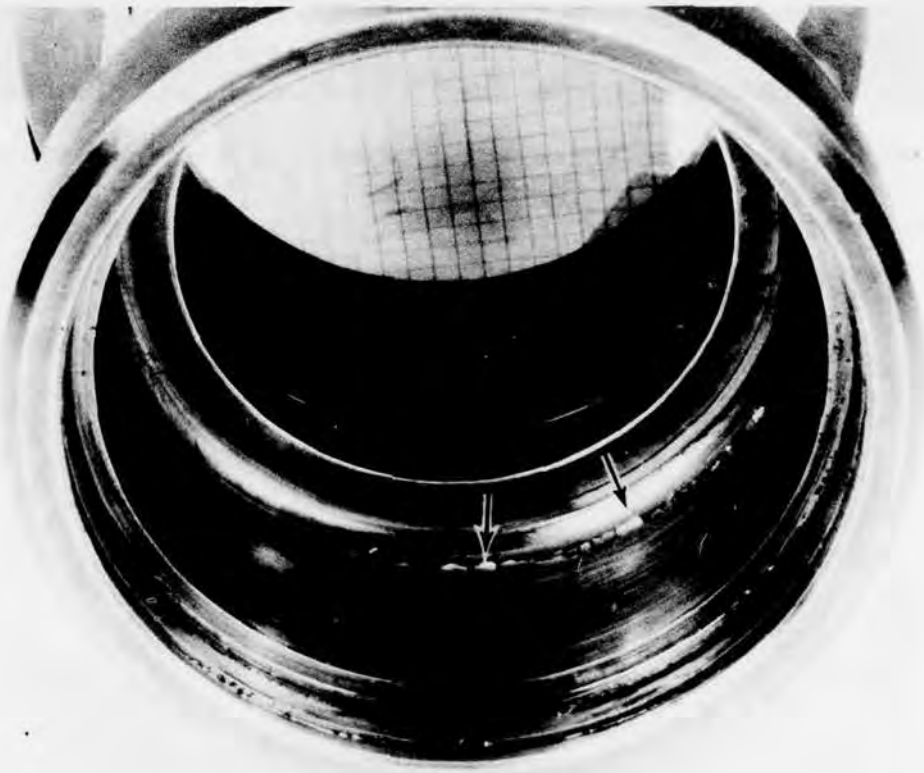

Figure 96. Ramp-Roller Clutch Outer Housing After Differential Speed Overrunning Test, Task I.

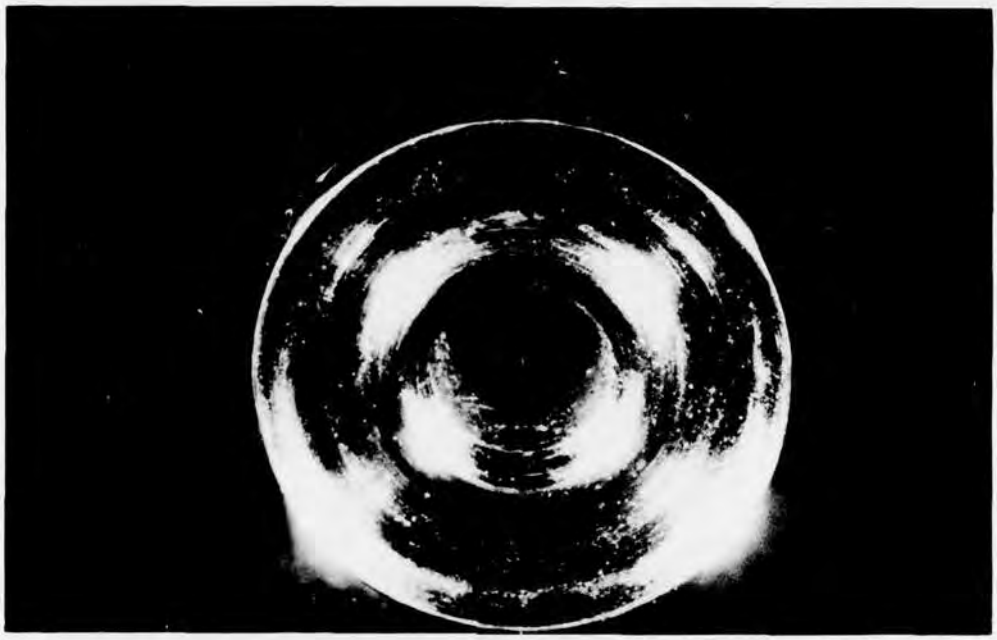

Figure 97. Ramp-Roller Clutch Roller, End Face Wear.

Figure 98. Roller Carrier After Differential-Speed Overrunning Test, Task I.

The retest consisted of 1 hour at 50% differential-speed, 1 hour at 67% differential-speed, and 1 hour at 75% differential-speed overrunning. At the conclusion of the retest, the ramp-roller clutch was disassembled and inspected. The cam shaft flats now showed new signs of wear at different contact points, as shown in Figure 99. Some degree of roller chattering and vibration was present, but to a much less extent, which showed that the heavier springs helped solve the problem. The roller end wear problem was showing up again, but to a much lesser extent, as seen in Figure 100. The typical roller seen in Figure 101 did not exhibit the surface roughness seen previously, and the wear pattern on the carrier was confined to a small bandwidth. From this evidence, it was concluded that the heavier spring had helped correct the roller chattering problem, and it was decided to use this configuration for further testing.

The ramp-roller clutch retest completed all overrunning tests of Task I. The results of drag-torque measurements are presented in Figure 102. Drag torque is induced in overrunning clutches by viscous frictional drag and by centrifugally-induced rolling resistance. During differential-speed overrunning, when the input shaft speed is low, viscous effects are maximum because the difference in shaft speeds is maximum. As the input shaft speed increases, viscous friction decreases until the time when the input shaft speed is equal to the output. The opposite is true with rolling resistance. When the input shaft is fixed, as in full-speed overrun, rolling resistance will have a fixed value. As the input shaft speed increases during differential-speed overrun, rolling resistance will increase because centrifugal force acting on the spinning components will increase. As with the viscous friction, rolling resistance is zero when the input and output shafts are rotating together in a locked position.

As seen in Figure 102, the ramp-roller clutch follows the theoretical drag curves in the predicted manner by starting at a fixed value, increasing in drag to about one-half speed and then decreasing to zero drag at the locked position. However, the sprag clutch did not follow the theoretical drag curve for sprag design. With increasing input shaft speed, the sprag clutch drag steadily decreased. The conclusion is that the viscous effects were so large as to completely overcome the rolling (or sliding in the case of the sprag clutch) effects of drag. The decreasing drag torque with increasing speed is an undesirable condition. The sprag should have enough centrifugal engaging moment to overcome sliding resistance, and the drag curve for differential-speed overrun should exhibit a shape similar to that of the ramp roller. Failure to do this may result in a condition where the sprag can lose contact with the inner race and be unable to produce

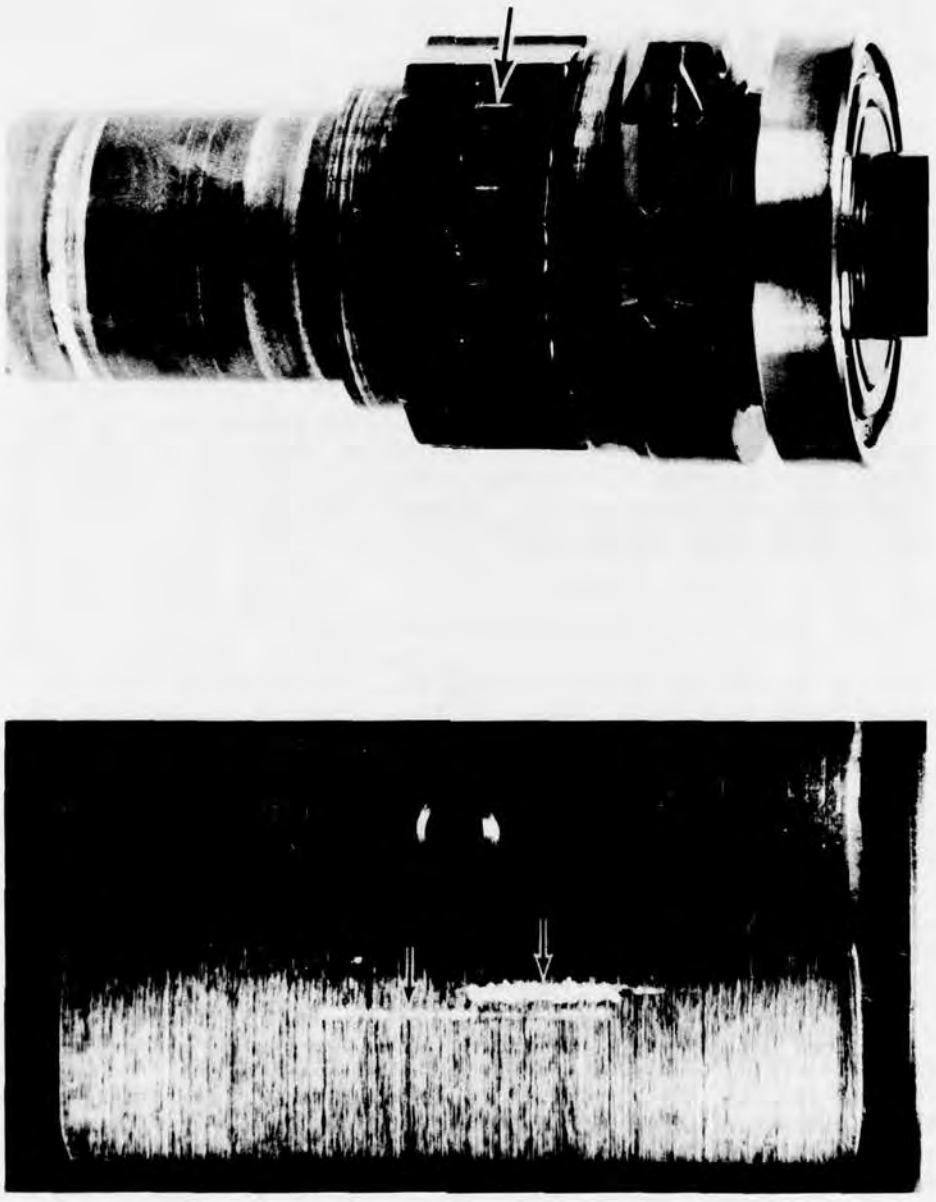

Figure 99. Ramp-Roller Clutch Cam After Differenctial-Speed Retest.

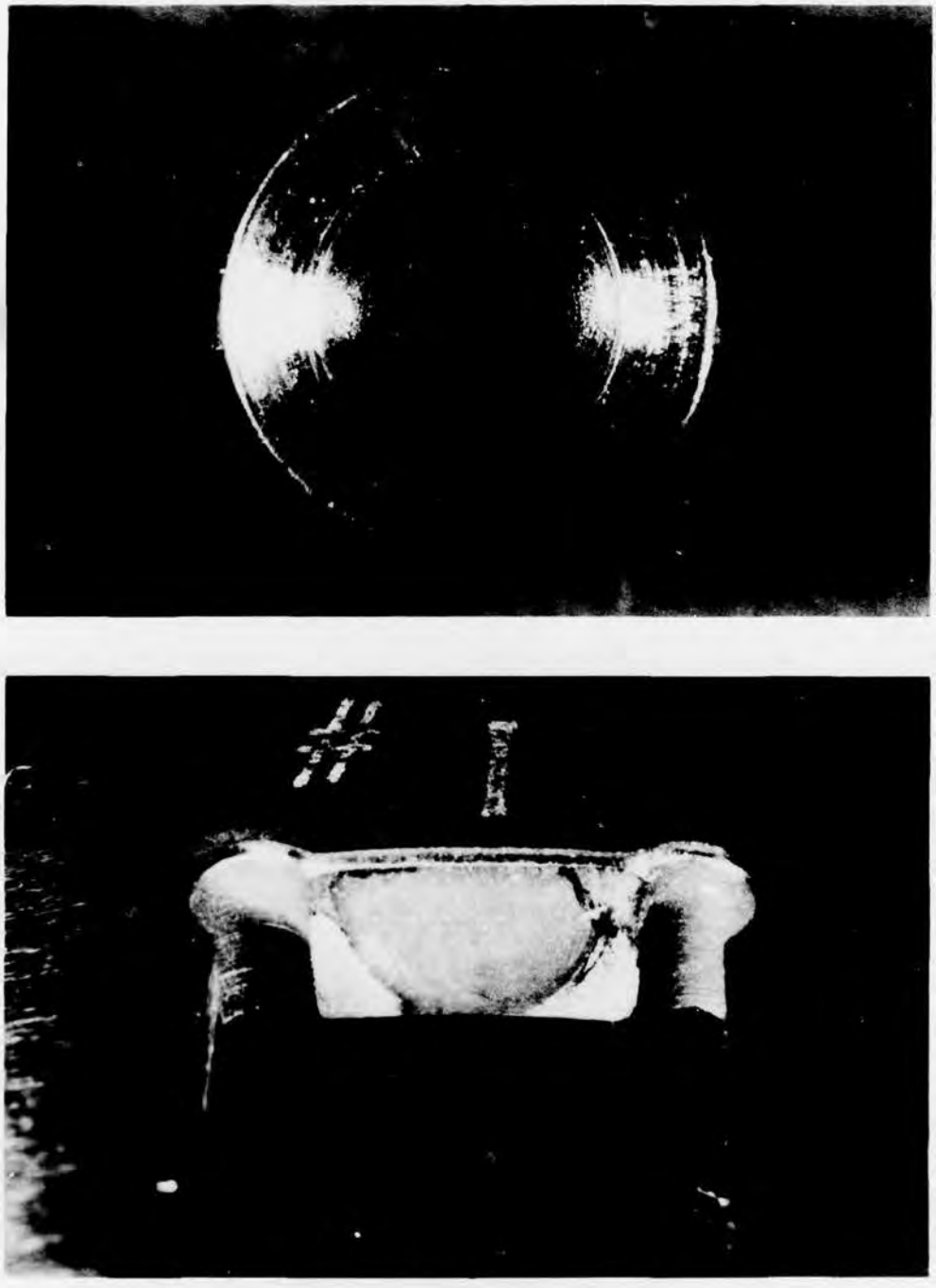

Figure 100. Roller End Wear and Wear in Corresponding Slot in Cage After Differential-Speed Retest.

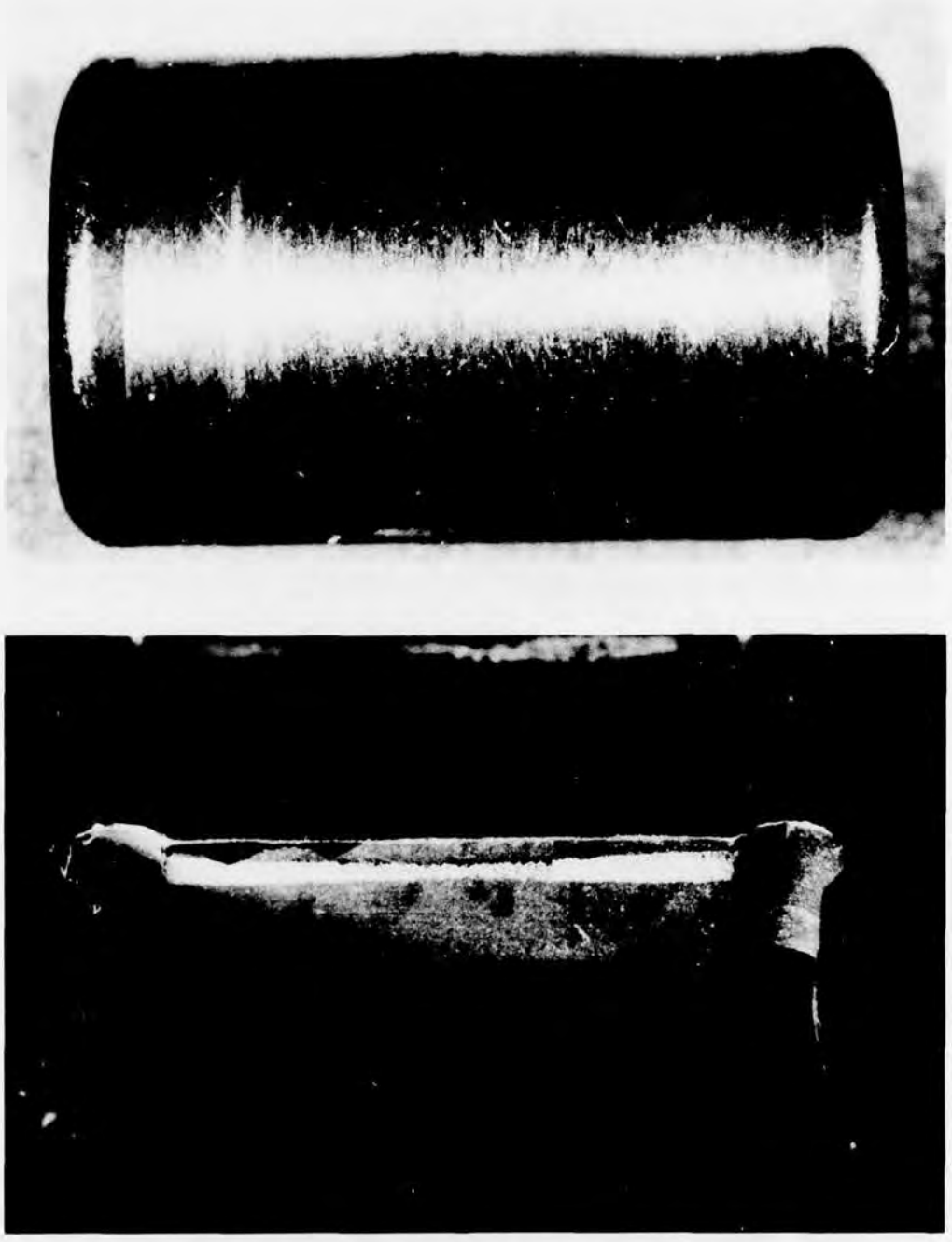

Figure 101. Typical Roller and Cage Slot Pattern After Differential-Speed Retest.

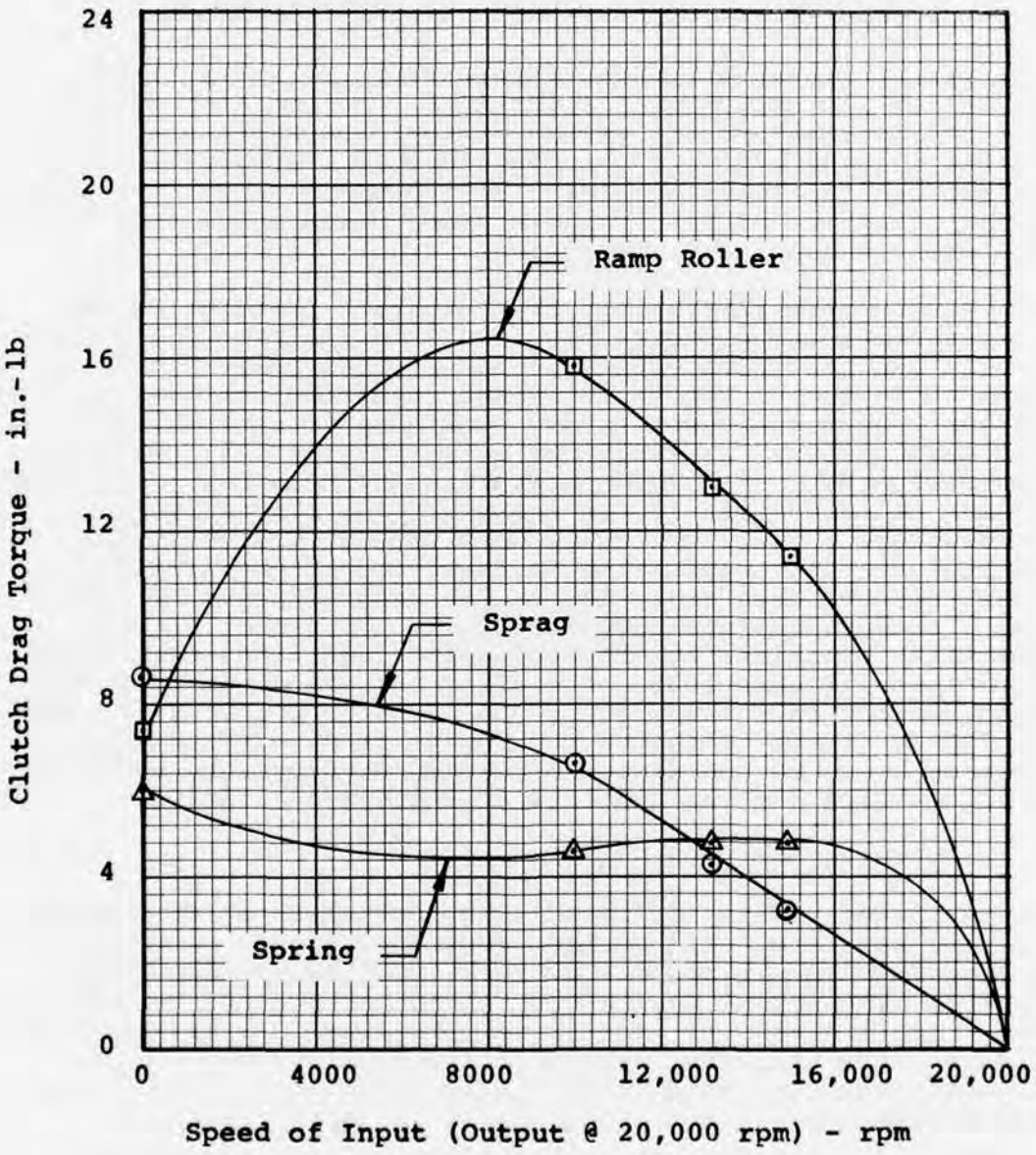

Figure 102. Drag Torque Versus Input Speeds With Output at 20,000 rpm for Spring, Sprag, and Ramp-Roller Clutches.

high-speed engagements. The sprag clutch was able to engage at high speed in all of the normal testing but did actually fail to engage in the cold temperature environmental test. The results are discussed in that chapter of the report.

The spring clutch exhibited a relatively flat drag torque curve for all overrunning conditions. Centrifugal effects are not as important in the spring clutch, and therefore, the sum of the sliding resistance and viscous drag effects remains almost constant throughout the entire speed range. This is a typical feature of the spring clutch, which makes it a candidate for even higher speed operation.

The clutch race temperature is shown as a function of the differential-speed overrunning condition in Figure 103. The spring and the sprag clutches both exhibit temperature versus time curve that exhibits a minimum condition, whereas the ramp-roller clutch race temperature continues to decrease with increasing flow. It should be noted that in the spring and sprag clutches, the race temperatures between input shaft speeds of 10,000 and 15,000 rpm are below the oil inlet temperatures; i.e., the races were cooling the oil. This is because the heat generation in these conditions is actually less than the heat rejection by the natural means of convection, conduction, and radiation. The phenomenon can be partially explained by the decreasing drag with input speed functions (Figure 102). A similar situation was prevalent with bearing race temperature, as shown in Figure 104. Here, the sprag clutch exhibited the lowest race temperatures, perhaps owing to the straddle-mounted arrangement, which is a good design for the bearings of the sprag clutch.

Dynamic Load Test Results

Dynamic load testing of Task I was conducted on the dynamic turbine test rig. The turbine test facility is comprised of a Lycoming T53 gas turbine engine, which drives the test clutch. The output of the test clutch is splined to a flywheel whose polar moment of inertia is 5373 lb-in.^{2} This moment of inertia simulates the inertia of the UTTAS's rotor head, transmission, and main rotor blades reflected to the engine's input speed by

$$Iin = Irh\left[\frac{rpmrh}{rpmin}\right]^2 + Ib\left[\frac{rpmb}{rpmin}\right]^2 + \sum_{i=1}^{n} Iti\left[\frac{rpmti}{rpmin}\right]^2$$

where

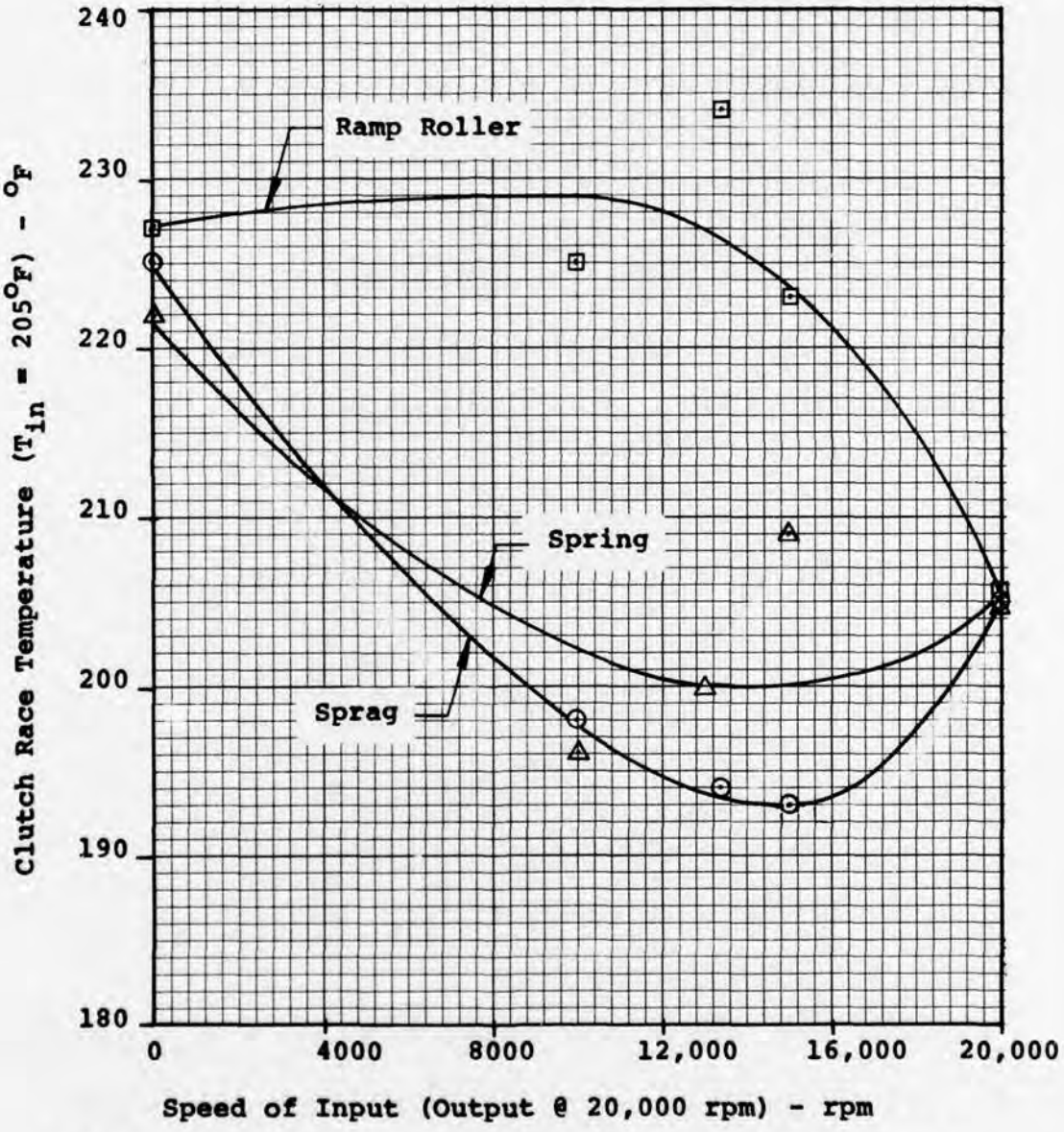

Figure 103. Clutch Race Temperature as a Function of Differential-Speed for Spring, Sprag, and Ramp-Roller Clutches.

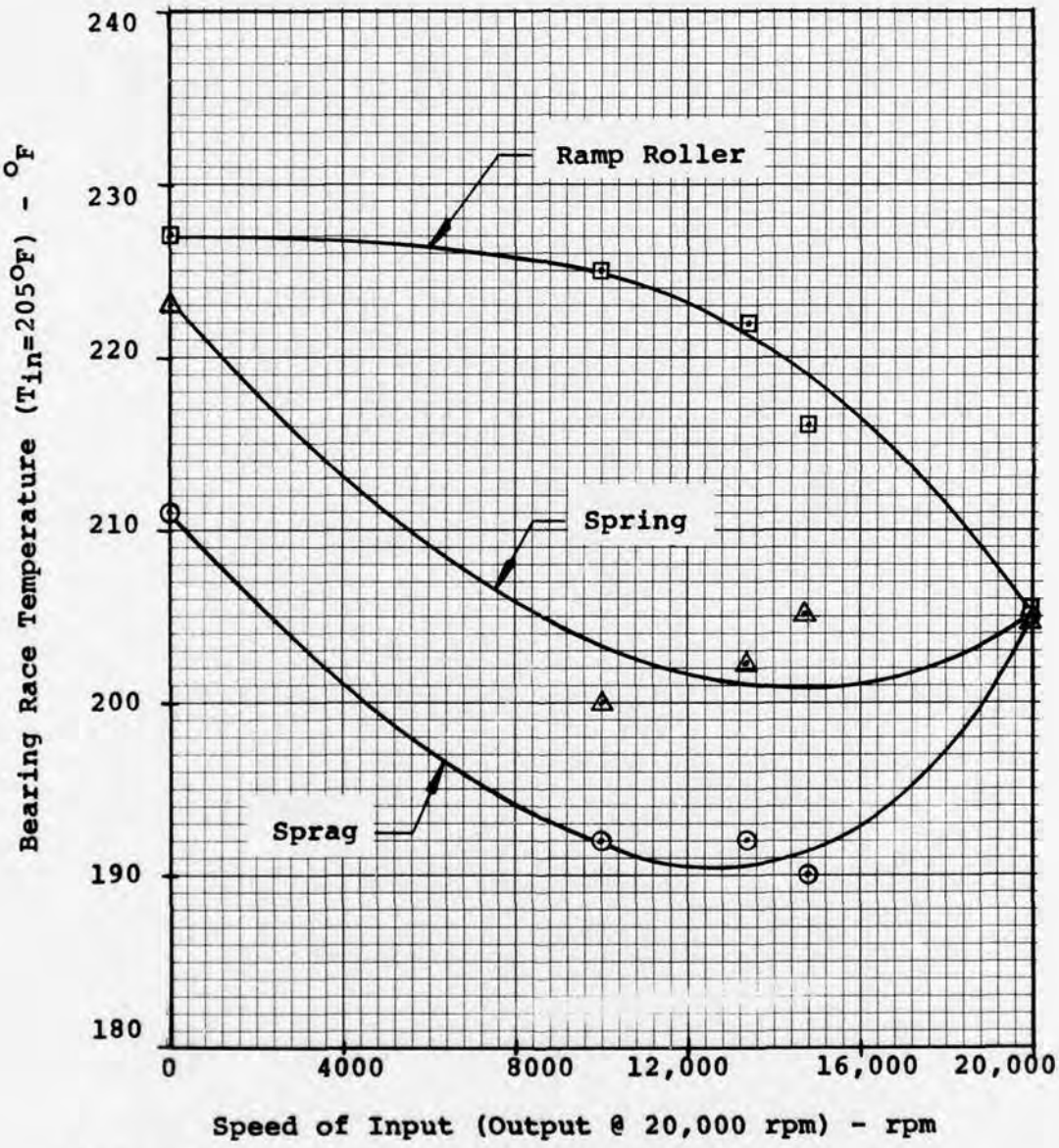

Figure 104. Bearing Race Temperature as a Function of Differential-Speed for Spring, Sprag, and Ramp-Roller Clutches.

Iin	=	moment of inertia of rotating system reflected to input speed
Irh	=	moment of inertia of rotor head
Ib	=	moment of inertia of blades
Iti	=	moments of inertia of individual transmission gears
rpmin	=	input speed
rpmrh	=	rotor head speed
rpmb	=	blade speed
rpmti	=	individual speed of transmission gears

In series with the flywheel and operating at the same speed is a waterbrake capable of operation of up to 20,000 rpm and 1500 horsepower.

The purpose of the Task I dynamic turbine testing was to simulate helicopter ground operation in all phases through the takeoff condition. Ground operations are the most critical period of operation for helicopter overrunning clutches since they must start from rest and pick up their loads, operate in full-speed and differential-speed overrunning, make high-speed engagements and disengagements, and operate to the full power rating upon takeoff. The Task I turbine tests simulated all of these operating conditions.

The first clutch to be tested in the Task I dynamic turbine test was the sprag clutch. The turbine was started and accelerated to 20,000 rpm at 400 hp. This condition simulates engine startup with rotors at flat pitch and was run for 5 minutes. After 5 minutes, the engine speed was reduced, causing the clutch to disengage since the flywheel with its high inertia continued to rotate the clutch output shaft. After the input speed dropped to approximately 12,000 rpm, the speed was then increased to 20,000 rpm, causing the test clutch to engage. This high-speed engagement simulates the start-up of the second engine and the engagement of its clutch in a twin turbine helicopter. During the period of disengagement, the test clutch is operating in the differential-speed over-running mode.

The disengagement and engagement procedure was repeated for a total of five engagements, whereupon the power was increased to 1500 hp (100% design) for approximately 1 minute to simulate takeoff. The turbine was then shut down, completing one test cycle. For each of the three test clutches, this test cycle was repeated three times during the Task I test.

The sprag clutch completed the three cycles as described above without any problems. At the completion of the test, the sprag clutch was disassembled and inspected. During the dynamic turbine load testing of Task I, the depth of wear increased but was negligible, and the conditions of the components were very similar to those prior to test. The bandwidth of sprag wear still measured approximately .015 inch wide, as it did prior to test. It was concluded after inspection of the parts that the sprag clutch was ready for Task II testing.

The second clutch to be subjected to the dynamic turbine test was the ramp-roller clutch. The test stand was started, and the flywheel was accelerated to 20,000 rpm at 400 horsepower to simulate flat-pitch rotor operation. This condition was held for 5 minutes. Next, the turbine speed was reduced to disengage the clutch, then accelerated to 100% speed; however, when the input speed was equal to the output speed, the clutch hesitated momentarily and then failed to pick up the load. The output speed continued to decay, while the input speed was held at approximately 20,000 rpm. At approximately 46 seconds after the disengagement, the clutch suddenly engaged. At the time of engagement, the input speed (turbine) was at approximately 18,900 rpm, while the output speed (flywheel) was at approximately 5900 rpm. Instantaneously, the input attempted to reach the same speed as the output and the clutch fractured.

Figure 105 is a plot of torque versus time. The torque spike at t = 46 seconds was at the moment of engagement.

The condition of the clutch after this fracture was that outwardly the unit was intact, still on its bearing supports and able to turn freely. However, the clutch was unable to transmit torque because the rollers had been crushed, as can be seen in Figure 106. The debris seen is from the 14 rollers, which fractured upon impact. The results of the force of the impact can be seen in Figure 107. The cam lobe became brinelled and shows obvious signs of metal flow. The roller retention cage, although showing some signs of distress, did not fracture, as seen in Figure 108. The snap ring that holds the oil dam was thrown from the housing and is seen in Figure 109 along with one of the bronze bushings for the carrier. This damage was considered secondary as the dam was forced to move axially out of position by the impact of the rollers. The cage of the inner support bearing closest to the roller area also fractured, as seen in Figure 110.

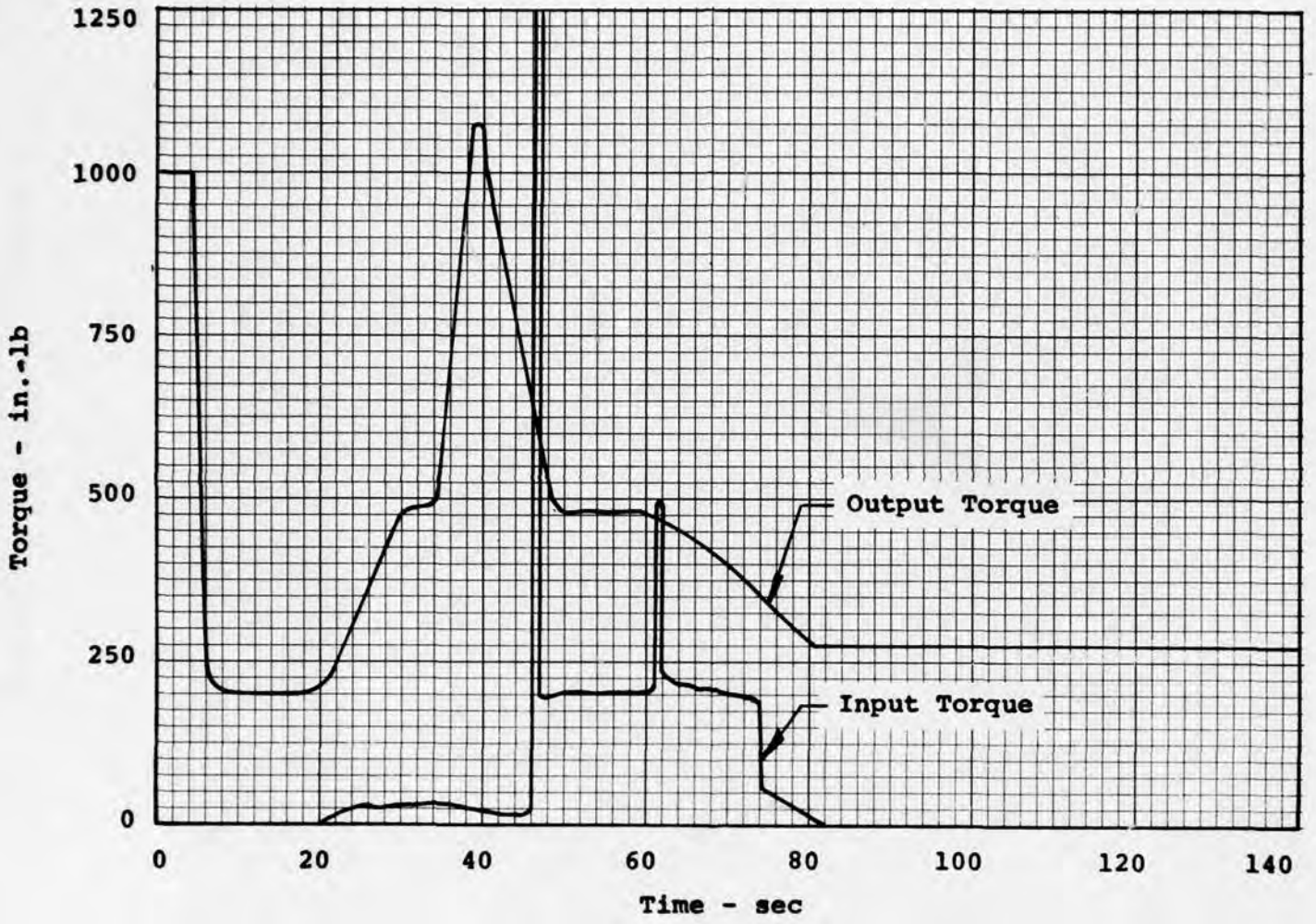

Figure 105. Torque Versus Time, Task I Turbine Dynamic Load Test, Ramp-Roller Clutch.

Figure 106. Ramp-Roller Clutch Outer Housing With Fractured Rollers, Task I Turbine Dynamic Load Test.

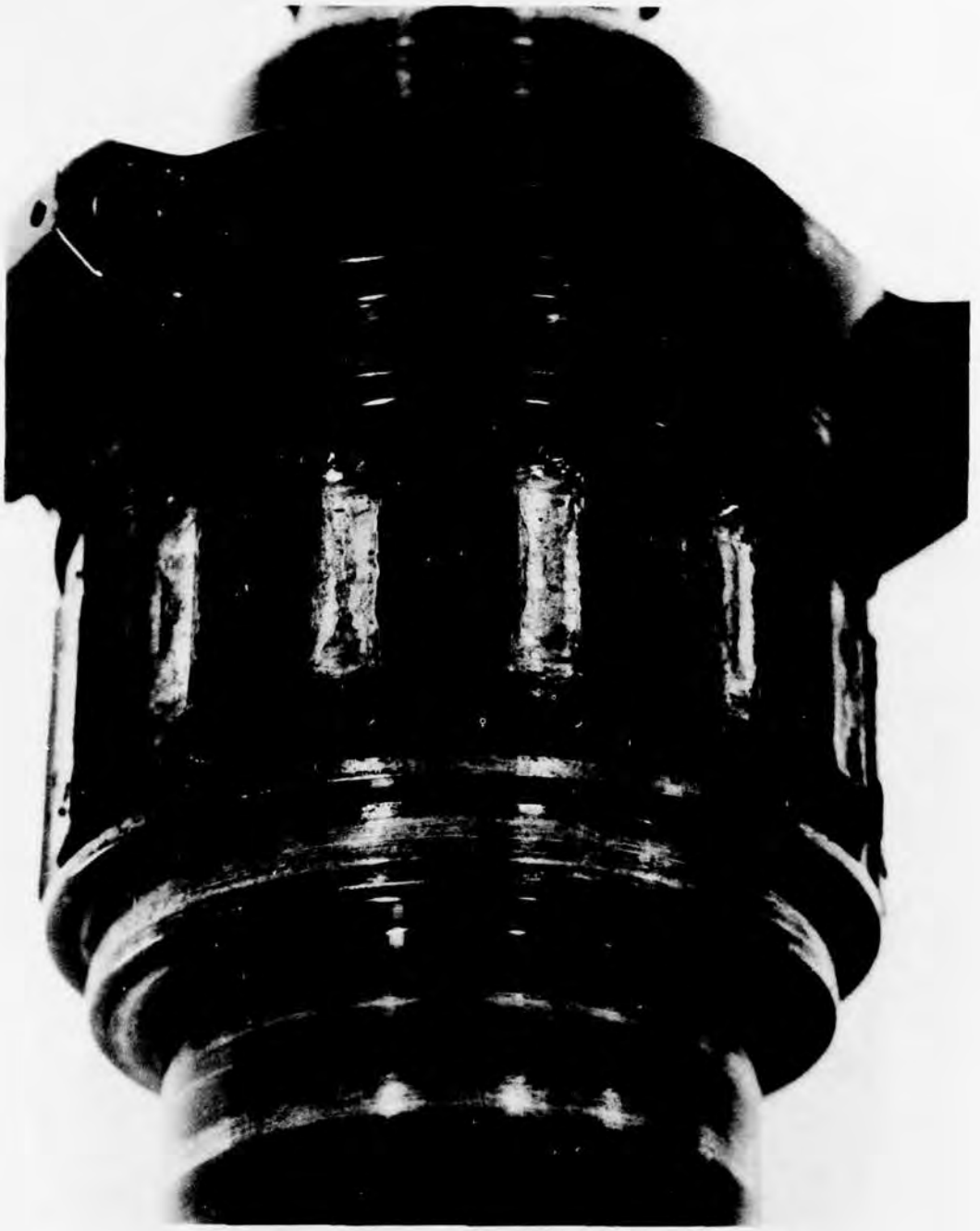

Figure 107. Cam Shaft Flats, Task I Turbine Dynamic Load Test, Ramp-Roller Clutch.

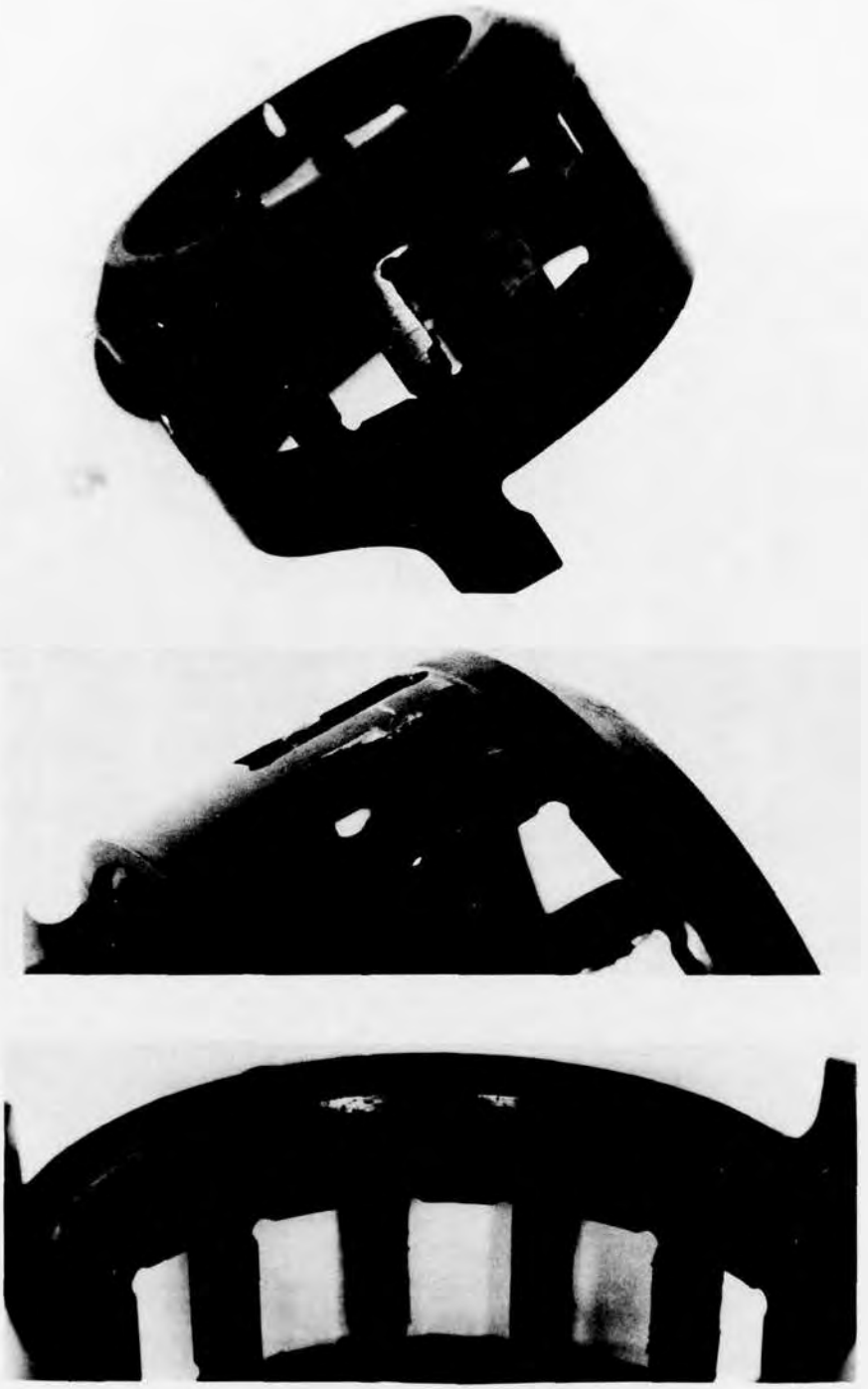

Figure 108. Ramp-Roller Clutch Roller Retention Carrier, Task I Turbine Dynamic Load Test.

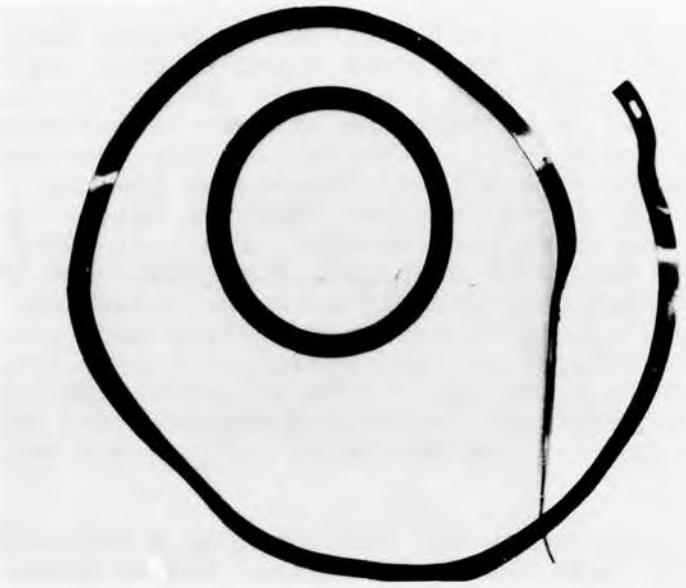

Figure 109. Oil Dam Snap Ring and Bronze Bushing, Task I Turbine Dynamic Load Test, Ramp-Roller Clutch.

Figure 110. Inner Support Bearing, Task I Turbine Dynamic Load Test, Ramp-Roller Clutch.

The reason that the ramp-roller clutch fractured was that it failed to engage when the input speed reached the speed of the output. The reason that the clutch did not engage can be seen in Figure 111. Note that the pattern of indentations on the cam flats are very similar except for the indicated one, which only exhibits some slight chipping on the top side of the flat. At first it was assumed that the roller associated with this flat must have been missing, i.e., it was left out of the assembly, but 14 major pieces were found and the weight of the pieces agreed very closely with the weight of 14 rollers, so it is concluded that all rollers were present during the test. Therefore, one roller must have been broken before the engagement occurred. The broken roller could have jammed the roller carrier, preventing movement and hence preventing engagement. The fractured rollers are shown in Figure 112.

A metalurgical examination was conducted on a new roller selected randomly from the spare parts. All rollers were manufactured from the same batch of material so that properties should be consistent throughout the batch of rollers.

The results of microhardness tests, shown in Figure 113, indicate a smooth hardness transition from case to core and an effective case depth from the outer surface of .020 inch. Depth from the inner wall was .028 inch. The inner wall was not machined after heat treat, as indicated by microstructure examination. This suggests that about .008 inch had been machined from the outer surface. Surface hardnesses were about RC 60 for the outer surface and RC 64 for the inner surfaces.

Microstructure was a fine martinsitic type with small patches of retained austenite. Two undesirable characteristics were found. Carbides were at grain boundaries to an almost continuous degree, which would have a considerable effect on strength. Lowering the carbon potential during carburizing or cooling the part more quickly in high temperature ranges is strongly recommended. The second problem is an oxidation of grain boundaries, which degrades fatigue strength. The condition occurs frequently, and as a result, it is good practice to remove .002 to .003 inch after heat treatment. This was not done on the hole of the hollow roller.

Figure 111 also shows another important piece of physical evidence. The journal located closest to the cam lug upon which the bronze bushing that guides the cage rides has two shiney spots on it where the finish is worn away. The centers of these spots are located 180 degrees apart and are also located precisely 90 degrees away from the center of the area

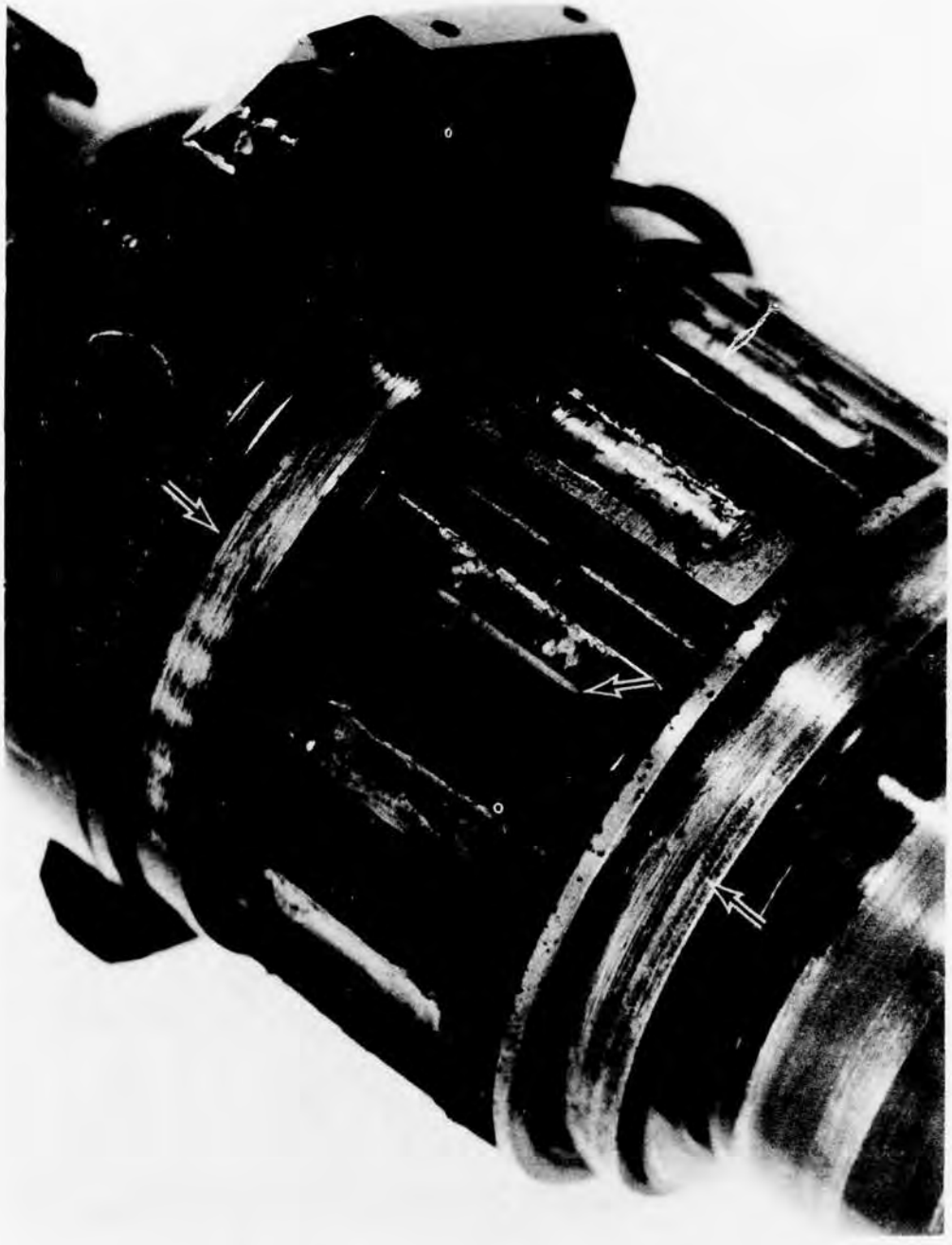

Figure 111. Ramp-Roller Clutch Cam Shaft Flats, Task I Turbine Dynamic Load Test.

Figure 112. Fractured Roller Pieces, Task I Dynamic Load Test.

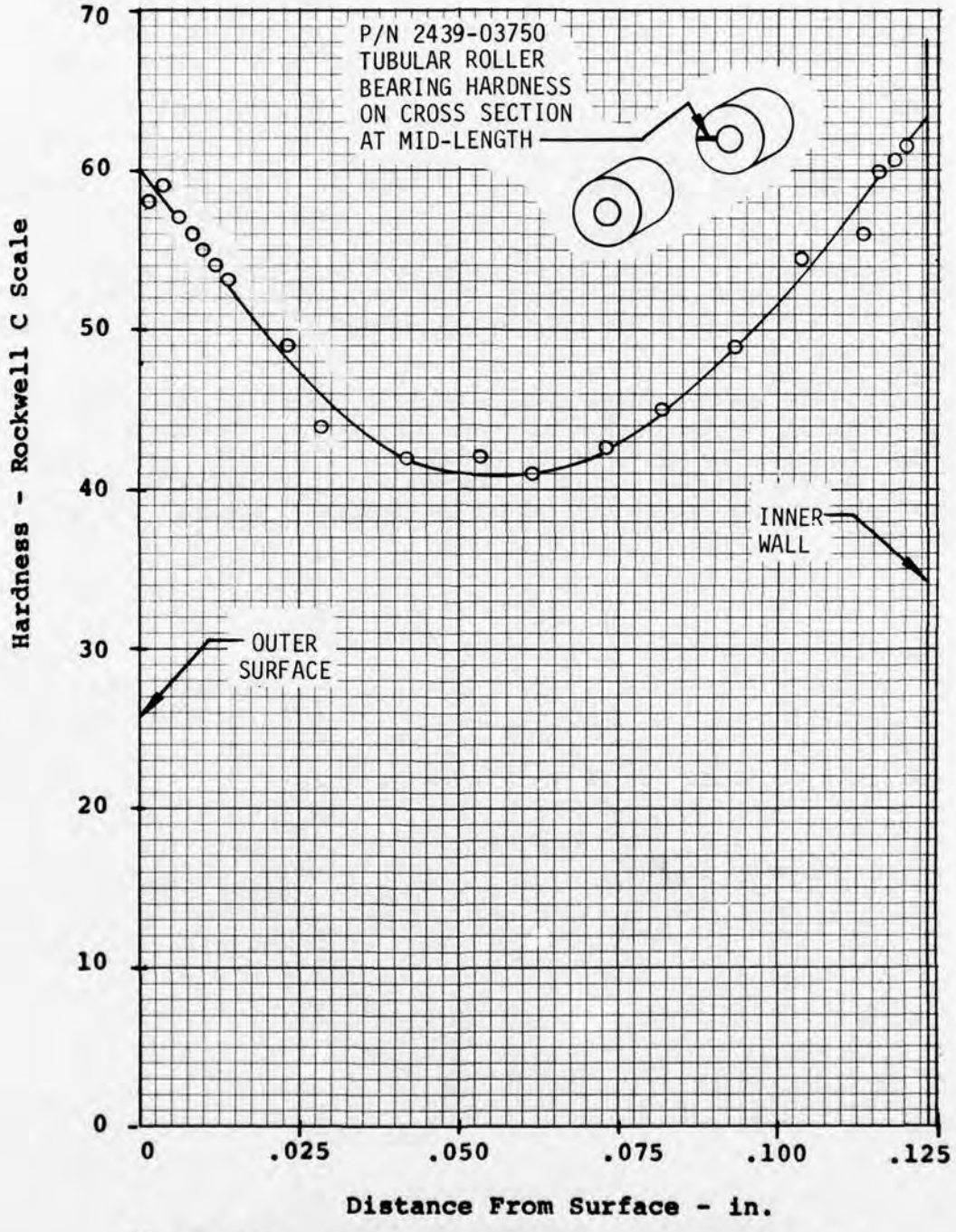

Figure 113. Hardness Versus Depth From Surface, Hollow Roller, Ramp-Roller Clutch.

in which the lugs on the cage operate. These areas of contact between the cam and the cage, being concentrated in these positions, led to the conclusion that the carrier was "pinching" the cam due to the action of centrifugal force on the cage's pin and spring lugs (stops). If an analysis of the cage is conducted, it is seen that the centrifugal force on the lugs is high compared to the stiffness of the ring portion of the cage, and as a result, forces the cage areas that are 90 degrees from the lugs inward until the cage touches on the journal of the cam and "pinches" the cage, preventing it from rotating. It is quite possible that this effect combined with the broken roller could possibly prevent the clutch from engaging at the proper time. This condition could also account for the roller chattering experienced during the overrunning testing.

An analysis of the lugs and cage deflection is presented in Appendix A. This analysis shows that the deflection at point A (see Figure 114) is .0095 inch at 20,000 rpm, which is greater than the radial clearance of .0020 inch, and therefore, the cage will grip the camshaft journal at these points.

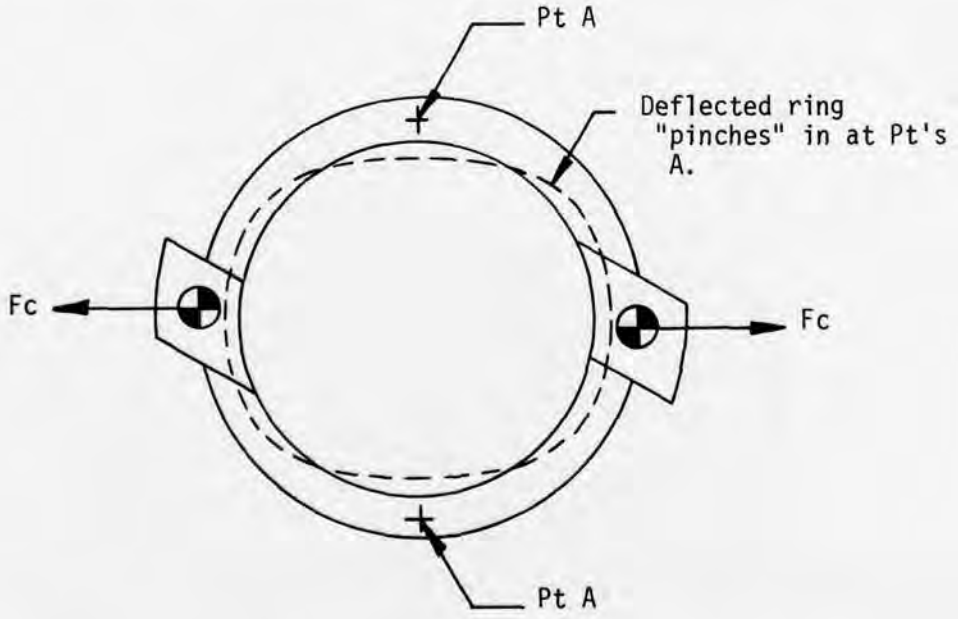

Figure 114. Ramp-Roller Clutch Carrier Centrifugal Effects of Lugs.

To prevent the cage from gripping the cam, the cage was redesigned, which accomplished two objectives. First, the mass of each lug was reduced from .0126 pound to .0072 pound by machining away all areas that were on the back side of the stop face that hit the pin of the pin and spring assembly. At 20,000 rpm, this change reduced the centrifugal force from 199 pounds to 114 pounds acting on the cage ring. Second, a steel ring was fabricated and pressed over the existing carrier with an interference fit of .003 inch to .005 inch. In effect, this ring restrained the innermost bushing area from outward expansion. The overall effect of the two changes was to reduce the radial expansion from .0095 inch in the original design to .0012 inch in the reworked design. The minimum radial clearance between the cage and cam is .002 inch; thus, the deflection of the original design exceeds the clearance whereas the redesigned cage deflection does not. Appendix A also presents the analysis of the reworked cage's centrifugally induced deflections. Figure 115 shows the reworked cage lugs and press-fitted strengthening ring. The redesigned roller retention cage was used on all further testing in the program.

The final clutch to be tested in the Task I dynamic load test was the spring clutch. Three cycles of dynamic load testing as previously described were completed on the spring clutch without problems. The spring clutch was disassembled after testing, and the end teaser coils were found to have experienced further deterioration in the form of silver-plate flaking. Figure 116 shows the scoring marks in the output housing incurred as a result of the silver plating particles wedging between the spring O.D. and housing I.D. during overrun. For the Task II tests, it was decided that a new spring would be used that had no silver plating on the ends so that the problem of chipped plating could be eliminated. The spring with flanged arbor used for the Task I turbine testing is shown in Figure 117.

At the same time that the dynamic load tests were being conducted on the spring clutch, another spring clutch was undergoing Task II static-cyclic testing. This clutch also contained the configuration using the flanged arbor design. Difficulty was experienced during this test with the spring gradually creeping towards the flange of the arbor and finally wedging itself so tightly against the flange that torque was lost. As a result of this test, it was decided to abandon the design using the flanged arbor and to revert to the original spring design for the rest of the testing in Task II.

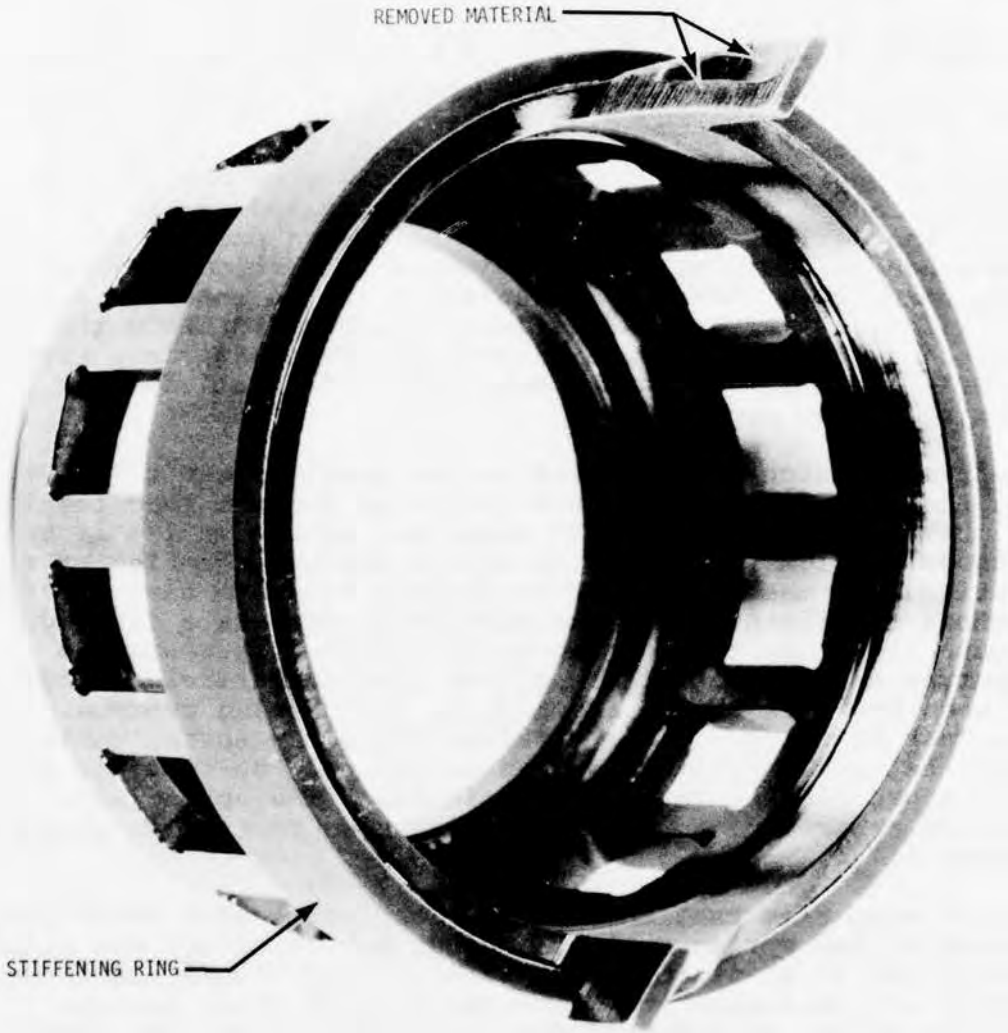

Figure 115. Redesigned Roller Retention Cage, Ramp-Roller Clutch.

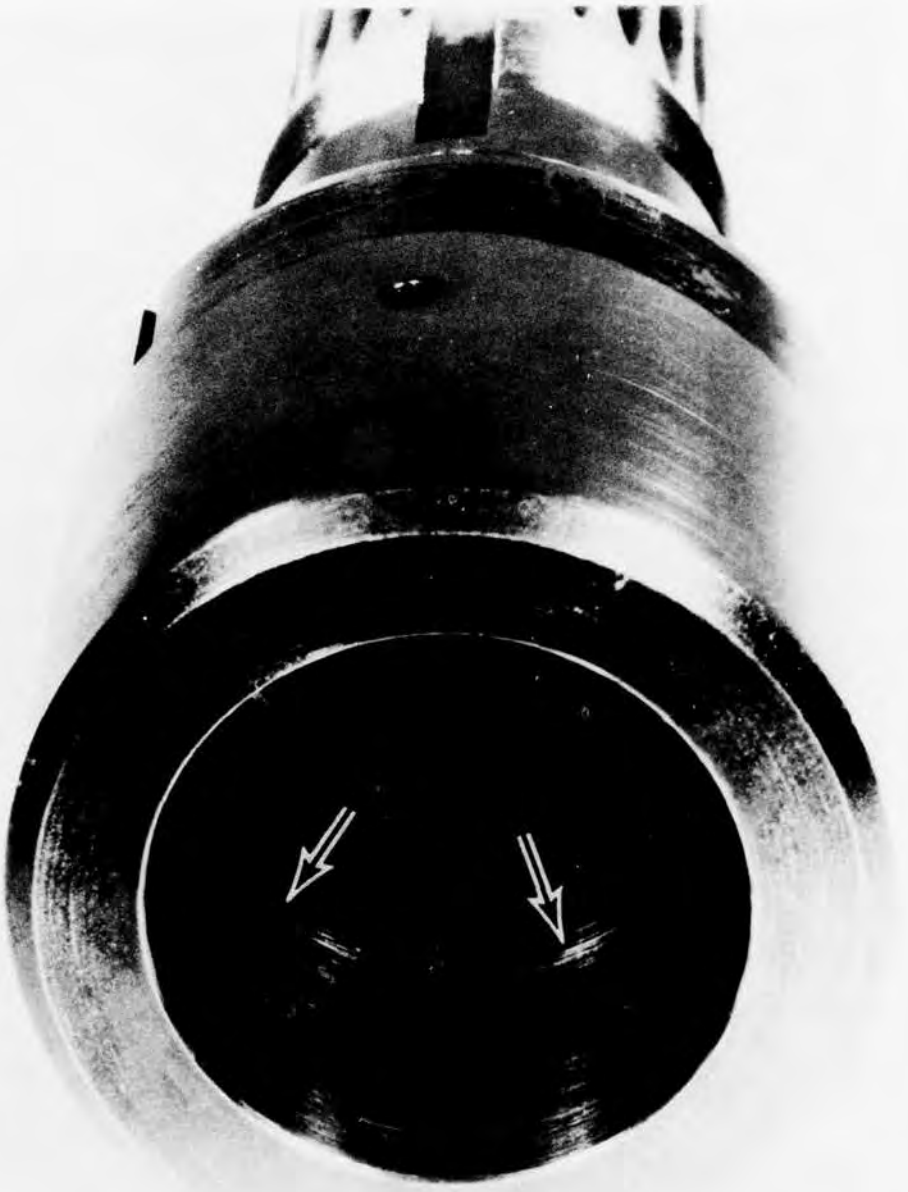

Figure 116. Scored Spring Clutch Outer Housing, Task I Turbine Dynamic Load Test.

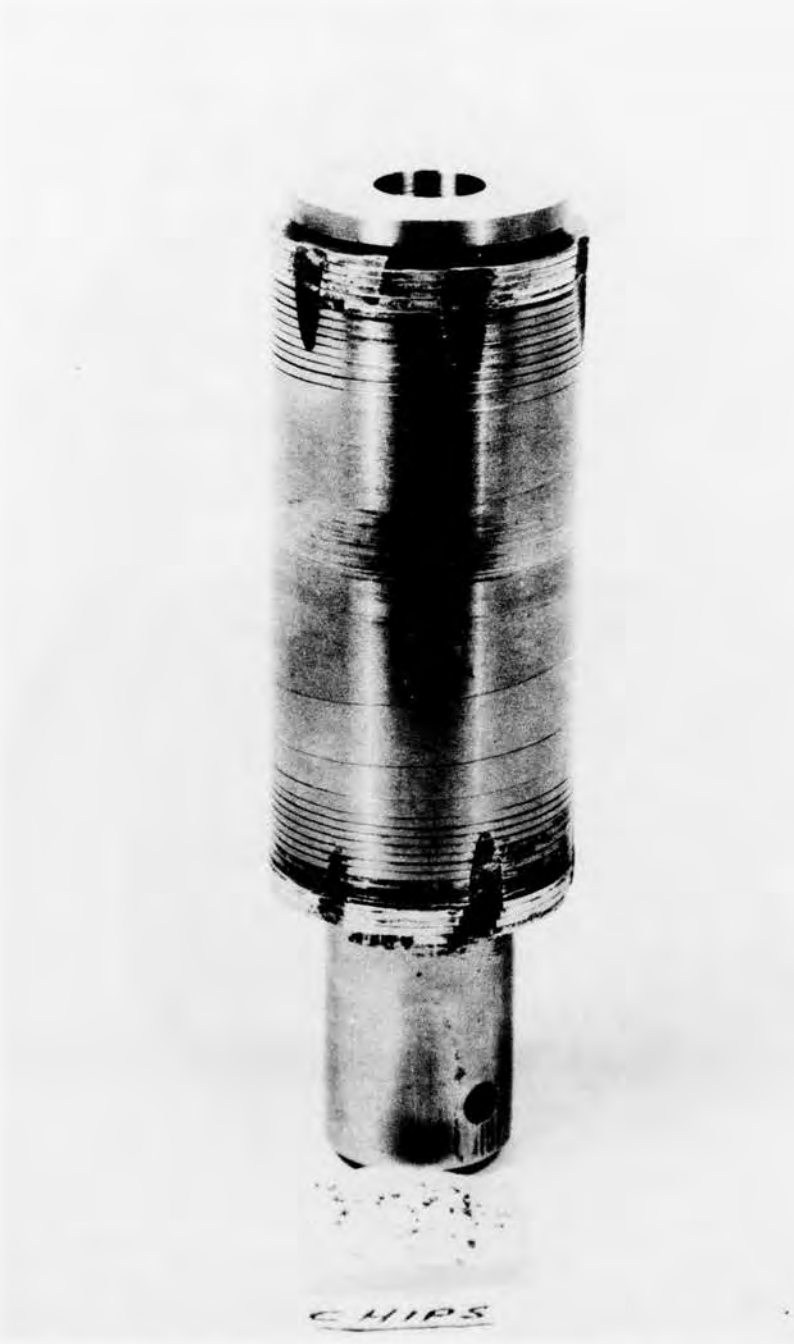

Figure 117. Spring Clutch Spring, Task I Turbine Dynamic Load Test.

TASK II TEST RESULTS

Full-Speed Overrun Test Results

The full-speed overrunning test of Task II consisted of two 25-hour test runs for a total of 50 hours on each clutch.

In terms of calendar date, the full-speed overrunning tests were actually conducted after the differential-speed overrunning tests. At the start of the differential-speed tests, the clutch hardware that had worn during Task I was replaced. The spring of the spring clutch was replaced with a new spring. This spring did not have silver plating on the teaser coils. The shouldered arbor was also removed and replaced with the slotted bronze spacer. In the sprag clutch, the inner race was replaced with a new shaft and the sprag unit was new; while, in the ramp-roller clutch, the rollers were new, as was the reworked and redesigned roller retention carrier and camshaft. Since this hardware was new for the differential-speed overrun tests, the photographs shown in this section (after full-speed overrun) represent the condition of the parts after 30 hours of differential-speed running in addition to 50 hours of full-speed overrunning.

The first clutch to undergo the full-speed overrunning tests was the sprag clutch. Fifty hours consisting of two 25-hour segments were completed without incident at the full-speed overrun condition. Very little wear or other apparent damage was evident or measured during this test. The bandwidth of wear of a typical sprag was approximately .015 inch, which is about the same as after the differential-speed test, indicating that no wear was measured during the test. Figure 118 shows the complete sprag assembly, while Figure 119 shows the inner shaft. Most of the score marks seen on the shaft in Figure 119 were incurred during differential-speed testing.

The second unit to undergo full-speed overrunning testing was the spring clutch. As with the sprag clutch, the spring clutch completed the two 25-hour tests without apparent difficulty. Figure 120 shows the output housing bore condition after testing. Note that the scoring marks are steadily spreading and are generally concentrated in an area just after the oil drain holes, indicating that the cause of the scoring is insufficient lubrication. Although the score marks continued to develop throughout the testing, they were not considered a serious problem. Operation of the clutch in both the drive mode and overrunning mode was unaffected by these conditions. The closeup of the spring shown in Figure 121 shows the area of the spring that was in contact with the score marks on the outer housing. Note that the scoring starts just where the oil drain slots taper to a solid section. The general overall condition of the spring was excellent,

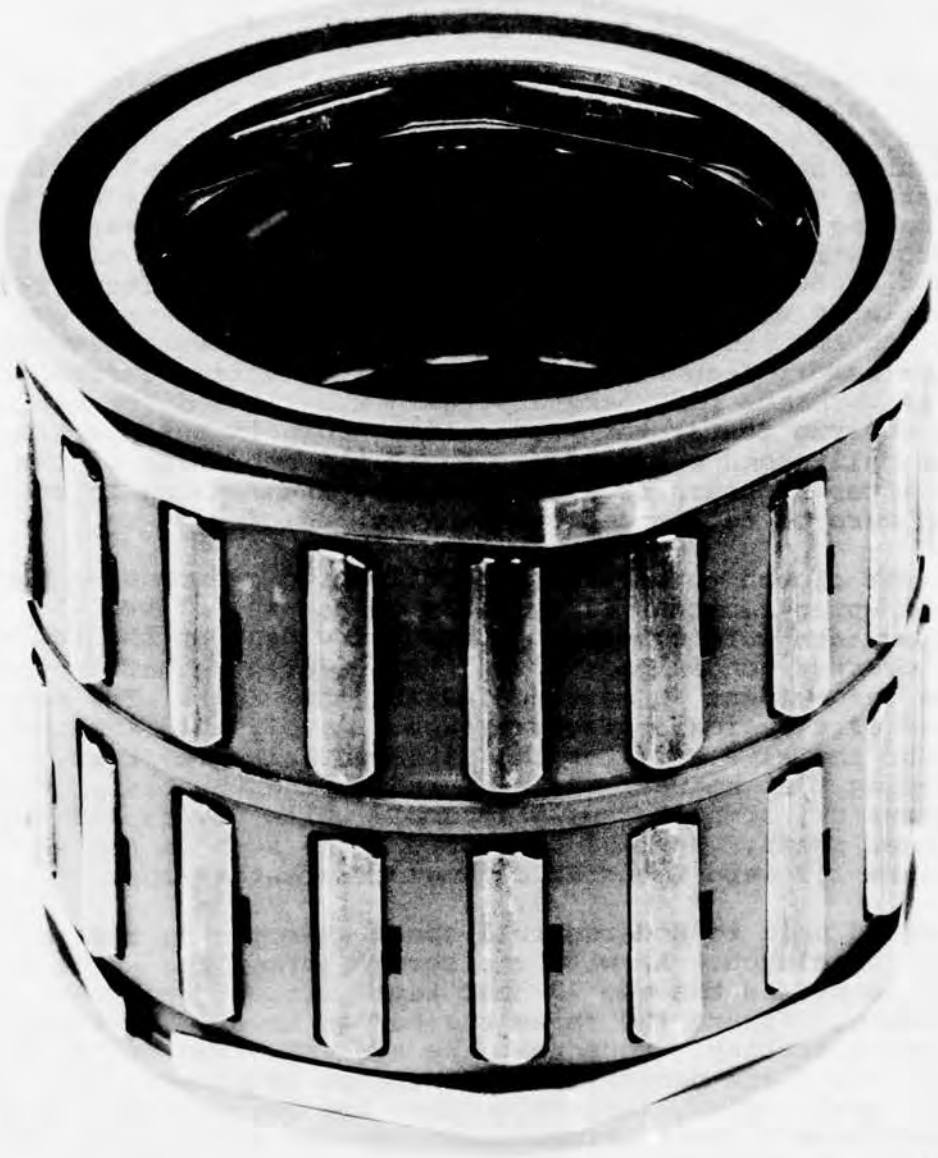

Figure 118. Sprag Assembly After Task II Full-Speed Overrun Tests.

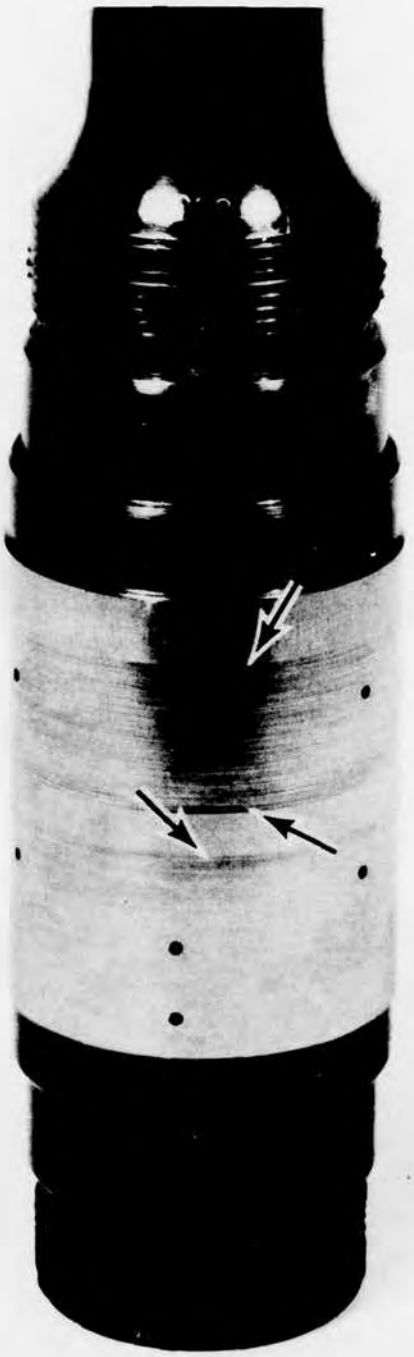

Figure 119. Sprag Clutch Inner Race After Task II Full-Speed Overrun Tests.

Figure 120. Spring Clutch Output Housing After Task II Full-Speed Overrun Tests.

Figure 121. Spring After Task II Full-Speed Overrun Tests.

with low teaser coil wear indicative of high overrunning wear life.

The ramp-roller clutch was the last clutch to be tested in the full-speed overrun testing of Task II. As with its predecessors, the roller clutch 50-hour full-speed overrun test was completed without difficulty. The same condition experienced in Task I testing was again occurring; several rollers were wearing on their end faces. The heaviest wear is shown in Figure 122 which shows the cage after testing.

It is interesting to note the harmonic nature typically found in the distribution of the roller end wear: The heaviest wear occurred in roller Number 1, whereas roller Number 7, located 180 degrees from roller Number 1, showed no signs of wear. The depth of wear is almost proportional to the angle from roller number 1. A closeup of the worst and best rollers is shown in Figure 123.

One notable outcome of the testing is seen in Figure 124. The wear pattern on the cam flats shows no signs of roller chatter, and since the cam flats shown are after 30 hours of differential overrun and 50 hours of full-speed overrun, the conclusion is that the redesigned roller cage completely solved the problem of roller vibration and chatter. Wear patterns on the cam shaft journal, which guides the cage were also uniform and were not concentrated in two positions 180 degrees apart, as noted in Task I. Compare the condition of this cam to the cam shown in Figure 111, which has the one flat without brinnell marks. In Task I, the cam-flat wear occurred in several different areas, from a single major area back to the pocket undercut, including at least two additional areas where significant amounts of overrunning wear had occurred. In the Task II cam, the wear area is confined to one small band of contact, which shows proper ramp-roller clutch operation.

During the full-speed overrun tests, temperatures were recorded at the bearing races of the overrunning bearings and also at the clutch races near the point in each clutch where the maximum rubbing or sliding was occurring. The temperature rise shown in the graphs which follow is defined as the stabilized operating temperature of the bearing race or clutch race minus the temperature of the oil in. Figure 125 shows the variation of the bearing-race temperature with test time. These results show that the temperature was not consistent throughout the test. On the other hand, clutch race temperature was fairly consistent as seen in Figure 126. On the spring clutch, race temperature appears to have two basic levels, one at approximately 0 for the first 25 hours

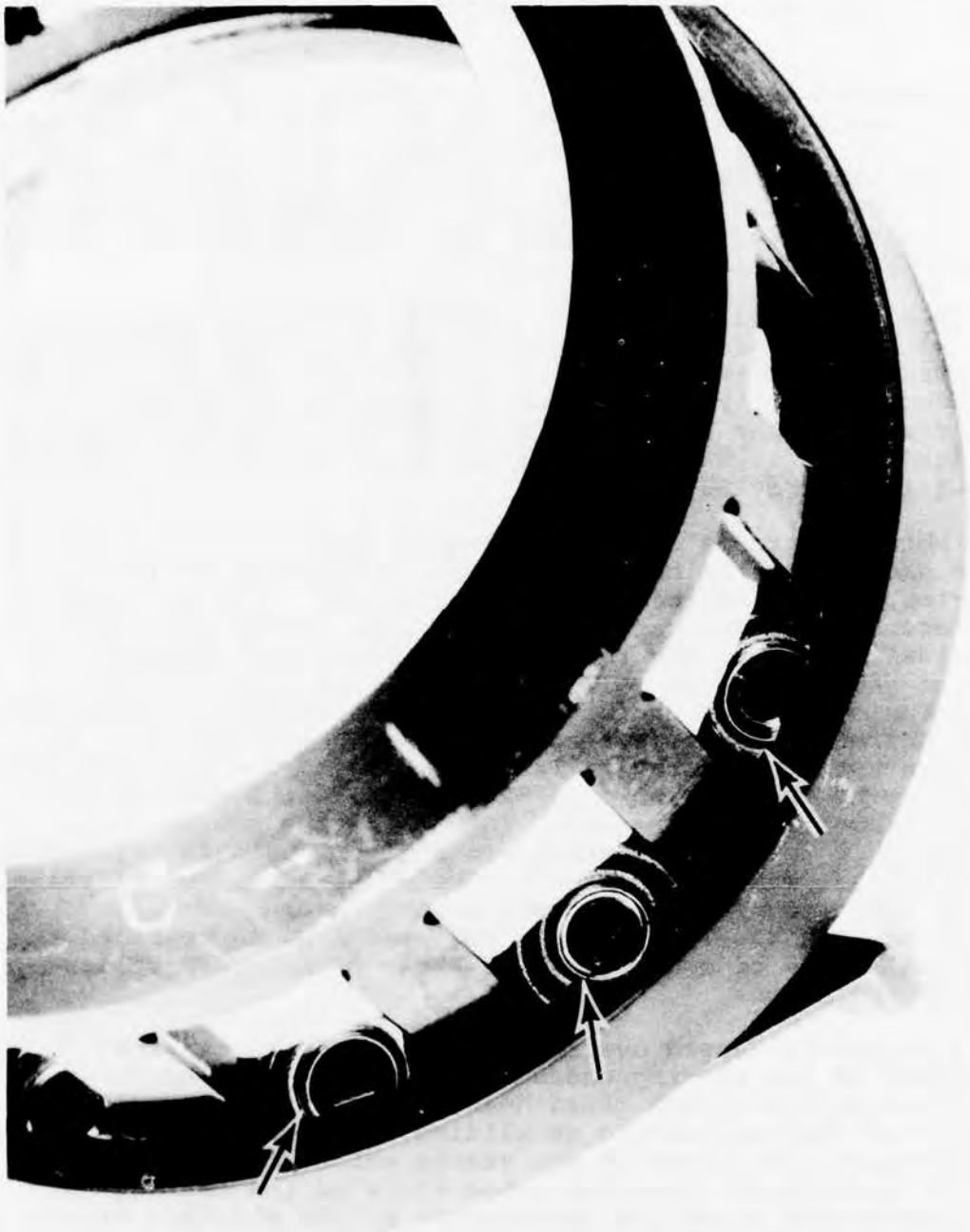

Figure 122. Roller Retention Cage End Wear After Task II Full-Speed Overrun Tests.

Figure 123. Rollers After Task II Full-Speed Overrun Tests.

Figure 124. Cam Shaft After Task II Full-Speed Overrun Tests.

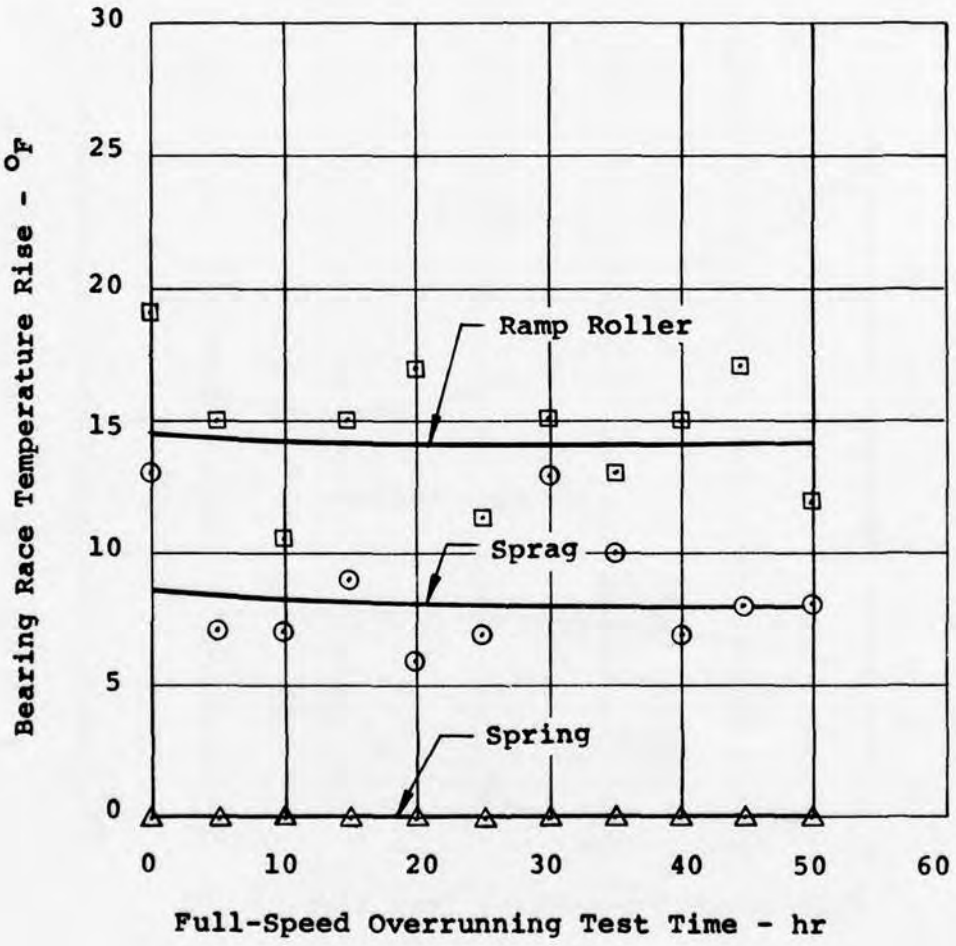

Figure 125. Bearing Race Temperature Versus Time, Full-Speed Overrun at 20,000 rpm.

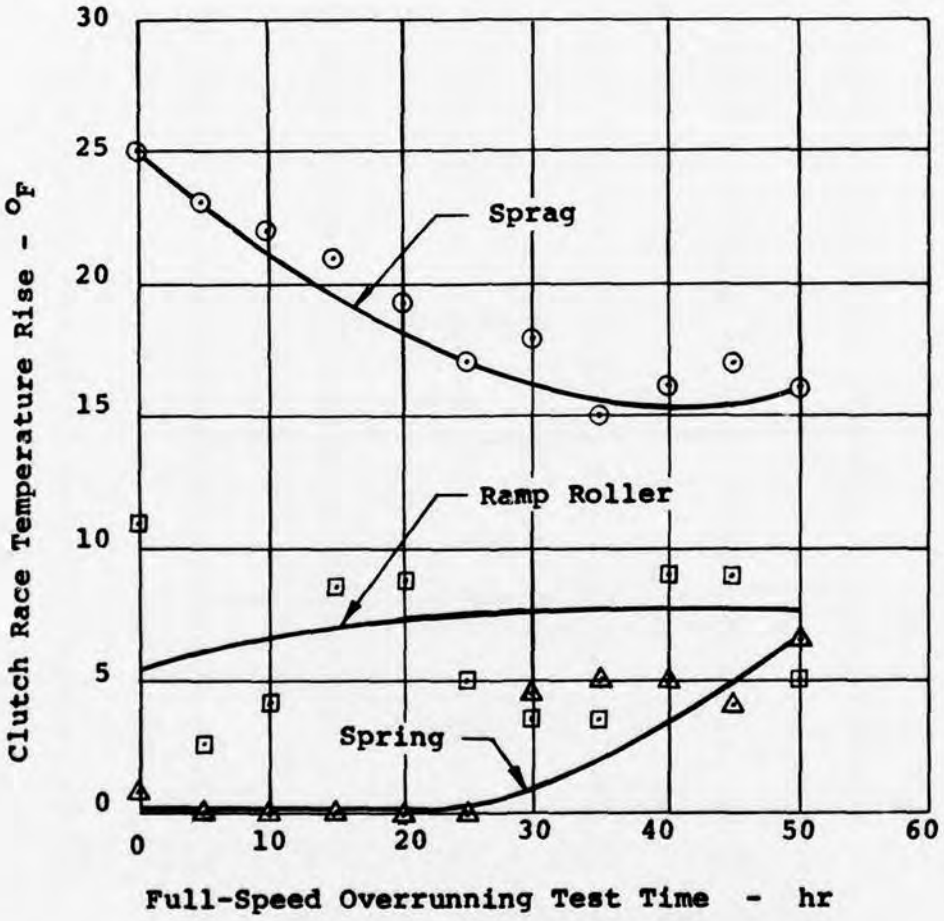

Figure 126. Clutch Race Temperature Versus Time, Full-Speed Overrun at 20,000 rpm.

and then a jump to approximately 5 degrees for the next 25 hours. This can possibly be explained by the difference in the hardware buildup after the 25-hour mark. The spring clutch was found to be very sensitive to support bearing preload (or looseness) and at times could be made to jam with heavy bearing preload. The decreasing temperature function of the sprag clutch may indicate a "wearing in" period.

Drag torque at full-speed overrun was found to be quite consistent for all clutches, as seen in Figure 127.

Differential-Speed Overrun Test Results

The differential-speed overrunning tests were the first tests to be conducted during Task II. These tests were conducted on the overrunning facility and consisted of two runs of 15 hours each for a total of 30 hours of differential overrunning operation on each clutch. Each 15-hour run consisted of 5 hours at 50% differential-speed overrun (input at 10,000 rpm, output at 20,000 rpm), 5 hours at 67% differential-speed overrun (input at 13,400 rpm, output at 20,000 rpm), and 5 hours at 75% differential-speed overrun (input at 15,000 rpm, output at 20,000 rpm).

The first clutch to be operated in the differential-speed overrunning mode was the sprag clutch. Prior to the start of this test, the sprag assembly and the inner race were replaced with new parts. The sprag clutch completed the first 15 hours, was disassembled, inspected, and reassembled, and then completed its second 15-hour test run without problems. The inner shaft was in essentially the same condition as it was after the full-speed overrun test and is shown in Figure 119. This shaft was new (unused) prior to the start of test so that all score marks were incurred during this test. Although these marks appear quite severe, the average depth measured less than .0001 inch, which is well within the allowable wear limits for the sprag, approximately .002 inch, indicating a long overrunning life.

Wear on the inner surface of the sprag incurred during the differential-speed overrun test was minimal. Figure 128 shows the outer race bore. The markings seen here are of negligible depth and are randomly oriented, indicating that a small degree of relative motion had taken place between the outer race and the sprag retainer unit.

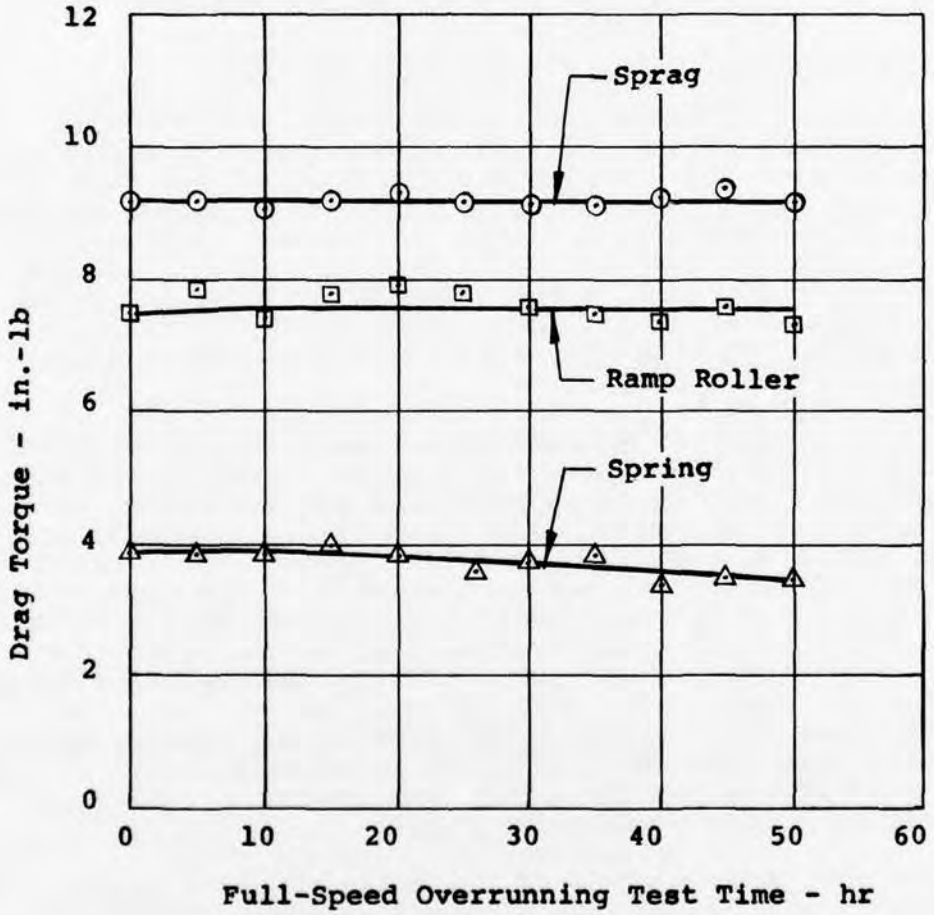

Figure 127. Clutch Drag Torque Versus Time, Full-Speed Overrun at 20,000 rpm.

Figure 128. Sprag Clutch Outer Race, Task II, Differential-Speed Overrun Tests.

Task II differential-speed overrun testing then continued with the spring clutch. Spring clutch testing was started with a new spring that did not have silver-plated end teaser coils. The flanged arbor design was also discarded in favor of the design using a slotted bronze spacer on the overrunning end of the spring. This decision was based on the results of static-cyclic torque testing of the spring clutch with the flanged arbor design that showed that, under cyclic load, the spring had a tendency to displace itself gradually toward the flange until it finally bound the teaser coils, rendering the spring inoperative. This phenomenon is discussed fully in the "Static Cyclic Test Results" section of this report. Even though the flanged arbor design was superior for overrunning, it was felt that load carrying reliability was a more important factor.

Testing was interrupted after 2.2 hours of 50% differential overrun on the spring clutch when the chip indicator warning light was activated. Inspection of the chip detector exhibited small metallic debris, slivers and fuzz; all were very light. Rotating the clutch by hand felt normal and it was decided to continue testing.

The overrunning steam turbine facility was restarted, and the remaining 3 hours of the 50% differential-speed test were completed. However, when the 67% differential speed (13,400 rpm on the input) test was attempted, difficulty was experienced with the "false engagement" type of problem that had been prevalent in Task I testing. Since no trouble was experienced at somewhat reduced speeds, the remaining 10 hours of testing were completed at 62% differential speed (12,400 rpm on input, 20,000 rpm on output).

Disassembly of the hardware revealed that some very slight scoring and rubbing was occurring at the overrunning end of the spring at the intersection of the end of the oil slots and the output housing bore. Figure 121 shows these score marks which were essentially the same after the full-speed overrun tests. Since the pressure at this point on the spring is less than in the teaser coils and since the velocity between the housing and spring is the same as for the teaser coils, it was deduced that the score marks were the result of poor lubrication in that area of the clutch. It should be noted that the drain holes in the outer housing are located just inside the end of the oil slots in the spring so that the lubricant will exit from the clutch prior to reaching the scored spring area. A solution to this problem would have been to extend the drain slots in the teaser coils to the center of the spring. However, the spring was not designed to withstand stress concentration effects of grooves in the more highly stressed center coil. Another solution would be the addition of a groove in the

housing; however, an oil groove in the housing was not considered feasible from a manufacturing standpoint because the housing was already in a hardened state. For these reasons and because of the long schedule delay that would be required to manufacture a new housing, it was decided to continue testing without altering the spring clutch.

The second 15-hour differential-speed overrun test was conducted with 5 hours at 50% speed and 10 hours at 75% speed. The spring clutch was able to operate at 75% speed without false engagement because the preload bearings were set to .001 end play, thereby allowing the arbor and the spring to better align themselves in the output and the input housings. Disassembly at the completion of the test showed that additional scoring had taken place between the spring and the housing. The scoring was taking place on the side of the oil drain holes opposite to the oil supply, i.e., most of the oil exits at the drain and very little was present in the scored area.

Although the scoring can eventually lead to spring clutch failure, it is estimated that this would take many hours of overrunning operation. During this time, normal operation in the drive mode would be unaffected. Thus, the condition was not of major concern and testing was continued.

The differential-speed overrun testing was then continued with the ramp-roller clutch. This test was the first test of Task II for the roller clutch and was also the first test with the redesigned roller cage. This cage had lighter stop lugs and a beefed-up, anti-expansion band press-fitted on the O.D. near the lugs. It was felt that this design would cure the roller chatter and vibration prevalent in the ramp-roller clutch during Task I testing. A new set of rollers was also installed.

The first 15-hour run, consisting of 5 hours each at 50%, 67%, and 75%, was completed without incident. The hardware was then disassembled and inspected. The wear on the cam shaft is like that shown in Figure 124 taken after all testing. The wear pattern area on the cam flats had improved greatly. The wear was confined to a small bandwidth in one area of the flat. This indicates that the rollers were operating in contact with the outer housing, and the cam and the cage were not vibrating in a rotational direction relative to the cam. Roller movement into the undercut area had been completely eliminated, indicating that the redesigned cage was a complete success.

Figure 129 is a photograph of the opposite side of the cam showing the peculiar pattern on flat number 3. This particular flat shows evidence of roller rotational movement relative to the cam; however, this is impossible without leaving identical marks on all the flats since the cage keeps all rollers in the same relative angular position. The only explanation is that roller number 3 must have been oversized such that it hit between the housing and the cam first, whereas the other rollers were not hitting. Centrifugal force would tend to keep the other rollers in contact with the outer housing. In effect, the clutch was freewheeling on only one roller. This roller then rapidly wore down to be equal in diameter to the other rollers, whereupon normal operation occurred. With only one roller in contact, wear would occur 14 times faster than would be normal if all 14 rollers were on contact. It is estimated that roller number 3 would have had to be approximately .002 inch larger than the other rollers for this to happen. This might have been possible if after carburization one roller was not final machined and was inadvertently left in with the finished parts. The only way to differentiate this roller from the rest would have been by measurement of the roller diameter.

Figure 130 shows the redesigned roller cage after 15 hours of differential speed operation. Just as in Task I testing, four rollers out of fourteen were wearing on their end faces. Figure 131 shows the worst and best rollers. It was decided to measure the end wear and keep track of it throughout testing. At this point, roller number 1 end wear measured approximately .040 inch in depth, which is quite severe for so short a test time. Later, at the end of all testing, it was found that the roller end wear subsided and eventually became negligible after reaching approximately .088 inch.

The ramp-roller clutch was then reassembled, and the second 15 hours of testing were conducted, with 5 hours at 50%, 5 hours at 67%, and 5 hours at 75% differential-speed overrun. As with the previous tests, this test was conducted without any apparent problems. When the clutch was disassembled, the parts were found to be in excellent condition. The roller end wear had progressed further, and was similar to the condition after full-speed overrun testing, as seen by the evidence of the cage roller slots shown in Figure 122. The depth of wear measured approximately .060 inch. It was decided that the roller clutch would not be changed for further Task II testing. This completed the Task II differential-speed overrun testing.

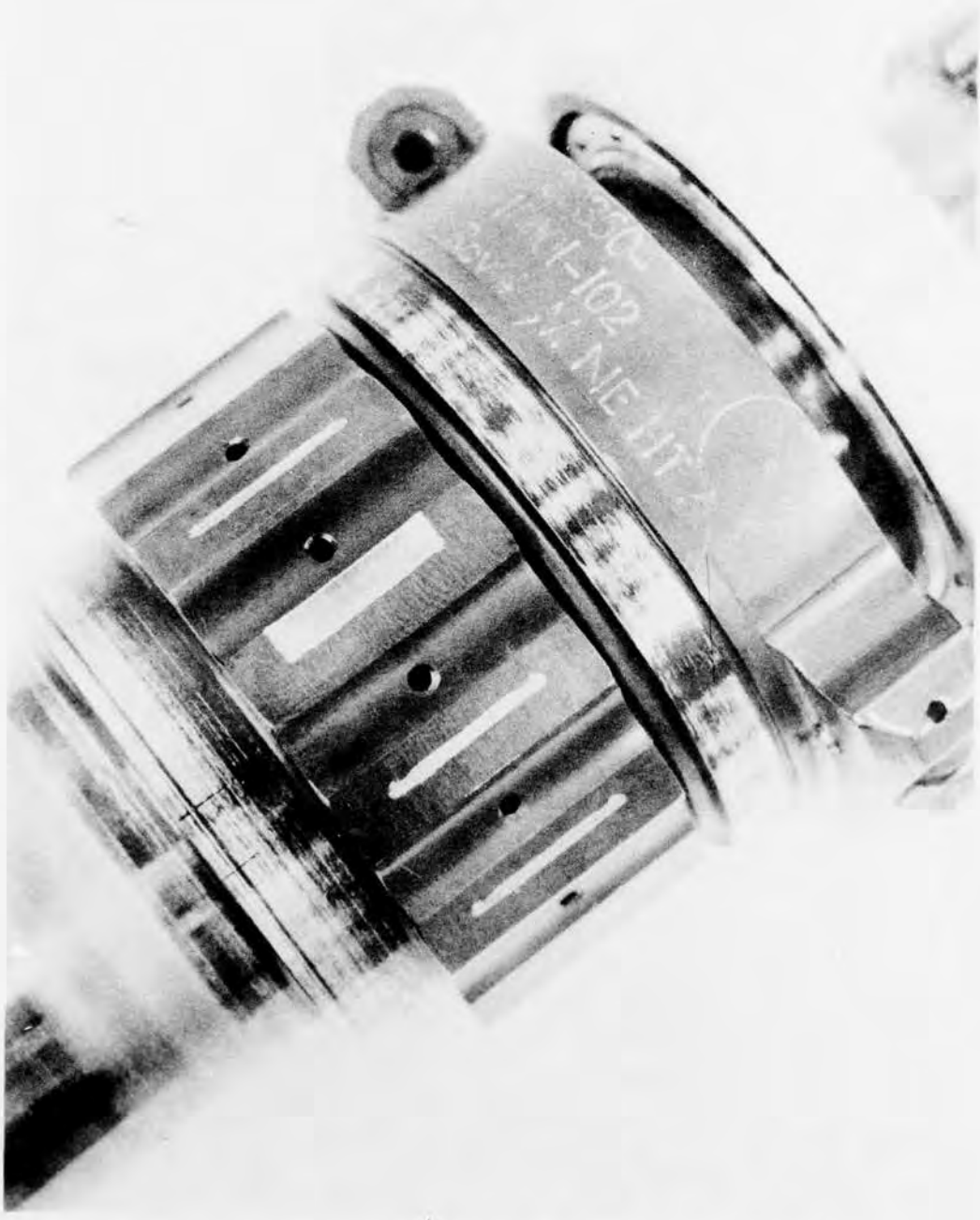

Figure 129. Cam Shaft Flat Number 3, Task II Differential-Speed Overrun Test.

Figure 130. Roller Retention Carrier After 15 Hours, Task II Differential-Speed Overrun Test.

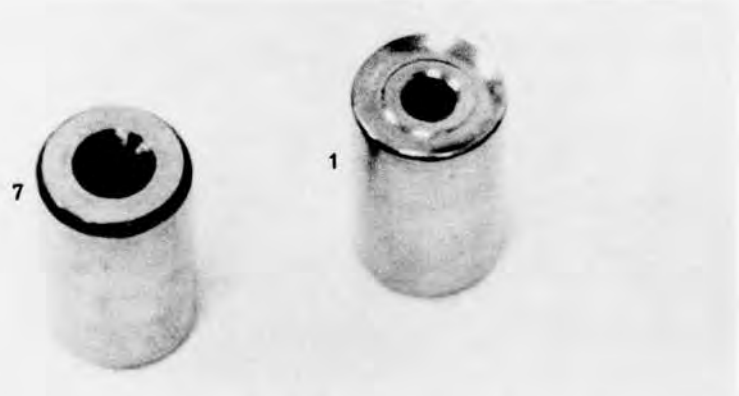

Figure 131. Rollers Number 1 and Number 7, Task II Differential-Speed Overrun Test.

Dynamic Load Test Results

Task II dynamic load testing was conducted on the dynamic turbine test rig. The procedure was essentially the same as that used in the Task I tests except that the duration of testing was much longer in Task II. In Task I, each clutch was subjected to three startups, 15 high-speed engagements, and three simulated takeoffs, whereas in Task II, each clutch was subjected to 75 startups, 750 high-speed engagements, and 150 simulated takeoffs. No disassemblies or inspections were conducted until the entire test was completed on each clutch.

The flywheel of the dynamic turbine facility simulated the inertia of the UTTAS rotor head, the transmission system, and the main rotor blades reflected to the clutch operating speed. The waterbrake provided power absorption to simulate flat pitch rotor operation (approximately 400 hp) and also full design takeoff power (1500 hp).

High-speed disengagements were accomplished by pulling back on the engine fuel control throttle after attaining full speed. This permitted the engine (clutch input) speed to be reduced to approximately ground idle, after which full throttle was again applied to increase turbine speed until the clutch engaged. Typical examples of a disengagement followed by an engagement for the spring, sprag, and ramp-roller clutches are shown in Figure 132. There were no significant differences in disengagement or engagement characteristics for any of the three types of clutches tested. Each clutch disengaged smoothly and evenly. Engagements were also smooth with each design.

The first clutch to undergo the Task II dynamic turbine testing was the sprag clutch. The testing was uneventful. At the completion of the test, the sprag clutch was disassembled and inspected. The typical band of wear on the sprags had not progressed significantly over what it was in the previous test, the 50-hour full-speed overrun, indicating that very little wear took place during the test. The sprag contact pattern on the inner bore of the outer housing was the result of wear on the surface finish of the housing only and was of negligible depth. The pattern is stationary, indicating that the sprag retainer assembly did not rotate relative to the housing during the test, which is as it should be. The inner shaft race showed very little change. An oscillograph record of a typical cycle is shown in Figure 133, which plots input and output rpm, output torque, and fuel flow against time.

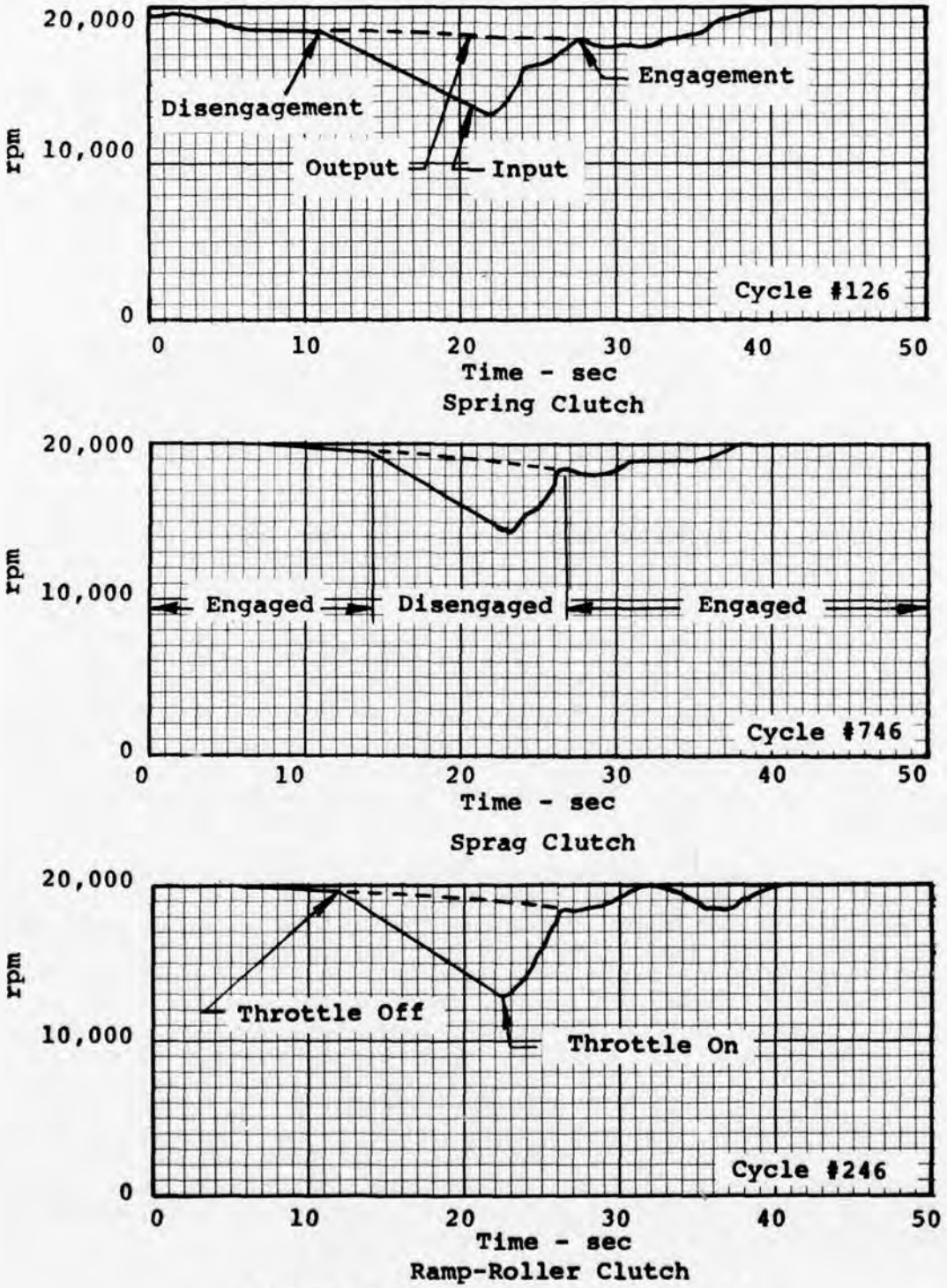

Figure 132. Typical Engagements.

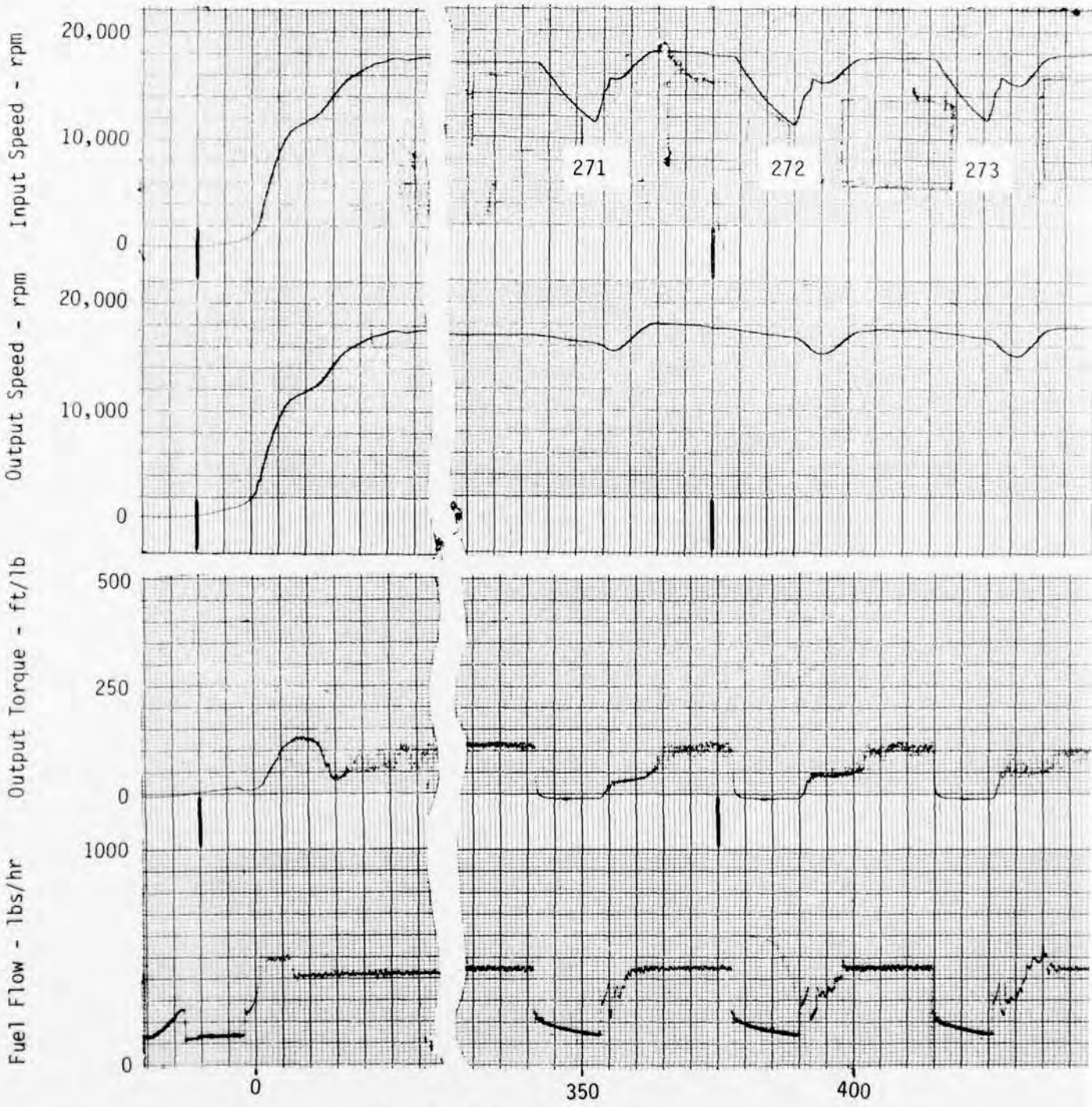

Figure 133. Typical Cycle, Sprag Clutch, Task II Dynamic Load Test.

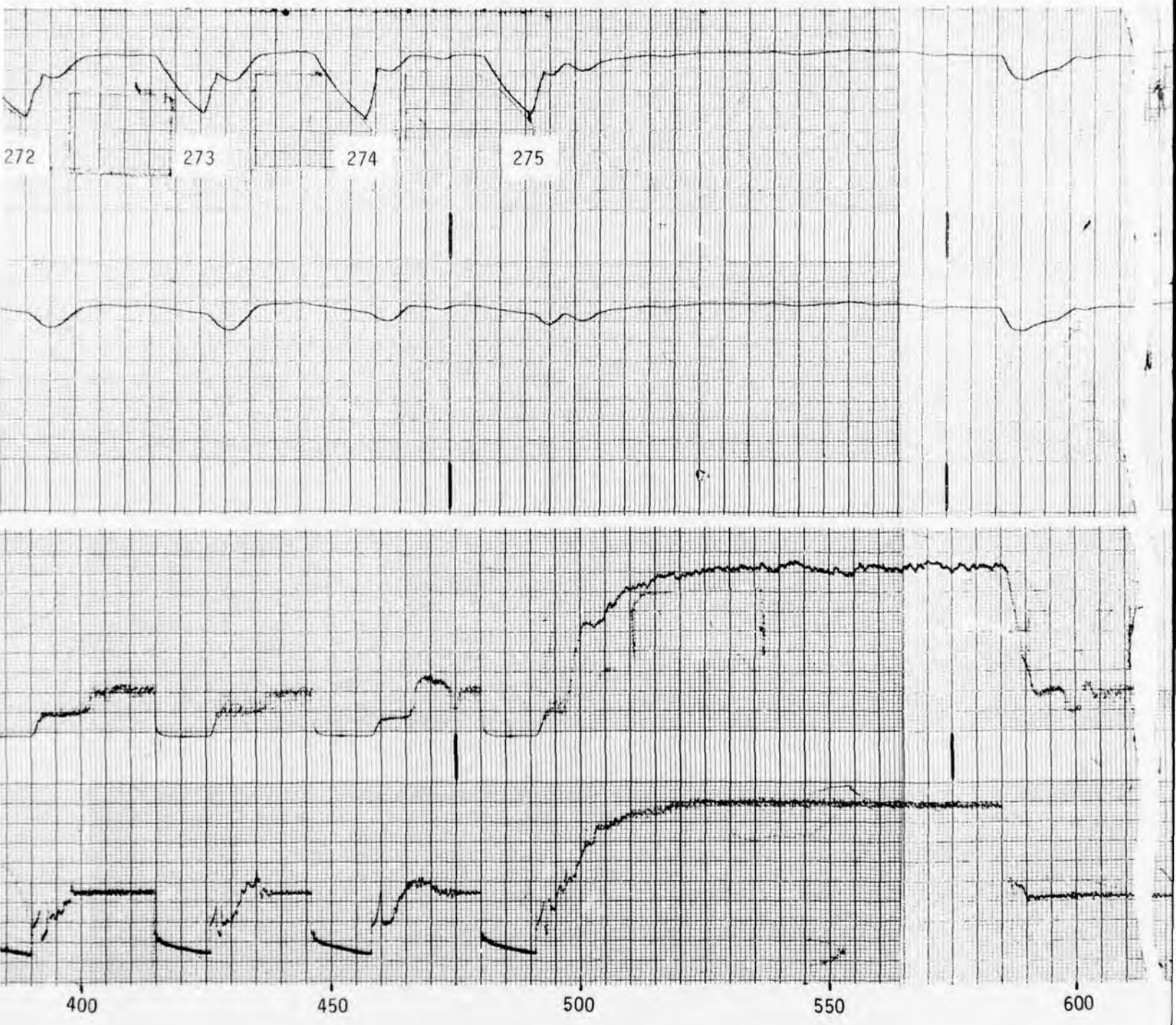

namic

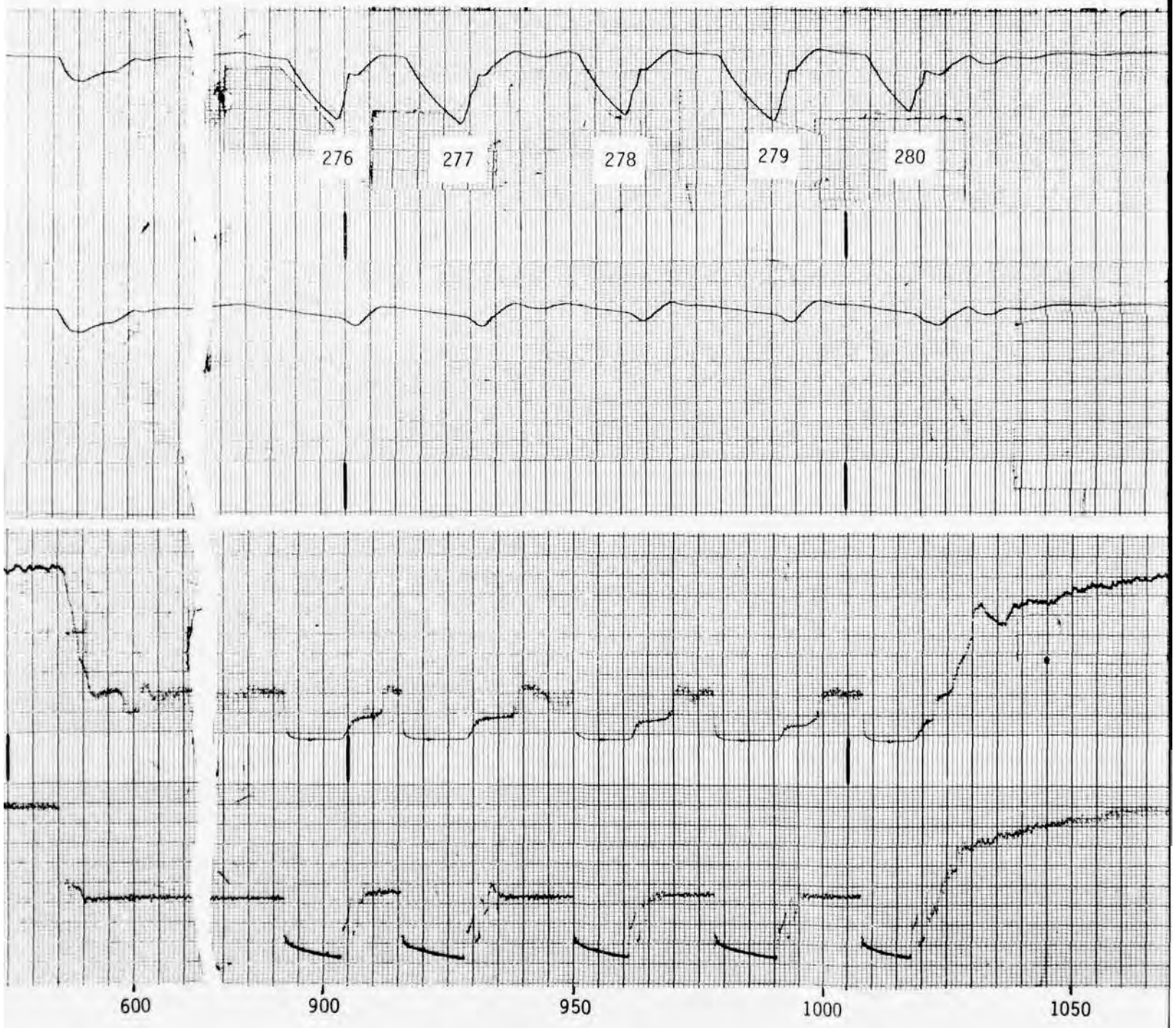
276
277
278
279
280

600
900
950
1000
1050

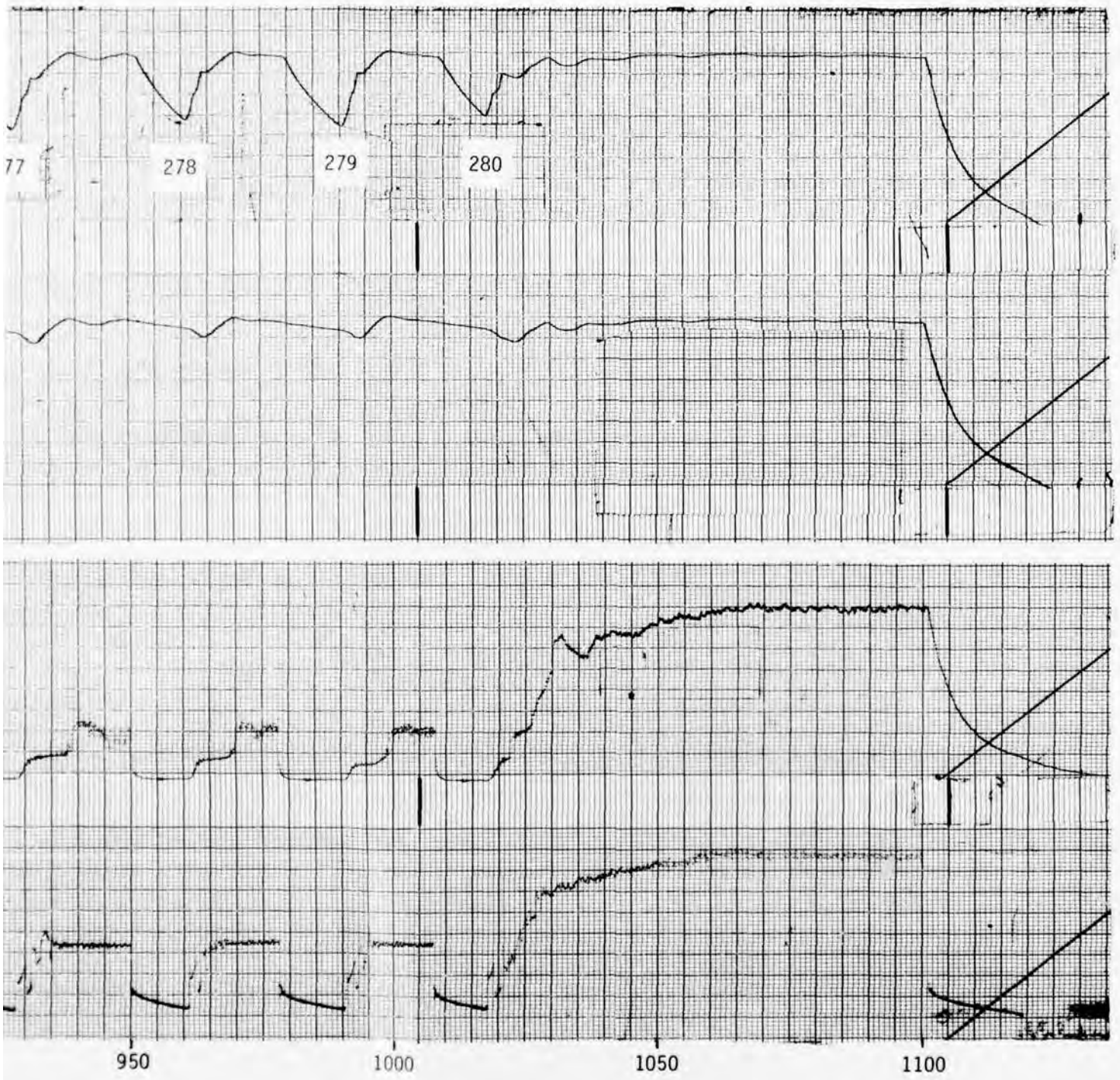
77
278
279
280
950
1000
1050
1100

The second clutch to be tested in the Task II dynamic load test was the ramp-roller clutch. As with the sprag clutch, the turbine testing was completed without incident. After the 750th engagement, the ramp-roller clutch was disassembled and inspected. Whereas roller diametral wear had been minimal up to this point, it was found that considerable wear had taken place during this test, although by no means approaching the "wear out" condition. Average roller diametral wear increased from approximately .0002 inch prior to testing to approximately .0007 inch after testing, indicating the severe nature of the test.

Figure 134 shows a typical roller retention carrier roller slot on the face that normally contacts the roller. The wear pattern is typical of this type of application. The roller end wear continued to progress throughout the test on roller number 1, but only by a small amount. Prior to the test, roller number 1 end wear measured .083 inch, and after testing, roller number 1 end wear measured to approximately .087 inch. The camshaft is shown in Figure 135. The wide wear pattern seen on flat number 3 (second from top) was from previous testing. A double wear pattern can be seen that was incurred during the dynamic load test. This double pattern appears to be the result of a high-load condition such as a shock engagement.

Figure 136 shows the outer housing, which sustained brinnel marks on the bore. These marks were of negligible depth; however, the bore of the housing was found to be worn to a depth of .0003 inch. The evidence seen, i.e., the brinnel marks on the housing bore and the markings high on the ramps of the camshaft would seem to indicate that the ramp-roller clutch had sustained one or more shock engagements or impact types of loading. Also, the wear sustained on the rollers, housing and carrier are typical of a condition caused by poor lubrication. However, a check of the lubrication design did not reveal any abnormalities. Also, a review of the oscillograph records did not indicate that any sudden shock engagements had occurred or, if they did, the magnitude of the speed difference would have been very low (in the order of 50 to 100 rpm).

A typical cycle for the Task II dynamic load test on the ramp-roller clutch is shown in the oscillograph record of Figure 137. It was concluded that although the ramp-roller clutch had worn throughout the test, the critical dimensions were still well within the allowable wear limits, and testing was continued.

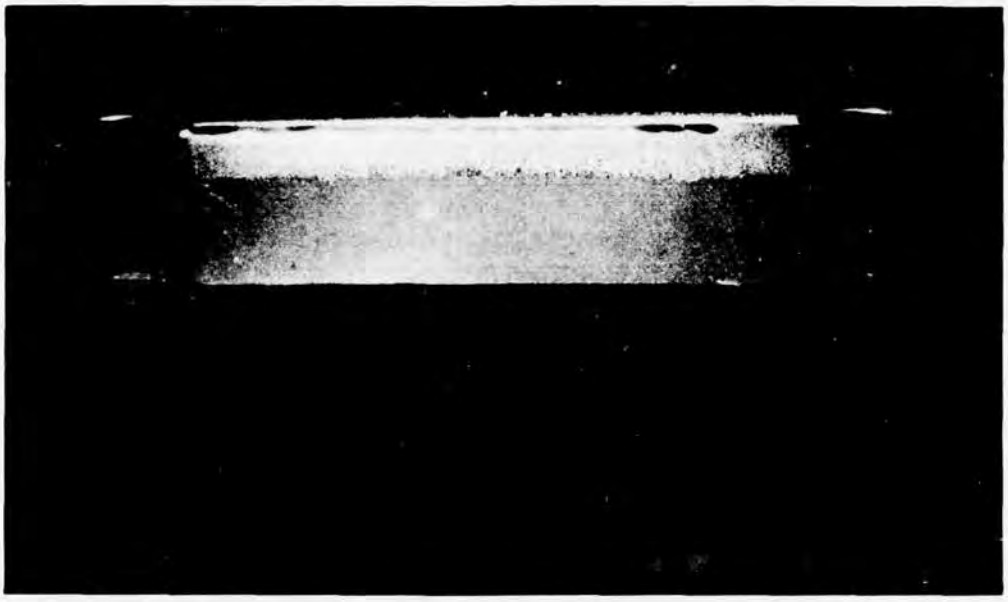

Figure 134. Ramp-Roller Clutch, Roller Slot at Completion of Task II Dynamic Load Test.

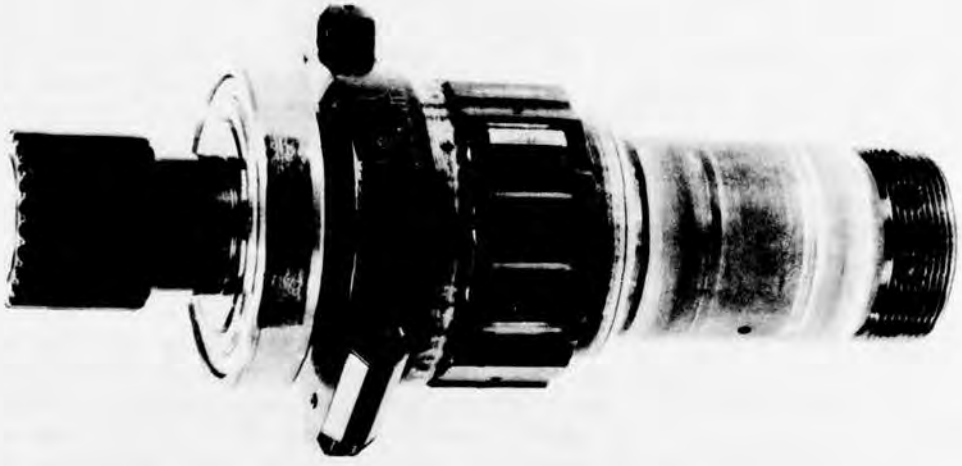

Figure 135. Ramp-Roller Clutch, Cam Shaft at Completion of Task II Dynamic Load Test.

Figure 136. Ramp-Roller Clutch, Outer Housing at Completion of Task II Dynamic Load Test.

The final clutch to be tested in the Task II dynamic load test was the spring clutch. As with the previous dynamic load tests, the spring clutch completed all testing without difficulty. Spring wear had increased throughout the test on the spring coils located in the output housing that were not receiving lubrication. This had been expected from the evidence found during overrunning testing. The magnitude of the wear was not significantly greater at the end of the test than it was at the beginning. Some new bands of wear had been formed near the center coils of the spring. The wear incurred was not considered significant. The overall spring condition was good, and the spring clutch was considered to be ready for further testing.

A typical cycle of the Task II dynamic load test conducted on the spring clutch is shown in the oscillograph record of Figure 138.

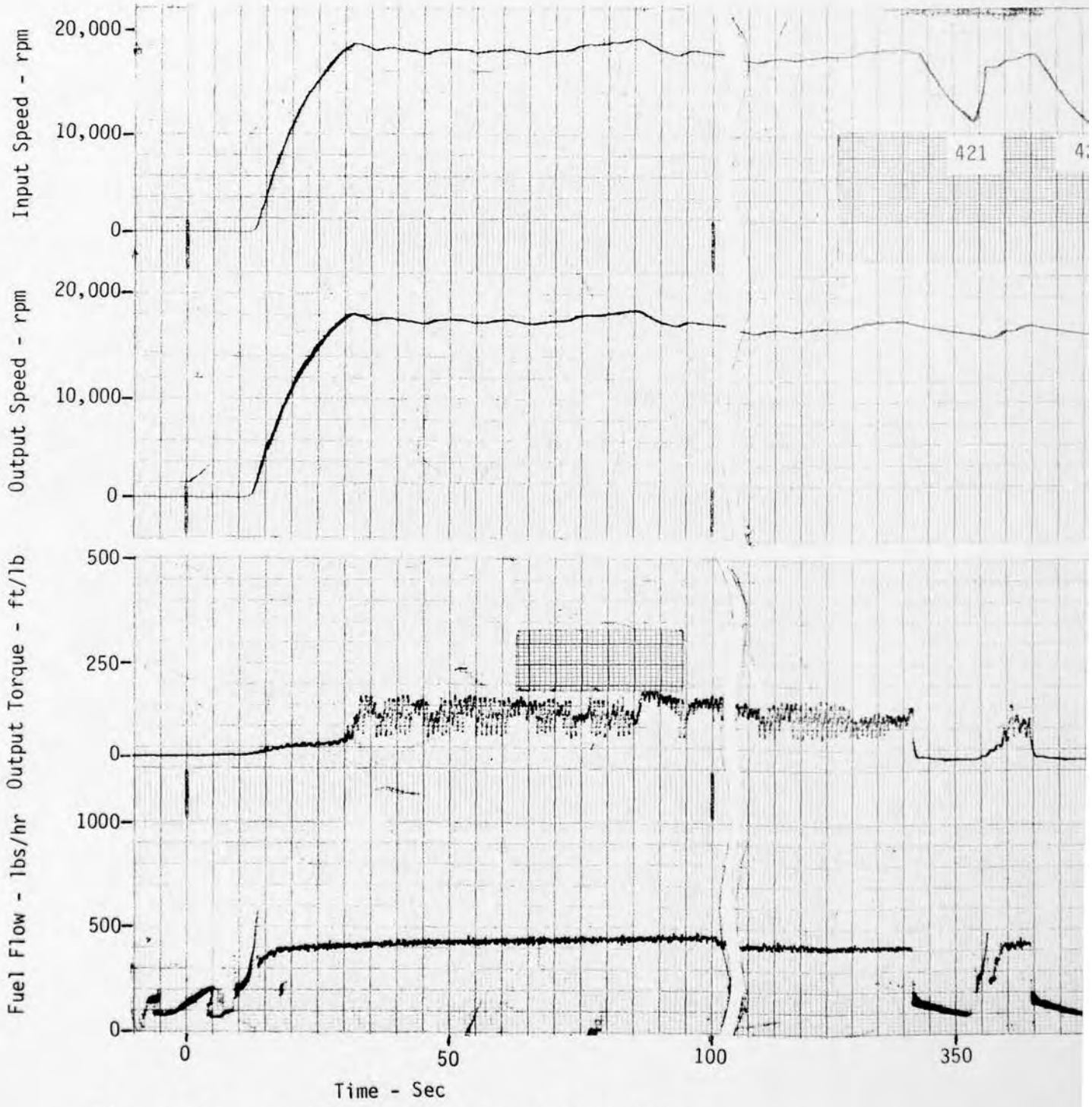

Figure 137. Typical Cycle, Ramp-Roller Clutch, Task II Dynamic Load Test.

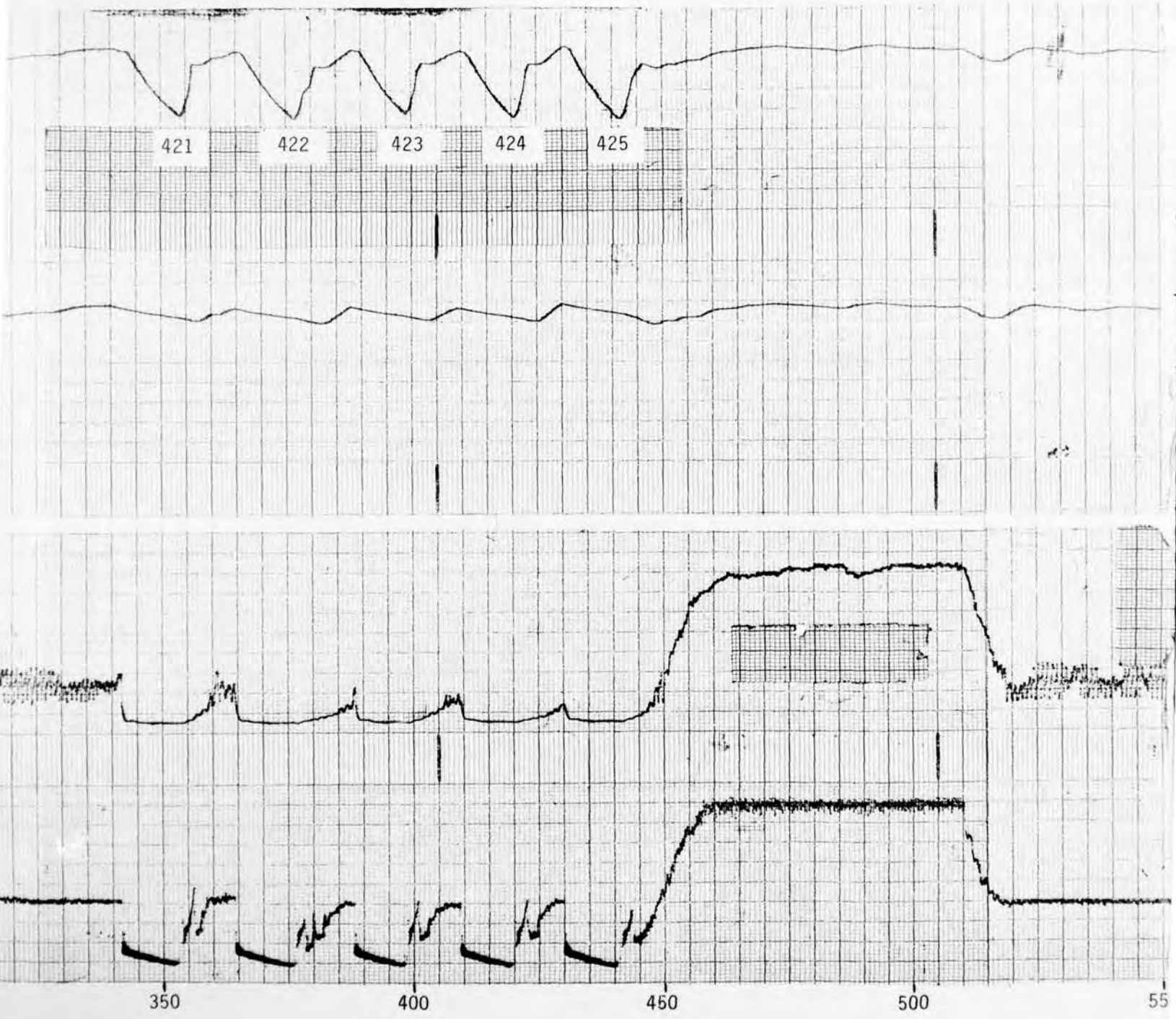

2

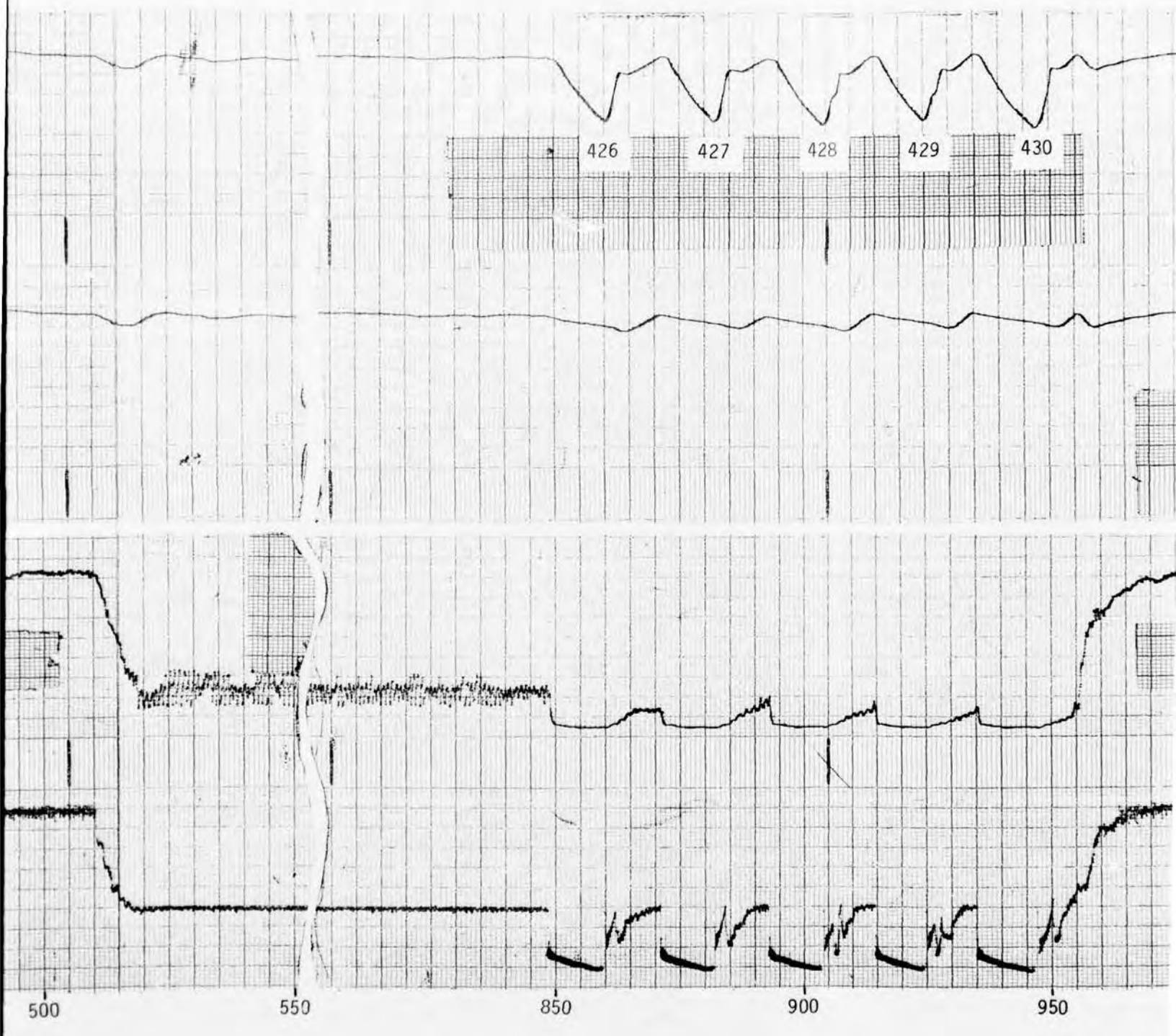
426
427
428
429
430
500
550
850
900
950

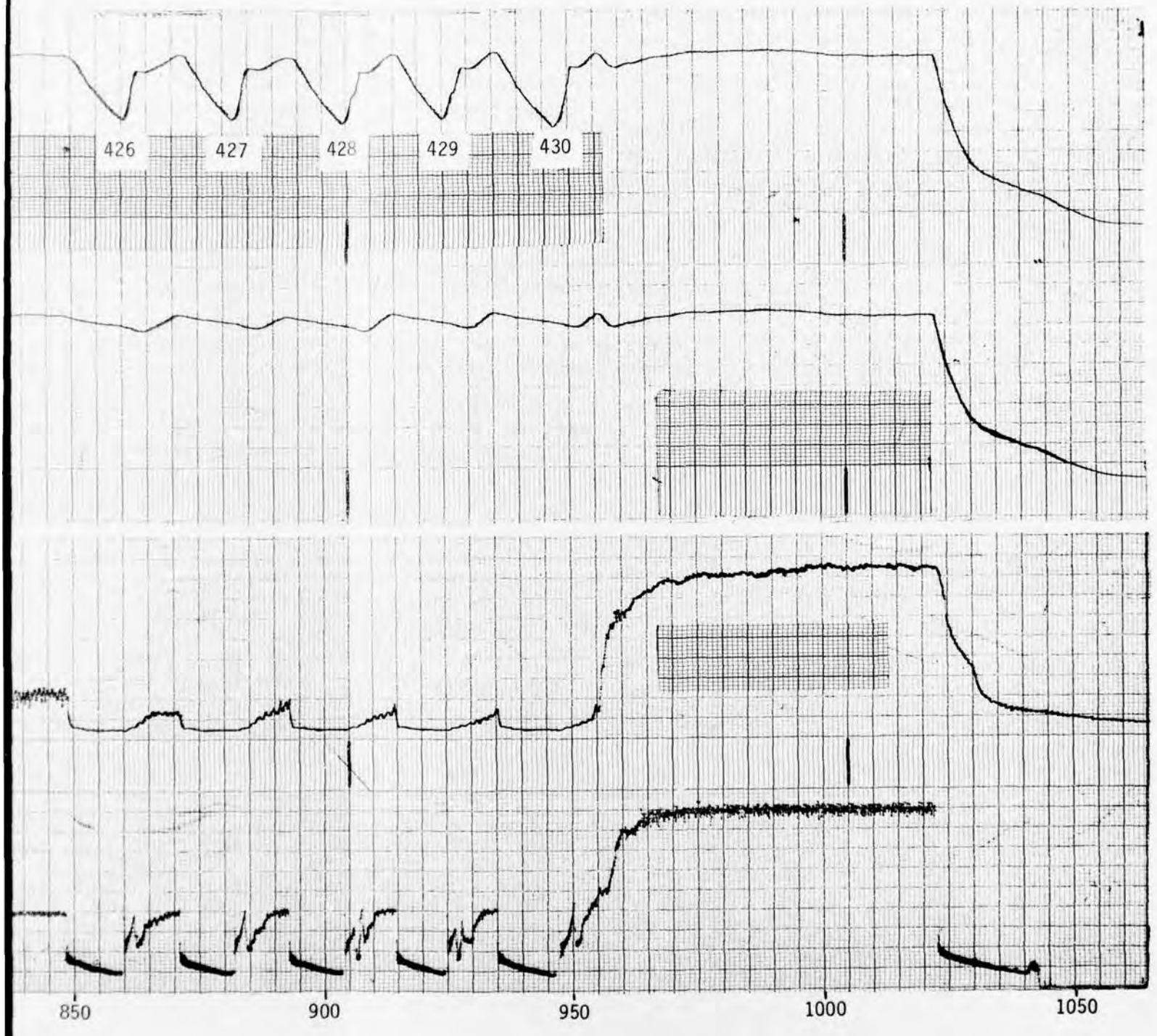
426
427
428
429
430
850
900
950
1000
1050

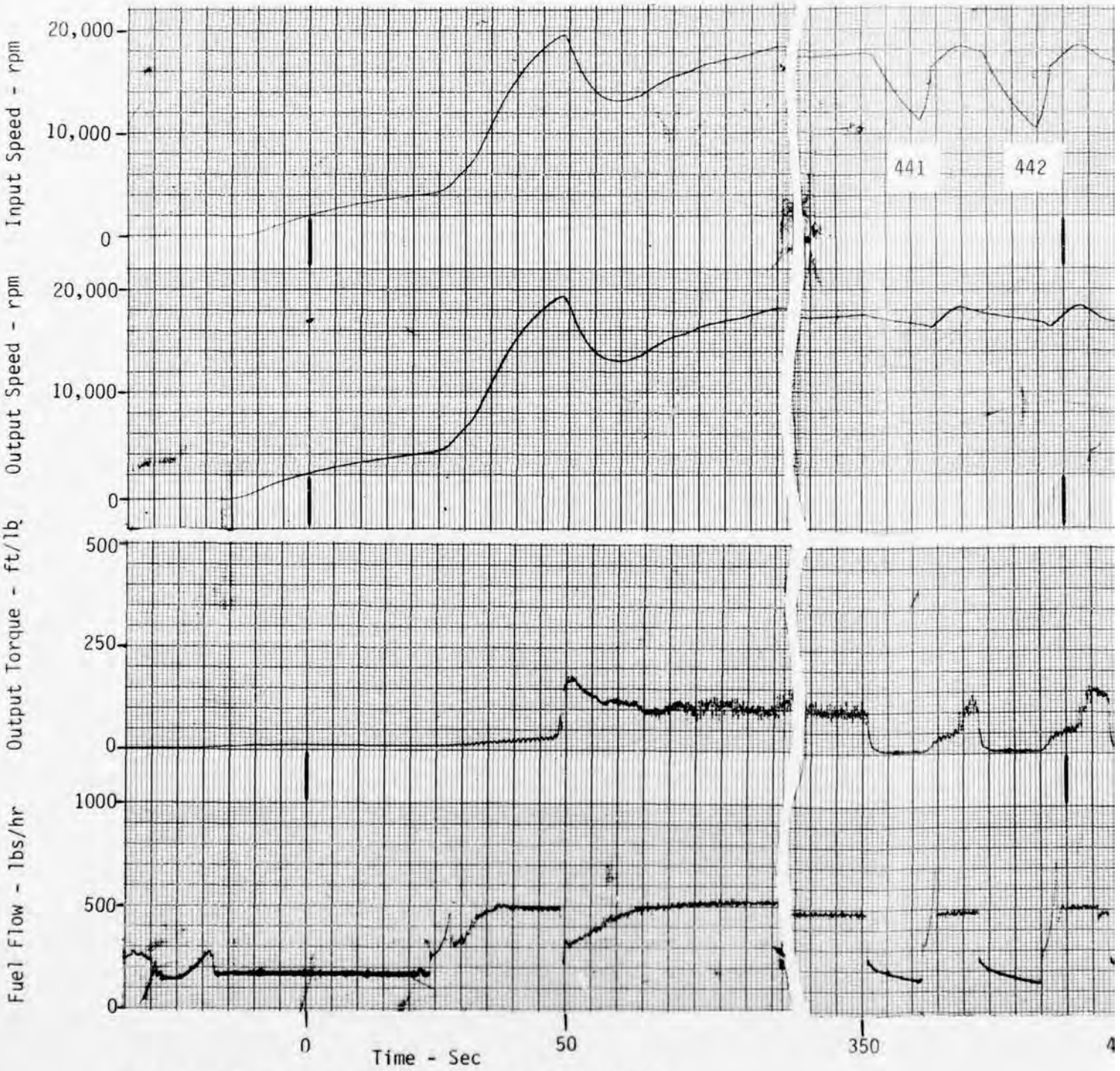

Figure 138. Typical Cycle, Spring Clutch, Task II Dynamic Load Test.

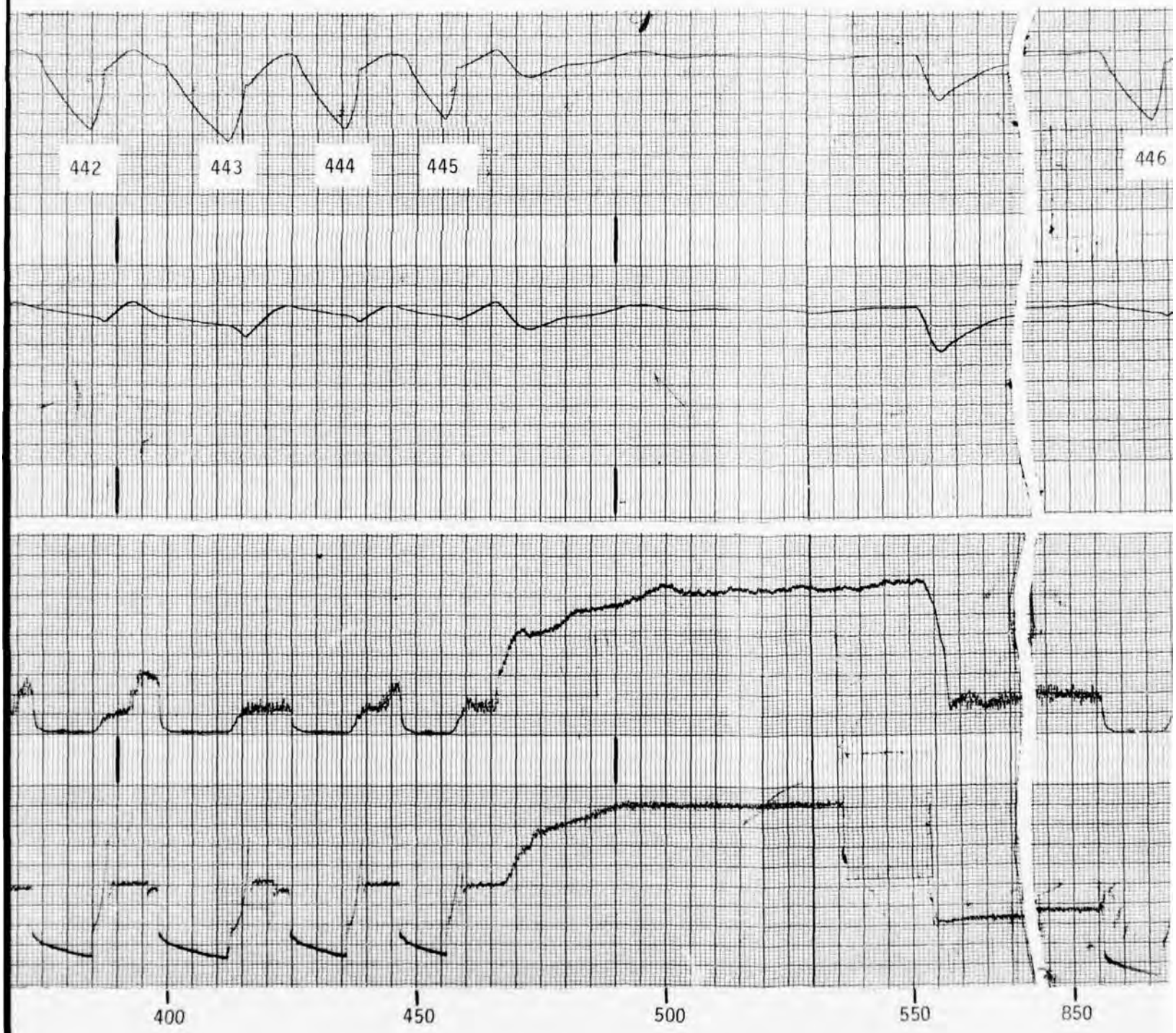
442
443
444
445
446
400
450
500
550
850

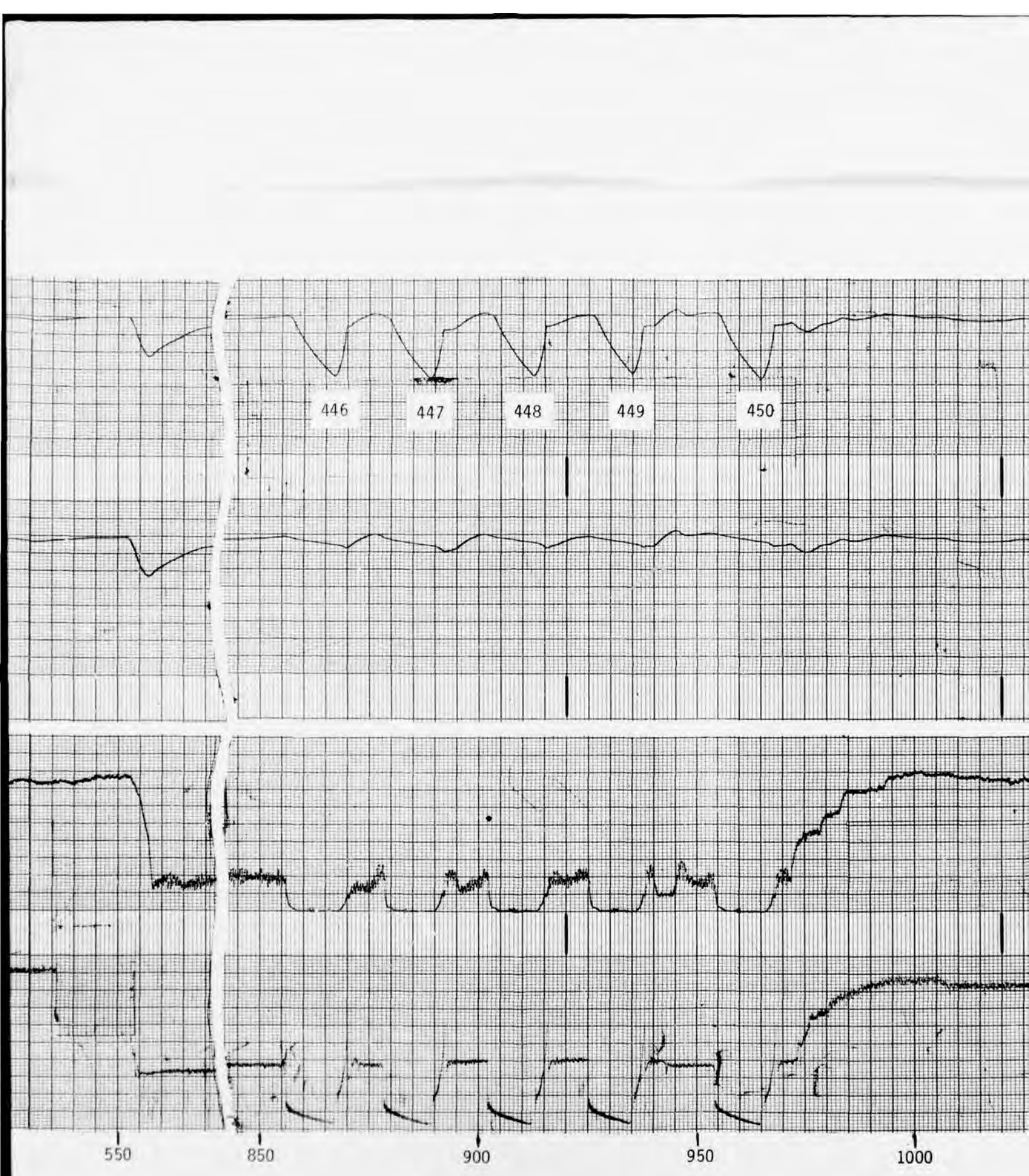

9

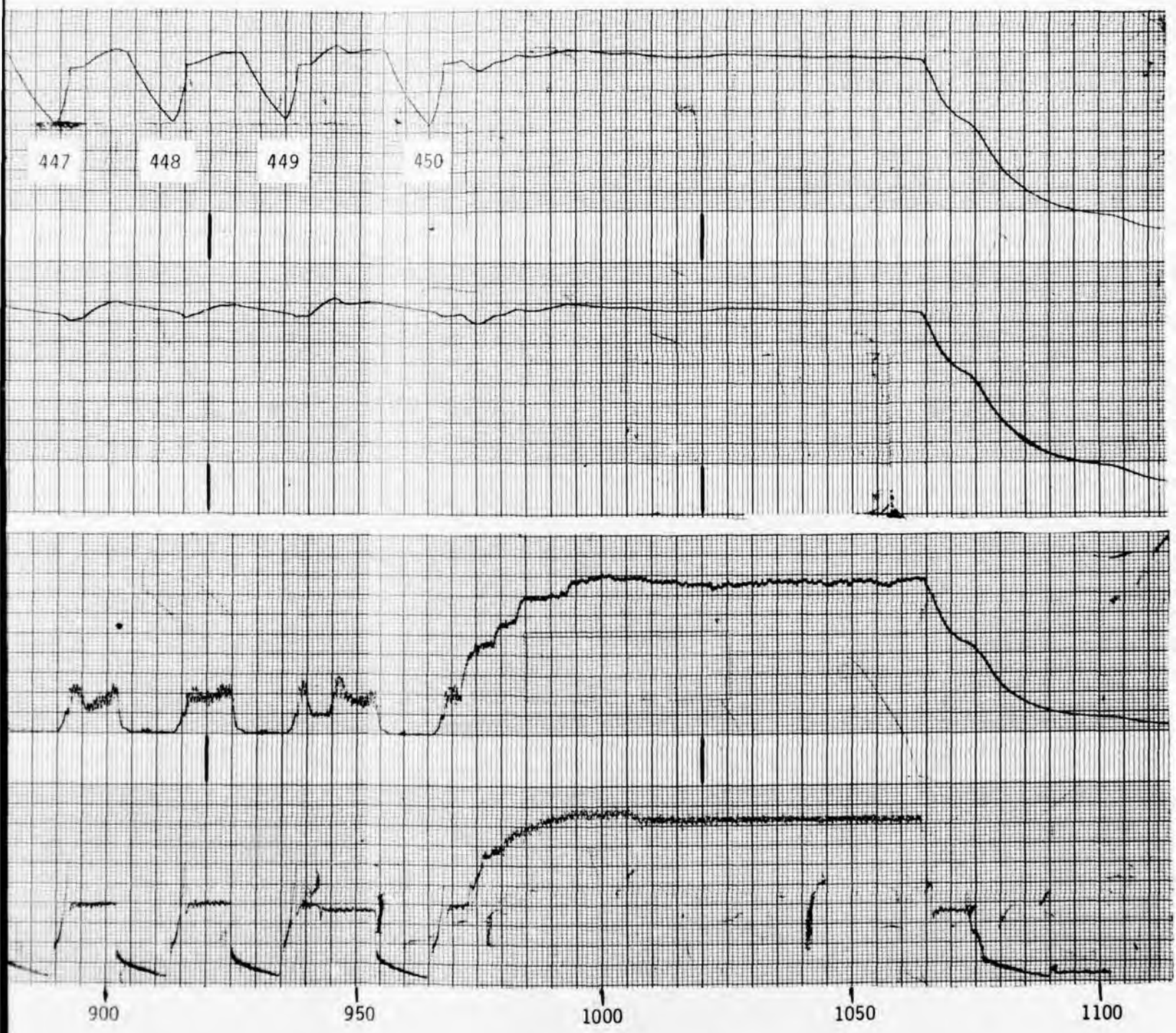

c1

Environmental Test Results

Environmental testing of the three clutch designs consisted of two parts: (1) testing with high-temperature oil, and (2) testing with low-temperature oil. Testing was conducted in the turbine test facility using a test cycle similar to that used in the dynamic load tests; i.e., run at simulated flat-pitch rotor, conduct five high-speed disengagements and engagements, operate at 1500 hp, and shut down. This procedure was repeated 10 times for a total of 50 engagements and disengagements.

Hot-Oil Environmental Test Results

In the high-temperature environmental test, the clutch oil supply was preheated to 300°F. The sprag clutch was the first clutch to be subjected to testing, and the test was completed without incident. Wear of the components incurred during the test was minimal.

The ramp-roller clutch was the second clutch to be tested in the high-temperature environmental test. The testing was uneventful. Deterioration of the ramp-roller clutch wear points throughout the course of the test was minimal. However, there were faint lines of wear progressing from the normal overrunning position back to the undercut pocket area, indicating that the rollers were transversing this area which they should not have been doing. There were also heavier areas of wear on each end indicating that the rollers were skewing as they "chattered" back and forth. Apparently the redesigned roller retention cage did not completely solve the roller chattering problem, as had been thought. The percentage of operation in the incorrect positions was small; however, it was decided that testing of the roller clutch would continue with the hardware as it was.

The last clutch to be tested in the high-temperature environmental test was the spring clutch. As with the previous high-temperature tests, the spring clutch high-temperature test was conducted without incident. Disassembly and inspection of the spring clutch components showed that no abnormalities had occurred during the test. The components were in essentially the same condition as they were prior to the start of test.

Cold-Oil Environmental Test Results

The second portion of the environmental tests consisted of low-temperature operation. In terms of calendar time, the low-temperature environmental test was actually conducted after the dynamic cyclic test (discussed in the next chapter). The objective of the low-temperature test was to simulate a start-up at -40°F, warm-up, engagement of the second engine in a twin-engine helicopter and takeoff. To meet these objectives, the procedure used was designed to simulate the actual conditions that would be felt by the helicopter clutch in a cold start in the field. First, the clutch housing was cold soaked to -40°F. This simulated the transmission standing at rest in an ambient air temperature of -40°F. Meanwhile, the oil supply was cooled to 0°F. The oil supply during this cooling period was shut off from the clutch. The turbine was then started and accelerated to ground idle at simulated flat-pitch rotor power (approximately 400 hp). The clutch was then operated in this condition for 5 minutes during which no oil was fed to the clutch. This simulated a start-up at -40°F, a pickup of load, and a warm-up period during which the actual helicopter clutch would not be receiving any oil because of the high oil viscosity involved and the inability of the conventional helicopter transmission lubrication pump to move any large quantities of oil at -40°F. After approximately 5 minutes of warming up, the valve that supplied oil to the clutch was opened, and the oil was permitted to flow to the clutch at 0°F. Again, this simulated the conditions that the helicopter clutch would experience in the field as the oil would have been heating up from -40°F to approximately 0°F in the warm-up period. After the oil was again flowing to the clutch, five disengagements and five engagements were conducted, followed by an increase in power to 1500 hp. This simulated the second engine start-up, pickup of the load, and takeoff. The turbine was then shut down, and the cold soaking was again started in preparation for the next cycle. The above cycle was conducted 10 times for a total of 10 cold starts, 50 engagements and disengagements, and 10 takeoffs for each clutch.

The ramp-roller clutch was the first clutch to be tested in the low-temperature environmental test. The testing was conducted without incident. When the ramp-roller clutch was disassembled, it was found to be moderately contaminated with what appeared to be metal filings. Analysis showed that the metal filings were of bronze material of the type used on the bushings that guide the roller retention carrier. These metal filings had not created any problems during the test and were more or less found at random on the cam flats, the outer housing, and the cage areas of the clutch. Inspection of the bronze bushings did not reveal any unusual or heavily worn

areas. The bronze material has a linear coefficient of thermal expansion higher than that of steel so that at the low temperature experienced during the test, the bushings had a tendency to bind on the cam due to differential thermal expansion. The conclusion was reached that the ramp-roller clutch was operational and that the bronze wear was a minor problem.

The spring clutch was the second clutch to undergo low-temperature environmental tests. The spring clutch low-temperature test was conducted without incident.

The final clutch to be tested in the low-temperature environment was the sprag clutch. During the initial, checkout run, in which the clutch housing had been cooled to -40°F, the sprag clutch was unable to engage after it had been disengaged. After several attempts to engage, the sprag clutch sustained an engagement, at which time the speed of the output was approximately 6200 rpm and the speed of the input was 7000 rpm. Instantaneously, the sprag clutch attempted to drive the output at the input speed. Since the inertias involved are very large in the turbine test stand, the torque transmitted instantaneously across the clutch exceeded the clutch capacity and the driveshaft fractured.

Figure 139 shows the results of the overspeed engagement. The output shaft sheared in an area between the sprag inner race and the spline connection. The fracture is typical of that experienced when a high-strength steel part fails in pure shear. The inner race was found to be in good condition from a dimensional standpoint, measuring 1.7497/1.7499 and 1.7502/1.7504 across each spragway. A hardness check found the hardness to be Rockwell "C" 62, which is the mean of the 60 to 64 drawing specification. Visually, the two spragways were in poor condition due to the presence of numerous high-load patterns that indicate slight brinnelling and galling. The number and locations of these high-pressure patterns suggest that the clutch bounced in and out of engagement approximately six times prior to shaft shear.

Figure 140 shows the sprags, which were in poor condition. The contact points in the high load region (.338 height) showed distress. In this region, the strut angles varied from 4.7 degrees to as high as 5.3 degrees, which represent increases of .5 degree and .8 degree, respectively. In the overrunning region at the .328 height, there was very little change in the strut angle curves, indicating an insignificant amount of distress that might cause improper engagements.

Figure 141 shows the outer race, which was found to be in poor condition both visually and dimensionally. The diameter

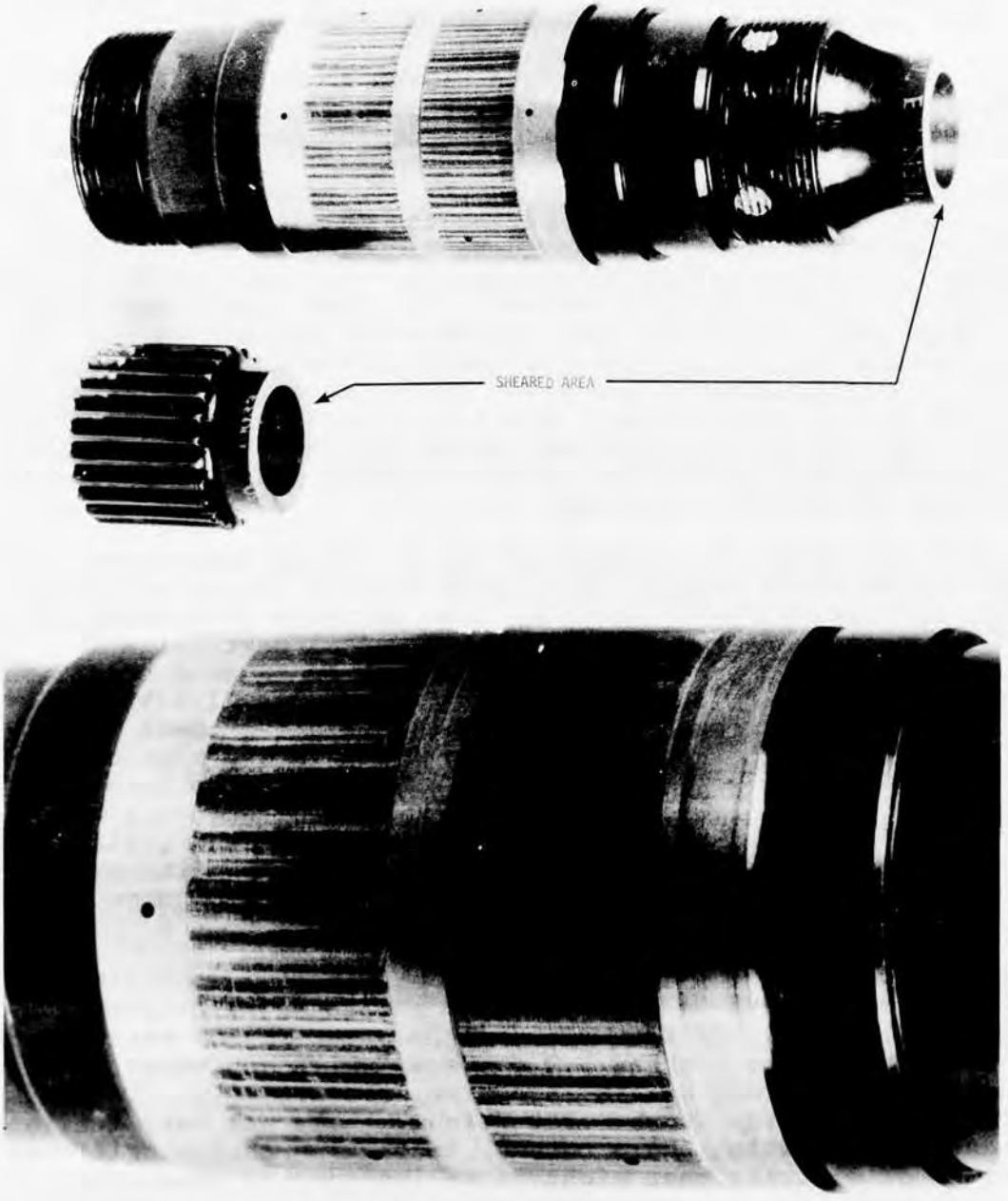

Figure 139. Sprag Clutch Inner Race at Completion of Low-Temperature Environmental Test.

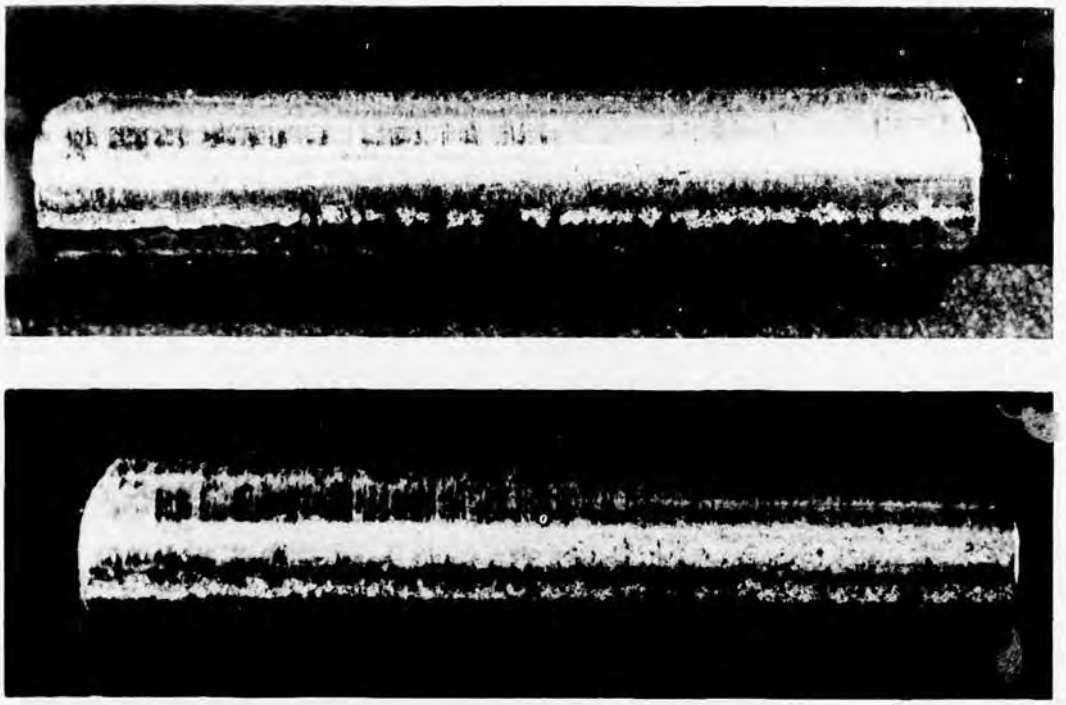

Figure 140. Typical Sprags at Completion of Low-Temperature Environmental Test.

Figure 141. Sprag Clutch Outer Race at Completion of Low-Temperature Environmental Test.

across the spragway measured 2.412/2.414 inches, indicating a permanent yield of .005/.007 inch. A hardness check showed that at the spragway, the hardness measured Rockwell C 31-32, which is well below drawing specifications of Rockwell C 60-64. This was caused by an error in heat-treating procedures when the housing was carburized but not placed back in the furnace for rehardening. A check of all the sprag clutch outer races showed that they were all in a similar state of heat treatment. Visually, there were eighteen high-pressure load patterns on each spragway in the form of brinnel marks, which measured approximately .002 inch deep. Although the outer housing was not hardened, as discovered during the cold-oil test, the housing showed no apparent signs of distress during all previous tests. Brinelling was less than .0001 inch prior to the cold test. Thus, the unhardened condition was not felt to be a contributing factor to the overspeed engagement.

Upon examination of the sprag retainer assembly after testing, it was found that the number 3 ribbon tab was broken off through the center of the formed wrinkle. It can be assumed that the tab broke sometime during the cold test because of the equal wear patterns present on all the sprags at the tab interface. The exact cause of the breakage cannot be determined since the broken tab was lost, probably upon disassembly, but it is possible that the tab fractured during the shock engagement. The conclusions reached regarding the reason that the sprag clutch did not engage are:

1. Insufficient sprag energizing to overcome the high viscosity of cold oil. This may result from the drag strip's tendency to lessen its load as the clutch speed increases.

2. The broken ribbon tab, if it occurred previous to the shock engagement, may have become wedged between the outer cam of a sprag and the outer race, which could also upset the balance of the sprags and prevent an engagement.

For future high-speed sprag clutch designs, it is important that the outer housing be designed so that all the oil in the spragway will drain out while retaining the flooded-oil feature. During cold starts, there would be no oil in the spragway area to reduce the sprag energizing. After warm up, the oil would again flow into the clutch.

Dynamic-Cyclic Test Results

The dynamic-cyclic testing conducted during the Task II portion of the program was run on the turbine test facility. The objective of the test was to operate each clutch in a forced torsional vibration mode at 95 ± 5% of design, which corresponds to 1425 ± 75 hp. To apply this magnitude of vibratory torque load on each overrunning clutch, a special fuel control valve was designed and built. The valve was connected to a fractional-horsepower, 60-rpm synchronous-speed electric motor. A cam was affixed to the output shaft of the motor so that, as the cam rotated, the cam follower opened and closed a valve in the fuel line. The fuel flows for the maximum and minimum settings on the valve were adjusted to produce 1500 hp and 1350 hp respectively. Each clutch was operated with the above arrangement for 3 hours, which, at 60 cycles per minute, represents 10,800 cycles of torsional fatigue loading.

The sprag clutch was tested without problems. Wear and brinelling incurred during the test was negligible. There was no noticeable or measured difference between any sprag clutch components before or after testing.

The ramp-roller clutch was the second clutch to undergo dynamic-cyclic testing. As with the sprag clutch, no problems were encountered during the testing, which went very smoothly. Post-test inspection and measurement did not reveal any abnormalities. The roller end wear did not progress during this test since the rollers were locked and did not rotate relative to the cage. A typical cam flat is shown in Figure 142.

The spring clutch was the final clutch to be tested in the dynamic cyclic test. As with the previous tests, 10,800 torque cycles were completed without incident. Post-test inspection and measurement of the hardware did not reveal any changes that occurred during the test.

Since the dynamic-cyclic test completed all of the dynamic testing in the program, it is informative to examine results obtained from the beginning of Task II dynamic testing to the end. Figure 143 depicts the key wear measurements for the clutches taken throughout the Task II tests.

For the spring clutch, the key wear parameter is the radial wear of the teaser coils on the overrunning (sliding) end of the spring. This measurement was obtained with a micrometer and is an average of measurements at two different positions, 90 degrees apart. These measurements were taken at the conclusion of each test.

Figure 142. Typical Cam Flat at Completion of Dynamic Cyclic Torque Test.

On the sprag clutch, the key measurement was the bandwidth of a typical sprag; in this case, sprag number 1. To measure the average bandwidth, a photograph was taken of the inner surface of sprag number 1 showing the bandwidth of wear after each test. From the photograph, a planimeter was used to measure area, and using appropriate scale factors, the average width was obtained by dividing the area by the sprag length. The average width of the wear band was then converted to depth of wear using the appropriate geometry of the sprag and the inner race. The depth of wear is plotted in Figure 143.

In the ramp-roller clutch, the key wear measurement was roller diameter. This was measured with a micrometer after each test. It is seen in Figure 143 that the roller clutch wear increased significantly during the dynamic load tests. A projection of the wear curve for the ramp-roller clutch will not give a long clutch life, whereas the projections of the sprag and spring clutch wear parameters would indicate long clutch overrunning lives.

Figure 144 is a series of photographs of sprag number 1 after the various tests conducted during Task II. The originals of these photographs were used to obtain the average bandwidth of wear as previously discussed.

The rollers of the ramp-roller clutch incurred a peculiar type of wear throughout the testing on the end faces of several of the rollers. The roller with the highest wear was roller number 1. The next worst case was roller number 2, which only experienced approximately half of the wear of roller number 1. A plot of roller number 1 end wear is shown in Figure 145.

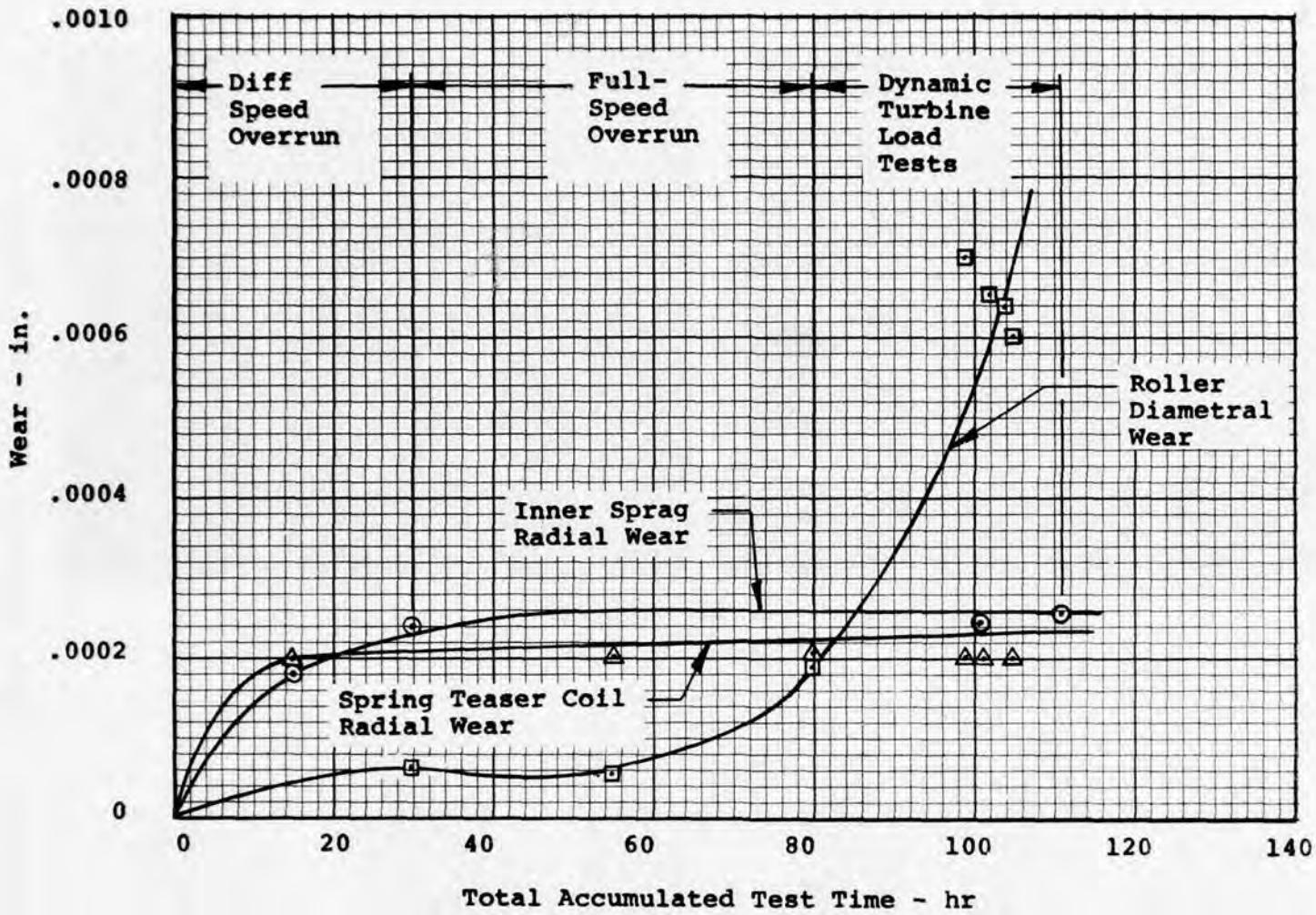

Figure 143. Wear Versus Time, Spring, Sprag, and Ramp Roller Clutches.

Sprag #1
After 15 Hours
Differential-
Speed
Overrun

Sprag #1
After 30 Hours
Differential-
Speed
Overrun

Sprag #1
After 50 Hours
Full-Speed
Overrun

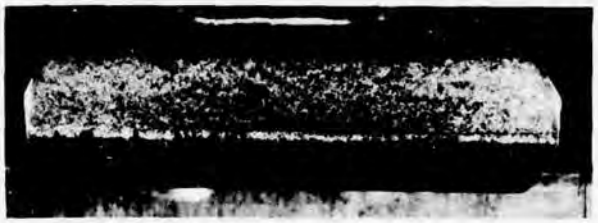

Sprag #1
After Dynamic
Load Tests,
750 Engagements

Sprag #1
After Dynamic
Cyclic Test,
10,800 Cycles
95±5%

Sprag #1
After High
Temperature
Environmental
Test
300°F

Figure 144. Sprag Condition Throughout Testing.

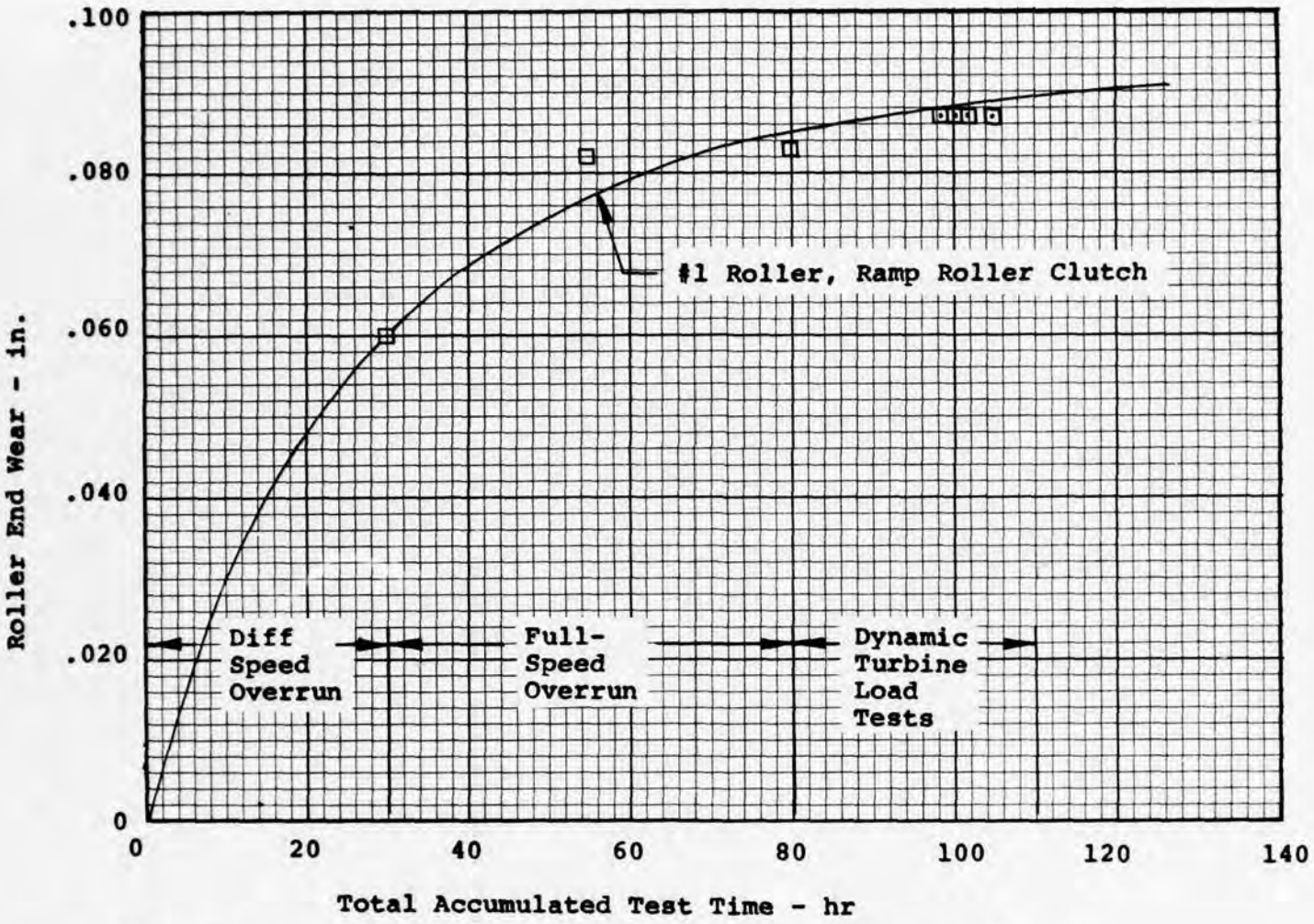

Figure 145. Roller End Wear Versus Time, Ramp-Roller Clutch.

Static-Cyclic Test Results

Static-cyclic testing was conducted on the static test facility. A typical clutch set up in the static facility is shown in Figure 38. Torque was applied through a hydraulic rotary actuator to the clutch input side. The output side of the clutch was bolted to the ground. Each clutch was strain gaged on its outermost shaft in eight equally spaced locations. These gages were used to center the clutch so that no side loads were produced as a result of eccentric torque application.

A torque load of 9450 $\pm$ 1000 inch-pounds was applied at a frequency of 10 cycles per second using a sine-wave excitation. Test duration was 10 million cycles or inability to sustain the applied torque load, whichever occurred first. Continuous oil flow was maintained within each clutch assembly using MIL-L-7808 oil at room temperature. The test rig included automatic shut-down devices in the event of torque loss or chip detection.

The first clutch to be tested in the static-cyclic torque test was the spring clutch. At the time of the test, the spring clutch used the flanged arbor that proved to be very good for overrunning but that restrained the spring axially so that the teaser coils could not touch the output housing in the axial direction. Relative motion during overrunning between the teaser coils and the output housing was restricted to the outside diameter of the spring only.

The spring clutch was operated for 753,860 cycles when the test was stopped by clutch slippage to the limits of the rotary actuator's travel (100 degrees maximum) and the inability of the clutch to sustain reapplied torque load. The spring's teaser coils on the overrunning end of the clutch had "jammed" against the flange of the arbor, causing the diameter of the teaser coils to reduce to the point where torque could no longer be transmitted. The spring clutch was cleaned, reassembled and testing resumed. After an additional 744,020 cycles, a chip was detected and the test stopped. Figure 146 shows fine metallic slivers and light metallic chips inside the spring's center slot. Figure 147 is a close-up of the spring arbor dowel-pin hole. Note the burr on the edge of the hole, which indicates that a high degree of working has taken place. Figure 148 shows that the silver plating applied to the spring's teaser coils had chipped off. These chips and silver pieces worked their way through the system to the chip detector. The system was again cleaned, a new spring was installed, and testing was resumed. This time the spring clutch sustained 133,050 cycles of operation before the limit of the actuator was reached. Repeated

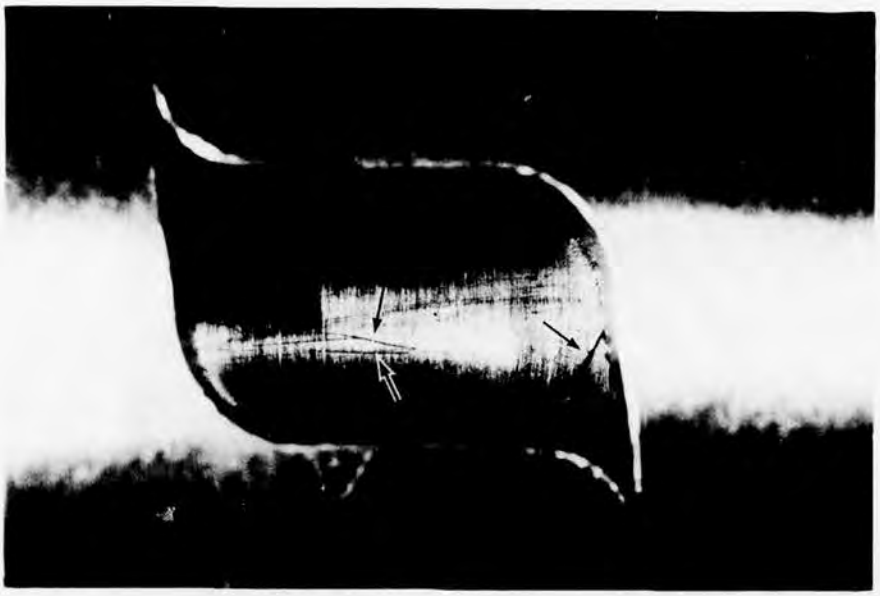

Figure 146. Spring Clutch Center Coil Hole, Static-Cyclic Test.

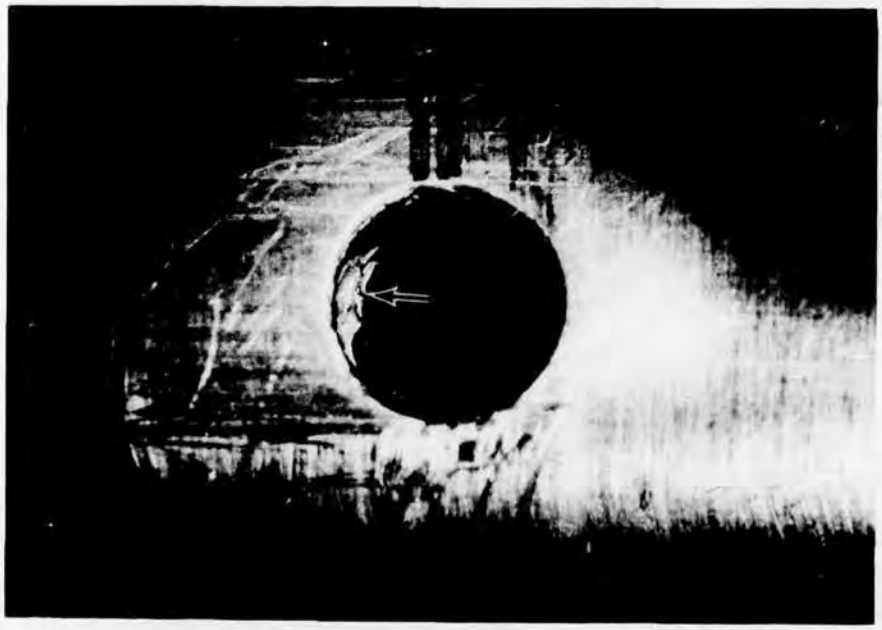

Figure 147. Spring Clutch Arbor, Retention Pin Hole, Static-Cyclic Test.

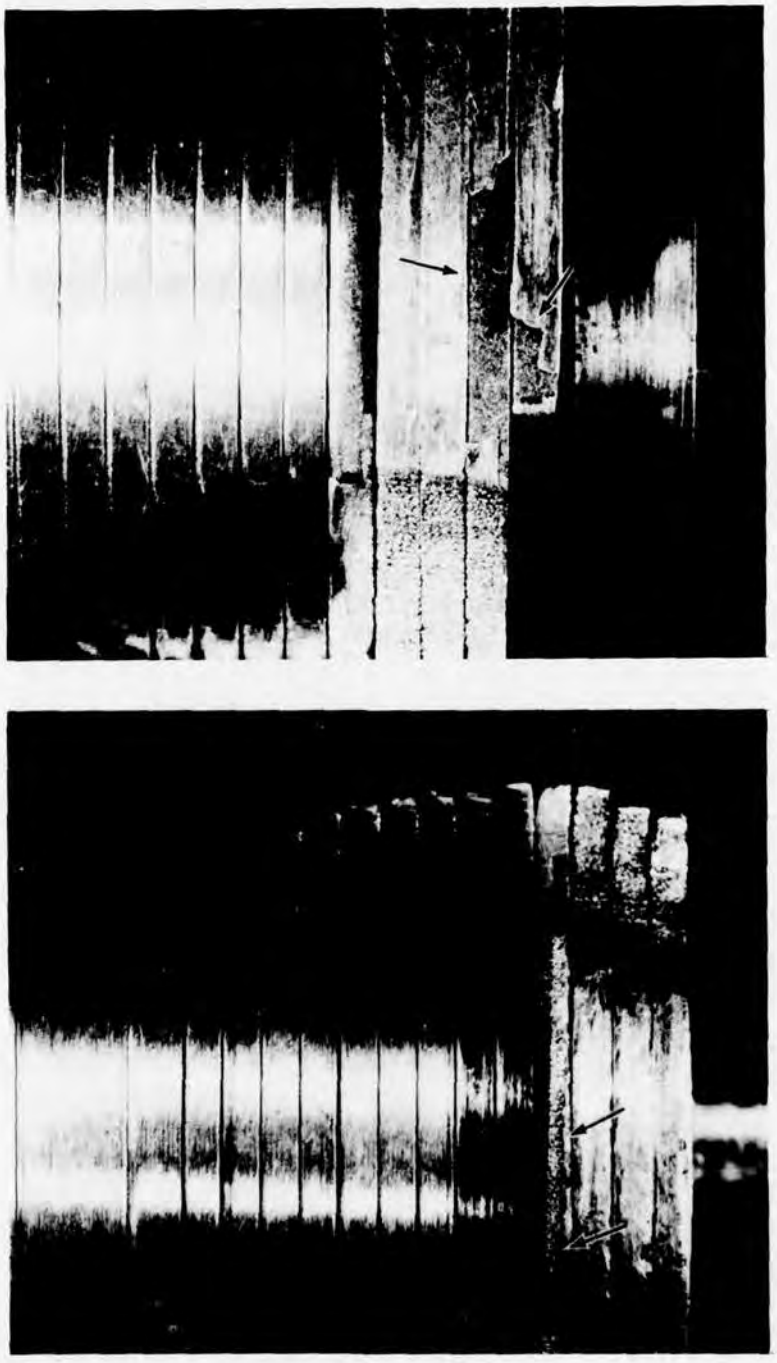

Figure 148. Spring Teaser Coils, Static-Cyclic Test.

attempts to reengage the clutch failed, and the clutch was disassembled and inspected. As in the first spring clutch test, the spring was unable to drive because the spring had "bunched up" against the flanged arbor and had jammed itself tightly against the flange, rendering drive-mode operation impossible. Figure 149 illustrates the jamming condition. Note the staggering of the end teaser coils with the progressively increasing offsets towards the free end. During each cycle of vibratory torque application, the spring had crept towards the flange. In operation on the helicopter, each time the engines are turned off after a flight, the spring clutch would return to its arbor and free itself of this jamming effect. However, because of the possibility of loss of torque, the flanged arbor design was abandoned in favor of the original design with slotted spacer, and all Task II dynamic testing was conducted with the slotted spacer design. In this design, the teaser coils will move in unison with the output housing, and the tendency to creep is reduced.

An additional static cyclic test was conducted with the spring clutch in its original configuration, with the slotted spacer. This test was conducted for 1,864,750 cycles before termination by loss of torque drive. Inspection showed that the spring had again crept towards the bronze spacer and had, in fact, wedged itself into the spacer, leaving an impression .012 inch deep where the end of the spring touched the washer. The condition of the spring is shown in Figure 150. The dark lines seen on the center coil sections are the result of permanent yielding. An analysis of the stresses present in the spring for the torque load being applied indicates that the spring should not yield at even twice the load tested. The conclusion was that the torque was not being applied uniformly to the spring clutch assembly, and since the spring clutch design is sensitive to housing bore misalignment, the loads induced in the spring were magnified. It was decided that the final configuration tested, i.e., the design with the bronze spacer between the output housing and the spring's overrunning end, would be used for all further testing.

The second clutch to be tested in the static-cyclic test was the ramp-roller clutch. It was operated at a torque of 9450 $\pm$ 1000 inch-pounds for 10,000,000 cycles without difficulty. Inspection of the roller clutch components after the test did not reveal any abnormalities. Figure 151 shows a typical roller at the completion of testing. The light line seen on the roller was the result of contact between the roller and the outer housing in a single continuous position and was of negligible depth. The camshaft, as shown in Figure 152, was in good condition. The brinell marks seen on the flats were of negligible depth.

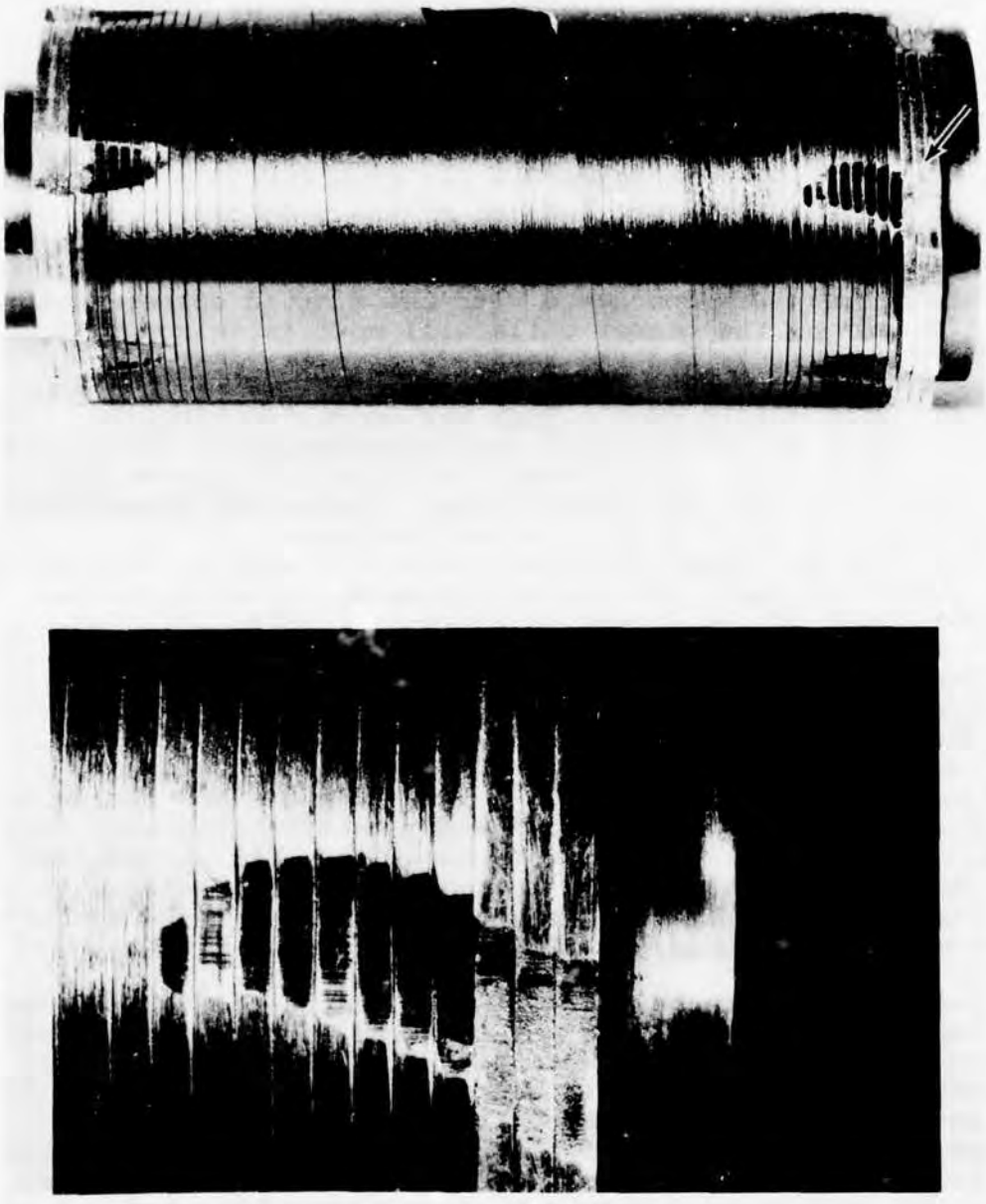

Figure 149. Spring Teaser Coil Jamming, Static-Cyclic Test.

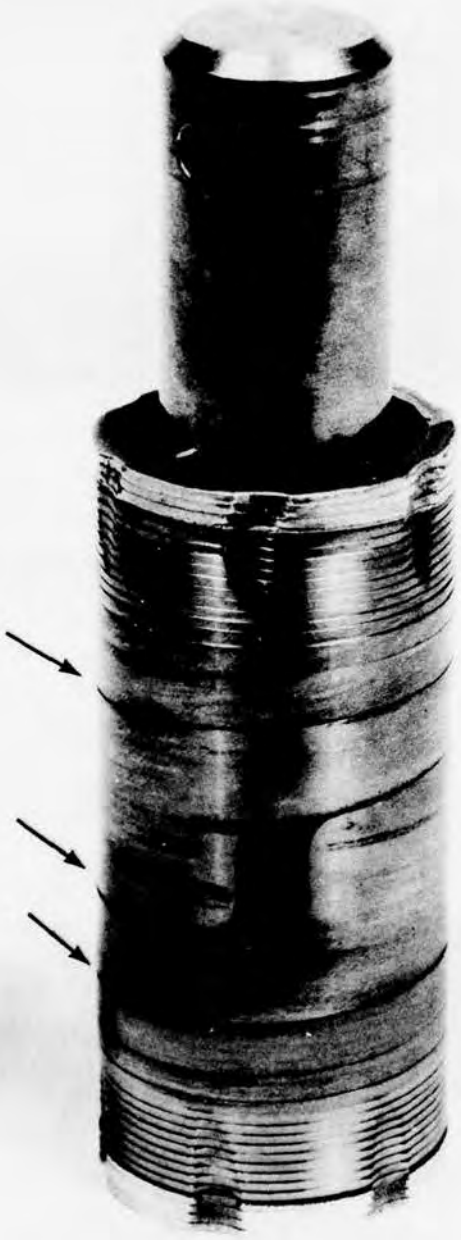

Figure 150. Spring at Completion of Static-Cyclic Test.

Figure 151. Roller at Completion of Static-Cyclic Test.

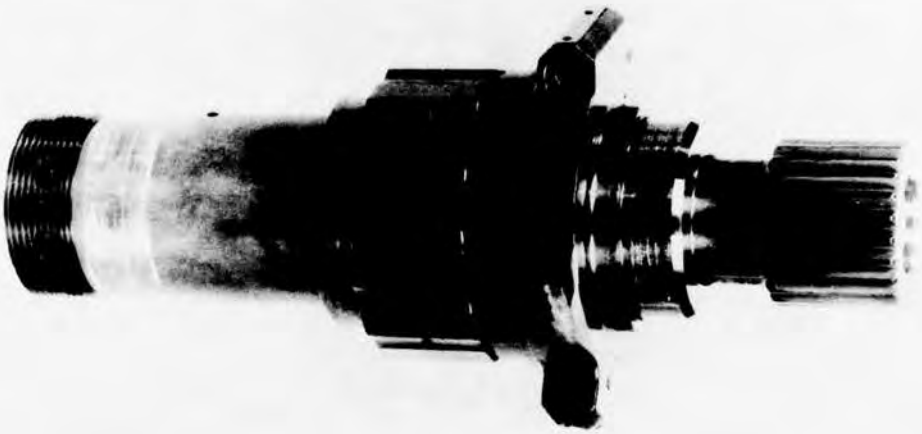

Figure 152. Camshaft at Completion of Static-Cyclic Test.

The final clutch to be tested in the static cyclic test was the sprag clutch. Testing went smoothly, and 10,000,000 cycles were completed without difficulty. Figure 153 shows the outer race. Brinell marks which measured .0004 inch deep can be seen at the contact points. Metalurgical inspection of the outer housing revealed that the bore hardness measured Rc 39, whereas the drawing requirement was Rc 60. During the manufacture of the part, in the heat-treating cycle, the housings were placed in the carburizing furnace and then cooled. However, they were never put back into the furnace for rehardening, leading to the softened state found. The brinelling marks incurred during the test were the result of the unhardened condition of the housing and probably would not have been present had the outer housing been properly heat-treated. It should be noted that the condition of the housing did not affect the test other than the slight brinelling that occurred.

Static Overload Test Results

The static overload tests of Task II were conducted on the static test facility. During this test, torque was applied to each clutch in increments of 500 inch-pounds to a maximum of 18,900 inch-pounds or until the clutch was unable to sustain the applied torque load, whichever occurred first. The 18,900-inch-pound torque level represents four times the maximum design torque and is equivalent to 6000 hp. This exceeds the static structural requirements of the transmission system. The internal clutch components were lubricated by soaking the parts in MIL-L-7808 oil prior to testing. No lubricant was applied to the clutch during the test.

Torque, angular displacement between input and output sides of the clutch, and the diametral growth of the outer race (sprag and roller clutches) and the output housing (spring clutch) were monitored during the overload test. Torque readout was observed using an oscilloscope, a digital voltmeter, and a load-amplitude measurement system. Angular displacement was measured with graduated scales located on the input and the output adaptor flanges (test fixtures) and with pointers attached to the ground. Diametral growth was determined by averaging the output of eight strain gages tangentially oriented and equally spaced around the circumference of the component measured.

The first clutch to be tested in the static overload test was the spring clutch. The spring clutch sustained a torque load of 12,000 inch-pounds and slipped 23 degrees to the end of the rotary actuator available rotation (100 degrees maximum) when 12,500 inch-pounds of torque was applied. In the spring clutch design, approximately 50 degrees of the available

Figure 153. Sprag Clutch Outer Race, Static-Cyclic Test.

rotation are used up at very low torque levels (less than 500 inch-pounds). To determine if the spring clutch would have reengaged after slipping if additional rotation had been available, the test was repeated with a pre-twist of 45 degrees at the clutch output side. The spring clutch again slipped to the end of the available travel at the same torque, 12,500 inch-pounds. Figure 154 shows the spring. The housing condition was unchanged during the test but the spring sustained scoring marks on the outermost 13 coils (.040 thick coils) on the input end. Since the geometrics of the input end and the output end are identical, it is a matter of chance as to which end will slip first.

The second clutch to undergo static overload testing was the ramp-roller clutch. The roller clutch sustained a torque load of 18,500 inch-pounds but fractured at 18,800 inch-pounds during the final load increment. The fracture occurred at the inner race camshaft through the cross section adjacent to the drive spline. Figure 155 shows the camshaft with the fracture. This type of fracture is typical for a high-strength steel part subjected to pure shear. The calculated strength of the section was in close agreement with the test results. Prior to total fracture, appreciable yielding of the shaft was evident at torque levels exceeding 17,500 inch-pounds.

The final clutch to be tested in the static overload test was the sprag clutch. The sprag clutch sustained 18,900 inch-pounds of torque without evidence of yielding or slipping. Figure 156 is a plot of torque versus angular displacement for the three clutches tested. The yielding of the roller clutch is plainly seen in this curve. The sprag clutch geometry is identical to the roller clutch geometry in the area of fracture. That is, the spline is the same, the outside and the inside diameters of the adjacent area are the

Figure 154. Spring, Static Overload Test.

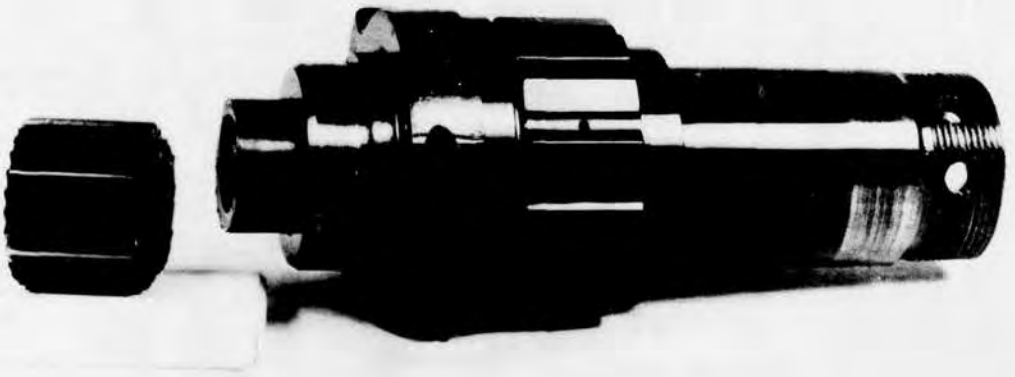

Figure 155. Camshaft, Static Overload Test.

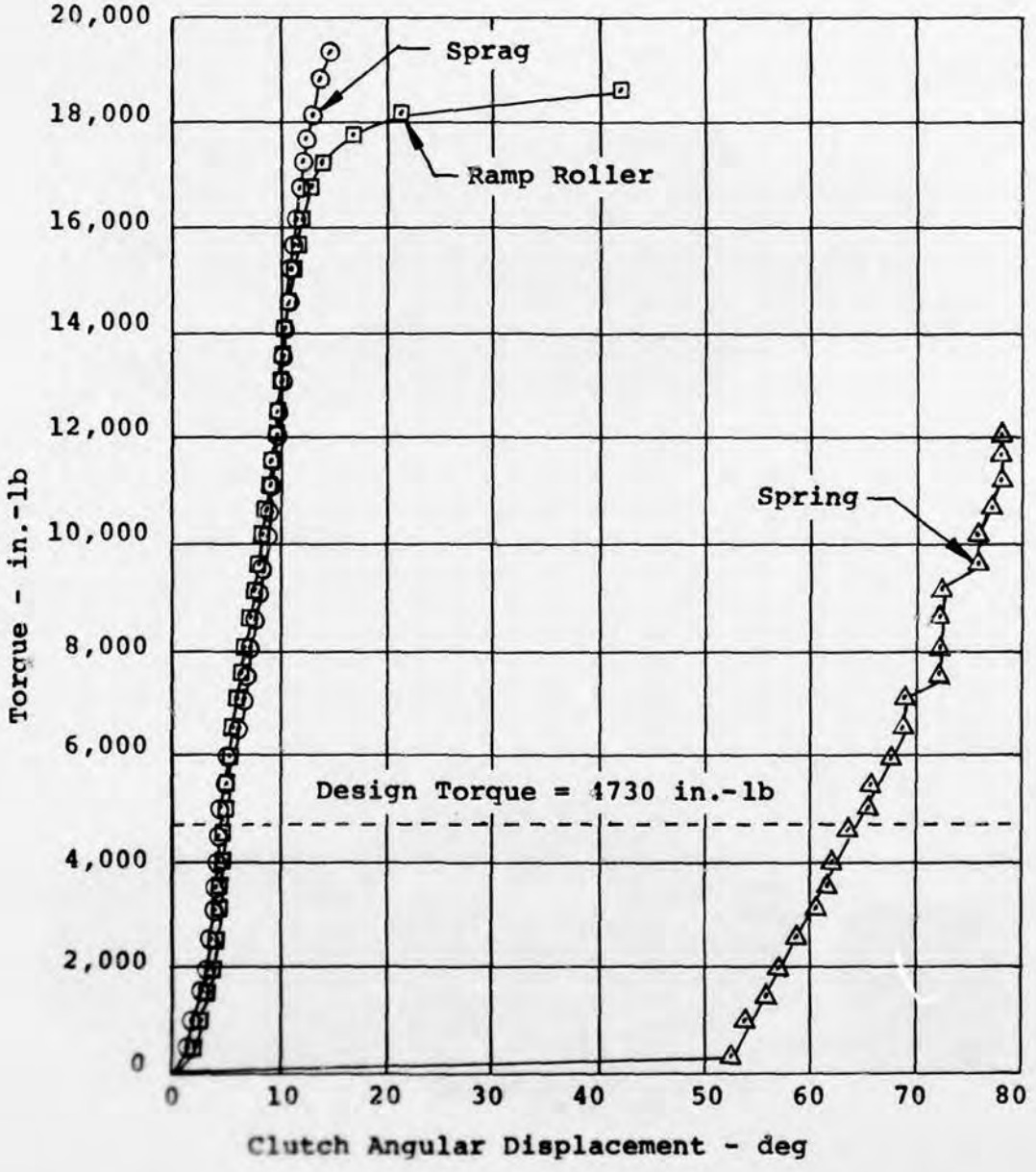

Figure 156. Static Torque Versus Angular Displacement, Spring, Sprag, and Ramp-Roller Clutches.

same, and the material and the heat treatment are the same. The conclusion can therefore be made that the sprag clutch was also on the verge of yielding in the area adjacent to the spline. In fact, the beginning of the change in slope of the sprag clutch (beginning of yield) can be seen in Figure 156, starting at approximately 18,000 inch-pounds.

Figure 157 is a plot of housing radial displacement versus torque. Note the similarity of the spring rates for each design.

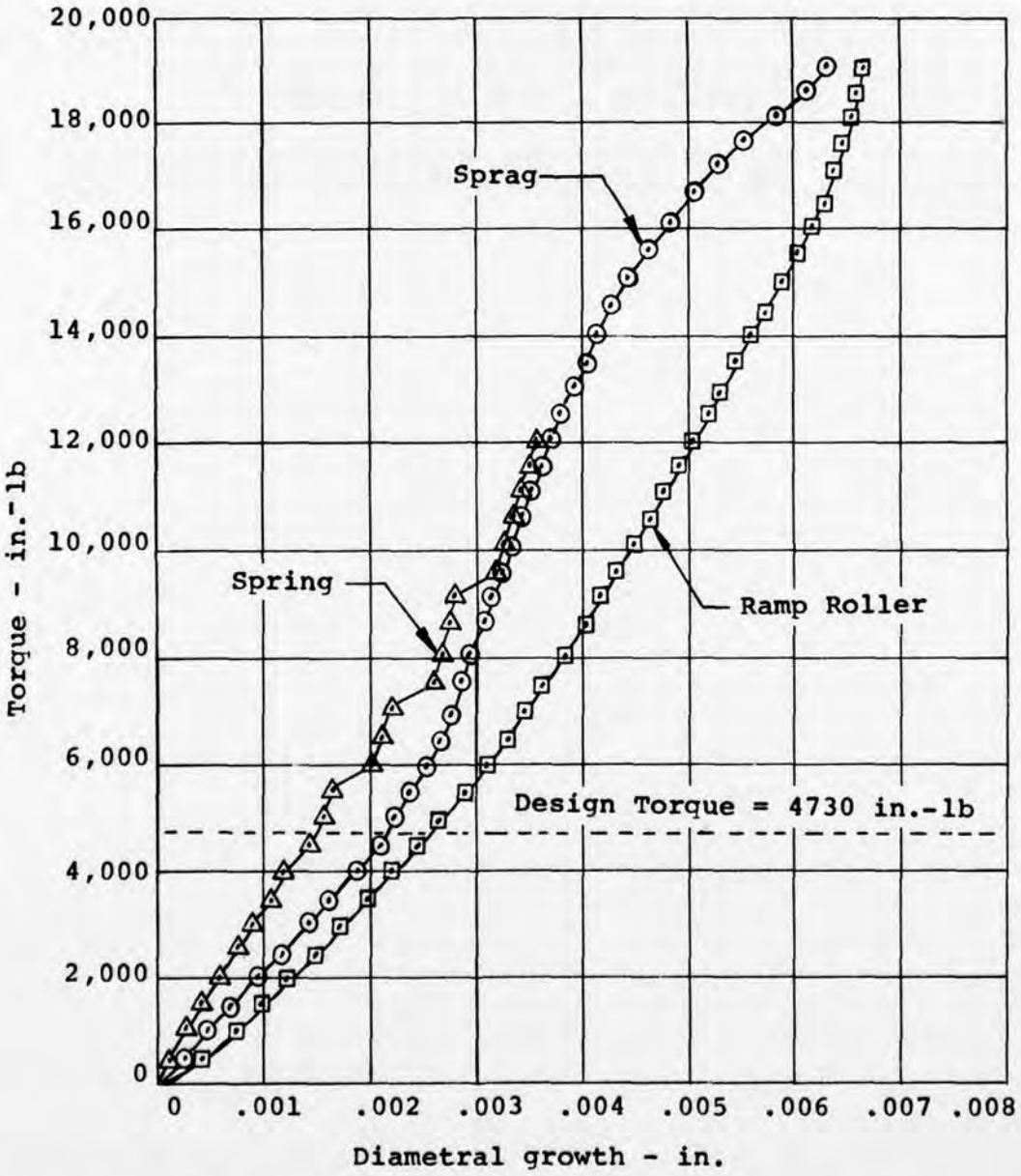

Figure 157. Static Torque Versus Radial Displacement, Spring, Sprag, and Ramp-Roller Clutches.

APPLICATION TO UH-60A

The spring, sprag, and ramp-roller clutch designs were applied to the UH-60A production transmission to compare high-speed freewheel units and conventional designs usually located on the first reduction gear. On the UH-60A main transmission, the freewheel unit is a ramp-roller clutch rotating at 5867 rpm. The clutch is located inside the output gear.

Figure 158 is a cross section of the input module of the UH-60A. The input is designed to transmit 1560 hp at 20,900 rpm, which is essentially the same torque requirement as the clutches developed in this program, i.e., 1500 hp at 20,000 rpm. The first reduction stage consists of a spiral bevel gear set of 3.56 to 1 reduction ratio. The ramp-roller clutch is located inside the shaft of the output spiral bevel gear and is of the design with the outer housing driving and cam output. This is the reverse of the ramp-roller clutch developed in this program that used the cam as the input with the outer housing as the output.

Attached to the output cam side of the ramp-roller clutch is a small spiral bevel pinion. This pinion is used to drive the accessory module consisting of a generator and hydraulic pump. Also on the output cam is a spline used to drive a quill shaft, which in turn drives the input of the main module. The input module as shown in Figure 158 is used on both the left- and the right-hand inputs by assembling the unit to the main module inputs in a plane 180° apart. This also necessitates reversing the external oil input and drain lines and plugs on the castings.

The input side of the assembly contains a pilot diameter and mounting bolts for mounting the engine gimbal. The centerline of the gimbal is located on the centerline of the input multiple disc coupling.

On the redesigned input modules, which have the spring, sprag, and ramp-roller clutches located on the high-speed input pinion, the interfaces are identical to those on the production UH-60A input module. Thus, the spiral bevel pinion which drives the accessory module is identical as is the accessory module mounting pad location and dimensions. The input interface is identical. This interface consists of the location and mounting of the engine gimbal mount and input flanges for the multiple disc coupling. The mounting of the input module to the main module is identical. However, a new quill shaft, shorter in length, is required.

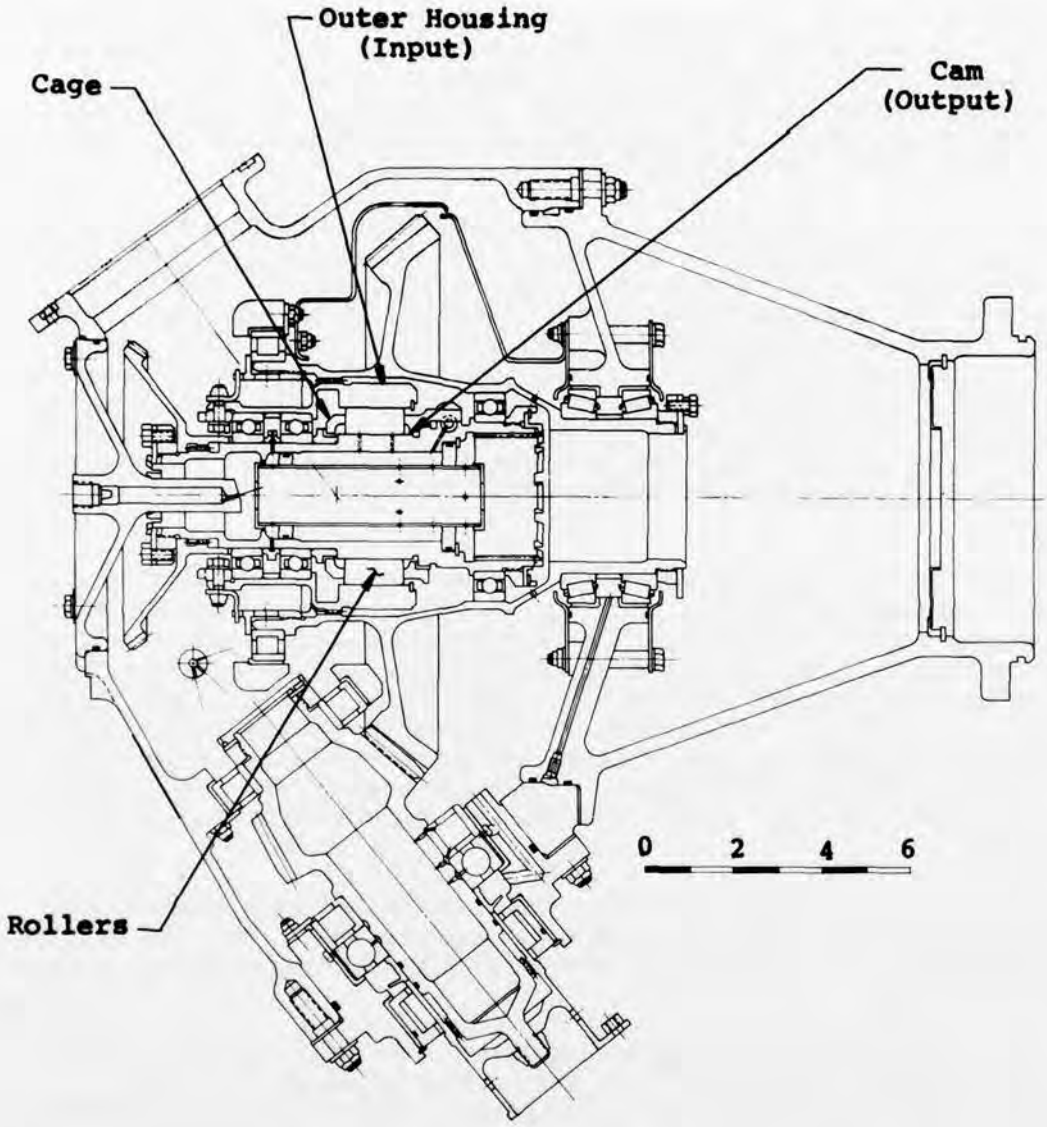

Figure 158. Production UH-60A Input Module With Ramp-Roller Clutch at 5867 rpm.

Figure 159 is a cross section of the input module redesigned with the spring clutch located inside of the input pinion. The major changes which become apparent when comparing the production design of Figure 158 to the spring clutch design of Figure 159 are as follows:

- The ramp-roller clutch assembly has been removed from the output gear.
- The shaft size of the output gear has been reduced.
- The roller bearing of the output gear is smaller.
- The accessory drive pinion is the same part and is in the same location.
- The ball and roller bearing combination on the input pinion is larger to accommodate the spring clutch components.
- The spring clutch is located on the inside of the input spiral bevel pinion.

Figure 160 is a similar cross section showing the sprag clutch inside the high-speed input pinion while Figure 161 shows the ramp-roller clutch. The design changes between the production input module and the redesigned sprag and ramp-roller clutch input modules are similar to those noted above for the spring clutch. In both the sprag and ramp-roller designs the input ball and roller bearing combination has been further increased in size to fit the clutch components inside of the pinion shaft.

The input pinion with the spring clutch is shown isolated in a larger size in Figure 162. The engine drive shaft coupling flange is splined directly to the spring clutch input housing shaft. The spring arbor is also pinned to this shaft which forces the spring to rotate with the input shaft since it is press fitted to the arbor. Thus, all sliding during overrunning will take place at the output end of the spring at the intersection of the spring teaser coils and the bore of the input pinion. The bore of the spiral bevel pinion serves as the output housing of the spring clutch. A slotted spacer is located at the overrunning end of the spring to provide a buffer for overrunning, since relative motion will take place at this location. Lubricant is fed inside the arbor which doubles as an oil distribution tube. Holes are provided in the arbor at the overrunning end of the spring and at the bearings to distribute oil to the required places. The spring size is identical to that used in the test program conducted herein. The bearing mounting is similar but is spread with a

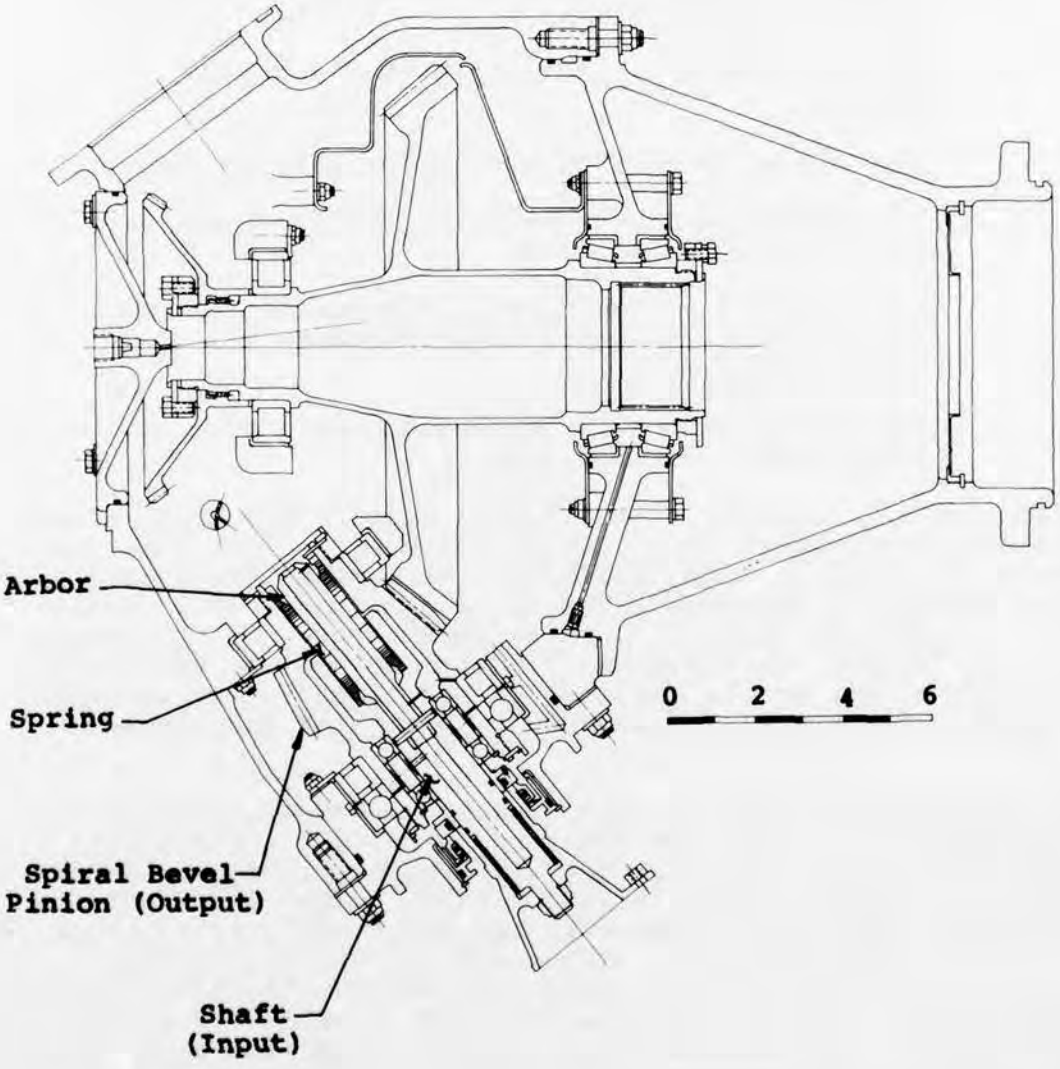

Figure 159. Input Module With Spring Clutch at 20,900 rpm.

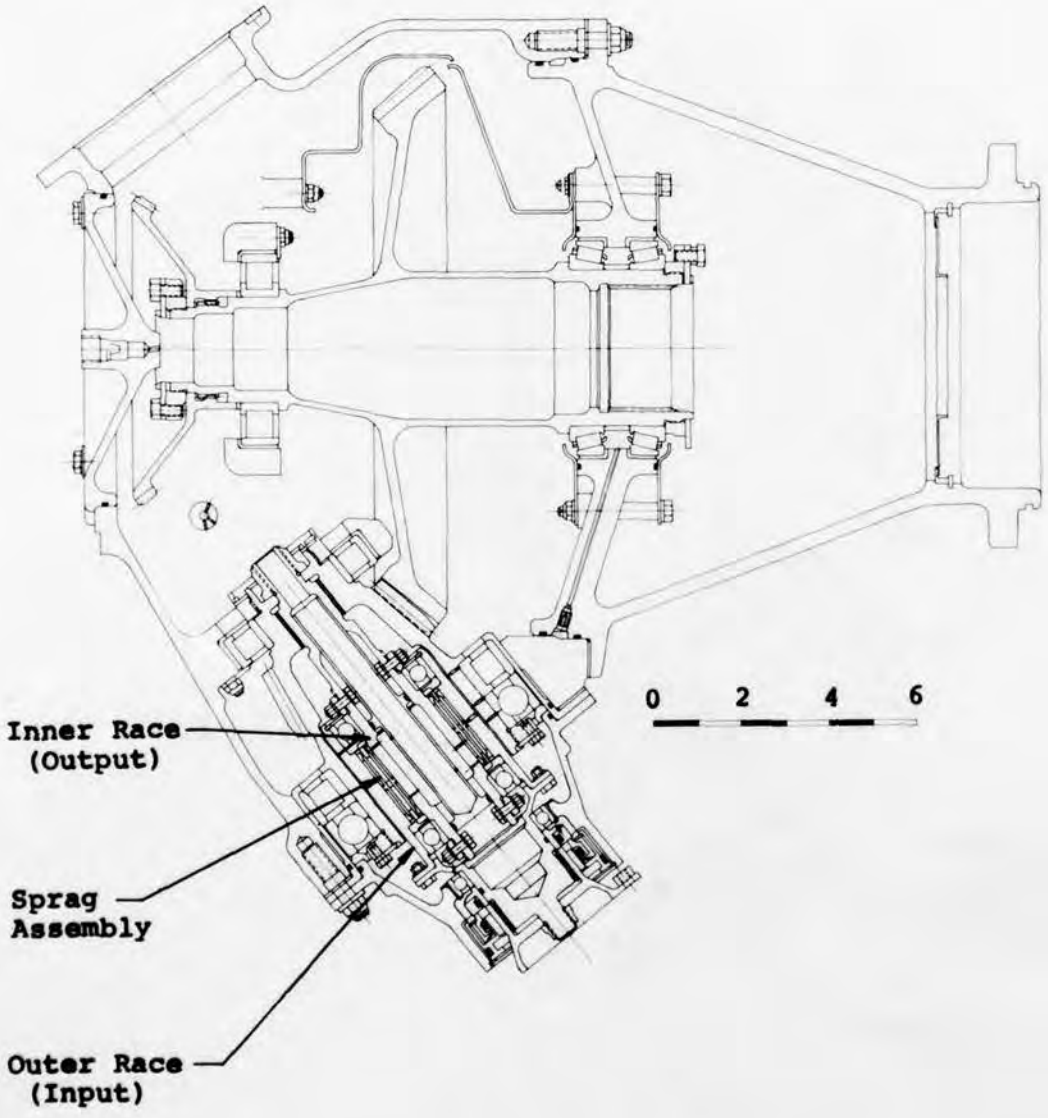

Figure 160. Input Module With Sprag Clutch at 20,900 rpm.

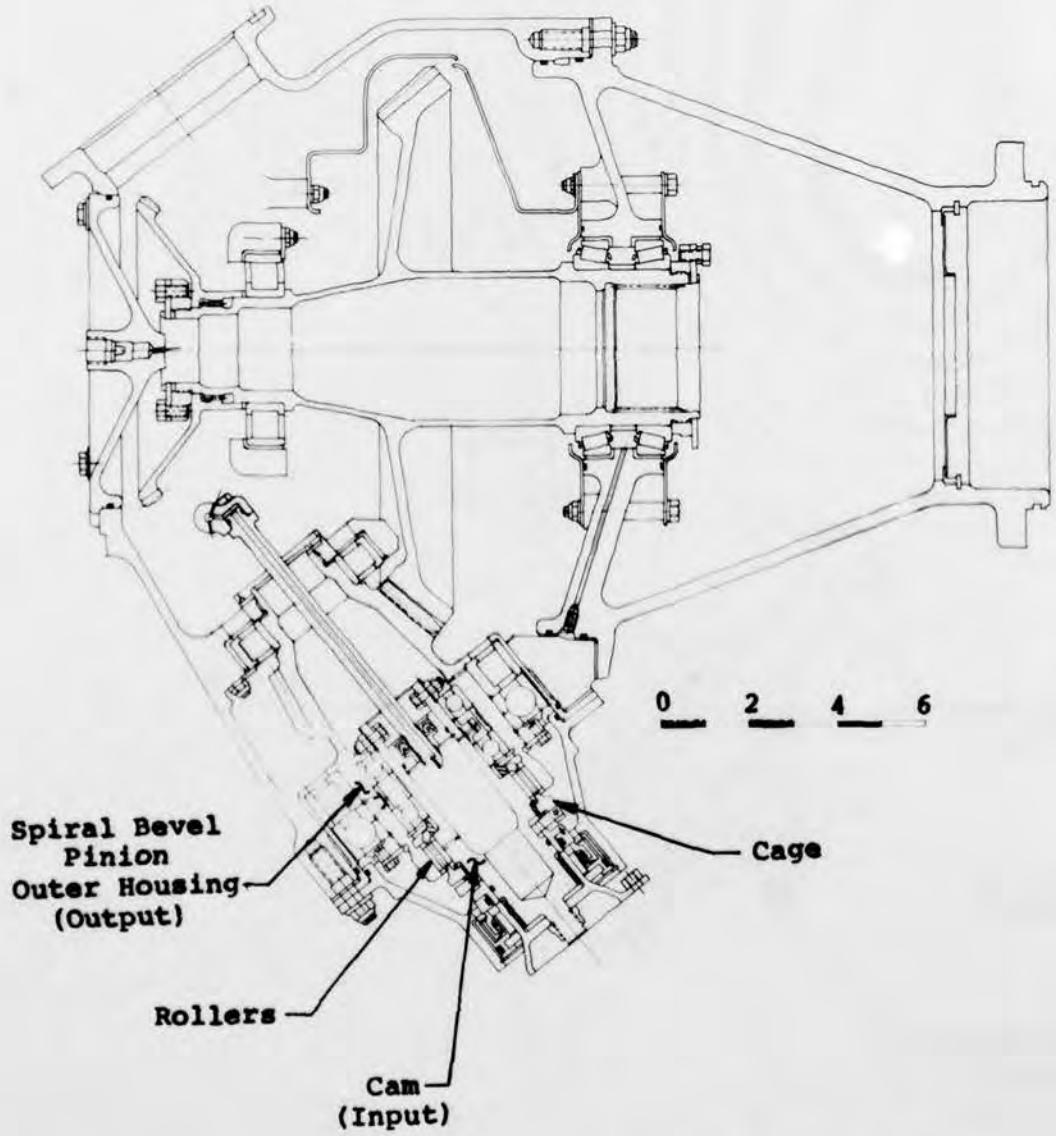

Figure 161. Input Module With Ramp-Roller Clutch at 20,900 rpm.

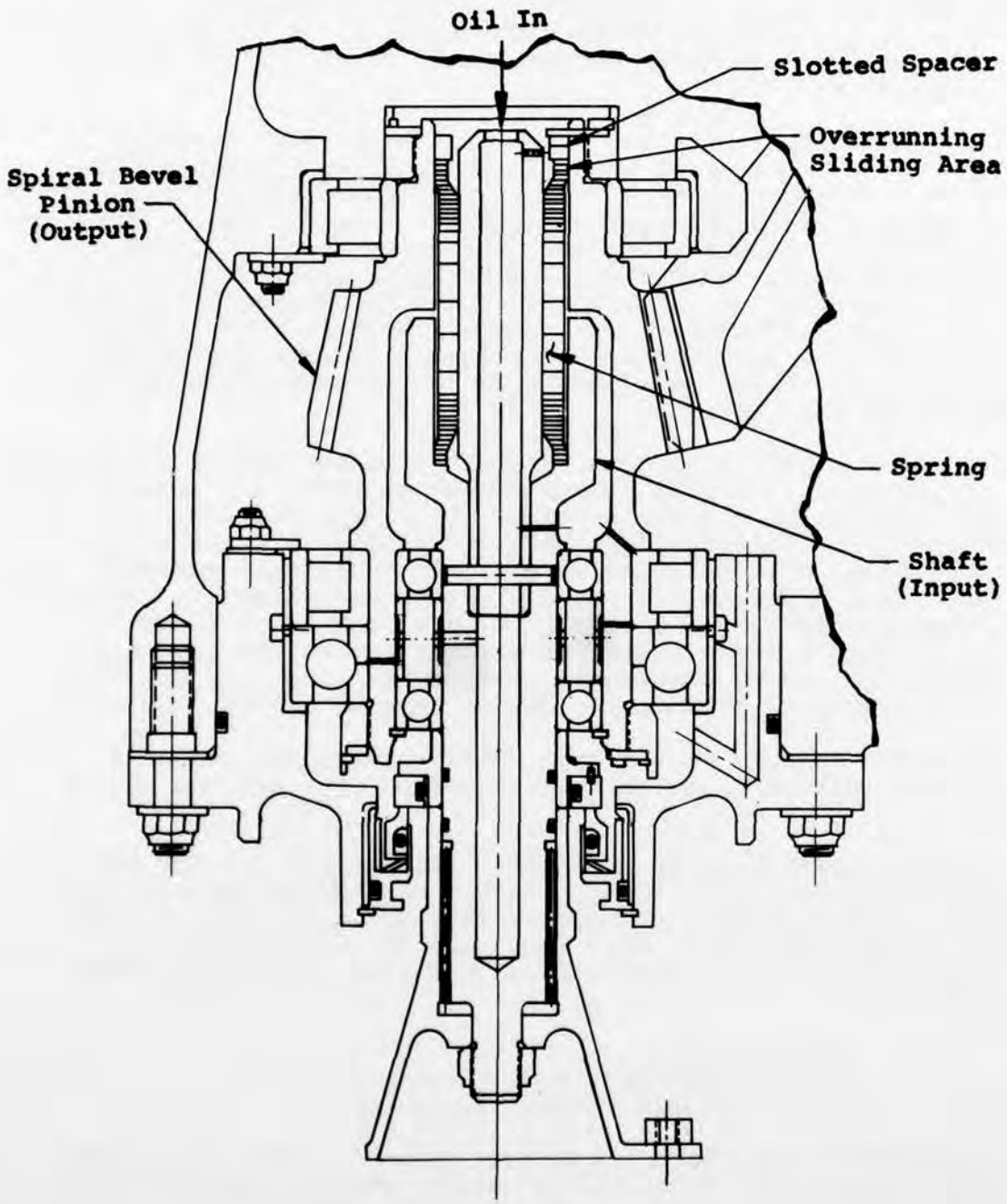

Figure 162. Spring Clutch in Input Pinion.

matched spacer set to provide a more rigid mounting. The bearings are designed with slight end play (0 to .001 inch) to permit the spring to center itself in the pinion during overrunning.

The input pinion with the sprag clutch is shown isolated in Figure 163. The sprag unit is identical to the one tested herein. The design itself is also similar from the standpoint of the straddled bearing arrangement. The oil dams also serve as a spacer for the bearings. The lips of the oil dams are below the sprag inner race diameter such that during rotation, a solid annulus of oil fills the cavity formed by the dams, inner race, and outer race. The oil distribution tube located inside of the sprag inner shaft seals the area inside the inner shaft so that oil cannot escape and must pass through the sprag assembly.

The input pinion with the ramp-roller clutch design is depicted in Figure 164. As with the previous designs, the size, number, and location of the key elements, i.e., the rollers, cam, and housing, are identical with the corresponding items in the ramp-roller clutch tested herein. To facilitate assembly, the lug, which contains the pin and spring mechanism, is removable. A seal and bushing assembly is used to guide the fixed jet and to form a pressurized oil chamber inside the camshaft. During full-speed overrunning, all rollers receive oil from the pressurized chamber and do not rely on splash lubrication.

The basic support of the ramp-roller clutch is through a duplexed set of ball bearings separated by a matched spacer set.

From the layouts shown in Figures 158 through 164 and from the production UH-60A hardware, weights were calculated for the three clutch designs. These weights are summarized in Table 24. Only major components are shown for simplicity. The input module can be broken down into three major component areas:

Center housing
Output housing and gear assembly
Input housing and pinion assembly

The miscellaneous hardware colums shown in Table 24 include items such as "O" rings, nuts, bolts, washers, spacers, oil jets, oil transfer tubes, shims, locking plates, snap rings, nameplates, shields, seals, and other small components.

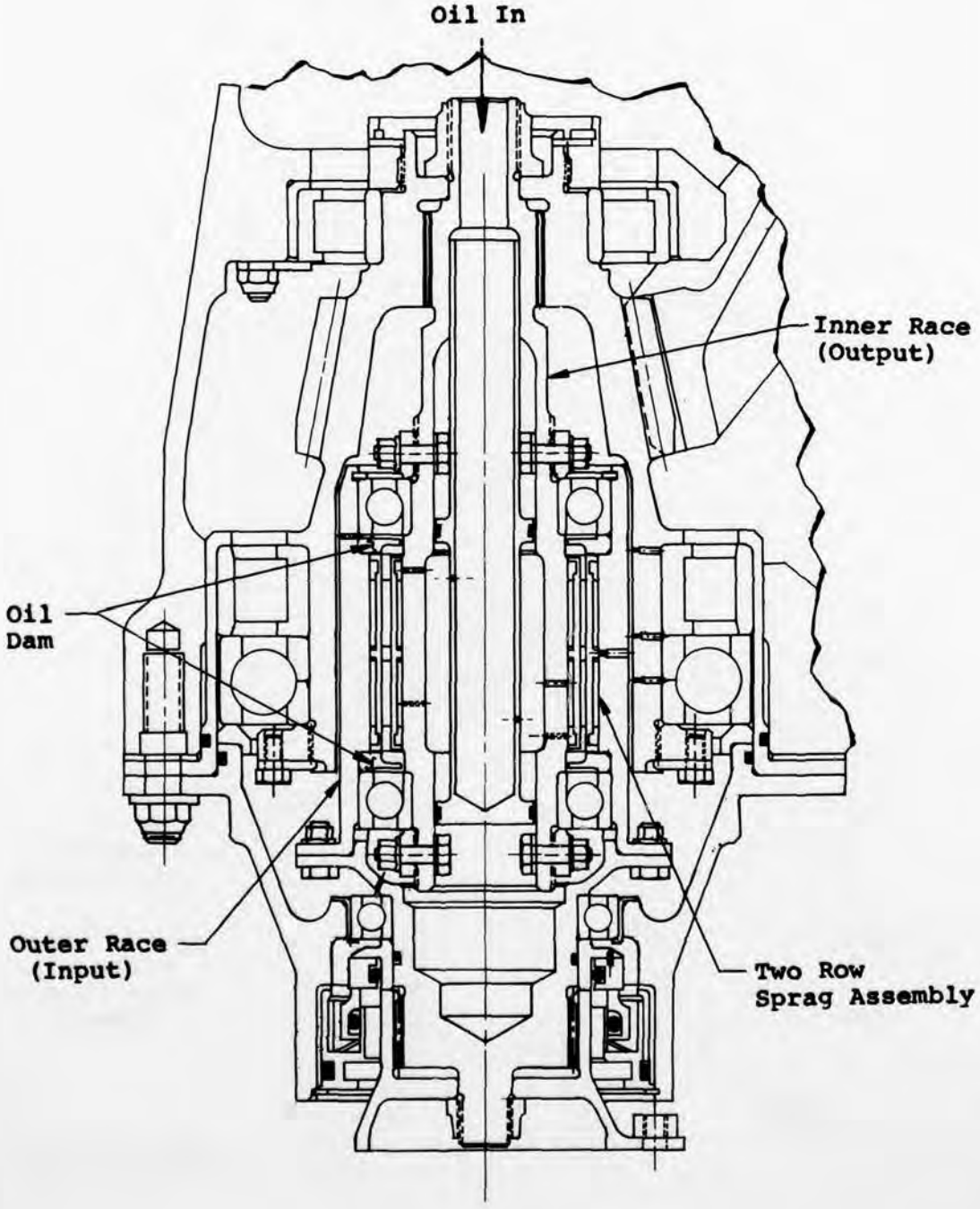

Figure 163. Sprag Clutch in Input Pinion.

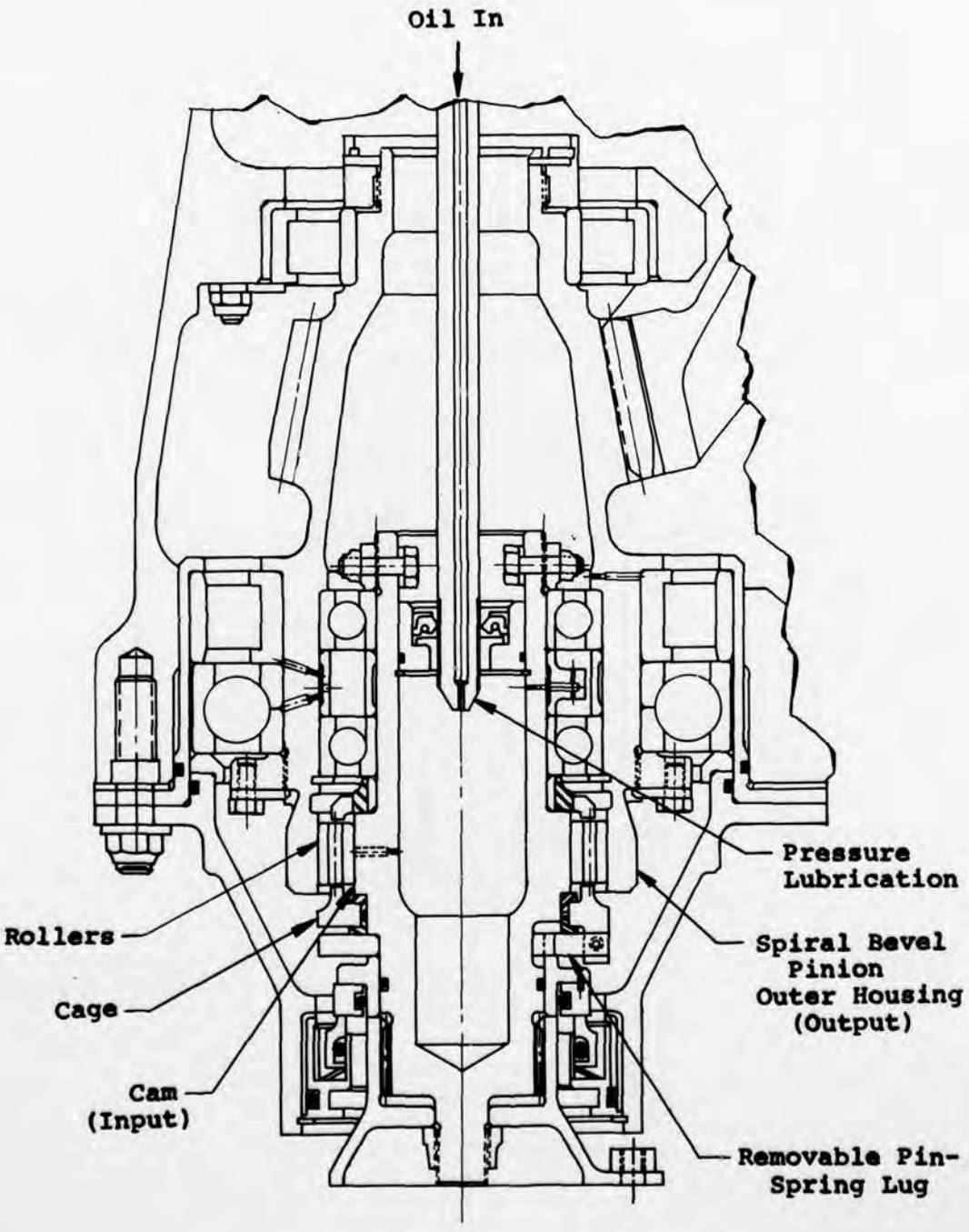

Figure 164. Ramp-Roller Clutch in Input Pinion.

TABLE 24. INPUT MODULE WEIGHT SUMMARY

Component Description	UH-60A Prod	Spring	Sprag	Roller
Quill Shaft	4.986	4.371	4.371	4.371
Center Housing & Misc. Hardware	30.765	30.100	30.100	30.296
Gear & Housing Assembly, Output				
Gear, Spiral Bevel	21.000	21.769	21.769	21.769
Housing Assembly	15.520	15.520	15.520	15.520
Clutch Assembly	19.370	-	-	-
Bearings	5.888	5.328	5.328	5.328
Miscellaneous Hardware	4.170	3.154	3.154	3.154
Pinion & Housing Assembly				
Flange Assembly	1.486	1.252	0.828	0.835
Pinion, Spiral Bevel	6.500	5.994	6.606	7.399
Housing Assembly, Input	4.024	3.980	2.371	2.371
Housing Assembly, Seal	-	-	1.618	1.202
Bearings	5.320	4.986	8.614	8.827
Arbor, Spring	-	.509	-	-
Spring	-	.690	-	-
Input Housing, Spring	-	2.338	-	-
Inner Shaft, Sprag	-	-	1.836	-
Sprag Retainer Assembly	-	-	0.850	-
Outer Race, Sprag	-	-	2.815	-
Adapter Shaft	-	-	1.394	-
Camshaft, Ramp Roller	-	-	-	2.693
Cage, Ramp Roller	-	-	-	0.503
Lug, Pin & Spring, Ramp Roller	-	-	-	0.251
Miscellaneous Hardware	1.449	2.204	3.029	3.225
Total Weight, Pounds	120.478	102.195	110.203	107.744

For the spring, sprag, and ramp-roller clutch designs, the output housing and gear assembly is lighter than in the production UH-60A version since the ramp-roller clutch has been removed from the output gear. Even though the redesigned output gear shaft is smaller in diameter, it is heavier than the production gear because it is longer.

The input housing and pinion assemblies for the spring, sprag, and ramp-roller clutches are, of course, heavier because they contain the clutch hardware.

As seen by the total input module weights, the spring clutch design is the lightest, being 18.28 pounds per input module lighter than the production UH-60A input module. Since there are two input modules per aircraft, this represents a total weight reduction of 36.56 pounds for the high-speed spring clutch. Table 25 summarizes the total weight savings for the three high-speed clutch designs.

TABLE 25. HIGH-SPEED CLUTCH WEIGHT SAVINGS SUMMARY

Configuration	Weight Difference per Module (lb)	Weight Difference per Aircraft (lb)
Production UH-60A	Baseline	Baseline
Spring Clutch	-18.28	-36.56
Sprag Clutch	-10.28	-20.56
Roller Clutch	-12.73	-25.46

The three clutch designs were also analyzed for estimated production cost differences between the new high-speed clutch designs and the UH-60A input module hardware. The differences are summarized in Table 26. The cost estimates were obtained from purchasing records, from estimation of part machining costs, setup time, and materials costs, and by comparison of costs between similar parts on other production helicopters. A production run of 400 units per year was assumed with manufacture occurring in lots of 50 units. With these quantities, setup time becomes small and can usually be neglected for most components. As seen from Table 26, all of the high-speed clutch designs are estimated to be less expensive to manufacture than the production UH-60A design. The largest single difference is in the elimination of the clutch assembly from the output housing and gear assembly of the production

TABLE 26. INPUT MODULE COST SUMMARY

Component Description	Cost Differences ($) UH-60A Prod	Spring	Sprag	Roller
Center Housing & Misc. Hardware	Baseline	- 48	- 48	- 25
Gear & Housing Assembly, Output				
Gear, Spiral Bevel	Baseline	+ 86	+ 86	+ 86
Housing Assembly	Baseline	0	0	0
Clutch Assembly	Baseline	-2230	-2230	-2230
Bearings	Baseline	- 221	- 221	- 221
Miscellaneous Hardware	Baseline	- 100	- 100	- 100
Pinion & Housing Assembly				
Flange Assembly	Baseline	+ 12	- 17	- 17
Pinion, Spiral Bevel	Baseline	- 65	- 51	- 68
Housing Assembly, Input	Baseline	- 13	- 267	- 267
Housing Assembly, Seal	-	-	+ 130	+ 114
Bearings	Baseline	+ 166	+ 203	+ 219
Arbor, Spring	-	+ 21	-	-
Spring	-	+ 532	-	-
Input Housing, Spring	-	+ 140	-	-
Inner Shaft, Sprag	-	-	+ 222	-
Sprag Retainer Assembly	-	-	+ 682	-
Outer Race, Sprag	-	-	+ 112	-
Adapter Shaft	-	-	+ 92	-
Camshaft, Ramp Roller	-	-	-	+ 233
Cage, Ramp Roller	-	-	-	+ 218
Lug, Pin & Spring, Ramp Roller	-	-	-	+ 49
Miscellaneous Hardware	Baseline	+ 10	+ 197	+ 131
Total Cost Difference Per Input Module, $	Baseline	-1710	-1210	-1878

design with a resultant cost savings of $2230. In the new designs, the addition of the various high-speed clutch parts to the input pinion and housing assemblies adds a lesser amount than the $2230 removed from the output gear and is $803 more for the spring clutch, $1303 more for the sprag clutch, and $612 more for the roller clutch. The difference in clutch hardware cost is due mainly to the smaller sizes found in the high-speed clutch designs. The total cost differences shown in Table 26 must be multiplied by 2 since there are 2 input modules per main transmission. Thus, the high-speed ramp-roller clutch is $3756 less expensive to manufacture per aircraft.

Table 27 summarizes the number of parts in each of the input module designs. In this table, the 14 rollers of the ramp-roller clutches in the UH-60A production design and in the high-speed clutch design have been considered to be one part. Similarly, the 44 pieces comprising the sprag retainer assembly have been considered to be one part. Note that the spring clutch design contains 19 less parts than its nearest competitor. Although not directly related, parts count can be thought of as a measure of reliability. Assemblies with fewer parts are usually more reliable than assemblies with many parts owing to the chain analogy. In mathematical terms, the assembly reliability is the product of the reliabilities of the individual components. Thus, more components will result in lower calculated reliabilities assuming all parts have approximately the same chance of failure.

TABLE 27. INPUT MODULE PARTS COUNT SUMMARY

Component Description	UH-60A Prod	Spring	Sprag	Roller
Center Housing & Misc. Hardware	97	97	97	97
Gear & Housing Assembly, Output				
Gear, Spiral Bevel	1	1	1	1
Housing Assembly	1	1	1	1
Clutch Assembly	29	-	-	-
Bearings	3	3	3	3
Miscellaneous Hardware	50	47	47	47
Pinion & Housing Assembly				
Flange Assembly	1	1	1	1
Pinion, Spiral Bevel	1	1	1	1
Housing Assembly, Input	1	1	1	1
Housing Assembly, Seal	-	-	1	1
Bearings	3	5	6	6
Arbor, Spring	-	1	-	-
Spring	-	1	-	-
Input Housing, Spring	-	1	-	-
Inner Shaft, Sprag	-	-	1	-
Sprag Retainer Assembly	-	-	1	-
Outer Race, Sprag	-	-	1	-
Adapter Shaft	-	-	1	-
Camshaft, Ramp Roller	-	-	-	1
Cage, Ramp Roller	-	-	-	1
Lug, Pin & Spring, Ramp Roller	-	-	-	5
Miscellaneous Hardware	17	19	42	33
Total Number of Parts	204	179	205	198

As seen in Figures 158 through 164 discussed previously, the size of the ball and roller bearing combination has been increased in all of the high-speed clutch designs to accommodate the clutch components within the input pinion. In moderate and slow speed bearing applications, an increase in bearing size will show a corresponding increase in bearing fatigue life. With high-speed bearings such as in the UH-60A input pinion, the converse is usually true. Fatigue life will increase with increased bearing size to a certain level depending on speed. At this level, the centrifugal forces on the larger rolling elements that are rolling on a larger bearing compliment pitch diameter, degrade the fatigue life of the outer race and decrease the overall bearing life.

The bearings of the input pinion and output gear were analyzed for the loads induced by the spiral bevel gear teeth. A prorated power of 1136 hp was used based on an estimated spectrum of usage for the UH-60A helicopter. The prorated power is defined as that power which, if continuously applied, would result in the same life as if the spectrum of varying powers and percent times had been applied. Table 28 summarizes the results of the bearing life analysis.

TABLE 28. BEARING LIFE SUMMARY

Configuration	Location	Basic Brg Size	B-10 Life (hr)
UH-60A Production	Pinion Front Roller	211	12,800
	Pinion Back Roller	212	28,620
	Pinion Back Ball	212	14,750
	Output Gear Roller	1831	19,510
Spring Clutch	Pinion Front Roller	211	12,900
	Pinion Back Roller	114	14,290
	Pinion Back Ball	114	8,550
	Output Gear Roller	212	60,070
Sprag and Roller Clutches	Pinion Front Roller	211	11,620
	Pinion Back Roller	119	19,540
	Pinion Back Ball	119	9,160
	Output Gear Roller	212	60,070

Table 28 shows that the pinion bearings for the high-speed clutch configuration have a reduced life, except for the front roller bearing which remains essentially unchanged. The fatigue lives of the ball and roller bearing combination for the spring clutch are approximately 58% and 50% of the corresponding ball and roller bearing combination of the production design. The lives of the bearings for the sprag and roller clutch configuration are higher than those for the spring clutch but are still 62% and 68% of the corresponding lives for the production ball and roller bearing configuration. The change to the roller bearing on the output gear from an 1831 size to a 212 size which is smaller but heavier resulted in a 300% increase in fatigue life.

The effect of these changes on the bearing system fatigue life of the input module and the entire gearbox is shown in Table 29.

TABLE 29. BEARING B-10 SYSTEM LIFE

Configuration	B-10 Life of Input Module (hr)	B-10 Life of Main Transmission (hr)
UH-60A Production	4900	317
Spring Clutch	4000	311
Sprag or Roller Clutch	4250	313

The system life for any group of bearings is calculated from the individual bearing lives by

$$\frac{1}{L_S} = \left\{ \sum_{i=1}^{n} \left[\frac{1}{L_i} \right]^{\frac{10}{9}} \right\}^{\frac{9}{10}}$$

where

L_S = system B-10 bearing life
L_i = individual B-10 bearing life

Thus, from Table 29, the B-10 life of the input module with the spring clutch is reduced to 82% of that for the production configuration and for the sprag and roller clutch 87% of the production configuration. The system life of the entire main transmission remains virtually unchanged due to the large number of lower life bearings on the main module.

The decrease in B-10 system life of the input module will result in a lower mean time between failures (MTBF). The mean bearing life is approximately five times the B-10 life. Therefore, for the production configuration, the mean time between bearing failures is 24,500 hours (5 x 4900). The MTBF of the UH-60A production input module has been established at 4200 hours. From the following relationship, the MTBF of all the other components in the input module is calculated to be 5070 hours.

$$\text{MTBF input module} = \frac{1}{\frac{1}{\text{MTBF(bearings)}} + \frac{1}{\text{MTBF(other)}}}$$

If it is assumed that the MTBF of the other components (gears, clutches, housing) will remain unchanged, then the predicted reduction of MTBF for the input modules with high-speed clutches is shown in Table 30 along with the effect on the entire transmission system.

TABLE 30. MTBF OF INPUT MODULES WITH HIGH-SPEED CLUTCHES

Configuration	Input Module MTBF (hr)	Main Transmission MTBF (hr)
UH-60A Production	4200	944
Spring	4041	927
Sprag	4093	933
Roller	4093	933

As seen from Table 30, the effect on the MTBF of the main transmission is small.

Another parameter that must be examined with high-speed bearings is related to pitch line velocity effects measured in DN values, where D is the diameter of the bearing bore in millimeters and N is the shaft rpm. The UH-60A input pinion bearings currently operate at a maximum DN of 1,255,000. This is well within the current state-of-the-art allowable DN for helicopter transmission bearings of 1,500,000. The spring clutch bearings operate at a DN of 1,464,000, which is approximately at the upper allowable limit; the sprag and roller clutch bearings operate at a DN of 1,986,000, which is above the allowable limit.

The sprag and roller clutch designs were re-examined to determine if the DN value could be reduced. If the same basic clutch geometry as previously tested is maintained, it is not possible to reduce the size of the ball and roller bearing combination on the input pinion. However, by using turbine engine technology such as bearing under-race cooling, the allowable DN can be increased to 2,200,000 and makes the sprag and roller clutch design a viable approach.

After evaluating the weight differences, cost differences, and MTBF differences between the baseline UH-60A input module and the three high-speed clutch designs, the effects of these parameters on aircraft cost, mission effectiveness, mission capability, and transmission cost factors still remained to be evaluated. To evaluate these data, the mathematical model was used that was developed during the Helicopter Transmission Modularization and Maintainability Analysis Program of Reference 6.

Aircraft mission capability is a measure of the performance of the aircraft and is usually measured in ton-knots. It is calculated as an average mission payload times speed. Knowing the mission capability of the baseline UH-60A helicopter, the mission capability can be calculated for the high-speed clutch designs by evaluating the weight differences and the partial derivative of mission capability with respect to weight. It is assumed that the efficiency of the baseline and high-speed clutch designs is the same since the losses will be low in the clutches when they are locked and driving. Mission capability is calculated by

---

6. Kish, Jules, G., Menkes, Paul, and Cormier, Kenneth R., HELICOPTER TRANSMISSION MODULARIZATION AND MAINTAINABILITY ANALYSIS, USAAMRDL Technical Report 73-82, Eustis Directorate, U. S. Army Air Mobility Research and Development Laboratory, Fort Eustis, Virginia, January 1974.

$$AMCAP = AMCAPB + DCAPWT\ (\Delta WT)$$

where

AMCAP	=	aircraft mission capability
AMCAPB	=	baseline aircraft mission capability
DCAPWT	=	partial derivative of aircraft mission capability with respect to weight
ΔWT	=	difference in transmission weight between baseline and new design

Aircraft mission effectiveness is defined as aircraft mission capability degraded by the aircraft's unavailability to fly a mission on demand, and by system failure aborting a mission after it is initiated. It is calculated from

$$AMEFF = AMCAP \times RELIA \times AVAIL$$

where

AMEFF	=	aircraft mission effectiveness
AMCAP	=	aircraft mission capability
RELIA	=	reliability
AVAIL	=	availability

It is assumed that aircraft reliability and availability will be essentially equal in the UH-60A baseline and in the high-speed clutch designs; thus, the only factor influencing mission effectiveness is change in weight since mission capability is a function of weight only. Table 31 summarizes the mission capability and mission effectiveness of the baseline and high-speed clutch designs.

TABLE 31. AIRCRAFT MISSION DATA HIGH-SPEED CLUTCH DESIGN

Configuration	Mission Capability (ton-kts)	Mission Effectiveness (ton-kts)
UH-60A Production	194.00	181.77
Spring	196.69	184.29
Sprag	195.51	183.19
Roller	195.87	183.53

Since the spring clutch design is the lightest weight, it has the highest mission capability and the highest mission effectiveness.

Fuel cost differences between the baseline and high-speed clutches were also evaluated. To evaluate the differences in fuel costs, the average mission fuel flow was required. As with mission capability, the average mission fuel flow was found by subtracting from the baseline fuel flow the change in fuel flow with weight, and was calculated by

$$FF = FFBA + DFFWT\ (\Delta WT)$$

where

FF	=	fuel flow
FFBA	=	fuel flow of baseline aircraft
DFFWT	=	partial derivative of fuel flow with respect to weight
ΔWT	=	difference in transmission weight between baseline and high-speed clutch designs

The total cost of fuel is then found as the product of fuel flow, life cycle flight hours, and fuel cost as

$$CPOL = CFUEL\ (LCFH)\ FF$$

where

CPOL	=	total cost of fuel
CFUEL	=	cost of fuel per pound
LCFH	=	life-cycle flight hours
FF	=	fuel flow

The life-cycle flight hours were calculated for a service life of 20 years assuming an annual utilization of 828 flight hours. Even though the weight changes between the baseline and high-speed clutch designs were significant, it was found that differences in fuel costs per aircraft were not high as shown in Table 32.

TABLE 32. FUEL FLOW AND COST, HIGH-SPEED CLUTCH DESIGN

Configuration	Fuel Flow (lb/hr)	Life-Cycle Fuel Cost ($)
UH-60A Production	1097.00	,162,644
Spring	1095.54	1,161,094
Sprag	1096.18	1,161,773
Roller	1095.98	1,161,565

Although the per aircraft differences are small, when considering the fleet of 1106 aircraft, the total fuel cost savings for the spring clutch amounts to $1,711,387 based on recent prices. This represents an energy savings of 4,397,458 gallons of fuel.

Transmission acquisition cost includes recurring and nonrecurring costs. Recurring cost is the cost of manufacture of the transmission and has been shown previously in Table 26. Nonrecurring costs include design engineering, test facilities, testing, prototype manufacturing, and other costs associated with development of the first transmission from inception to production. These development costs are then spread over the production run. The fleet size is assumed to be 1106 helicopters for this calculation. Assuming that the choice of design has been made prior to program initiation, there would be very little difference in development costs between any of the designs considered. When determining nonrecurring costs on a per-aircraft basis using a fleet size of 1106 helicopters, the difference between the high-speed clutch designs and the current designs will become negligible.

The cost of spares can conveniently be divided between initial spares and replenishment spares. Recurring acquisition cost and the reliability of the components establish the cost of spares. The high-speed clutch designs have two counterbalancing parameters in this respect since the recurring costs of the input modules are lower but the maintenance costs are higher. The overall effect is to produce almost a negligible change in cost of spares. Table 33 summarizes initial and replenishment spares cost.

TABLE 33. TRANSMISSION SPARES COST, HIGH-SPEED CLUTCH DESIGNS

Configuration	Initial Spares Cost ($)	Replenishment Spares Cost ($)
UH-60A Production	9,365	45,279
Spring	9,067	43,476
Sprag	9,154	44,193
Roller	9,034	43,579

Transmission maintenance costs are derived for each of the Army maintenance levels: field unit, intermediate, and depot. At each level of operation, the total maintenance man-hours per flight hour (MMH/FH) are calculated by summing the hours for inspection, removal, requisition, installation, and scrappage. At the field level, the MMH/FH required for daily scheduled inspection is also included while at the direct support level the scheduled periodic inspection MMH/FH is included. The cost of maintenance is then found as that required for labor and material. For the spring, sprag, and ramp-roller high-speed clutch designs, material and labor costs have a counterbalancing effect on maintenance since material costs are lower while labor costs are higher. Labor costs are higher because the bearing life of the input module is lower in the high-speed clutch designs; thus, the frequency of maintenance is increased. Total maintenance costs also include shipping costs for the sake of completeness and are summarized in Table 34.

TABLE 34. TRANSMISSION MAINTENANCE COSTS, HIGH-SPEED CLUTCH DESIGNS

Maintenance Item	UH-60A Prod ($)	Spring ($)	Sprag ($)	Roller ($)
Shipping	3,674	3,720	3,705	3,705
Field	16,281	16,123	16,168	16,103
Intermediate	34,258	33,138	33,466	33,056
Depot	140,806	140,757	140,720	140,125
Total	195,019	193,738	194,059	192,989

As seen in Table 34, there is only a $2030 difference between the highest and lowest total maintenance cost. However, all high-speed clutch designs have maintenance costs which are lower than the baseline UH-60A in spite of higher maintenance frequencies on the input modules. This is because the lower cost of materials for the high-speed designs offsets the increased labor costs.

In determining life-cycle costs for the UH-60A helicopter with high-speed freewheel units in the input module, all of the cost parameters previously discussed are included; i.e., nonrecurring, recurring, initial GSE tooling, replenishment GSE tooling, initial spares, replenishment spares, maintenance, cost of fuel, and training costs. The cost differences between each of the above items in the high-speed designs and the baseline are added or subtracted from the baseline life-cycle costs. Since there are no major differences in any of the items discussed, the life-cycle cost is only slightly lower in the high-speed designs and does not show a significant difference on a per aircraft basis as seen in the summary of Table 35.

TABLE 35. LIFE-CYCLE COST DIFFERENCE SUMMARY, HIGH-SPEED CLUTCH DESIGNS

Configuration	Difference in Life-Cycle Cost ($)
UH-60A Production	Baseline
Spring	-9,000
Sprag	-6,000
Roller	-10,000

However, when considering the fleet of 1106 aircraft, the spring, sprag, and ramp-roller clutches save $9,954,000, $6,636,000, and $11,060,000, respectively.

The effects of the weight savings and cost savings of the spring, sprag, and roller clutch designs do not significantly affect the cost of fuel, acquisition cost, GSE tooling costs, spares costs, maintenance costs or life-cycle costs. The aircraft cost effectiveness is defined as aircraft mission effectiveness per life-cycle dollar and is found by dividing aircraft mission effectiveness by the life-cycle cost of the aircraft. Aircraft cost effectiveness combines performance and cost and is a useful means in evaluating the overall effect of the high-speed clutch designs on the UH-60A.

Fleet effective cost is an equivalent measure of aircraft cost effectiveness on the fleet level. It is defined as the cost to operate a fleet of aircraft for the service life of 20 years. Usually, fleet effective cost is found by multiplying the life-cycle cost of the aircraft by the size of the fleet. However, when comparing fleet effective costs, aircraft of equal performance capabilities must be compared. Fleet size is adjusted for the same mission effectiveness by

$$FEC = NBA\ (AMEFFB/AMEFF)LCCA$$

where

FEC	=	fleet effective cost
NBA	=	number of baseline aircraft = 1106
AMEFFB	=	aircraft mission effectiveness of the baseline aircraft
AMEFF	=	aircraft mission effectiveness of the high-speed clutch design
LCCA	=	life-cycle cost

As shown in Table 36, it is in fleet effective cost the spring clutch design results in a cost savings of greater than 106 million dollars. This is due almost in whole to the 36.56-pound weight savings of the spring clutch compared to the UH-60A production design.

TABLE 36. AIRCRAFT COST EFFECTIVENESS AND FLEET EFFECTIVE COST DIFFERENCES, HIGH-SPEED CLUTCH DESIGNS

Configuration	Aircraft Cost Effectiveness ton-kts/mega $	Difference in Fleet Effective Cost $
UH-60A Production	28.402	Baseline
Spring	28.834	-106,219,000
Sprag	28.650	- 61,270,000
Roller	28.719	- 78,172,000

CONCLUSIONS AND RECOMMENDATIONS

1. The spring clutch is recommended as a candidate for helicopter high-speed overrunning clutches for speeds up to 27,000 rpm.

2. The sprag clutch is recommended as a candidate for helicopter high-speed overrunning clutches that do not exceed 20,000 rpm.

3. The ramp-roller clutch is recommended as a candidate for helicopter high-speed overrunning clutches that do not exceed 12,000 rpm.

4. In all future transmission designs, the freewheel units should be located on the highest speed shafts. This will save weight, reduce cost, and improve reliability.

5. Full-speed overrun testing (input fixed, output at 20,000 rpm) showed that if proper precautions are taken in the design phase in the areas of centrifugal effects and lubrication, all clutches can operate in the full-speed overrunning mode for long periods of time without structural or functional problems.

6. Differential-speed overrun testing (input rotating at some speed between 10,000 to 15,000 rpm, output at 20,000 rpm) showed that centrifugal effects induced during differential overrunning when both input and output are rotating create the most severe overrunning environment. The spring clutch is the design least susceptable to centrifugal effects. Wear in the ramp-roller clutch induced during differential-speed overrun would limit the overrunning life of the ramp-roller clutch.

7. Turbine dynamic engagement, disengagement, and full-load testing showed that the operation of all three clutch designs was satisfactory. All clutches engaged and disengaged smoothly and evenly. Full-load testing proved to be no problem for any of the designs.

8. High temperature environmental tests showed that all clutches could operate without difficulties at a 300^{o}F oil-inlet temperature.

9. Low-temperature environmental tests showed that start-up and high-speed engagements conducted in a simulated environment of -40°F can be a problem for some designs. The spring clutch concluded the low-temperature environmental tests without difficulty. The roller clutch experienced heavy wear of components, which had a variety of thermal expansion coefficients (bronze and steel), while the sprag clutch failed to engage, possibly due to low energizing torque and high oil viscosity.

10. Dynamic-cyclic torque testing at 95% ± 5% of maximum for 10,800 cycles did not present any problems for any of the clutches tested.

11. Static-cyclic torque testing at 200% ± 20% of maximum for 10 million cycles was not a problem for the sprag and roller clutches. The spring clutch experienced spring creep leading to eventual loss of torque drive. In operation on a helicopter, this type of spring creep is avoided when the spring overruns during engine shutdown after each flight.

12. Static overload testing showed that the sprag and the ramp-roller clutches sustained approximately four times the design torque. The spring clutch exhibited a characteristic curve of torque versus angular displacement that showed areas of angular rotation where the spring coils suddenly slip to new positions in the housing. The maximum torque sustained by the spring clutch was approximately two and one-half times the design torque.

13. When designing a high-speed spring overrunning clutch, the following features are recommended:

    - Concentricity between spring, arbor, input bore, and output bore is critical and should be held as close as practical machining tolerances permit.

    - There must be a lubricant flow path on the overrunning end of the spring from the free end to the center of the spring. This can be accomplished by slots in the spring or slots in the housing, but slots in the spring are preferred

    - Silver plating and other forms of plating on the overrunning teaser coils should be avoided.

14. When designing a high-speed sprag overrunning clutch, the following features are recommended:

    . The design should be centrifugally engaging. The drag produced by the centrifugal engagement must exceed the drag created by oil churning; i.e., drag should increase with increasing differential-speed overrunning.

    . Oil drainage should be such that when the clutch is at rest most of the oil in the sprag area is drained.

    . Clutch diameters should be as small as possible commensurate with stress levels. Thus, a tandem, two-row design should be considered. Smaller diameters reduce centrifugal effects.

    . The mounting arrangement with clutch bearings straddling the sprag unit is preferred.

15. When designing a high-speed ramp-roller overrunning clutch, the following features are recommended:

    . Circularity of the cage must be maintained at operating speed. The deflection of the cage due to centrifugal force on the cage lugs must not exceed the clearance between the cage and its mounting pilot on the cam.

    . The effect of centrifugal force on the pin and spring mechanism must be fully evaluated.

    . Hollow rollers are recommended to reduce centrifugal roller load and to reduce Hertz stresses. The cage slot design must be such that a maximum amount of material contact area exists between the ends of the rollers and the end of the roller slots.

    . Clutch diameters should be as small as possible commensurate with stress levels. Smaller diameters reduce centrifugal effects.

16. A spring clutch operating at 20,900 rpm is recommended as a candidate design to replace the ramp-roller clutch design operating at 5867 rpm in the UH-60A helicopter transmission.

17. A high-speed spring clutch design in the UH-60A input module can save approximately 36.56 pounds and cost approximately $3424 less to manufacture for each main transmission.

18. Based on fleet effective cost and a fleet size of 1106 aircraft, a high-speed spring clutch design in the UH-60A input module is estimated to cost 106 million dollars less than the current ramp-roller clutch design for the same mission effectiveness.

19. Maintenance costs, spares costs, nonrecurring cost, total cost of fuel, and aircraft life-cycle costs are not significantly different in the baseline UH-60A and the high-speed spring clutch design. Input module bearing life and MTBR are lower in the high-speed spring clutch design by 19% and 2% respectively.

20. A high-speed sprag clutch or a high-speed ramp-roller clutch are not recommended as candidate designs to replace the baseline UH-60A ramp-roller clutch because the input pinion bearing DN value would exceed current state-of-the-art values in helicopter transmission bearing design.

LITERATURE CITED

1. Kish, Jules G., HELICOPTER FREEWHEEL UNIT DESIGN GUIDE, Sikorsky Aircraft, USAAMRDL Technical Report 77-18, U. S. Army Air Mobility Research and Development Laboratory, Fort Eustis, Virginia, October 1977.

2. Lynwander, P., Meyer, A. G., Chachakis, S., SPRING OVERRIDING AIRCRAFT CLUTCH, Avco Lycoming Division, USAAMRDL Technical Report 73-17, Eustis Directorate, U. S. Army Air Mobility Research and Development Laboratory, Fort Eustis, Virginia, May 1973, AD 766309.

3. Lynwander, P., Meyer, A. G., Chachakis, S., SPRAG OVER-RIDING AIRCRAFT CLUTCH, Avco Lycoming Division, USAAMRDL Technical Report 72-49, Eustis Directorate, U. S. Army Air Mobility Research and Development Laboratory, Fort Eustis, Virginia, July 1972, AD 747807.

4. Kish, Jules G., AIRCRAFT CLUTCH ASSEMBLIES, RAMP ROLLER, Sikorsky Aircraft, USAAMRDL Technical Report 72-31, Eustis Directorate, U. S. Army Air Mobility Research and Development Laboratory, Fort Eustis, Virginia, July 1972, AD 747816.

5. Wirth, Charles J., POSITIVE ENGAGEMENT CLUTCH, Kaman Aerospace Corporation, USAAMRDL Technical Report 73-96, Eustis Directorate, U. S. Army Air Mobility Research and Development Laboratory, Fort Eustis, Virginia, December 1973, AD 775835.

6. Kish, Jules, G., Menkes, Paul, and Cormier, Kenneth R., HELICOPTER TRANSMISSION MODULARIZATION AND MAINTAINABILITY ANALYSIS, Sikorsky Aircraft, USAAMRDL Technical Report 73-82, Eustis Directorate, U. S. Army Air Mobility Research and Development Laboratory, Fort Eustis, Virginia January 1974, AD 775834.

APPENDIX A

ANALYSIS OF CENTRIFUGAL EFFECTS ON ROLLER RETENTION CAGE LUGS, RAMP-ROLLER CLUTCH

Under the action of centrifugal force, the cage of the ramp-roller clutch is subjected to two diametrically opposed forces as shown in Figure A-1.

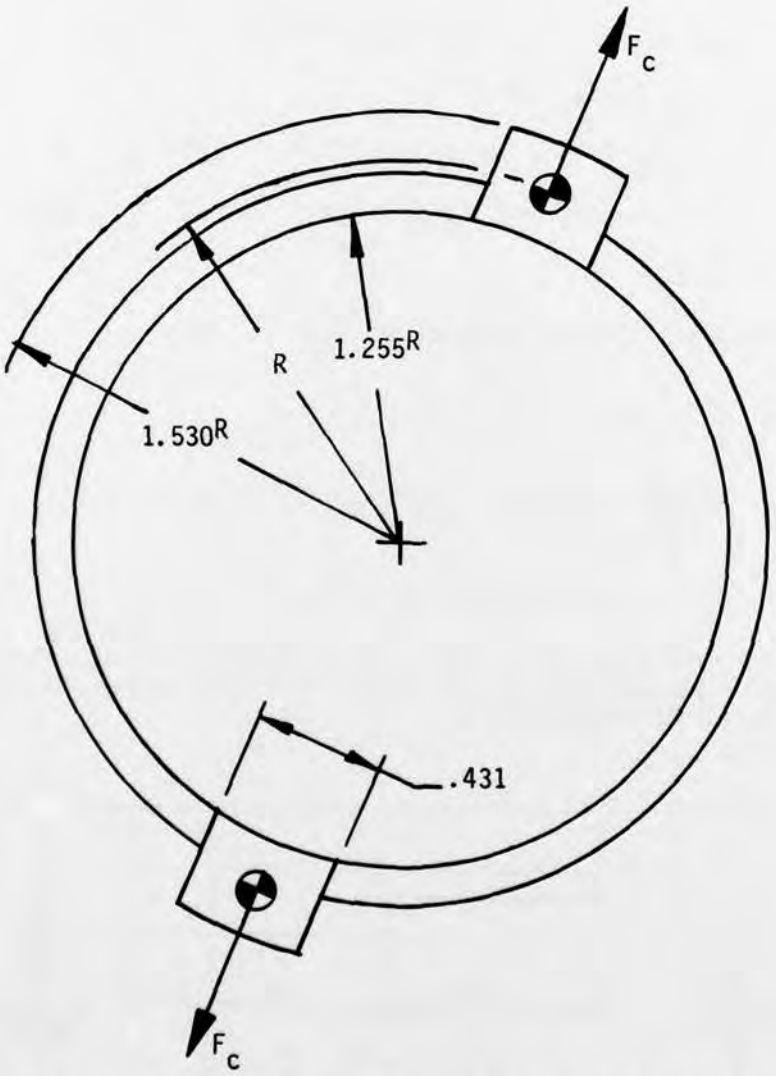

Figure A-1. Centrifugal Force on Cage, Ramp-Roller Clutch.

Even though the loads are inherently balanced, at high speeds the centrifugal load, Fc, may become so high that the cage deflections exceed the clearance between the shaft journal and the cage. If this happens, the cage will be restrained from rotation, and the ramp-roller clutch will be unable to function properly in the overrunning mode.

The carrier originally designed for this program is analyzed as follows

$$R = \text{Ave Radius} = \frac{1.530 + 1.255}{2} = 1.392$$

Weight of lug = WL

$$WL = \left\{(1.530 - 1.255)\ (.431)\ (.312) + (1.363 - 1.255)\ (.431)\ (.136)\right\}\ .29$$

$$WL = .0126 \text{ lb}$$

Centrifugal force acting on lug = Fc

$$Fc = \frac{w}{g} R\ \omega^2$$

$$Fc = \frac{.0126}{386}\ (1.392)\ \left(\frac{20000\pi}{30}\right)^2$$

Fc = 199 lb acting on each lug

The cage is analyzed as a ring with diametrically opposed loads of 199 pounds each. A cross section taken through the cage is shown in Figure A-2.

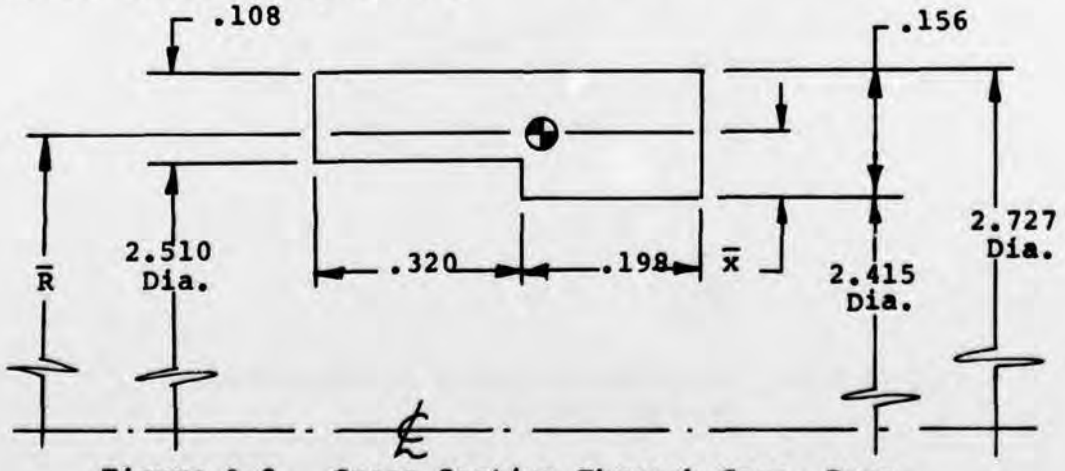

Figure A-2. Cross Section Through Cage, Ramp-Roller Clutch.

From the Figure

$$\bar{X} = \frac{\Sigma AXi}{\Sigma A}$$

$$\bar{X} = \frac{(.320)(.108)(.048+.108/2) + (.198)(.156)(.156/2)}{(.320)(.108) + (.198)(.156)}$$

$$\bar{X} = .091 = \text{centroidal distance}$$

$$\bar{R} = 1.208 + .091 = 1.299$$

$$I\bar{X} = \frac{.320\ (.108)^3}{12} + (.320)(.108)(.102 - .091)^2 +$$

$$\frac{.198\ (.156)^3}{12} + (.198)(.156)(.078 - .091)^2$$

$$I\bar{X} = .000105\ \text{in.}^4 = \text{moment of inertia of cross section about c.g.}$$

$$Z\bar{X} = \frac{IX}{C} = \frac{.000105}{.091} = 00115\ \text{in.}^3$$

$$\delta = \frac{K\ P\ R^3}{EI}$$

K is a function of the position at which the deflection is desired.

At the load points

$$K = .07439 \text{ (+outward)}$$

At 90 degrees from the load

$$K = -.06831 \text{ (inward)}$$

$$\delta = \frac{(-.06831)(199)(1.299)^3}{(30 \times 10^6)(.000105)}$$

$$\delta = -.00946 \text{ in.}$$

Since the radial clearance between the cage and journal on the cam is .002 inch and the deflection is .0095 inch, the cage will hit the journal and pinch tightly, not allowing cage rotation.

To correct this situation, the lug was redesigned by removing weight from the lugs and by adding a stiffening ring to the outside of the cage. The redesigned lug is shown in Figure A-3.

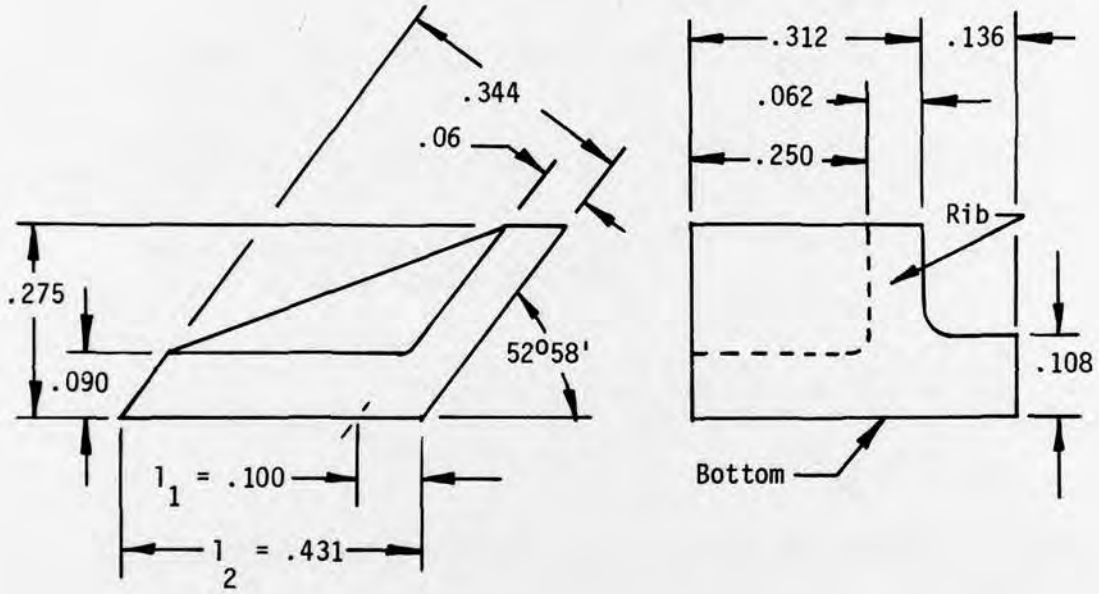

Figure A-3. Redesigned Lug of Cage, Ramp-Roller Clutch.

$$l_1 = \frac{.06}{\sin 52^\circ 58'} = \frac{.06}{.79828} = .075$$

$$l_2 = \frac{.344}{\sin 52^\circ 58'} = \frac{.344}{.79828} = .431$$

Weight of solid lug = WL = .0126 lb

Weight of hollowed out lug = Wh

$$Wh = \rho \left[V_{bottom} + V_{front} + V_{rib} + V_{lug} \right]$$

$$V_{bottom} = .250\ (.090)(.432 - .075) = .00801\ in.^3$$

$V_{front} = (.275/\cos 37^{\circ}\ 2')(.06)(.250) = .00517\ in.^3$

$V_{rib} = .00531\ in.^3$

$V_{lug} = (.136)(.431)(.108) = .00633\ in.^3$

$\rho = .29$ = density of steel

$W_h = .29 \left[.00801 + .00517 + .00531 + .00633 \right]$

$W_h = .00720$ lb

$F_c = 199 \frac{W_h}{W_L} = 199 \frac{.00720}{.0126}$

$F_c = 114$ lb = centrifugal force on redesigned lug

A cross section through the cage with the new press-fitted ring is shown in Figure A-4.

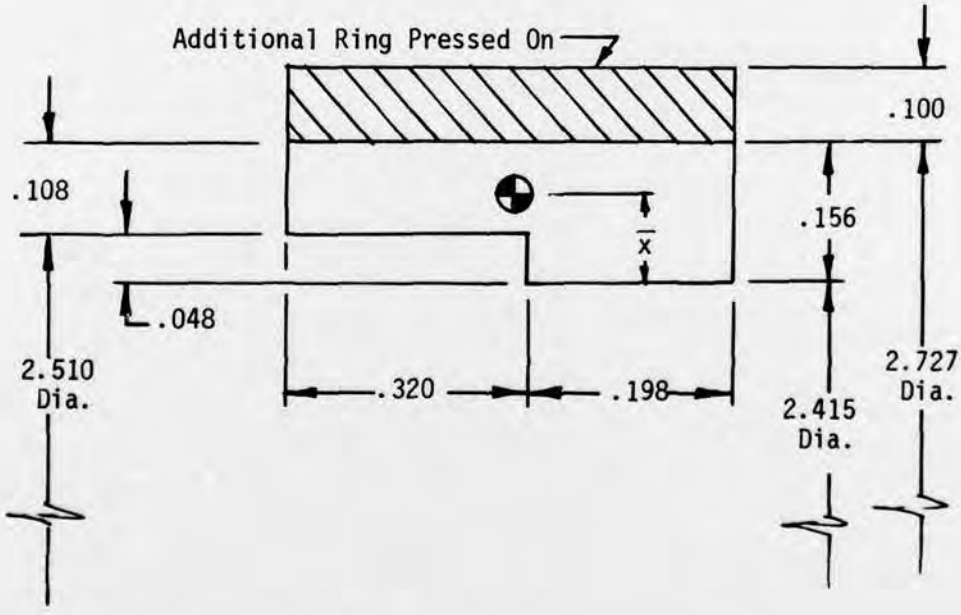

Figure A-4. Redesigned Cage With Press-Fitted Ring, Ramp-Roller Clutch.

$$\bar{X} = \frac{\Sigma AXi}{\Sigma A}$$

$$\bar{X} = \frac{(.208)(.320)(.208/2 + .048) + (.198)(.256)(.256/2)}{(.208)(.320) + (.198)(.256)}$$

$\bar{X}$ = .1416 in. = new centroidal distance

$\bar{R}$ = 2.415/2 + .1416 = 1.349

$$I\bar{X} = \frac{.320(.208)^3}{12} + (.320)(.208)(.208/2 + .048 - .1416)^2 + \frac{.198(.256)^3}{12} + (.198)(.256)(.256/2 - .1416)^2$$

$I\bar{X}$ = .000533 in.^{4} = moment of inertia of cross section about c.g.

$$\delta = \frac{K P R^3}{EI}$$

$$\delta = \frac{(-.06831)(114)(1.349)^3}{(30 \times 10^6)(.000533)}$$

δ = .00120 in.

Since the radial clearance between the cage and the journal on the cam is .002 inch, the cage will be free to rotate at 20,000 rpm with the redesigned parts.

The following analysis is performed to determine if the ring will remain on the cage under the action of centrifugal force. Figure A-5 is a cross section of the ring press-fitted onto the cage.

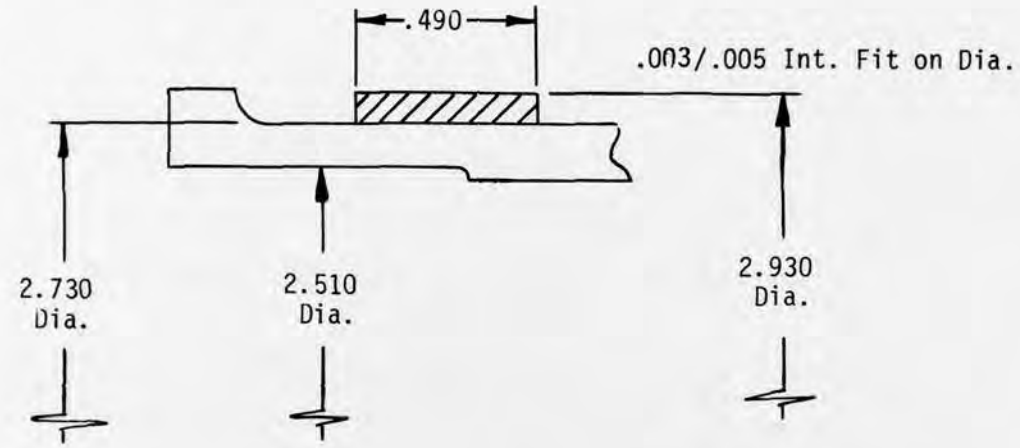

Figure A-5. Cross Section of Cage With Press-Fitted Ring, Ramp-Roller Clutch.

The classical two-ring press-fit formula is used as follows

$$p12 = \frac{\Delta 12/R12}{\underbrace{\frac{1}{E_1}(\eta_1 - \nu_1)}_{\text{inner}} + \underbrace{\frac{1}{E_2}(\eta_2 + \nu_2)}_{\text{outer}}}$$

$$\eta = \frac{b^2 + a^2}{b^2 - a^2}$$

$$\eta_1 = \frac{2.73^2 + 2.51^2}{2.73^2 - 2.51^2} = 11.930$$

$$\eta_2 = \frac{2.93^2 + 2.73^2}{2.93^2 - 2.73^2} = 14.168$$

$E_1 = E_2 = 30 \times 10^6$ psi for steel

$\nu_1 = \nu_2 = .32$ = Poisson's ratio

$$p12 = \frac{.005/2.73}{\frac{1}{30x10^6}(11.93-.32) + \frac{1}{30x10^6}(14.168 + .32)}$$

$p12 = 2105$ psi

$f_1 = p12\ \eta_1 = 2105\ (11.93)$

$f_1 = 25{,}100$ psi = stress in cage from press fit

$f_2 = p12\ \eta_2 = 2105\ (14.168)$

$f_2 = 29{,}800$ psi = stress in strengthening ring from press fit

The centrifugal growth of the outer strengthening ring is found by converting the centrifugal force into an internal pressure acting on the outer ring and conservatively neglecting the centrifugal growth of the inner ring.

$$Fc = \frac{W}{g} R \omega^2$$

$$\text{Internal pressure} = Pi = \frac{\text{Fc of entire ring @ R}}{\pi\ di\ \ell}$$

$$W = \frac{\pi}{4}(2.93^2 - 2.73^2)(.49)(.29) = .1263 \text{ lb}$$

$$Fc = .\frac{1263}{386}\left(\frac{2.83}{2}\right)\left(\frac{2000\pi}{30}\right)^2 = 2030 \text{ lb}$$

$$Pi = \frac{2030}{\pi(2.73)(.49)} = 483 \text{ lb/in.}^2$$

Δa = centrifugal growth of stiffening ring

$$\Delta a = \frac{Pia}{E}\left[\eta_1 + \nu_1\right]$$

$$\Delta a = \frac{483(2.73)}{30 \times 10^6}\left[11.93 + .32\right]$$

$\Delta a = .0005$ in. (diametral)

Thus, the outer stiffening ring will grow by .0005 inch in diameter when rotating at 20,000 rpm, but it will remain on the cage because the minimum interference fit is .003 inch.